ラン藻の鉄輸送機構の研究

加藤　大和

博士（理学）

総合研究大学院大学

生命科学研究科

分子生物機構論専攻

平成 13 年度

(2001)

目次

略語表

略語

ABC: ATP-binding cassette

CBB: coomassie brilliant blue

CCCP: carbonylcyanide *m*-chlorophenylhydrazone

DCCD: N, N'-dicyclohexylcarbodiimide

DTT: dithiothreitol

EDTA: ethylenediamine-N, N, N', N'-tetraacetic acid

FCCP: carbonylcyanide *p*-(trifluoromethoxy)phenylhydrazone

GST: glutathione S-transferase

IM: inner membrane

IPTG: isopropyl-β-D-thiogalactopyranoside

OD: optical density

ORF: open reading frame

OM: outer membrane

PBS: phosphate-buffered saline

PEG: poly (ethylene glycol)

PP: periplasmic space

PS I: Photosystem I

PS II: Photosystem II

rFutA1: recombinant FutA1

RT-PCR: reverse transcription-polymerase chain reaction

SDS: sodium dodecyl sulfate

SDS-PAGE: SDS-polyacrylamide gel electrophoresis

TES: N-tris(hydroxymethyl)methyl-2-aminoethanesulfonic acid

Tris: Tris(hydroxymethyl)aminomethane

第 1 章　緒論

全ての細胞および細胞内小器官は脂質膜を介して外界から分けられている。細胞が生存するためにはこの膜を介した物質の透過が良く調節され選択的に行われなければならない。物質の膜透過には、単に栄養物の取り込みと老廃物の排出のみにとどまらず様々な制御因子の行き来も含まれる。自然環境下において生存競争を勝ち抜いて生育するために、バクテリアが非常に効率良く栄養物を取り込みまた不必要なものを排出できる能力を持っていることは容易に想像できる。これは、例えば大腸菌において生育培地中にアミノ酸が存在すれば、そうでない場合に比べてより早く生育できることからも明らかである。すなわち、必要な化合物を自ら合成するよりも外界から取り込むことの方がエネルギー的にずっと有利なのである。たとえば、ヒスチジンの合成には 41 分子の ATP が必要であるが、細胞内へヒスチジンを輸送するにはわずか 1, 2 分子の ATP で事足りるのである (Ames, 1986)。それゆえバクテリアが多種多様な物質輸送系を持っていることは驚くにあたらない。膜を横切った物質の能動輸送にはそれを担う膜に組み込まれた特異的なタンパク質の存在が必要である。このようなタンパク質の同定とその細胞生理学上の機能の解明に重点を置いた研究が多くの研究者によって行われたきた。その結果これら多数の膜輸送系は幾つかのファミリーに分類できることが分かった。それぞれのファミリーの中でそのメンバーはアミノ酸配列および輸送の分子機構においてお互いに類似しており、進化的に同一起源を持っていると考えられている。輸送体ファミリーには、先に述べたヒスチジン輸送体のように基質の輸送に際し ATP 加水分解エネルギーを必要とする ABC (ATP-binding cassette) 型輸送体ファミリーをはじめ、他にも幾つかのものが知られている。原核生物および真核生物両方で見られる 12 回膜貫通ヘリックス型輸送体ファミリーは様々な分子種を輸送し、その構造上 ABC 型輸送体と若干の類似性を示すが輸送のエネルギーは膜を介した電気化学的勾配または他の分子との共輸送/対向輸送により供給される。これゆえ 12 回膜貫通ヘリックス型輸送体は ABC 型輸送体と異なり、その溶質を勾配に応じて膜のどちら側へも透過し得る。また、PTS (phosphotransferase) システムは膜輸送に際しその基質のリン酸化によりエネルギーが供給される。この機構で働く輸送体ファミリーは主に糖およびその誘導体の輸送に限られている

(Lengeler, et al., 1990)。ところで大腸菌においては同一の物質が ABC 型輸送体と 12 回膜貫通ヘリックス型輸送体の両方で輸送される例が知られているが、このことによって細胞は置かれた条件によってどちらの輸送体を使うのがエネルギー的に有利になるかを選択できると考えられている。しかし一般的に言えば 12 回膜貫通ヘリックス型輸送体はタンパク質当たりの輸送速度は大きいが溶質に対する特異性が低く、また熱力学的な理由から大きな濃度勾配に逆らった溶質の膜内側への蓄積は困難である (Hengge and Boos, 1983)。これに対して ABC 型輸送体は輸送速度は小さいが非常に高い親和性を持ったシステムであり、高い濃度勾配に対しても基質を蓄積する事が可能である。基質に対する高親和性は特に物質の排出の際に重要となる性質である (Silver, et al., 1989)。

ABC 型輸送体の最初の研究は、グラム陰性細菌における結合タンパク質依存性輸送体に関するものであった。この能動輸送体ファミリーの特徴は浸透圧ショック感受性であることである (Berger, 1973, Berger and Heppel, 1974)。浸透圧ショックとは細胞をショ糖溶液中で原形質分離させた後、冷蒸留水で急激に希釈する方法である。原形質分離を EDTA とトリス緩衝液存在下で行うことで細胞外膜を少しだけ弱くし、次の希釈による水の急速な細胞内への流入によって膜が部分的に破壊される。この浸透圧ショックにより、いわゆるペリプラズムタンパク質と呼ばれる一群のタンパク質が細胞外へと放出される。ペリプラズムタンパク質はその名の通り細胞の外膜と内膜の間に位置するペリプラズム内に存在していると考えられている。もちろんペリプラズム内の全てのタンパク質がこの操作で放出される訳ではなく、明らかに細胞質で働くタンパク質が放出される場合もある。またグラム陽性細菌においては結合タンパク質は脂質基によって膜に固定されている。引き続く遺伝学的な研究により、ペリプラズムタンパク質はこれを含む膜透過系に必要な構成要素であることが確かめられた。ペリプラズムタンパク質は比較的簡単に精製が可能で、かつ多量に存在している場合が多く、また精製後も著しく安定でその生化学的な機能も検定し易いことから、詳細な解析が進められてきた。これらのタンパク質は分子量およそ 25 kDa から 56 kDa のモノマータンパク質として存在し、幾つかのものは熱に対しても安定である。結合基質となる化合物に対する親和性が高く、基質と結合することでコンフォメーションが変化する。幾つかのタンパク質は結晶化されその 3 次元構造が決定された (Adams and Oxender, 1989)。ペリプラズ

ムタンパク質は 2 つの球状ドメインとこれらが形成する溝から成り、柔軟性をもったヒンジ領域で結合されている。この窪みの部分に基質が結合することでコンフォメーションが変わる。このコンフォメーション変化は、基質結合タンパク質と後で述べる ABC 型輸送体の膜タンパク質との相互作用を可能にする。バクテリアの取り込み系の ABC 型輸送体は全てこのペリプラズムタンパク質が存在するが、輸送に際して必須ではない場合も知られている (Tam and Saier, 1993)。排出系の ABC 型輸送体でペリプラズムタンパク質を必要とするものは知られていない。

ABC 型輸送体が複数のタンパク質から構成されていることが示されたのは、ヒスチジン輸送体の野生型結合タンパク質を持つにも関わらずヒスチジン輸送活性を持たない変異株が得られたことからであった (Ames and Lever, 1970)。その後ヒスチジン透過酵素、マルトースや分枝鎖アミノ酸、オリゴペプチド等の膜透過酵素の遺伝子構造解析から、一般にバクテリアの膜透過酵素はペリプラズム基質結合タンパク質と 4 つの膜結合タンパク質から構成されていることが明らかになった。この 4 つの膜タンパク質のうち 2 つは非常に疎水性が高いのに対し、残り 2 つはそれほど疎水性が高いものではないことも分かった。疎水性でない膜サブユニットはおよそ 200 残基のアミノ酸で構成されており、アミノ酸一次配列中には多種の膜透過酵素間で非常に保存性の高い領域が何カ所か存在している。これらの領域はこの輸送体ファミリーに共通の作用機構と深く関係しているだろうと考えられた。Higgins ら (1985) はこの保存性の高い配列の一部がプロトントランスロケーティング ATP アーゼの α および β サブユニットや、ミオシン、アデニレートキナーゼ、RecA タンパク質などに見られる ATP 結合部位と有意な相同性を持つことを発見した (Walker, et al., 1982)。実際この ATP 結合部位に ATP およびそのアナログ化合物が結合することが実験的に示され (Hobson, et al., 1984)、さらに結合した ATP が加水分解されることが基質の輸送に必須であることが証明された (Bishop, et al., 1989, Dean, et al., 1989)。これらの知見から基質結合ペリプラズムタンパク質依存性の膜透過酵素は ABC 型輸送体と呼ばれることとなったのである。ATP 結合タンパク質 (ABC タンパク質) は細胞膜の細胞質側の表面に存在しており、通常ホモあるいはヘテロ二量体を形成している。残り 2 つの膜タンパク質は先にも述べたように著しく疎水性が高いことが特徴である。実際これらのタンパク質

はそのアミノ酸配列から膜を貫通する複数の α-ヘリックスから成っていると推測されている。一つの膜貫通タンパク質は普通 6 本の膜貫通領域を持っており、N 末端および C 末端は膜の細胞質側に存在していると考えられている。また 2 つの膜貫通タンパク質は膜内で二量体を形成しており、合わせて一つの輸送体につき 12 本の膜貫通領域が存在している。この 2 つの膜タンパク質が基質を透過する経路を形成し、かつ輸送される基質の特異性を決定していると考えられている。また、膜貫通タンパク質は各輸送体間でそれほど配列が保存されてはいない。

ABC 型輸送体のサブユニットは特に原核生物においては別々のポリペプチドとしてコードされていることが多いが、個々のサブユニットが種々の組み合わせをもってひとつのポリペプチドとしてコードされている場合も少なくない。代表的な ABC 型輸送体のサブユニット構成を Fig. 1-1 に示す。 Fig. 1-1, A, B はそれぞれ *Salmonella typhimurium* のヒスチジン輸送体とオリゴペプチド輸送体であり、これらは 3 種あるいは 4 種の膜サブユニットとペリプラズムタンパク質が別々にコードされている。Fig. 1-1, C は *Escherichia coli* のリボース輸送体であり、2 つの ABC タンパク質が一本のポリペプチドとしてコードされている。同じく *E. coli* の鉄化合物輸送体 FhuB (Fig. 1-1, D) は膜貫通タンパク質が一つのポリペプチドとしてコードされている。ヒトペプチド輸送体は RING 4 と RING 11 の 2 つのポリペプチドがら成っており、これらはそれぞれ N 末側に疎水性の膜貫通領域を持ち、C 末側に ABC 領域が存在する (Fig. 1-1, E)。また、ヒトの多剤耐性 (Mdr) P 糖タンパク質 (Fig. 1-1, F) やのう胞性繊維症膜貫通調節タンパク質 CFTR (Fig. 1-1, G) においては、4 つのタンパク質領域が一本のポリペプチドとしてコードされている (Higgins, 1992)。

近年、ヒトをはじめとしてシロイヌナズナや酵母、大腸菌等々、様々な生物の全ゲノム塩基配列が決定されてきているが、ABC 型輸送体は動物、植物、バクテリアを問わず普遍的に存在しており、最も大きなタンパク質ファミリーの一つと言える。実際 *E. coli* や *Bachillus subtilis* においては全 ORF の 1〜2% 程度が ABC 型輸送体ファミリーで占められていると予測されている (Holland and Blight, 1999)。また、ヒトの遺伝病の原因遺伝子の幾つかがこのファミリーに属しているため、医学的な重要性からも注目されている。しかし大規模ゲノム解析から明らかになった輸送体遺伝子の多くは、未だその正確な機能すなわ

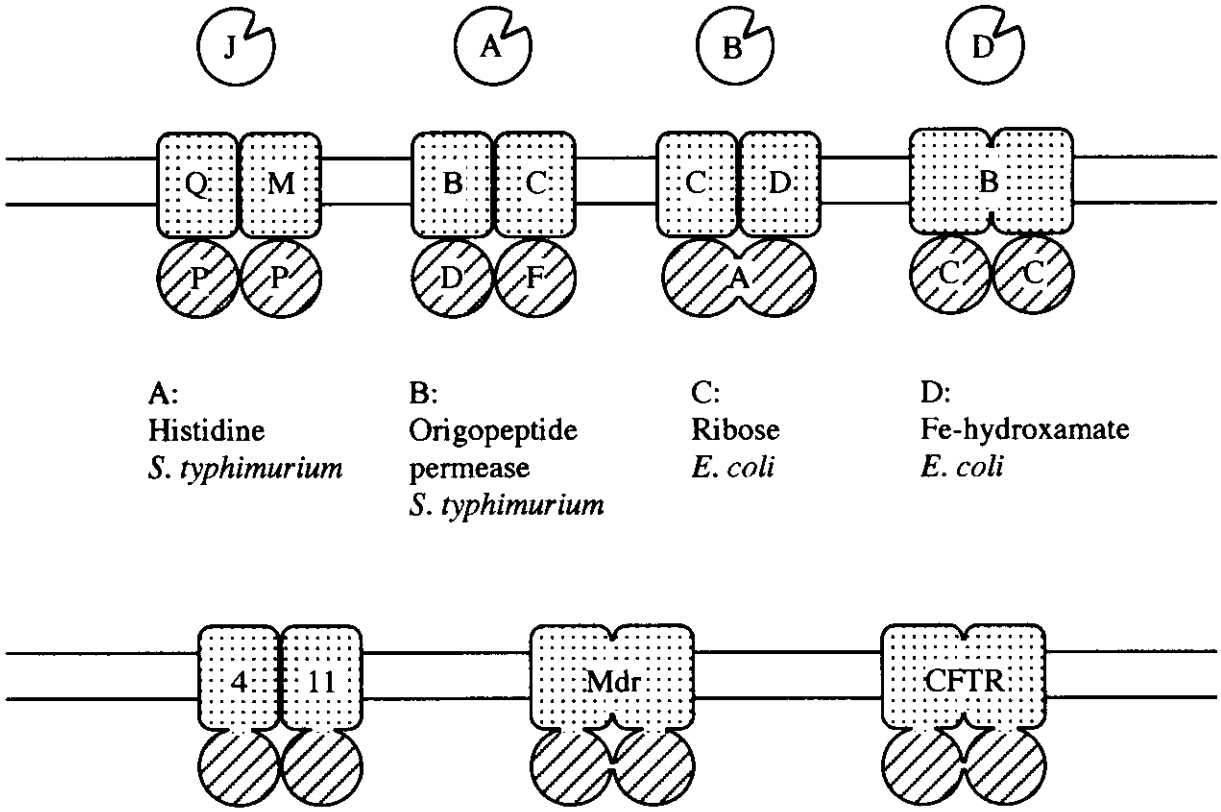

Fig. 1-1. Domain organization of ABC transporters. A typical ABC transporter consists of four domains, two highly hydrophobic membrane-spanning domains (shaded), which form the translocation pathway, and two peripheral membrane domains (shaded) which couple ATP hydrolysis to the transport process. The domains are often encoded as separate polypeptide; however, they may also be fused together in one of several alternative combinations. See text for further details.

ち輸送される基質が何であるか明らかでない場合が多く、今後はそれらの生理学的な機能をひとつひとつ解明していくことが非常に重要である。そこで私は既にゲノム解析が完了しているラン藻 *Synechocystis* sp. strain PCC 6803 において機能未知の輸送体遺伝子の機能解析を試みた。ラン藻 (シアノバクテリア) は、水を電子供与体として酸素を発生する植物/藻類型の光合成を行うグラム陰性原核生物である。細胞内に良く発達したチラコイド膜を持ち、ここに光合成のための光捕集、エネルギー変換、電子伝達等を司るタンパク質複合体が埋め込まれている。このグループの生物は地球上のあらゆる生態学的地位に生活し、また栄養性や光強度、光波長、温度、湿度等あらゆる物理化学的パラメーターが著しく変動するような場所において見ることができる。ラン藻は形質転換などの遺伝子工学的手法を適用することで遺伝子の機能や発現制御機構を比較的簡単に解明することができる。また、ラン藻が持つ独立栄養の能力は細胞内共生によって藻類や植物へ受け継がれたと考えられているため、高等植物における光合成研究のモデル生物として研究されてきた。特に単細胞性ラン藻 *Synechocystis* sp. strain PCC 6803 は、(1) 細胞外の DNA を容易に細胞内に取り込んで相同組換えにより形質転換する、(2) 暗所で従属栄養的に生育できる、(3) ゲノム塩基配列が既に決定されている、という特徴を持つ。PCC 6803 株は Kaneko ら (1996) により、全 3,168 ORF のうち 158 ORF が輸送/結合タンパク質カテゴリーに分類されており、その大部分が ABC 型輸送体遺伝子ファミリーに属すると考えられる。中でも ABC タンパク質はそのアミノ酸配列の保存性の高さから ABC 型輸送体のサブユニットであることは推定し易いが、一方で何を輸送するタンパク質をコードしているのか不明な ORF が非常にたくさん残されている。先ず私はこれらの ABC タンパク質に着目し、細胞の栄養要求性の観点から解析を進めることにした。

ラン藻における栄養要求性と物質輸送に関してはこれまでに数多くの研究がなされてきている。ラン藻を栄養素欠乏状態にして、種々の生理学的な応答が調べられた。それらの細胞応答は、ある栄養物の欠乏に特異的な応答と様々な栄養物の欠乏に共通なものとに分けられる。特に前者の応答の一つとして、それぞれの栄養素欠乏に応答した特異的なタンパク質の合成が古くから観察されていた。これらのタンパク質のうち幾つかはその栄養素に特異的な輸送体であり、また幾つかは細胞の栄養要求度を変化させる様々な代謝酵素であることが

分かった。

多くのラン藻種は無機炭素源として二酸化炭素と炭酸イオンを能動的に取り込んで、外界の 1,000 倍程度までその細胞内濃度を高めることができる (Kaplan, et al., 1991)。生育が制限されるような無機炭素濃度では細胞の無機炭素の取り込み活性が上昇する (Badger and Price, 1990)。はじめに *Synechococcus* sp. strain PCC 7942 において炭素源制限条件下で 42 kDa の膜タンパク質が合成されることが報告された (Omata and Ogawa, 1986)。この 42 kDa タンパク質遺伝子の欠損株 M42 は低 CO_2 通気条件下で誘導される無機炭素輸送活性が低下していることから、細胞の無機炭素取り込み活性の上昇にはこのタンパク質が必要であることが示唆された (Omata, et al., 1987)。このタンパク質の遺伝子はクローニングされ *cmpA* と名付けられたが、その後の解析から *cmpA* の下流には 3 つの遺伝子 *cmpB*、*cmpC*、*cmpD* から成る遺伝子クラスターが存在し、遺伝子の推定アミノ酸配列から *cmpABCD* オペロンは ABC 型輸送体をコードしていると予想された。しかし PCC 7942 株は低 CO_2 通気条件下で誘導される複数の無機炭素輸送系が存在しているため、*cmpABCD* オペロンのプロモーター領域を次に述べる硝酸/亜硝酸イオン輸送体のもので置換し、高 CO_2 通気条件下で *cmpABCD* を強制発現させた変異株を用いた無機炭素輸送活性の解析によって、*cmpABCD* オペロンが ABC 型炭酸イオン輸送体をコードしていることが実験的に証明された (Omata, et al., 1999)。

これに先立って PCC 7942 株では ABC 型の硝酸/亜硝酸イオン輸送体遺伝子が同定されている。ラン藻はアンモニア、硝酸塩、亜硝酸塩だけでなく、尿素等の有機化合物を窒素源として利用することができ、また空気中の窒素を固定する種も知られている。窒素源としてアンモニアが優先的に使われるため、培地中にアンモニアが存在すると他の窒素化合物の取り込み系および同化に必要な酵素類の合成は抑制されている (Flores and Herrero, 1994)。PCC 7942 株において窒素源として硝酸塩のみを用いて培養した細胞は、アンモニアを窒素源として培養した細胞では見られない 45 kDa のタンパク質の多量の蓄積が細胞質膜に認められる。このタンパク質遺伝子は *nrtA* と命名され、さらにその後の解析から *nrtA* は *nrtBCD* と共に ABC 型の硝酸/亜硝酸イオン輸送体をコードしていることが分かった (Omata, 1991, Omata, et al., 1993)。さらに *nrt* 遺伝子の周囲には硝酸塩還元酵素遺伝子と亜硝酸塩還元酵素遺伝子が存在しているこ

とも明らかとなった。これらの遺伝子クラスターは mRNA の転写レベルで発現が調節されており、アンモニア培地での培養では転写が抑えられており、硝酸培地で培養することにより転写されることが示された (Suzuki, et al., 1992)。

ラン藻における硫黄の利用の分子機構は詳細に調べられている。*Synechococcus* は硫酸塩、チオ硫酸塩、システイン、シスチン、還元型グルタチオン、チオシアン酸等、種々の無機および有機含硫化合物を利用可能である (Schmidt, et al., 1982)。初期の研究において硫酸塩輸送系はエネルギー要求性でかつ光依存性であり、また温度や pH にも影響されることが報告されている (Utkilen, et al., 1976, Jeanjean and Broda, 1977)。DCCD や CCCP のような代謝阻害剤、セレン酸塩やクロム酸塩のような硫酸塩類縁体、チオ硫酸塩や亜硫酸塩といった含硫化合物により硫酸塩の細胞内への輸送は阻害を受け、また硫黄欠乏により細胞の硫酸取り込み活性は上昇する。Utkilen らの報告によれば、*Synechococcus* の硫黄欠乏下での硫酸輸送系の $K_{1/2}$ 値および V_{max} 値は 42°C でそれぞれ 0.75 μM および 0.7 pmol(10^6 cells×min)$^{-1}$ であった (Utkilen, et al., 1976)。この輸送系は浸透圧ショック感受性であることから、ペリプラズムタンパク質の関与が示唆された。この硫酸輸送に必要な遺伝子領域が明らかになったのは、硫黄源として硫酸塩を与えた場合に生育に必要な *S. typhimurium* の遺伝子領域をプローブとして、PCC 7942 株ゲノム中の類似遺伝子を探索した研究からであった (Green, et al., 1989, Laudenbach and Grossman, 1991)。ここで得られた DNA 断片において、最初に詳しい解析がなされたのは、*cysA* と呼ばれる遺伝子である。*cysA* 遺伝子産物の推定アミノ酸配列内には ABC 型輸送体ファミリーの ABC タンパク質に特徴的な ATP 結合モチーフが存在した。続いて *cysA* 遺伝子の上流領域が解析され、ペリプラズム基質結合タンパク質遺伝子 *sbpA*、膜結合タンパク質遺伝子 *cysT*、*cysW* が同定された。これらの遺伝子の破壊株の表現型から、*cycA*、*sbpA*、*cysT*、*cysW* が ABC 型硫酸イオン輸送体の構成遺伝子であることが示された。更に、*E. coli* のチオ硫酸イオン結合タンパク質遺伝子 *cysP* の相同遺伝子が PCC 7942 株の *cysW* の下流に存在し、その下流にはそれぞれ *cysT* と *cysW* の相同遺伝子と考えられる *cysU* と *cysV* の存在も示された。この事実から *cysP*、*cysU*、*cysV* 遺伝子がチオ硫酸イオン輸送体の各サブユニットをコードしていると推定された。ここで硫酸イオン輸送体の ABC タンパク質 CysA の相同遺伝子は同定されなかったが、他の予備

的な実験から、 PCC 7942 株において CysA タンパク質は硫酸イオン輸送体とチオ硫酸イオン輸送体の両方で ATP 結合タンパク質の役割を持っているだろうと推定されている (Grossman, et al., 1994)。

マンガンはラン藻の光合成において水の分解に必須な微量金属元素である。*Synechocystis* sp. strain PCC 6803 においては、少なくとも 3 つのマンガン輸送系の存在が確認されている。このうちの最初に遺伝子が同定されたのはナノモルオーダーのマンガン濃度で発現が誘導されてくる ABC 型マンガン輸送体で、これは *mntCAB* オペロンにコードされている (Bartsevich and Pakrasi, 1995)。これとは別にマイクロモルオーダーのマンガン濃度での生育時には基質特異性の高い第二のマンガン輸送系が機能している。この輸送系の存在は *mnt* 遺伝子破壊株が特異性の高いマンガン輸送活性を持っていることから示されたが、遺伝子の同定には至っていない。さらにマンガン輸送活性の速度論的解析から第三のマンガン輸送系の存在も示されたが、これはマンガンに対する親和性は低いものであった。ABC 型マンガン輸送体はもともと光合成活性の低下した変異株のスクリーニングによって明らかにされたものである。それぞれ *mntA* が ABC タンパク質を、*mutB* が膜貫通タンパク質を、*mntC* が基質結合タンパク質をコードしている (Bartsevich and Pakrasi, 1996, Bartsevich and Pakrasi, 1999)。

以上で述べたように、ラン藻における物質輸送は、多量栄養元素に関してはリンを除いて良く解析されている。*Synechococcus* においては 3 つのリン酸輸送体の存在が示唆されているが、分子機構の解明は進んでいない (Grillo and Gibson, 1979)。一方微量栄養元素の輸送については、マンガン輸送体 MntABC 以外に輸送系の分子機構が解明された例は報告されていない。特に鉄や銅に関しては、それらの欠乏に対する細胞の応答機構は詳細に解析されてきた。鉄欠乏下では鉄含有光合成電子伝達鎖の構成要素であるフェレドキシンは、鉄を含まないフラボドキシンで置き換えれらる (Laudenbach, et al., 1988, Bottin and Lagoutte, 1992)。銅欠乏に対しラン藻は銅を含んだ光合成電子運搬タンパク質プラストシアニンの役割をヘムを含んだシトクロム c_{553} で置き換えることが報告されている (Briggs, et al., 1990)。これらのタンパク質の発現制御は mRNA の転写レベルで調節を受けている。しかしこの 2 つの応答はいずれも栄養素欠乏条件下で細胞の栄養素の要求度を低下させるもので、先に述べたいわゆる欠乏ストレス下での代謝酵素等の新規合成の範疇に入ると言える。鉄欠乏に関し

ては細胞の鉄輸送活性が上昇すること、新たな細胞質膜タンパク質と外膜タンパク質が蓄積すること等も観察されたが、ラン藻および光合成藻類における膜を介した鉄輸送の分子機構は謎のままである (Scanlan, et al., 1989)。

本研究では、まず *Synechocystis* sp. strain PCC 6803 の基質未同定の ABC 型輸送体サブユニットをコードすると考えられる 35 個の遺伝子に着目した。モチーフ検索の結果、これらのうち ATP 結合モチーフを持つものは 32 個存在した。この 32 個の遺伝子についてそれぞれ欠損変異株を作製し、種々の栄養素欠乏培地上での生育特性を野生株と比較した。その結果低濃度鉄培地上で生育が遅い変異株 Δ*futC* (Δ*sll1878*) を得た。さらに野生株とこの変異株を用いて、細胞の鉄輸送活性の解析を行った (第 2 章)。次に、ラン藻の鉄輸送機構に着目し、他の生物の鉄輸送体遺伝子と相同性の高い PCC 6803 の推定遺伝子をそれぞれ破壊した変異株を作製した。これらの表現型の解析から、PCC 6803 における ABC 型三価鉄輸送体遺伝子群 *futA1*, *futA2*, *futB*, *futC* (*slr1295*, *slr0513*, *slr0327*, *sll1878*) と、ABC 型二価鉄輸送体遺伝子 *feoAB* (*ssr2333*, *slr1392*) を同定した。また、*fut* 遺伝子群は恒常的に発現していること、これに対し *feoAB* 遺伝子は鉄欠乏ストレスにより発現が誘導されることを明らかにした (第 3 章)。さらに、三価鉄輸送体 (Fut 輸送体) の基質結合タンパク質をコードしていると予測される *futA1* 遺伝子を大腸菌に組み込み、タンパク質を過剰発現させた。精製したリコンビナント FutA1 タンパク質 (rFutA1) 溶液を用いた分光学的解析から、FutA1 タンパク質が三価の鉄イオンとモル比 1 : 1 で結合すること、すなわち Fut 輸送体 の基質が鉄イオンであることを証明した (第 4 章)。なお、本論文においては、Kaneko ら (1996) により推定された ORF を便宜上遺伝子と同義とし、遺伝子名として ORF 番号 (例：*slr1234*) を用いた。また遺伝子の推定翻訳産物を示す際には ORF 番号の頭文字を大文字とした (例：Slr1234)。

第 2 章　*Synechocystis* sp. strain PCC 6803 の輸送体遺伝子の機能解析

序論

ラン藻は栄養条件、光の強度や波長、温度条件等に対して応答性を示す。様々な栄養素の欠乏に対する共通の応答として、細胞の形態的な変化、細胞内部での栄養素の貯蔵、代謝活性の低下などが挙げられる。これに対して、ある栄養素に特異的な応答として、その栄養素に対する特異的な輸送系や細胞がその栄養素を利用しやすい化合物へと代謝するための酵素の発現誘導がある (Grossman, et al., 1994)。

近年、ラン藻 *Synechococcus* sp. strain PCC 7942 や *Synechocystis* sp. strain PCC 6803 において、環境応答に関連した基質特異的輸送体の遺伝子が幾つか同定されるようになった。低濃度 CO_2 条件下で発現が誘導される高親和性炭酸イオン輸送体は *cmpABCD* 遺伝子によりコードされている (Omata and Ogawa, 1986, Omata, et al., 1999)。窒素源として硝酸塩を用いて培養した細胞は *nrtABCD* 遺伝子産物である硝酸イオン輸送体を発現しているが、これはアンモニアを窒素源として培養した細胞では発現していない (Omata, et al., 1989, Omata, et al., 1993)。硫黄欠乏下で発現が誘導される *cys* 遺伝子クラスターの中には硫酸イオン輸送体をコードする遺伝子 *cysA*, *cysT*, *cysW*, *sbpA* が含まれている (Laudenbach and Grossman, 1991)。これらはいずれも基質の輸送に際して ATP 加水分解エネルギーを必要とする ABC 型輸送体であった。グルコースや中性アミノ酸の輸送体遺伝子についても報告がある (Schmetterer, 1990, Montesinos, et al., 1997)。また、光合成活性の低下した変異株の遺伝子解析から ABC 型のマンガン輸送体遺伝子 *mntCAB* が同定された (Bartsevich and Pakrasi, 1995)。特に硫酸イオンや無機炭素、マンガンの輸送には光によるエネルギー供給が必要であることが報告されている (Utkilen, et al., 1976, Ogawa, et al., 1985, Bartsevich, et al., 1996)。

Synechocystis sp. strain PCC 6803 は既にゲノム全塩基配列が決定され、遺伝子コード領域の推定が行われた。さらに推定された全 3,168 個の ORF はそのアミノ酸配列をもとに遺伝子データーベースに対して相同性検索が実施され、そ

の結果 PCC 6803 株には多数の輸送体相同体遺伝子が存在することが示された (Kaneko, et al., 1996)。Kaneko らにより輸送体/結合タンパク質カテゴリーに分類された ORF は 158 個であり、これは全遺伝子のおよそ 5% にものぼる。このことから PCC 6803 株が非常に複雑な物質輸送系を発達させてきたことは容易に理解できる。これらの ORF のうち 123 個については配列の類似性から基質に関する何らかの情報が類推されているが、一方で ABC 型輸送体とアノテーションされているだけで基質に関する情報が示されていない ORF が 35 個も残されている。これは主に、それらの遺伝子翻訳産物が ABC 型輸送体の ABC タンパク質である場合には、その機能上の制約から配列内に基質に関する情報を含んでいないことが多いためと考えられる。さらに ABC タンパク質であれば分子内に必ず ATP 結合領域を持つため、配列情報のみからでも推定し易いこともその理由の一つであろう。そこで、これら基質未同定の輸送体の ATP 結合タンパク質サブユニットをコードしていると予測される ORF に着目し、各欠損変異株を作製して各栄養素欠乏ストレス下における表現型を解析することにより、各輸送体遺伝子産物の機能の解析を試みた。さらに、ここで得られた鉄要求性の高いひとつの変異株 *Δsll1878* を用いて、細胞の鉄輸送活性を測定し、野生株との比較を行った。

材料及び方法

2-1. ラン藻の培養条件

ラン藻はグルコース耐性の *Synechocystis* sp. strain PCC 6803 を用いた。PCC 6803 の野生株 (GT 株) 及び各変異株は 20 mM TES-KOH (pH 8.0) の緩衝液を含む BG-11 培地中で、3% (vol/vol) CO_2 (空気に CO_2 ガスを混合して最終 CO_2 濃度を 3% [vol/vol] としたもの、以下 3% CO_2 と略す) を通気し、 30°C、白色光 (蛍光管 60 $\mu Em^{-2}s^{-1}$) 連続照射下で培養した (Stainer, et al., 1971)。固形培地は上記 BG-11 培地中に 12 mM チオ硫酸ナトリウムと 1.5% 寒天 (Bacto-agar, Difco) を加えて調製した。

2-2. 形質転換用プラスミドの構築

推定アミノ酸配列内に ATP 結合モチーフを持つ 32 個の遺伝子 (Table 2-2) それぞれについて、以下の方法で形質転換用プラスミドの構築を行った。

目的とする遺伝子の 5'-側と 3'-側にそれぞれ相当する約 500～700 bp の DNA 断片を PCR により増幅した。5'-側の DNA 断片を増幅する際にはリバースプライマーの 5'-末端に制限酵素サイトと 3 つの付加塩基を持ったプライマーを用いた。同様に、3'-側の DNA 断片の増幅にはフォワードプライマーの 5'-末端に制限酵素サイトと 3 つの付加塩基を持ったプライマーを用いた。前者の酵素サイトは形質転換に用いた薬剤耐性遺伝子 (Elhai and Wolk, 1988) の 5'-側の酵素サイトと同じものを、後者の場合は薬剤耐性遺伝子の 3'-側の酵素サイトを持つように設計した。薬剤耐性遺伝子は pUC18 プラスミドのマルチクローニングサイト内の Hinc II サイトにクローニングしたものを用いた。目的遺伝子領域由来の 2 種類の DNA 断片と薬剤耐性遺伝子をそれぞれ特異的な制限酵素で切断し、0.8% アガロースゲル電気泳動により精製した。ゲルからの DNA 断片の精製には QIAquick Gel Extraction Kit (QIAGEN) を用いた。制限酵素処理した 3 種類の DNA 断片を pGEM-T ベクター (Promega, WI) にライゲーションし、この溶液を用いて大腸菌 DH5α 株を形質転換させた。得られた薬剤耐性大腸菌から、薬剤耐性遺伝子の両端に目的遺伝子特異的配列を持ったプラスミド DNA をアルカリ-SDS 法により精製した。

2-3. ラン藻の遺伝子破壊株の作製

材料及び方法 2-2 で構築したプラスミド DNA を用いて PCC 6803 野生株を相同組み換え法により形質転換した (Williams and Szalay, 1983)。対数増殖期の野生株細胞を遠心 (1,600×g, 30°C, 8 分間) して集め、波長 730 nm の吸光度 (OD 730 nm) が 2.0 になるように BG-11 培地に懸濁した。この細胞懸濁液 100 μL に形質転換用のプラスミド DNA を 100 ng 加えて 1 晩、30°C、暗所で静置した後、BG-11 固形培地上に塗布した。1 日後、ゲル表面がラン藻により淡緑色になりはじめたところで適当な抗生物質をゲル底面に添加し、さらに約 2 週間培養を続け、薬剤耐性ラン藻のコロニーを形成させた。各コロニーを抗生物質を含む新しい BG-11 固形培地で生育させ、ゲノム上の目的遺伝子が全て薬剤耐性遺伝子を挿入したものと置き換わるまで経代した。形質転換体のセグリゲーションは、材料と方法 2-4 の方法で単離したゲノム DNA を鋳型に PCR 反応を行い、目的遺伝子領域由来の PCR 産物の分子量により確認した。抗生物質はそれぞれカナマイシン (終濃度 10 μg/mL)、スペクチノマイシン (20 μg/mL)、ハイグロマイシン (50 μg/mL)、クロラムフェニコール (30 μg/mL)、エリスロマイシン (15 μg/mL) を用いた。

2-4. ゲノム DNA の単離

ラン藻細胞を遠心 (1,600×g, 30°C, 8 分間) して集菌し、200 μL の TE 溶液 (10 mM Tris-HCl, 1 mM EDTA, pH8.0) に懸濁した。これにトリス飽和フェノール (pH 8.0) (等量)、10% (w/v) SDS (25 μL)、ガラスビーズ (Acid-Washed, 粒径 150-212 μm を 100 mg) を添加した後激しく混合した。遠心分離 (15,000×g, 4°C, 3 分間) 後、上清を別のチューブに移し、再度フェノール (200 μL) を添加して混合し、遠心分離 (15,000×g, 4°C, 3 分間) して上清を別のチューブに移した。この操作をもう一度繰り返した後、フェノールを除去するため水飽和エーテル (上清と等量) を加えて激しく撹拌後、遠心 (15,000×g, 4°C, 1 分間) し、上層を除去した。エーテル抽出を 3 回繰り返した後、50°C で 10 分間加熱しエーテルを除去した。得られた溶液に 10 M 酢酸アンモニウム (1/5 量)、エタノール (2 倍量) を加えて混合した後、遠心 (15,000×g, 4°C, 15 分間) してゲノム DNA を回収した。

2-5. 栄養素欠乏 BG-11 培地の作製と変異株の生育特性の検定

BG-11 培地の各栄養素を含まない固形培地の作製は Table 2-1 に示すように、各栄養素を含んだ化合物を、それを含まない化合物で置き換えることで他の栄養素の含量を大きく変えることなく作製した。液体培地についても同様に作製した。鉄については、材料及び方法 3-1 に従い Chelex 100 陽イオン交換樹脂 (日本バイオラッドラボラトリーズ、東京) で処理した培地 (以後これを鉄欠乏培地と称す) を用いた。これらの培地上で各変異株を材料及び方法 2-1 に従い寒天固形培地上で生育させた。なお、炭素の欠乏には通常の BG-11 培地を使用し、3% CO_2 の代わりに空気を通気した。各種栄養素欠乏固形培地上での生育比較実験において、1 次スクリーニングにより若干でも野生株と差の認められた株は、さらに細胞を新しい栄養素欠乏培地に塗りひろげ、2 次スクリーニングを行った。

2-6. ラン藻細胞の鉄輸送活性の測定

後期対数増殖期 (OD 730 nm = 1～1.3) の細胞を遠心 (1,600×g, 30°C, 8 分間) して集め、等量の Chelex 100 処理した 20 mM TES-KOH (pH 8.0) 緩衝液に再懸濁し、細胞を洗浄した。もう一度洗浄を行った後、細胞の OD 730 nm が 7 (細胞数約 1×10^9 mL^{-1} に相当) となるように鉄欠乏培地に懸濁した。細胞懸濁液 (250 μL) を分注し、鉄欠乏培地に終濃度の二倍濃度になるように ^{59}Fe 放射標識塩化鉄溶液 (Amersham Pharmacia Biotech, Buckingham, UK) を添加した標識培地溶液を細胞懸濁液に直ちに等量加え良く混合することで、細胞による鉄の取り込みを開始させた。取り込み反応は 30°C、光照射下 (600 W ハロゲンランプ、Cabin Co., Tokyo, Japan、700 $\mu Em^{-2}s^{-1}$) あるいは暗所で行った。三価の鉄の取り込み量のみを測定するため、反応液中には鉄濃度の 100 倍濃度の二価鉄特異的キレーターであるフェロジンをあらかじめ加えた (Ecker and Emery, 1983)。取り込み反応を停止させるため、サンプルを氷上に移し、遠心 (11,000×g, 4°C, 1 分間) 後、上清を取り除いた。細胞を等量 (500 μL) の洗浄用緩衝液 (20 mM TES-KOH, pH 8.0, 10 mM EDTA) に懸濁し、室温で 5 分間静置した後、遠心 (11,000×g, 4°C, 1 分間) し、上清を取り除いた。この操作をもう一度繰り返した後、ガンマカウンター (model ARC-380, Aloka, Tokyo, Japan) を用いて細胞内の ^{59}Fe から発する γ 線量を測定した。

鉄取り込み量測定に際し、必要に応じて鉄欠乏ストレスを与えた細胞を使用した。すなわち、細胞を洗浄後、鉄欠乏培地で約 20 時間培養を続け生育させることで、培地中の微量残留鉄あるいは細胞内の貯蔵鉄を消費させた (材料及び方法 3-1 参照)。

2-7. その他の方法

液体培地におけるラン藻細胞の濁度は細胞懸濁液の OD 730 nm を測定した。細胞数は実際に細胞懸濁液を希釈し、固形培地で生育させコロニー数を数えることから得た、次の計算式から算出した。

懸濁液 1 mL 当たりの細胞数 = OD 730 nm × 1.5 × 10^8

吸光度の測定には紫外/可視分光光度計 V-550 (Jasco, Tokyo, Japan) を使用した。

特に言及していない実験操作は一般的な実験書に従い行った (Sambrook, et al., 1989)。塩基配列の解析ソフトウェアには DNASIS (日立ソフトウェア) を、モチーフ検索には MOTIF (京都大学化学研究所) を使用した。特に明記していない各種酵素などは宝酒造、東洋紡、ベーリンガーマンハイム、及びシグマから購入し、その他の試薬については和光純薬から購入したものを使用した。

Table 2-1. Composition of nutrient-deficient BG-11 media used in this study.

		-N	-P	-S	-Na	-Mg	-Ca	-Fe[a]	-A_6 microcomponents
Stock solution 1	Citric Acid							-	
	Ammonium iron (III) citrate	$FeCl_3$						-	
	Na_2EDTA								
Stock solution 2	$NaNO_3$	NaCl			KNO_3				
	K_2HPO_4		KCl						
	$MgSO_4$			$MgCl_2$		K_2SO_4		(K_2SO_4)	
Stock solution 3	$CaCl_2$						NaCl	(-)	
A_6 solution	H_3BO_4								-
	$MnCl_2$								-
	$ZnSO_4$			$Zn(CH_3COO)_2$					-
	$CuSO_4$			$Cu(CH_3COO)_2$					-
	Na_2MoO_4								-
	$Co(NO_3)_2$								-
	$Na_2S_2O_3$			-	$K_2S_2O_3$				

[a] Iron deficient media were treated with Chelex 100 resin before adding Mg and Ca (See Materials and Methods 3-2).

Table 2-2. Growth characteristics of *Synechocystis* mutants on various nutrient-deficient BG-11 media under 3% CO_2.

ORF	Segregation	BG-11	Air	N	P	S	Na	Mg	Ca	Fe	A_6
Wild type		+	+	+	+	+	+	+	+	+	+
sll0182		+	+	+	+	+	+	+	+	+	+
sll0240		+	+	+	+	+	+	+	+	+	+
sll0385		−	−	−	−	−	−	−	−	−	−
sll0415		+	+	+	+	+	+	+	+	+	+
sll0484		+	+	+	+	+	+	+	+	+	+
sll0489		+	+	+	+	+	+	+	+	+	+
sll0739		+	+	+	+	+	+	+	+	+	−
sll0759	×	+	+	+	+	+	+	+	+	+	+
sll0778		+	+	+	+	+	+	+	+	+	+
sll0912	×	+	+	+	+	+	+	+	+	+	+
sll1001		+	+	+	+	+	+	+	+	+	+
sll1041		+	+	+	+	+	+	+	+	+	+
sll1276	×	+	+	+	+	+	+	+	+	+	+
sll1623	×	+	+	+	+	+	+	+	+	+	+
sll1725		+	+	+	+	+	+	+	+	+	+
sll1870		+	+	+	+	+	+	+	+	+	+
sll1878		+	+	+	+	+	+	+	+	−	+
slr0075	×	+	+	+	+	+	+	+	+	+	+
slr0251	×	+	+	+	+	+	+	+	+	+	+
slr0354	×	+	+	+	+	+	+	+	+	+	+
slr0544		+	+	+	+	+	+	+	+	+	+
slr0615		+	+	+	+	+	+	+	+	+	+
slr0864		+	+	+	+	+	+	+	+	+	+
slr0982		+	+	+	+	+	+	+	+	+	+
slr1113		+	+	+	+	+	+	+	+	+	+
slr1149		+	+	+	+	+	+	+	+	+	+
slr1488		+	+	+	+	+	+	+	+	+	+
slr1494		+	+	+	+	+	+	+	+	+	+
slr1735	×	+	+	+	+	+	+	+	+	+	+
slr1901		+	+	+	+	+	+	+	+	+	+
slr2019		+	+	+	+	+	+	+	+	+	+
slr2044		+	+	+	+	+	+	+	+	+	−

Air means that cultures were aerated with 3% (v/v) CO_2.

The symbol of each element represents deficiency of that in culture medium (see Table 2-1).

× represents the gene that could not be inactivated completely.

+ means that the mutant grew as fast as wild-type cells.

− means that the mutant grew slowly than wild-type cells.

結果

輸送体遺伝子破壊株の作製

Synechocystis sp. strain PCC 6803 のゲノム塩基配列をもとに、基質未同定の輸送体遺伝子の推定アミノ酸配列内のモチーフを検索した結果、Table 2-2 に示した 32 個の ORF が ATP/GTP 結合モチーフ (コンセンサス配列 ; [AG]-x(4)-G-K-[ST]) を持っていた (Walker, et al., 1982)。これらの遺伝子を破壊するため形質転換用のプラスミド をそれぞれ構築し、これらを用いて野生株の形質転換を試みた。その結果、24 個の遺伝子についてゲノム中の野生型遺伝子が全て薬剤耐性遺伝子を挿入したものに置き換わった変異株を得ることができた (Table 2-2)。残りの 8 個については、野生型遺伝子全てが薬剤耐性遺伝子を挿入したものに置き換わった変異株を得ることは出来なかった (Table 2-2, ×で示した)。

輸送体遺伝子破壊株の生育特性

輸送体遺伝子が破壊された上記 32 株を、それぞれ炭素、窒素、リン、硫黄、ナトリウム、マグネシウム、カルシウム、鉄、微量栄養素 A_6 を除いた固形培地上で生育させ、その生育特性を野生株と比較した。野生株では上記のどの栄養素を欠乏させた培地でも、通常の BG-11 培地上と同程度に生育した。これは、BG-11 培地は野生株細胞の生育に必要などの栄養素も過剰に含んでおり、野生株は各栄養素欠乏培地中にわずかに残った低濃度の栄養素を効率的に利用できること、あるいは、細胞内の貯蔵分でしばらくは十分に生育可能であることを示している。ほとんどの変異株は野生株と同様に生育したが、4 つの変異株が野生株と異なる生育特性を示した。Table 2-2 において、各栄養素欠乏培地上で＋は野生株と同程度に生育したことを、－は野生株に比べて生育が遅かったことを表している。すなわち、*sll1878* 破壊株（以後 Δ*sll1878* と記す、他の ORF についても同様）は鉄欠乏培地上で、Δ*sll0739* と Δ*slr2044* は A_6 欠乏培地上で、また Δ*sll0385* は実験に用いた全ての条件で、野生株と比較して明らかに生育が遅かった。さらに、Δ*sll0385* 以外の 3 つの破壊株は他の栄養素欠乏下では野生株と同程度に生育することも示された。Fig. 2-1 に Δ*sll1878* の鉄欠乏培地上での生育状態を示す。他の変異株と比較しても明らかに生育が遅い

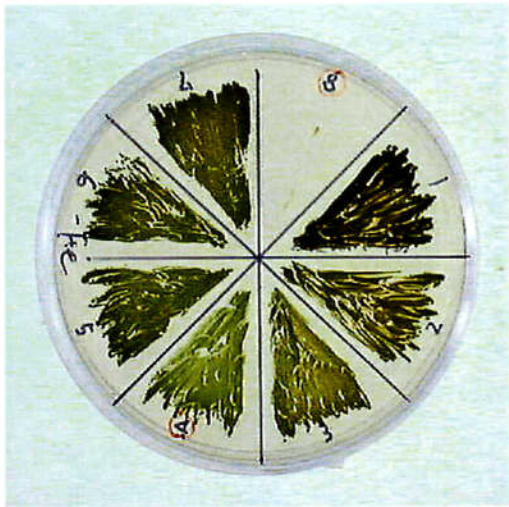

Fig. 2-1. Growth of the wild-type and mutants on solid iron-deficient BG-11 medium. Wild-type (WT) and mutants cells of *Synechocystis* were spread on agar plate containing iron-deficient BG-11 medium at pH 8.0, and plate was incubated under 3% (vol/vol) CO_2 in air for 14 days. 1: WT, 2: Δ*sll0240*, 3: Δ*sll0415*, 4: Δ*sll0484*, 5: Δ*sll0739*, 6: Δ*sll0759*, 7: Δ*sll1870*, 8: Δ*sll1878*.

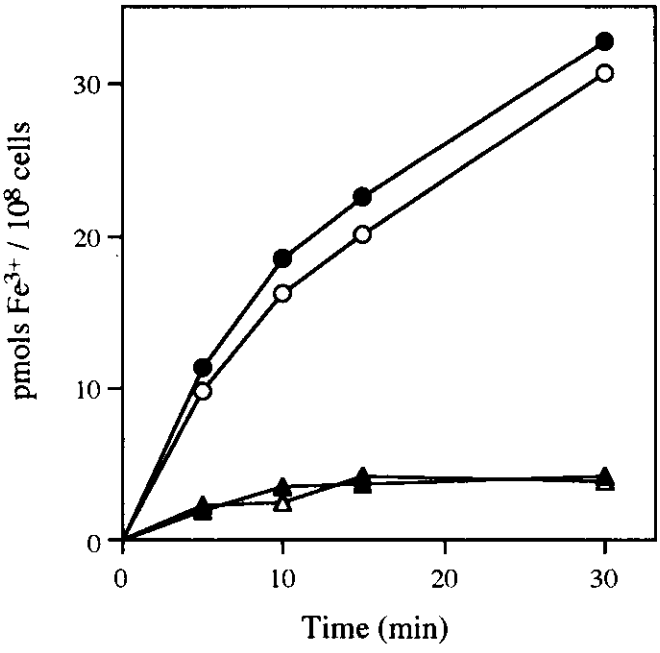

Fig. 2-2. Time course of $^{59}Fe^{3+}$ uptake by iron–deprived wild-type (circles) and Δ*sll1878* (triangles) cells, either in the dark (filled symbols) or in the light (open symbols).

ため、細胞の鉄輸送系が十分に機能していないことが推測された。

野生株と Δ*sll1878* 株の三価鉄取り込み活性

鉄欠乏培地上で生育の遅かった Δ*sll1878* 株において、実際に細胞の鉄輸送活性が低下しているのか、あるいは別の理由による二次的な表現型なのかを明らかにするため、野生株と Δ*sll1878* 株を用いて、細胞の鉄輸送活性を測定した。鉄欠乏ストレス下における活性を比較するため、細胞は約 20 時間、鉄欠乏培地で前培養したものを用い、活性測定溶液中の鉄濃度を 10 μM に固定して細胞内への鉄の蓄積量の時間変化を調べた (Fig. 2-2)。その結果、野生株細胞 (○; 光照射下, ●; 暗所) 内への鉄の取り込み量は、30 分間でおよそ 32 pmols $Fe^{3+}/10^8$ cells に達したのに対し、Δ*sll1878* 株 (△; 光照射下, ▲; 暗所) では約 5 pmols $Fe^{3+}/10^8$ cells であった。野生株においては、反応開始後 5 分間は鉄取り込み量の直線的な増加が認められた。またいずれの株においても暗条件による取り込み量の低下は見られなかった。

次に、通常の BG-11 培地 (○, △) と鉄欠乏培地 (●, ▲) の両条件で前培養した野生株 (○, ●) と Δ*sll1878* 株 (△, ▲) を用い、活性測定溶液中の鉄濃度を 0.1 μM から 20 μM まで変化させ、細胞の鉄取り込み活性の濃度依存性を調べた (Fig. 2-3)。取り込み反応時間は 5 分間に固定した。通常の条件下で培養した野生株細胞を用いた場合、鉄取り込み活性は鉄濃度 20 μM では飽和に達していたのに対し、鉄欠乏培地で培養した場合では同濃度でも飽和に達していなかった。このことから、野生株細胞では鉄欠乏培地で前培養することで各鉄濃度における取り込み速度が大きく上昇することが明らかになった。一方、Δ*sll1878* 株では、鉄欠乏培地で前培養することでわずかに鉄取り込み速度の上昇は認められたが、上昇の程度は野生株ほどではなく、両培養条件下において鉄輸送活性が野生株と比べて著しく低下していることが示された。

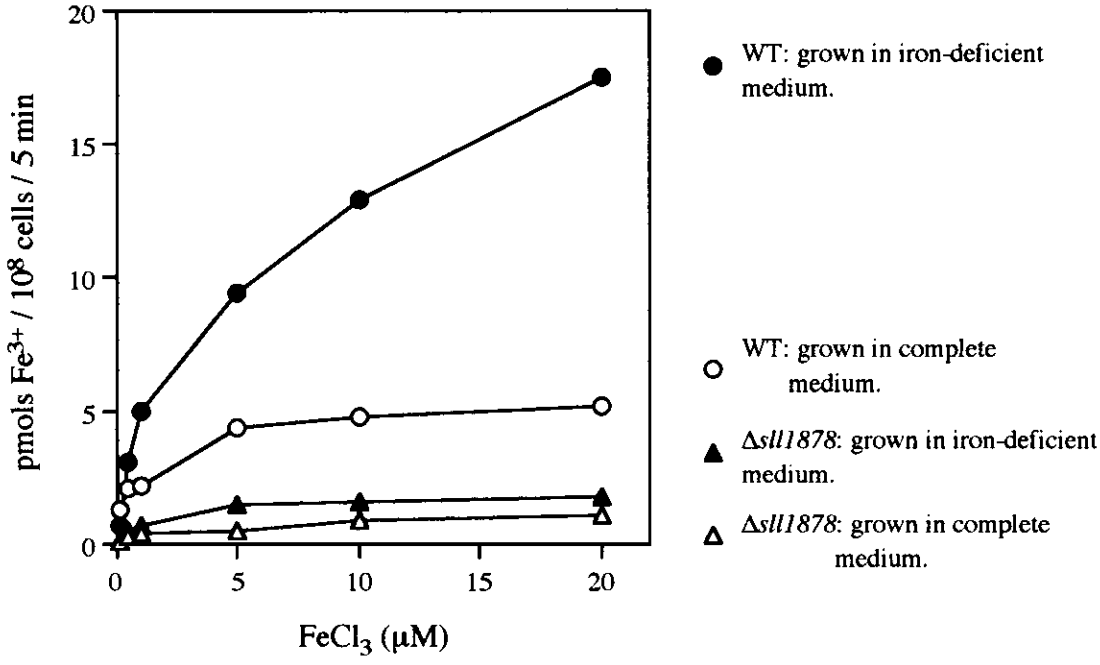

Fig. 2-3. Concentration-dependent uptake of $^{59}Fe^{3+}$ by wild-type (circles) and Δ*sll1878* (triangles) cells grown in complete medium (open symbols) or in iron-deficient BG-11 medium (filled symbols) during a 5 min incubation in the light.

考察

バクテリアにおける ABC 型輸送体は一般に、ペリプラズムに存在して基質と結合する結合タンパク質、内膜を貫通する膜タンパク質、および ATP 結合タンパク質から構成されている (Ames, 1986, Linton and Higgins, 1998)。本章では、*Synechocystis* sp. strain PCC 6803 ゲノム解析の結果明らかになった多数の基質未同定輸送体遺伝子の中から ATP 結合タンパク質サブユニットをコードすると予想された ORF に着目し、遺伝子破壊株を作製してそれらの表現型解析を行った。32 系統の遺伝子破壊株の中で 4 つの株において、野生株と表現型の異なる破壊株を見出すことができた。

Δ*sll1878* 株は鉄欠乏培地上で野生株と比較して明らかに生育が遅く、また細胞の三価鉄輸送活性も非常に低下していたことから、PCC 6803 における ABC 型三価鉄輸送体の ATP 結合タンパク質サブユニットをコードしていると考えられた。さらに、細胞の三価鉄輸送に際し光によるエネルギーの供給は必要ではなく、測定条件の範囲内では呼吸や他の代謝反応による ATP の供給で十分であると考えられた。これは同じ微量金属元素であるマンガンの場合と大きく異なっている (Bartsevich, et al., 1996)。通常の BG-11 培地で前培養した場合、野生株は Δ*sll1878* 株よりも高い三価鉄取り込み活性を示した。これは、*sll1878* 遺伝子が通常の培養条件下でも発現し、その翻訳産物が細胞の鉄輸送において機能していることを示している。野生株を鉄欠乏培地で前培養すると鉄輸送活性が上昇することから、野生株では鉄欠乏ストレスに応答して細胞の鉄輸送活性を高める機構が存在することが考えられる。今のところこのストレス応答機構が単に *sll1878* 遺伝子産物を含んだ輸送体の発現の量的な増加によるものか、あるいはそれ以外の鉄欠乏ストレス応答性遺伝子の新たな発現によるものなのかは明らかでない。いずれにしても、Δ*sll1878* 株においても細胞の鉄輸送活性が低レベルながら残存していることから、*sll1878* 遺伝子翻訳産物を含んだ ABC 型三価鉄輸送体以外にも鉄の輸送系が存在していることは確かである。

Δ*sll2044* 株と Δ*sll0739* 株は A_6 微量要素を欠いた BG-11 培地上で生育が遅いことが示された。A_6 微量要素にはホウ素、マンガン、亜鉛、銅、モリブデン、コバルトが含まれている。両変異株においてはおそらくこれらの微量要素のいづれかの輸送系の機能が低下しているものと推測される。PCC 6803 ゲノ

ム上で *slr2044* 遺伝子の直上には *slr2043* 遺伝子が、直下には *slr2045* 遺伝子がそれぞれ存在しており、これらはオペロン構造をとっていると考えられる。*slr2043* 推定翻訳産物は PCC 6803 のマンガン輸送体における基質結合タンパク質 MntC (Sll1598) と相同性があり、また細胞の亜鉛輸送に関与しているという報告 (Pakrasi, 2000) があることから、*slr2044* は ABC 型亜鉛輸送体の ATP 結合タンパク質サブユニットをコードしている可能性が高いと考えられる。*sll0739* 遺伝子のすぐ上流に存在する *sll0738* の推定翻訳産物は *Escherichia coli* の ABC 型モリブデン輸送体の基質結合タンパク質 ModA と非常に相同性が高い (Rech, et al., 1995)。このことから *sll0739* 遺伝子は PCC 6803 における ABC 型モリブデン輸送体の ATP 結合タンパクサブユニットをコードしている可能性が考えられる。

Δ*sll0385* 株は実験に用いた全ての培地上で十分に生育しなかった。この遺伝子が破壊されると細胞は、生育に必要な栄養素を過剰に含んだ通常の BG-11 培地でも生育速度が遅くなることから、この遺伝子産物は細胞の生育のための要求度が非常に高いと考えられる。この遺伝子の上流にはコバラミン生合成系の遺伝子のホモログが存在することから、*sll0385* 翻訳産物は微量要素コバルトの輸送に関与しているのかもしれない。

上記 4 系統の変異株以外に 20 株の遺伝子完全破壊株が得られたが、これらは調べた全ての条件で野生株と同程度に生育したため、輸送体の基質の同定には至らなかった。この理由のひとつには、同一基質あるいは同一栄養素を含んだ種々の化合物を輸送できる複数の輸送体が細胞に存在する可能性が挙げられる。ラン藻においては、無機炭素や窒素化合物、硫黄化合物の輸送に複数の輸送体の関与が報告されている (Grossman, et al., 1994)。すなわち、主要な輸送体をひとつ破壊しても別の輸送体による輸送活性で十分に細胞が生育できるため、表現型として現れなかったと考えることができる。また、別の理由として、本章で基質を同定できなかった輸送体遺伝子は、実は糖類や有機酸、アミノ酸、ペプチド等の輸送体をコードしており、実験で用いた、光独立栄養条件下では生育に必要のない遺伝子群であった可能性も考えられる。

残りの 8 つの遺伝子については、遺伝子を完全に薬剤耐性遺伝子で置き換えた変異株を得ることができなかった。これらの遺伝子は、先の 20 の遺伝子とは逆に、光独立栄養条件下で必須の機能を持っていると推定できる。ところ

で、細胞は外界からの物質の取り込み系だけでなく、ニッケルやカドミウムなどの細胞毒性を示す物質の積極的な排出経路を持っている(Silver, et al., 1989)。本実験で機能を推定できなかった 28 個の遺伝子の内には、物質を細胞の中から外へ排出する輸送体をコードしているものの存在も当然考えられる。どちらにしても、さらなる遺伝子機能解析を行うためには、複数の遺伝子を同時に破壊すること、従属栄養条件下での表現型を調べること、生育培地に大過剰の栄養素や金属などを投与すること、あるいは遺伝子を過剰発現させて表現型を調べることなどが必要であると言える。

第 3 章　*Synechocystis* sp. strain PCC 6803 の鉄輸送体遺伝子と鉄輸送機構

序論

鉄は生体にとって必須な元素であり、また地球上で 4 番目に豊富な元素である。鉄イオンは二価 (Fe^{2+}; ferrous) または三価 (Fe^{3+}; ferric) のイオン型で存在するが、通常の酸化的な水環境では二価の鉄は速やかに三価の鉄へと酸化され、生理的な pH (pH 7 付近) では不溶性の水酸化鉄として沈殿する。このため生物は頻繁に鉄欠乏の状況に直面する (Boyer, et al., 1987, Straus, 1994)。光合成や呼吸、窒素代謝といった、基本的な細胞生理に関わるタンパク質の多くは、補因子としてヘムや鉄-硫黄クラスターを必要とする。しかし環境中の利用可能な鉄が常に充分ではないため、生物は効率的に鉄を利用するための様々な機構を進化の過程で発達させてきた (Guerinot and Yi, 1994, Straus, 1994)。

微生物の鉄輸送機構はこれまで非光合成微生物である大腸菌や病原性バクテリア、あるいは 酵母等を用いて詳細に研究されてきており、数多くの鉄輸送体遺伝子もクローニングされている。バクテリアや菌類は主に、(1) シデロフォアの生産と利用、(2) ヘム、トランスフェリン、ラクトフェリンなど、ホストの鉄化合物の利用、(3) 三価の鉄から二価の鉄への還元と二価鉄の輸送、という 3 種類の鉄輸送経路をそれぞれ発達させることにより、鉄欠乏ストレスを克服してきた (Braun, et al., 1998)。シデロフォアとは三価鉄をキレートして可溶化する低分子有機化合物の総称で、多くのバクテリアや菌類は鉄欠乏条件下で鉄を効率的に細胞内に取り込むため、これらの化合物を合成し細胞外へ分泌する (Crosa, 1989, Neilands, 1995)。可溶化された鉄はその特異的な輸送体により細胞内に輸送される。グラム陰性細菌においてシデロフォア-鉄複合体は、まず細胞外膜に存在する特異的なレセプタータンパク質と結合し、細胞膜の電気化学ポテンシャルにより供給されるエネルギーを用いて外膜を通過する。次にシデロフォア-鉄複合体はペリプラズムにおいて特異的な基質結合タンパク質と結合し、さらに、細胞膜に存在する膜タンパク質-ATP 結合タンパク質複合体と相互作用することにより、細胞質側へと輸送される (Braun, et al., 1998)。*Escherichia coli* ではシデロフォア-鉄複合体のレセプター遺伝子として *fhuA*,

fhuE, *iutA* が報告されている。同様に基質結合タンパク質遺伝子として *fhuD* が、膜貫通タンパク質遺伝子として *fhuB* が、ATP 結合タンパク質遺伝子として *fhuC* 遺伝子が同定された (Braun, et al., 1983)。すなわちシデロフォア-鉄複合体は ABC 型輸送体を通して細胞内へ輸送されるのである。クエン酸は鉄イオンをキレートするが、*E. coli* はクエン酸鉄複合体のレセプタータンパク質 FecA と ABC 型クエン酸鉄輸送体 FecBCDE も持っている (Pressler, et al., 1988, Staudenmaier, et al., 1989)。これらに加えて、二価鉄特異的な ABC 型輸送体遺伝子 *feoAB* の存在も報告されている (Hantke, 1987, Kammler, et al., 1993)。病原性バクテリアである *Serratia marcescens* や *Neisseria gonorrhoeae* においては、ペリプラズムに存在するフリーの三価鉄イオンを細胞内へ輸送するタンパク質複合体 SfuABC や FbpABC の存在が報告されている (Angerer, et al., 1990, Berish, et al., 1990, Adhikari, et al., 1996)。これらは典型的な ABC 型輸送体であり、*sfuA*/*fbpA* 遺伝子が鉄結合タンパク質を、*sfuB*, *C*/*fbpB*, *C* 遺伝子がそれぞれ膜貫通タンパク質と ATP 結合タンパク質をコードしている。

ラン藻や微細藻類において古くから鉄欠乏ストレスに対する応答機構が研究されてきたにも関わらず、光合成微生物における鉄輸送の分子機構はほとんど解明されていない。ラン藻 *Synechocystis* sp. strain PCC 6803 のゲノム解析の結果 PCC 6803 株には、他の生物で鉄輸送体をコードする遺伝子と相同性の高い ORF が複数個存在することが示された (Kaneko, et al., 1996)。さらに前章において、ABC 型輸送体の ATP 結合タンパク質をコードすると推定される *sll1878* 遺伝子が PCC 6803 株の三価の鉄輸送に必要であることが示された。そこで本章では PCC 6803 株の鉄輸送体相同遺伝子に着目し、まず鉄欠乏ストレスに対する各 mRNA の発現パターンを調査し、次に各遺伝子の網羅的な破壊株を作製して、鉄欠乏培地上での生育特性と細胞の三価鉄と二価鉄の輸送活性を調べた。また野生株における鉄輸送活性の速度論的解析を試み、さらにエネルギー供給系、および輸送される基質の特異性についても解析した。

材料及び方法

3-1. ラン藻の培養条件

Synechocystis sp. strain PCC 6803 の野生株 (GT 株) および各変異株は、材料及び方法 2-1 に従い BG-11 培地で培養した。必要に応じて鉄欠乏 BG-11 培地を用いた。鉄欠乏培地は以下のように作製した。ストック溶液 1 からはクエン酸とクエン酸鉄アンモニウムを省略し、ストック溶液 2 は硫酸マグネシウムの代わりに硫酸カリウムを使用し、これらを 20 mM TES-KOH (pH 8.0) 緩衝液と混合した後、 Chelex 100 陽イオン交換樹脂 (日本バイオラッドラボラトリーズ、東京) を充填したカラムに通して鉄、銅、亜鉛等の微量金属を除去した。Chelex 100 処理後、高純度の塩化マグネシウム (99.9%) と塩化カルシウム (99.99%) (高純度化学研究所、埼玉)、および A_6 溶液を必要量加えて鉄欠乏 BG-11 培地を調製した。細胞を液体培地中で鉄欠乏ストレスに適応させるためには、以下の操作を実施した (この操作を鉄欠乏処理と呼ぶ)。対数増殖期の細胞を遠心 (1,600×g, 30°C, 8 分間) して集め、等量の Chelex 100 処理した 20 mM TES-KOH (pH 8.0) 緩衝液に再懸濁し、細胞を洗浄した。もう一度洗浄を行った後、細胞の OD 730 nm が 0.2〜0.3 となるように鉄欠乏培地に懸濁し、光照射下、3% CO_2 通気条件下でおよそ 20 時間前培養することで、培地中の微量残留鉄と細胞内貯蔵鉄を消費させた。

3-2. ラン藻細胞からの全 RNA の調製

PCC 6803 野生株からホットフェノール法 (Aiba, et al., 1981) により全 RNA を調製した。対数増殖期にあるラン藻細胞を遠心 (1,600×g, 4°C, 8 分間) して集め、RNA 調製用緩衝液 (50 mM Tris-HCl (pH 8.0), 5 mM EDTA, 0.5% SDS) を添加後激しく撹拌した。この試料にあらかじめ 65°C に加熱しておいたトリス飽和フェノールを等量添加して混和した後、65°C で 10 分間静置した。遠心 (15,000×g, 4°C, 10 分間) 後、上清を新しいチューブに移した。さらにフェノール・クロロホルム抽出を数回繰り返し、試料中のタンパク質を変性させて除去した。核酸をエタノール沈殿により精製した後、滅菌水に溶解した。DNA を除去するため 10 M LiCl を 1/4 量添加して激しく混合し、氷上に 1 時間静置した。遠心分離 (15,000×g, 4°C, 20 分間) 後、再度エタノール沈殿の操作を繰

り返して全 RNA を調製した。

3-3. Riverse transcription - PCR

材料及び方法 3-2 で得た全 RNA 溶液中に混入した DNA を分解するため、全 RNA 2 μg を RNase-free DNase I (BOEHRINGER MANNHEIM) で 25°C、30 分間処理し、フェノール・クロロホルム抽出、エタノール沈殿により精製し、滅菌水に溶解した。この RNA 溶液 100 ng と第 1 鎖 cDNA 合成用プライマー 2 pmols を混合し、滅菌水を加えて容量を 12.5 μL とし、70°C で 10 分間静置した後氷上に移して急冷し、RNA の二次構造を変性させた。第 1 鎖合成用プライマーにはそれぞれの遺伝子の mRNA と相補的な配列を持つ合成オリゴヌクレオチドを用いた。変性 RNA 溶液に 5 倍濃度の第 1 鎖合成用緩衝液を 4 μL、0.1 M DTT を 2 μL、2.5 mM dNTP mixture を 1 μL、逆転写酵素 SuperScript II (GIBCO BRL) を 0.5 μL、それぞれ加えて 42°C で 50 分間逆転写反応を行い、第 1 鎖 cDNA の合成をした。次いで、逆転写酵素を不活性化させるため、70°C で 15 分間処理した。各遺伝子の転写産物の検出のため、第 1 鎖合成 cDNA を鋳型とし、rTaq polymerase (宝酒造) により PCR 反応を行った。ゲノム DNA 由来の PCR 産物が増幅されていないことを確認するため、コントロール実験として第 1 鎖合成時に逆転写酵素を添加しなかった試料を用いて同様の操作を行った。得られた PCR 産物を 0.8% アガロースゲル中で電気泳動し、エチジウムブロマイドで染色して検出した。ポジティブコントロールとして、ストレス条件下においてそれほど発現量が変動しないと考えられる *RNase P* 遺伝子を用いた (Agustin, 1992)。

3-4. ラン藻形質転換用プラスミドの構築と遺伝子破壊株の作製

推定アミノ酸配列に基づき、他の生物で同定された鉄輸送体と一次配列において相同性の高い 13 個の遺伝子 (Table 3-1) について、材料及び方法 2-2, 2-3 に従い形質転換用プラスミドを構築し、これを用いて PCC 6803 の遺伝子破壊株を作製した。

3-5. ラン藻変異株の生育特性の検定

材料及び方法 3-1 に従い鉄欠乏処理した細胞を遠心 (1,600×g, 30°C, 8 分間)

して集め、波長 730 nm の吸光度が 0.1, 0.01, 0.001 となるように鉄欠乏培地に懸濁した。それぞれの細胞懸濁液 2 μL を鉄欠乏 BG-11 培地上にスポットし、7 日間培養して生育状況を比較した (希釈スポット法と呼ぶ)。

3-6. ラン藻細胞の鉄輸送活性の測定

細胞の鉄輸送活性の測定は材料及び方法 2-6 に従い行った。取り込み反応液中に鉄濃度の 100 倍濃度のフェロジンを加えることで三価の鉄の取り込み量を、500 倍濃度のアスコルビン酸を加えて鉄を還元することで二価の鉄の取り込み量を測定した (Ecker and Emery, 1983, Kammler, et al., 1993)。また、鉄取り込み反応の阻害実験においては、あらかじめ細胞懸濁液に FCCP (終濃度 10 μM), DCCD (終濃度 100 μM) をそれぞれ加え、30 分間暗所に置いたものを使用した。各種金属による鉄取り込み阻害実験では、取り込み反応開始直前に 100 μM の各金属塩化物を細胞懸濁液に加え、直ちに放射標識鉄 (終濃度 1 μM) を加えて測定を行った。

3-7. その他の方法

特に言及していない試薬および実験操作は、材料及び方法 2-7 に従った。遺伝子産物の相同性検索には BLASTP 2 を、各配列のマルチプルアライメントには CLUSTAL X (Thompson, et al., 1997)を使用した。

結果

ラン藻の鉄輸送体相同体遺伝子と遺伝子産物局在性の推定

Synechocystis sp. strain PCC 6803 において輸送体サブユニットをコードすると予測された ORF の推定アミノ酸配列を用い、他の生物で同定された鉄輸送体と一次配列において類似性の高い ORF を相同性配列解析ソフトウェア BLASTP 2 を使用して相同性探索した結果、15 個の ORF が見出された (Kaneko, et al., 1996, See CyanoBase: http://www.kazusa.or.jp/cyano/cyano.html)。

バクテリアにおける鉄の膜透過機構には 4 種類のタンパク質が関与している。すなわち (1) 細胞外膜に存在するレセプタータンパク質、(2) ペリプラズムに存在する基質結合タンパク質、(3) 細胞膜貫通タンパク質、(4) ATP と結合する ABC タンパク質、である。このことを念頭において 15 個の PCC 6803 の ORF の分類を BLASTP による相同性検索の結果に基づいて次のように行った。(1) *sll1206*, *sll1406*, *sll1409*, *slr1490* の推定翻訳産物は、*E. coli* の FhuA、FhuE あるいは *Alcaligenes eutrophus* の IutA と相同性が高かった (Fig.3-1, A, B)。FhuA, FhuE, IutA はいずれもシデロフォア-鉄複合体輸送体の外膜レセプターである (Coulton, et al., 1983, Sauer, et al., 1987, Gilis, et al., 1996)。すなわち、これら 4 つの遺伝子は、細胞の外膜に存在するシデロフォア-鉄複合体レセプターをコードしていると推定された。(2) *sll1202*, *slr1319*, *slr1491*, *slr1492* 推定翻訳産物は *E. coli* の FecB、FepB、FhuD と相同性が高かった(Fig. 3-1, C)。FecB はクエン酸鉄輸送体の基質結合タンパク質である (Staudenmaier, et al., 1989)。FepB と FhuD はそれぞれシデロフォア-鉄複合体輸送体の基質結合タンパク質である (Elkins, and Earhart, 1989, Coulton, 1987)。従ってこれら 4 つの遺伝子はペリプラズムに存在する鉄輸送に関わる基質結合タンパク質をコードしていると推定された。*slr0513*, *slr1295* 推定翻訳産物は *S. marcescens* の鉄イオン輸送体のペリプラズムタンパク質 SfuA と相同性が高く (Angerer, et al., 1990)、両遺伝子ともペリプラズムに存在する鉄結合性基質結合タンパク質をコードしていると推定された (Fig. 3-1, D)。(3) *slr1316*, *slr1317* 推定翻訳産物は *E. coli* のクエン酸鉄輸送体膜貫通タンパク質 FecC および FecD と相同性が高い (Staudenmaier, et al., 1989) ことから、これらは PCC 6803 においてもクエン酸鉄輸送体の細胞質膜貫通タンパク質サブユニットをコードしている可能性が推定された

```
Sll1406           ----------MNTKISLGLTICCLCSGLVAP-----------LPILAQINNSG-----
Sll1409     (1)   MWGAQKMIKILEQTSLAVLIGLTALHSGVALGSVGESNLSEKEKLEDQELQNEYK-----
Slr1490           ---MQGVIMNQVQWSVLLMGIVSLLCAPRAWAETNPNQLNRTNILESGNLERTKAGDLLP
FhuA_E.coli       ------------------------------------------------------------

Sll1406     (33)  AQTKIQ------AQVGSILVTGVNLKSTEKGLELELANNSPIPVQPLIYPQGNLLIIELT
Sll1409     (56)  ANVKIENWQQQISQAQIKEVIQIELKDTQTGIELILKTADQSQLIPLIISEDNILIIDIL
Slr1490     (58)  VATTVDEWITQIAQASIIEIKEARINLTEAGLELTLATTGR-LSTPTTSVVGNALIVDIP
FhuA_E.coli       ------------------------------------------------------------

Sll1406     (87)  DALLDIPGGE-FNQENPSPQIAAIAITQGENNIVRITVTGVDNNLPEVTVSSVDQNLVLS
Sll1409     (116) DAVLRLPDGENFIVENPSEQISQITAVQTSSNSLRITVTGNG-TVPAAQVIPSSENLILS
Slr1490     (117) NAILALPDSDGLQQENPTEEIALVSVTALPDNIVRIAITGVN-VPPTVEVNATDQSLVLG
FhuA_E.coli       -----MARSKTAQPKHSLRKIAVVVAT---------AVSGMS-VYAQAAVEPKEDTITVT
                        :. ..    ::.  :*: :  .         :::* .   . . * . .:.: :

Sll1406     (146) LTSSSTAIAPENPESEIEVVATQEG-QGEASYFVPSASTATGLDTPLLDIPQSIQVVPQQ
Sll1409     (175) LTPPINTVESEE---EIEIVATREEEAAVQEFFVPNTSVATGTDTPIMDTPFSAQVVSEE
Slr1490     (176) LSPGKGVADEEDGNDAIQVVVTGEQ---DEGYAVDDATTATLTDTPLRDIPQSIQVVPQQ
FhuA_E.coli (46)  AAPAPQESAWGP---------------AATIAARQSATGTKTDTPIQKVPQSISVVTAE
                   :.                                . .::..*  ***: . * * .**. :

Sll1406     (205) VLQDRNVTELGPALQTVPGVSPAGGRG--TSVFGPGFLIRGFPVNNSIFRDGIPYQS---
Sll1409     (232) VIRSQQAITLEDVLTNVSSVTFGGTTGGRETIFGIRGFGNQFSDTVPILRDGFRLYGGF-
Slr1490     (233) VLEDRQIIRASEALQNVSGVQRGNTVGGTSEIFNIR----GFQQFGGTLRDGFKFRDN--
FhuA_E.coli (90)  EMALHQPKSVKEALSYTPGVSVGTRGASNTYDHLIIRGFAAEGQSQNNYLNGLKLQGNFY
                   :  ::       .*  ...*  .   .     .                   :*:   .

Sll1406     (260) -LAPLNTTDIEQIEVLKGPSSIVFGAGEPGGSINLISKKPLDEPYYNAAVSLGNYNDYRL
Sll1409     (291) -QGITEVSHLQQVEVLKGPSSILYGQIEPGGVINLNSKKPLNEPFAEVEVQLGNQGLVRP
Slr1490     (287) -FSIPDTANLQRIEVLKGPASVLYGNLDPGGVINYITKQPLSEPFYEVAMQAGNFGLVRP
FhuA_E.coli (150) NDAVIDPYMLERAEIMRGPVSVLYGKSSPGGLLNMVSKRPTTEPLKEVQFKAGTDSLFQT
                    .  :   ::: *:::** *:::*  .*** :*  :*:*  **  :. .. *. .  :

Sll1406     (319) DVDLSGPLLPEAIDTVNYRLNVSYETSGSFRDFVYG-DLWVVSPTLTWNIGPDTKLNIYG
Sll1409     (350) RFDISGGLNPS--GNLRYRLNGVYSNEASFRDFNQPLERFAYAPIVTYAITDDTDLSLAV
Slr1490     (346) TIDLSGPLNSQ--RTALYRLNAAYEGGGNFRDFDTEVARFFISPVVTWQISDQTDLRFEW
FhuA_E.coli (210) GFDFSDSLDDD--GVYSYRLTGLAR-SANAQQKGSEEQRYAIAPAFTWRPDDKTNFTFLS
                   .*:*. *  .      ***.      .. ::       :  :* .*:    .*.: :

Sll1406     (378) QYTTNRETLDEGIPAP--NIADLPSNR------FLGERFSKFEQDQYLIGYTFNHDFNEN
Sll1409     (408) EYINDTNPADFGLSSFGDGVAPVPRSR------VINDPSDIVNKNFISAGYNLEHRFNEN
Slr1490     (404) DYLYDRRPFDRGIVAFGTGIADIPFDR------VLGELDDFDARTNFSAGYRLEHRFSDN
FhuA_E.coli (267) YFQNEPETGYYGWLPKEGTVEPLPNGKRLPTDFNEGAKNNTYSRNEKMVGYSFDHEFNDT
                   :  : ..   *  .    :  :* .:        .   .   :     ** ::* *.:.

Sll1406     (430) LKLRHAMQYLAYAP-----------------VRYAPLFDFFDEDTGELNRFEYYGGGNYQ
Sll1409     (462) WKLRNAFRYMSYN-----------------YDYNVIALPTIVNGPTVTRFFADQDGQQG
Slr1490     (458) WKLRNRFRFSYLDQ-----------------AAEQTELVRLDETTGNLSRQFSRNEQQIR
FhuA_E.coli (327) FTVRQNLRFAENKTSQNSVYGYGVCSDPANAYSKQCAALAPADKGHYLARKYVVDDEKLQ
                   .:*: :::     .  .      ..  . .                 : *       :

Sll1406     (473) RFFTNAELIGEFYTGPVKHRVLFGLEYR--NDTETPEFQFSNTFAPINVFNPVYTNTPF-
Sll1409     (504) SYSFYTNAVGKFSTGSVKHELLAGIDYN--WSEESILTLFGGPTS-INVFDPDYNAIPK-
Slr1490     (501) NYELQTDLIGKFSTGPIQHTLLFGVDLS--WQSAPFIFRGGVAAPTINIFNPVYGTVAR-
FhuA_E.coli (387) NFSVDTQLQSKFATGDIDHTLLTGVDFMRMRNDINAWFGYDDSVPLLNLYNPVNTDFDFN
                   :   ::  .:* ** :.* :* *::     .        . . . :*:::*
```

```
Sll1406      (530)  PIAP--EFFRD--DQVNRFAVYLQDQMDLFDNLKLLVGLRYDSATQNRS-TQSITDPREE
Sll1409      (560)  PNRSDLPLFGDTFTSSNRLGIYLQDQVSLLENLILVAGLRYDTITQNTNNLQTDFNQGGN
Slr1490      (558)  PSINDFPDVFSSEGQTNTLGIFLQDQVTLTDNLKLLMGGRFDTIDQSSS------SNGES
FhuA_E.coli  (447)  AKDPANSGPYRILNKQKQTGVYVQDQA-QWDKVLVTLGGRYDWADQESLN----RVAGTT
                    .             . :  .:::***    ::: :  * *:*   *.

Sll1406      (585)  FNQTDNQLTPRVGIIYQPIPTVSLYGSYTTSFNPSFAASLNADGSTFDPQTGRQFEVGVK
Sll1409      (620)  TQQTDSAVTPRIGLLYRPIPEISFFSNYSQSFTP--NSGIDISGNPLEPERGEGFEIGVK
Slr1490      (612)  DERYDQAFSPRLGIVYQPIEPVSLYASFSRSFQP--NFGTRFDGSLLEPVFGTQYEVGVR
FhuA_E.coli  (502)  DKRDDKQFTWRGGVNYLFDNGVTPYFSYSESFEP--SSQVGKDGNIFAPSKGKQYEVGVK
                     :: *. .: * *: *     :: : .:: ** *        .*. : *  *  :*:**:

Sll1406      (645)  ADITDK-LSVTFSAFDIRKQNVPTIDPANLLFTIQTGEQTSRGVELYLGGEILPGWNIVT
Sll1409      (678)  AELFEQQLLTTLTYFNISKNNVAVSDPVNPLFLSTIGTQQSQGIELDIVGEILPGWKIIG
Slr1490      (670)  GEFLDGRLIANLAAYEITVSNLAVTDPENPNFSIPSGEQRSKGVEFDIAGEILPGWNIIA
FhuA_E.coli  (560)  YVPEDRPIVVTGAVYNLTKTNNLMADPEGSFFSVEGGEIRARGVEIEAKAALSASVNVVG
                        :  : .. : :::   *    ** .  *    *   ::*:*:   . : .. :::

Sll1406      (704)  GYSYLDAFVSQD-NTDIVDNTLSNVPSNQFSLWTTYEIQSGNLQGLGFGLGLFYVDQREG
Sll1409      (738)  NYSYINAKVTEDTDPNFVDNRLFGIPYNMANLWTTYEIQSGALQGLGFGIGFNYVGDRFG
Slr1490      (730)  SYAYTDARVTKD-DNLEPGNLLEGVPFNSASLWSTYEIQAGDLQGLGFGLGLFYVGERQG
FhuA_E.coli  (620)  SYTYTDAEYTTD--TTYKGNTPAQVPKHMASLWADYTFFDGPLSGLTLGTGGRYTGSSYG
                    .*:* :*  : *      .*    :* :  .**: * :  * *.** :* *  *...  *

Sll1406      (763)  DLDNTFVLPSYFRTDAAIFYRRE-----NWELQLNIENLFNTQYLAESNDFDLSVYPGAP
Sll1409      (798)  DLANTYTVGDYIIGNAAIFYQRD-----KYRVALNLRNFTNANYVRAVSGNQTGIEPGEP
Slr1490      (789)  DLNNSFQIPSYLRTDISVFYRRN-----NWRAAINVNNLFNIDYIEATQR-RTRVDPAAP
FhuA_E.coli  (678)  DPANSFKVGSYTVVDALVRYDLARVGMAGSNVALHVNNLFDREYVASCFN-TYGCFWGAE
                    *  *:: : .*   :  : *       .  .  :::.*: : :*:            .

Sll1406      (818)  FTVVGKIGVTF
Sll1409      (853)  FIIIGSFSVQF
Slr1490      (843)  LTVRGTISVEF
FhuA_E.coli  (737)  RQVVATATFRF
                      : ..  . *
```

Fig. 3-1, A. Sequence alignment of the *Synechocystis* ORFs (Sll1406, Sll1409, and Slr1490) with ferrichrome-iron receptor FhuA in *E. coli*. Identical amino acids are marked with asterisk; conservative substitutions are marked with colons or dots as defined by CLUSTAL X.

```
IutA_A. eu          ------------------MTHSYSTTGNRVGAAARDYGRRGSMAALAAAVLMSVAVAPVA
S111206     (1)     MGGRDMKTRLVRFGWTIALGIVMETMAMPLGAQEIISEPSPSVTVELDQGTSLVQVQEVR
                                      :    .* .  :**         *::.        * *  *

IutA_A. eu (43)     AQTPRGDVPIHIEAQPLADALLQLGRQTSLQLYFPPELVAGKRAPAVNGTMRPEAALDSL
S111206    (61)     LEPSGPGLEIILVTAGGAIASPNLQTVGNALIIDLPNTLMALPGGQGFEEVSPTADIAFV
                     :..  .: * : :   * *  :*    .  :   *: : .  .      : * * :  :

IutA_A. eu (103)    LKGSGIQYQRSGNQGFVLRPVSGTSRSTAGAIRYAPRHGPAHHRAGPGGSHRVTDIERSG
S111206    (121)    SVTQMTDNQVRLAITGVNGPPEAEVKPNSQGLQLLIRPGVAGTTAEIEESEALQIVVSAT
                       .  : *       *  * ..  :..: .::   * * *   *    *. :  :  :

IutA_A. eu (163)    PPDAAID-------VLERTELEELKTGSDSLATVLSKVIPGMADSSHTVTDFGQTLRGRG
S111206    (181)    RTEEEIANIPRSVTVIERAEIEQQTQVYSSLADILGQLVPGLAPSTGSASQFGQALRGRN
                     .:  *        *:**:*:*: .   .*** :*.:::**:* *: :.::***:****.

IutA_A. eu (216)    MLVLLDGIPLNTNRDSARNLANIDPALVERVEVLRGSSAIYGGGPTGGIVSITTRPAGGE
S111206    (241)    VLVLIDGVPQTTNRNAFRDLQTIAPSAIERIEVIQGPTAIYGDGATGGVINIITRGPAPE
                    :***:**:* .***:: *:* .* *: :**:**::*.:****.*.***::.* ** .. *

IutA_A. eu (276)    PKADTTVTMSTPLSRLRRGRLERQRAAALFGQQRDARLCVRPRRAPYRQSYDAKGHALRR
S111206    (301)    PFLASTRLAINTDFDSVSNSLGRMVEQYVGGTLDYADYAFTASYESVGGFFDALGNRIPP
                    *   :*    ..      . * *     : *    *  .. .   .    :** *: :

IutA_A. eu (336)    SQARATCSTRTTTTSAASSASFAPDQRIQLASSAILTPSRTRAGRRIRAWPNCRRAACPR
S111206    (361)    DPNGQGGVSDTDSFNVLGKLGINMTDEQRLQITINHFQATQNTDFTVDPSITAIAGRQRS
                    .       : * : .. .. .:   :. :*  :     :  .:.  : .  ..  .

IutA_A. eu (396)    RALDGLQLADQNQIRNTLVNLEYEHRDLLGSQLSAQFYYRNYYSRFTPFDARAVPVRGGN
S111206    (421)    QAIDGLDLDTPQTSNNTVVSLDYSHSNVLNGNLKGQIYYRDYLTRFFPFDGRASVSLGNS
                    :*:***:*   :  .**:*.*:*.* ::*..:*..*:***:* :** ***.**    *..

IutA_A. eu (456)    VDQAMQDSEVFGSRLTVKTPLGRDKRTRVIWGMDFEQETSDMPIDIFDLKAYDASGGRIF
S111206    (481)    IFQSEIDSTEWGGRLQLDTPLTGEKNLRLLWGADYNNESTAQPVNIFDPVTFDSSGGLSY
                    : *:  **  :*.** :.***  :*. *::** *:::*::  *::***  ::*:***  :

IutA_A. eu (516)    NKIGTLTYMPPITTRSIGALPSCRHKFNEQWSTEGGLRYQYARASFSDFVPLSQSRVTNP
S111206    (541)    RNTGKRTWVPSLNQDSLGLFGQLNWRANDWLTLLGGIRHEQVGLSVDDFTTLGGN-----
                    .: *. *::*.:.  *:* : . . : *:  :  **:*:: .  *..**..*. .

IutA_A. eu (576)    ATVSGGAVDYSAVLGNIGVAYKPVKDHEFYAAFSQGFNLPDIGLQVGNARAGFDIGSSDL
S111206    (596)    -TVQGGDLSYDATLFNLGGVVDVTDNISLFASFAQGFSLADVGLVLRNAPAGFSLATLQP
                    .**.** :.*.*.* *:* . . ..: .::*:*:***.*.*:** : ** ***.:.: :

IutA_A. eu (636)    QPVKTNNYELGWRGAFGNTLGSLAIFYTTSDLGDVQSFNNGLILTRTAEKIYGVEASADY
S111206    (655)    EAQRVNNYEIGVRGNWQNLRFSLAGFYNSSDLG--TTFTAPGEILRAPERVYGVEATMDA
                    :. :.****:* ** : *   *** **.:****   :*.    : *:.*::*****: *

IutA_A. eu (696)    LSTDERWGAGGTFTWMQGRETPQGR-DSQQMTGYRIPPLKLTGYVQYRPVPQWNNRLQAT
S111206    (713)    R-VGESWQLGGTFSLSAGEIDRLNTGNYTPLDGFRIAPVKLTAYVQHQTTPGWQNRLQLL
                     ...* *  ****:   *.    .  :   : *:**.*:***.***::..* *:****

IutA_A. eu (755)    FFAGYDYRLNGVTSFGRRDVSSYTTLDLISSYQVTKKDTVTVGIQNLLNRYYYPLYSQLL
S111206    (772)    YSGDRDVFSN-NTVFGQLPVSSYVTLDYISRINVGP-GKLEIGIANLLNTDYFPVVSQLQ
                    : .. *   *  * **:  ****.*** **  :*   ..: :** ****  *:*: ***

IutA_A. eu (815)    RNSNNTSHLRRPASRSPPPTAPLVTA
S111206    (830)    PNELSNAAARGRFLRIGYAFEW----
                     *. ..:  *    *   .      .
```

Fig. 3-1, B. Sequence alignment of the Sll1206 with ferric aerobactin receptor IutA in *A. eutrophus*. Identical amino acids are marked with asterisk; conservative substitutions are marked with colons or dots as defined by CLUSTAL X.

```
Slr1491      (1)    MHRSGRRFRLFTLTILTIVFFSACVGSTSQNLDQSTELLSVDCRIVEHSLGKTCVPLEPR
Slr1492             ------------------MLVVACQNPSQREAVKNSE----DCVIVNQPEDQACVPKTID
Slr1319             -----MKSKLIIFTFCLVLFGCAKQVPVEFSPGETIQSN-LTQRTIAHAMGVTAVPNEPQ
FecB_E.coli         -----------MLAFIRFLFAGLLLVISHAFAA----------TVQDEHGTFTLEKTPQ
Sll1202      (1)    MKKYKINYFSTLMIFMTSLLTSCNTNIDRSSHLQQSDKK--GCRIIEHKMGETEICGIPQ
                                      ::                        : .  .   :

Slr1491      (61)   RVVALDGATVGNLLALGMMPAG-VASNL---------LPEITRLIP----NVPRLGQSSQ
Slr1492      (39)   RLVTLDGAAFEYAIALGLEPIATVPSNF---------QAQLPALMTNA-ENIQNIGKGEQ
Slr1319      (55)   RIVVLTNEATDMVLALGVTPVGAVKSWSG--------DPYYEYLAKDM-LGVPIVGDEMQ
FecB_E.coli  (39)   RIVVLELSFADALAAVDVSPIGIADDNDA--------KRILPEVRAHL-KPWQSVGTRAQ
Sll1202      (59)   RVVVLGPYLLEPLLALNIQPIAYADHIAFHKEDYDHPTEQIPYLGQYINKPIANVGIAYM
                    *:*.*         *:.: * . .                  :          :*

Slr1491      (107)  INLETLAVLQPDLIIGAVWEMKGIYNKLSAIAPTVAFEMQTP--ADWQRPFRFDGQVLGL
Slr1492      (89)   PNLEAILGTNPDLIVG-LDSHQSIYPQLSQIGPTVLFPFEHS--GQWKEVFASVGNALHR
Slr1319      (106)  PNLEKIVALQPDLIIGSRLRQGQIYKSLSAIAPTVFSETIG---ESWQDNLRLYGQALDR
FecB_E.coli  (90)   PSLEAIAALKPDLIIADSSRHAGVYIALQQIAPVLLLKSRNETYAENLQSAAIIGEMVGK
Sll1202      (119)  PSLEGIFKAKPDLILSPDHNK-NEYQKFSQLAPTLMLSWNEP-----TENLEKIAQAVKQ
                     .** :   :****:.        *  :. :.*.:                   .: :

Slr1491      (165)  ETQAEKVLEQYQMRVNKLRAQVSD--SPLQISLVRIRAESGQMSLYLKNCFGGAILADLG
Slr1492      (146)  QAATQSALAAYQARSTDFRTQMGDRLDNLQVSVIRLYPDG--INLYLKDSFAGTVLQDAG
Slr1319      (163)  EAEAEQLLNDWDTRVAQMRQKLSA--KDLTISLVRFMPRG--ARIYLQNSFPGQILQAVG
FecB_E.coli  (150)  KREMQARLEQHKERMAQWASQLPK---GTRVAFGTSREQQ--FNLHTQETWTGSVLASLG
Sll1202      (173)  EEKVEQLLQETQQEIEKAKQEFSKIVAGYPKMLLLHAQNLQELSIANNEDLCSSLIEELG
                    :   : *   . .  .   :.         .          :  ::   . ::   *

Slr1491      (223)  FARPPSQDQGTPDQP-----PFAKSISRESMTEADGDVIFLFTFGHTPQIAAAA------
Slr1492      (204)  LARPPSQNISAVEAQQKFGNPIQTRISREVLEQADGDVIFLWTGENTPQGNEEA------
Slr1319      (219)  LERPASQANHG----------FAEHVSFEQIPQMEADALFYFIYTGDSGDQTPG------
FecB_E.coli  (205)  LNVPAAMAGAS----------MPSIGLEQLLAVNPAWLLVAHYREES------------
Sll1202      (233)  FELVSLPGAGTSTNSR----LPLSLESLPKLNNANSIIILGYNFQEFNKSKSRQNFTEHQ
                    :   .                      .   :   :   ::

Slr1491      (272)  -EAQLERLDTDPLWQSLGAVQKNRVYSVG-HYWGAGNSPLAADWVLDDVEQYLLEVPGNG
Slr1492      (258)  -KKRLQQLQQDPLWGQLRAVKAGKVYEVP-SYW-IGSGPIAANAILDDLYKYLLGEN---
Slr1319      (263)  -SITNPWLN-HPLWQQLEVVQSGKAYAVSDVVWTTAGGIQAAHLLLDDLERHLEP-----
FecB_E.coli  (242)  ---IVKRWQQDPLWQMLTAAQKQQVASVDSNTWARMRGIFAAERIAADTVKIFHHQPLTV
Sll1202      (289)  LSNLQQQWSENAITQSMKASRENRVYYIPTYLCTGLPGFFGTKLYLNELKKQLLTNQKP-
                           . ..:   : . :  :.  :         .  .:.    :  : :

Slr1491      (330)  V-
Slr1492             --
Slr1319             --
FecB_E.coli  (299)  VK
Sll1202             --
```

Fig. 3-1, C. Sequence alignment of the *Synechocystis* ORFs (Slr1491, Slr1492, Slr1319, and Sll1202) with ferric-dicitrate-binding protein FecB in *E. coli*. Identical amino acids are marked with asterisk; conservative substitutions are marked with colons or dots as defined by CLUSTAL X.

```
Slr1295    (1)    MVQKLSRRLFLSIGTAFTVVVGSQLLSSCGQSPDAPIADTPGEQQEINLYSSRHYNTDNE
Slr0513    (1)    MTTKISRRTFFVGGTALTALVVANLPRRAS-----------AQSRTINLYSSRHYNTDDA
SfuA_S.ma  (1)    MKLRISSLGPVALLASSMMLAFGAQAASAD--------------QGIVIYNAQHENLVKS
                  *  ::*    .   ::   :. .     ..              : * :*.::* *  .

Slr1295    (61)   LYAKFTAETGIKVNLIEGKADELLERIKSEGANSPADVLLTVDLARLWRAEEDGIFQPVQ
Slr0513    (50)   LYDAFG-----EVNLIEASAEELIERIQSEGANSPGDILFTVDAGMLWRAEQAGLFQPVR
SfuA_S.ma  (47)   WVDGFTKDTGIKVTLRNGGDSELGNQLVQEGSASPADVFLTENSPAMVLVDNAKLFAPLD
                      *      :*.* :.  .** ::: .**: **.*:::* :   :  .::  :* *:

Slr1295    (121)  SEILETNVPEYLRSPDGMWFGFTKRARVIMYNKGKVKPEELS-TYEELADPKWKGRVIIR
Slr0513    (105)  SGKLNERIPENLRHPDGLWYGFTQRARVLYYSRDRVNPADLS-TYEALADPQWRGKILVR
SfuA_S.ma  (107)  AATLAQVEPQYRPS-HGRWIGIAARSTVFVYNPAKLSDAQLPKSLLDLAKPEWKGRWAAS
                  :  *    *:     .* * *:: *: *: *.  ::.  :*. :   **.*:*:*:

Slr1295    (180)  SSSNEYNQSLVASLVVADGEESTLAWAKGFVSNFAREPQGNDTAQIEAVSSGEADLTLAN
Slr0513    (164)  PSSNVYNLSLTASRIAIHGEPETRRWLQGLVGNFARQPEGNDTAQIRAIAAGIGDVAIAN
SfuA_S.ma  (166)  PSGADF-QAIVSALLELKGEKATLAWLKAMKTNFTAYK--GNSTVMKAVNAGQVDSGVIY
                  .*.  :  ::.:: :  .**  *  * :.:  **:     .::: :.*: :*  *  :

Slr1295    (240)  TYYMGRLLESEDPAQKAIAENVGVFFPNQEG--RGTHVNVSGVGVVKTAPNREGAVKFIE
Slr0513    (224)  SYYYIRLQKSTDPADQEVVEKVSLFFPNTGSGERGTHVNVSGAGVLKNAPNRDAAIAFLE
SfuA_S.ma  (223)  HYYP----FVDGAKTGENSNNIKLYYFKHQD--PGAFVSISGGGVLASSKHQQQAQAFIK
                   **        ..      ::: ::: :  .   *:.*.:** **: .: ::: *  *::

Slr1295    (298)  FLVSEPAQAFLAQN-NYEYPVLAGVPLNKSVASFGEFKSDTTSLDKLGPALAPATKIMNE
Slr0513    (284)  YLASDDAQRYFAEG-NNEYPVIPGVPIDPVLAAHGQLKGDPLNVSNLGRYQPDSARLMNE
SfuA_S.ma  (277)  WITGKQGQEILRTNNAFEYAVGVGAASNPKLVPLKDLDAPKVDAAQLNSKK--VVELMTE
                  ::... .*  :  .   **.*  *.. :  :..  ::..   .  :*.      ..:*.*

Slr1295    (357)  AGWK
Slr0513    (343)  VGWQ
SfuA_S.ma  (335)  AGLL
                  .*
```

Fig. 3-1, D. Sequence alignment of the *Synechocystis* ORFs (Slr1295 and slr0513) with iron-binding periplasmic protein in *S. marcescens*. Identical amino acids are marked with asterisk; conservative substitutions are marked with colons or dots as defined by CLUSTAL X.

```
FecC_E. coli          ------------MTAIKHPVLLWGLPVAALIIIFWLSLFCYSAIPVSGADATRALLPGH
Slr1316       (1)     MPFLQCIMRSSLYFRAKSPGYLALGLVLGATVLFACLISSILLGAADISPQTVWQALFQF
                                  : * .   *  ** :.* :::  *      . .  ..::.   *  .

FecC_E. coli  (48)    TPTLPEALVQNLRLPRSLVAVLIGASLALAGTLLQTLTHNPMASPSLLGINSGAALAMAL
Slr1316       (61)    DGSTDHLIIRTVRLPRAILAIVVGASLAVAGAITQGLTRNPLAAPDILGVNVGASLAVVL
                        :  . ::::.:****:::*:::*****:**:: * **:**:*:*.:**:* **:**:.*

FecC_E. coli  (108)   TSALSPTPIAGYSLSFIAACGGGVSWLLVMTAGGGFRHTHDRNKLILAGIALSAFCMGLT
Slr1316       (121)   ATFIGGDGSNQWAFAFIGAAIAAVVVYGLGTLG---RSGLTPIKLVIAGAALSYFLGSLT
                      :: :.      ::::**.*. ..*    : * *   *      **::** *** *  .**

FecC_E. coli  (168)   RITLLLAEDHAYGIFYWLAGGVSHARWQDVWQLLPVVVTAVPVVLLLANQLNLLNLSDST
Slr1316       (178)   TGILLLNQRTLDDIRFWLAGSLGGQDWNGLTAVLPYIMVGLVSSLSLGRQLTLLTFGEEV
                         *** :    .* :****.:.   *:.:  :** ::..:   * *..**.**.:.:..

FecC_E. coli  (228)   AHTLGVNLTRLRLVINMLVLLLVGACVSVAGPVAFIGLLVPHLARFWAGFDQRNVLPVSM
Slr1316       (238)   AQGLGLKTAWVKLGAATVLVLLAGSAVALAGPIGFVGLIVPHVVRFGVGVDYRWILPYAM
                      *: **:: : ::*    :::**.*:.*::***:.*:**:***:.** .*.* * :** :*

FecC_E. coli  (288)   LLGATLMLLADVLARALAFPGDLPAGAVLALIGSPCFVWLVRRRG-
Slr1316       (298)   VMGGIFLSVADMAARLLISPQELPVGIMTALVGAPFFIYLARSQIK
                      ::*. :: :**: ** *  * :**.* : **:*:* *::*.* :
```

Fig. 3-1, E. Sequence alignment of the Slr1316 with ferric-dicitrate transport system permease protein FecC in *E. coli*. Identical amino acids are marked with asterisk; conservative substitutions are marked with colons or dots as defined by CLUSTAL X.

```
FecD_E. coli          ----------------------MKIALVIFITLALAG-CALLSLHMGVIPVPWRALLT--
Slr1317       (1)     MFAPRPWIVVRLRSLPLSFRLDRHVPLVMGLLTALALLLFILNISWGEYPVPPLAMLQAI
                                             ::.**: :  ***    :*.:  *  ***  *:*

FecD_E. coli (36)     -DWQAGHEHYYVLMEYRLPRLLLALFVGAALAVAGVLIQGIVRNPLASPDILGVNHAASL
Slr1317      (61)     FGLSTDADHEFVVRTLRLPRSLVALLVGMGLAIAGGILQGITRNPLAAPEIIGVNAGASL
                       . .:. :* :*:   **** *:**:** .**:** ::***.*****:*:*:*** .***

FecD_E. coli (95)     ASVGALLLMPSLPVMVLPLLAFAGGMAGLILLKMLAKTH--QPMKLALTGVALSACWASL
Slr1317      (121)    VAVTFIVLLPGISPSLLPVAAFCGGLTAAIAIYVLAWNQGSAPVRLILVGIGLAALASSL
                      .:*  ::*:*.:.  :**: **.**::. * : :** .:   *::* *.*:.*:*  :**

FecD_E. coli (153)    TDYLMLS-RPQDVNNALLWLTGSLWGRDWSFVKIAIPLMILFLPLSLSFCRDLDLLALGD
Slr1317      (181)    TSLMVTFGEISVVSQALVWLTGSVHGRGWEHLLPLLPWLALFIPLSLALARELDTLNLGD
                      *. ::   . . *.:**:*****: **.*..:   :* : **:****::.*:** * ***

FecD_E. coli (212)    ARATTLGVSVPHTRFWALLLAVAMTSTGVAACGPISFIGLVVPHMMRSITGGRHRRLLPV
Slr1317      (241)    NLARGLGSRVEWMRGLLLVCSVALAGSCVATAGNIGFVGLMAPHLARHLVGPSHGGMIPV
                        *  **  *   *   *: :**::.: **:.* *.*:**:.**: * :.*  *  ::**

FecD_E. coli (272)    SALTGALLLVVADLLARIIHPPLELPVGVLTAIIGAPWFVWLLVRMR--
Slr1317      (301)    AALTGACITELADLIGRTVFAPIEIPCGVITAIVGAPYFLWLLYRNRNQ
                      :***** :  :***:.* :..*:*:* **:***:***:*:*** * *
```

Fig. 3-1, F. Sequence alignment of the Slr1317 with ferric-dicitrate transport system permease protein FecD in *E. coli*. Identical amino acids are marked with asterisk; conservative substitutions are marked with colons or dots as defined by CLUSTAL X.

```
HitB_H. in          ----------MPRRPPFWLTLLIILIGLPLCLPFLYVILRATEVGLTRSVELLFRPRMAE
Slr0327     (1)     MFNFLTVLPSPPKVLLNFWVLTSLLIAVWIAVPVIFVFLGIFSWQG-EIFSHLWATVLGE
                              *:    : .*  :**.: :.:*.::*:*   .    . .. *: . :.*

HitB_H. in  (51)    LLSNTMLLMVCVTIGAISLGTFCAFLLERYRFFGKAFFEVAMTLPLCIPAFVSGFTWISL
Slr0327     (60)    YIRNSLALMLGVGAGVFVLGVGTAWLVTMCRFPGCRWLEWALLLPLSAPAYLLAYGYSNL
                     : *:: **: *  *.: **.  *:*:   ** *  ::* *: ***. **:: .: : .*

HitB_H. in  (111)   T-----------------------FRVEVFWGTIGIMTLSSFPLAYLPVSAILKRLDRS
Slr0327     (120)   LDFYGPVQTLLRSIFGWQSAPEYWFPQIRSLWGAIAILALVSYPYVYLLARIAFLEQGVC
                                           ::. :**:*.*::* *:* .** .   : . . .

HitB_H. in  (147)   LEEVSLSLGKSPVYTFWYAISPQLKPAIGSSILLIALHMLVEFGAVSILNYQTFTTAIFQ
Slr0327     (180)   TLEASRSLGCNPWQSFSRVALPLARPAIAAGLALVMMETLNDFGTVQYFGVNTFTTGIYS
                      *.* *** .*  :*  .  *  :***.:.: *: :. * :**:*. :. :****.*:.

HitB_H. in  (207)   EYEMSFNNSTAALLSAVLMAICILIVFGEIFFRGKQTLYHSGKGVTRPYLVKTLSFGKQC
Slr0327     (240)   TWFGFGERQGATQLAAFLMIFVFLLVVLERWSRRQAKFYQSS-SPHQNLPRYQLRGLRAI
                     :    :.. *: *:*.** : :*:*. * : * : .:*:*. .  :      *   :

HitB_H. in  (267)   LTFGFFSSIFILSIGVPVIMLIYWLIVGTSLESAGDFSEFLSAFSNSFIISGLGALLTVM
Slr0327     (299)   GALAFCLFPFLLGFLIPASYLLYLTVSYAQEVRN---NNFFQLASHSLILSFLTAAIALV
                     ::.*    *:*.: :*.  *:*  :  :.       .:*:.  *:*:*:* * * ::::

HitB_H. in  (327)   CALPLVWAAVRYRSYLTIWIDRLPYLLHAVPGLVIALSLVYFS----------------I
Slr0327     (356)   IGLILVYGQRLSRQPLTSFAVKVASMGYAIPGSVIAVGVLIPAGNFDNWLADWWENMWGV
                     .* **:.    *. ** :  ::. : :*:** ***:.::  :                :

HitB_H. in  (371)   HYANDLYQTFFVIIIAYFMLYLPMAQTTLRASLEQLSDQIEKVGQSLGRNPFYIFRTLTL
Slr0327     (416)   KIGLLLSGTIAILVYAYLVRFLAVALGSLEGSLGKIKPTLDDAARSLGKSPSQILWQVHT
                     : .  *  *: ::: **:: :*.:*  :*..** ::.  ::...:***:.*  *:  :

HitB_H. in  (431)   PAILPGVAAAFALVFLNLMKELTATLLLTSNDIKTLSIAVWEHTSDAQYAAATPYALMLV
Slr0327     (476)   PLMTGGLLTAVMLVFVDVMKELPATLVIRPFNFDTLAIRVYQYASDERLIEAAAPALTII
                     * :  *: :*. ***::*****.***:: . ::.**:* *::::** :   *:. ** ::

HitB_H. in  (491)   LFSGIPVFLLKKYAFK------
Slr0327     (536)   LAGMLPVIFLSVQIARSRPSEG
                     * . :**::*.    :
```

Fig. 3-1, G. Sequence alignment of the Slr0327 with iron transport system permease protein HitB in *H. influenzae*. Identical amino acids are marked with asterisk; conservative substitutions are marked with colons or dots as defined by CLUSTAL X.

```
FeoB_E. coli          ---------------MKKLTIGLIGNPNSGKTTLFNQLTGSRQRVGNWAGVTVERKEGQF
Slr1392       (1)     MVSHCQRGSVQSSRPDVKKRVAFIGQPNTGKSTFFNRITKANAAIANWPGLTVDLFRAVV
                                      *  :.:**:**:**:*:**::* :.  :.**.*:**:  .. .

FeoB_E. coli  (46)    STTDHQVTLVDLPGTYSLTTISSQTSLDEQIACHYILSGDADLLINVVDASNLERNLYLT
Slr1392       (61)    PLQGELIEFVDLPGIYDLNGFS----EDERVVQRFLANYAVNLVVVVVNAAQIDRQIRLL
                      .  .. : :***** *.*. :*     **::. ::: .  .:*:: **:*::::*:: *

FeoB_E. coli  (106)   LQLLELGIPCIVALNMLDIAEKQNIRIEIDALSARLGCPVIPLVSTRGRGIEALKLAIDR
Slr1392       (117)   LQVQTLGIPAITLLNLADEAKRYGVQIDVAALQERLGLPLYPISAKYGTGCSRAMDAIGR
                      **:  ****.*. **: * *:: .::*:: **. *** *: *: :. * * .    **.*

FeoB_E. coli  (166)   YKANENVELVHYAQPLLNEADSLAKVMPSDIPLKQRRWLGLQMLEGDIYSRAYAGEASQH
Slr1392       (177)   AVK-----------------------------------------------------DQP
                                                                              .*

FeoB_E. coli  (226)   LDAALARLRNEMDDPALHIADARYQCIAAICDVVSNTLTAEPSRFTTAVDKIVLNRFLGL
Slr1392       (183)   EAYQIPNLVNVLSDHPVAIADMETALAG-----VVQMPSPNARTLTNVIDGVMLHPVFGL
                          :..* * :.* .: *** .    .     * :  :.:.  :*..:* ::*: .:**

FeoB_E. coli  (286)   PIFLFVMYLMFLLAINIGGALQPLFDVGSVALFVHGIQWIGYTLHFPDWLTIFLAQGLGG
Slr1392       (238)   PIFFASMFGVFWVIWHVG--LPSADPVDAVTGWVQSNILEPLFSPLPTILQGLLLDGIWT
                      ***:  *: :* :  ::*  * .   *.:*: :*:.         :*  *  :* :*:

FeoB_E. coli  (346)   GINTVLPLVPQIGMMYLFLSFLEDSGYMARAAFVMDRLMQALGLPGKSFVPLIVGFGCNV
Slr1392       (296)   GFAALLSFVPLVAIFFIVMGILEGSGYLSRAAYLMDALMGRLGLDGRSFVLQMMGFGCNV
                      *: ::*.:** :.::::.:.:**.***::***::** **  *** *:***  ::******

FeoB_E. coli  (406)   PSVMGARTLDAPRERLMTIMMAPFMSCGARLAIFAVFAAAFFG-QNGALAVFSLYMLGIV
Slr1392       (356)   PAIMGTRVMRSRGMRLLSMLVIPFSLCSARLQVFVFILAAVMPGTQGAIALFLLYLMSFV
                      *::**:*.: :   **:::::: **  *.*** :*..: **.:   :**:*:* **::.:*

FeoB_E. coli  (465)   MAVLTGLMLKYTIMRGEATPFVMELPVYHVPHVKSLIIQTWQRLKGFVLRAGKVIIIVSI
Slr1392       (416)   AAFTVAAILSRFHYFQARDPFVLELPPYRLPTFKQVFLRVWGEMREFVARLSMFMVIGSS
                       *. .. :*.         ***:*** *::* .*.:::::.* .:: ** * . .::* *

FeoB_E. coli  (525)   FLSAFNSFSLSGKIVDNINDSALASVSRVITPVFKPIGVHEDNWQATVGLFTGAMAKEVV
Slr1392       (476)   LIWFLTSFPQGSTGLETFAG----RIGSVFQPLMNPLGINP---FLTISLIFGFVAKEVQ
                      ::  :.**. ... ::.: .     :. *: *:::*:*::      *:.*: * :****

FeoB_E. coli  (585)   VGTLNTLYTAENIQDEEFNPAEFNLGEELFSAIDETWQSLKDTFSLSVLMNPIEASKGDG
Slr1392       (529)   IAALTVIYGLNNSE-----------------------------------------------
                      :.:*..:*  :* :

FeoB_E. coli  (645)   EMGTGAMGVMDQKFGSAAAAYSYLIFVLLYVPCISVMGAIARES-SRGWMGFSILWGLNI
Slr1392       (543)   -----AVSDQIHSTVTFAQGFSYCLFSLIYIPCLTTLGAIWGESKSLAYTAISVATPLVT
                           *:.   :.  : * .:** :* *:*:**::.:***  ** * .: .:*:   *

FeoB_E. coli  (704)   AYSLATLFYQVASYSQHPTYSLVCILAVILFNIVVIGLLRRARSRVDIELLATRKSVSSC
Slr1392       (598)   AWLFSFIFYQSFSWLGW-------------------------------------------
                      *: :: :***  *:

FeoB_E. coli  (764)   CAASTTGDCH
Slr1392               ----------
```

Fig. 3-1, H. Sequence alignment of the Slr1392 with ferrous iron transport protein FeoB in *E. coli*. Identical amino acids are marked with asterisk; conservative substitutions are marked with colons or dots as defined by CLUSTAL X.

```
FecE_E. coli          -------MTLRTENLTVSYGTDKVLNDVSLSLPTGKITALIGPNGCGKSTLLNCFSRLLM
Slr1318       (1)     MLDVATPIALTTRKLSLAYDSHLIIQGLDLAINQGEITTLVGPNGCGKSTLLRGMARLLK
                             ::* *.:*:::*.:. :::.:.*::  *:**:*:***********. ::***

FecE_E. coli (54)     PQSGTVFLGDNPINMLSSRQLARRLSLLPQHHLTPEGITVQELVSYGRNPWLSLWGRLSA
Slr1318      (61)     PQGGTVYLEGEAIAHLPTKELAKRLGILPQSPPAPEGLTVRELVAQGRYPHQNWLQQWSK
                      **.***:* .:.*  *.:::**:**.:***   :***:**:***: ** *  .   : *

FecE_E. coli (114)    EDNARVNVAMNQTRINHLAVRRLTELSGGQRQRAFLAMVLAQNTPVVLLDEPTTYLDINH
Slr1318      (121)    QDELKVEEAIATTDLHQFANRPLDSLSGGQRQRAWIAMALAQDTEILLLDEPTTYLDLAH
                      :*: :*: *:  * ::::* * * .**********:**.***:* ::**********: *

FecE_E. coli (174)    QVDLMRLMGEL-RTQGKTVVAVLHDLNQASRYCDQLVVMANGHVMAQGTPEEVMTPGLLR
Slr1318      (181)    QIEVLDLLHWLNREAGRTIVMVLHDLNLACRYSHRLIALRDGKLLAQGRPQAIVTEELVR
                      *:::: *:  * *  *:*:* ****** *.**..:*:.: :*:::*** *: ::*  *:*

FecE_E. coli (233)    TVFSVEAEIHPEPVSGRPMCLMR-----
Slr1318      (241)    QVFGLESRIIADPVTGTPLCVPVSRHLK
                       **.:*:.* .:**:* *:*:
```

Fig. 3-1, I. Sequence alignment of the Slr1318 with ferric-dicitrate transport system permease protein FecE in *E. coli*. Identical amino acids are marked with asterisk; conservative substitutions are marked with colons or dots as defined by CLUSTAL X.

(Fig. 3-1, E, F)。*slr0327* と *slr1392* の推定翻訳産物はそれぞれ *Haemophilus influenzae* の Sfu/Fbp 型鉄輸送体の膜貫通サブユニット HitB と、*E. coli* の二価鉄輸送体の ATP 結合モチーフを含んだ膜貫通サブユニット FeoB と相同性が高く (Sanders, et al., 1994, Kammler, et al., 1993)、どちらも鉄輸送に関わる膜貫通タンパク質をコードしているであろうと推定された (Fig. 3-1, G, H)。(4) *sll1318* 推定翻訳産物は *E. coli* のクエン酸鉄輸送体の ABC タンパク質 FecE (Staudenmaier, et al., 1989) と相同性が高かった (Fig. 3-1, I)。このことから *slr1318* は ABC 型クエン酸鉄輸送体の ATP 結合タンパク質サブユニットをコードしていると推定された。

上記の 15 個の PCC 6803 の鉄輸送体相同体遺伝子のうち *slr1316* と *slr1317* については、ゲノム上で *slr1316, slr1317, slr1318, slr1319* の順でタンデムに存在しオペロン構造をとっていると予測されることから、これら 4 つの遺伝子をそれぞれ個別に破壊しても同一の表現型を示すものと考えられるため、以下の各実験を省略した。以後、これら 13 個の遺伝子と第 2 章で同定した *sll1878* に着目し、各 mRNA の発現パターンと遺伝子破壊株 (M1 - M10)の表現型を調査した。

Fig. 3-2 は BLASTP による相同性解析結果に基づいて本章で対象とする各遺伝子の翻訳産物の局在性を推定したものであり、かつ実験に用いた遺伝子破壊株 M1 – M10 においてどの ORF が破壊されているかを示している。縦の矢印はそれぞれの遺伝子を単一で (M1, M2, M3, M4, M7, M10)、横の矢印は枠で囲った複数の遺伝子を同時に (M5, M6, M8, M9)、薬剤耐性遺伝子で置換したことを表している。すなわち、M1 は Δ*sll1878* 単一破壊株、M2 は Δ*slr0327* 単一破壊株、M3 は Δ*slr1295* 単一破壊株、M4 は Δ*slr0513* 単一破壊株、M5 は Δ*sll1878*Δ*slr0327* 二重破壊株、M6 は Δ*slr0513*Δ*slr1295* 二重破壊株、M7 は Δ*slr1318* 単一破壊株、M8 は Δ*sll1202*Δ*slr1319*Δ*slr1491*Δ*slr1492* 四重破壊株、M9 は Δ*sll1206*Δ*sll1406*Δ*sll1409*Δ*slr1490* 四重破壊株、M10 は Δ*slr1392* 単一破壊株である。なお、M1 は第 2 章で作製した Δ*sll1878* である。Table 3-1 は各遺伝子内の欠失した領域と、そこに挿入した各薬剤耐性遺伝子を示している。これらの遺伝子全てについて、完全に薬剤耐性遺伝子と置き換わった変異株を得ることができた。

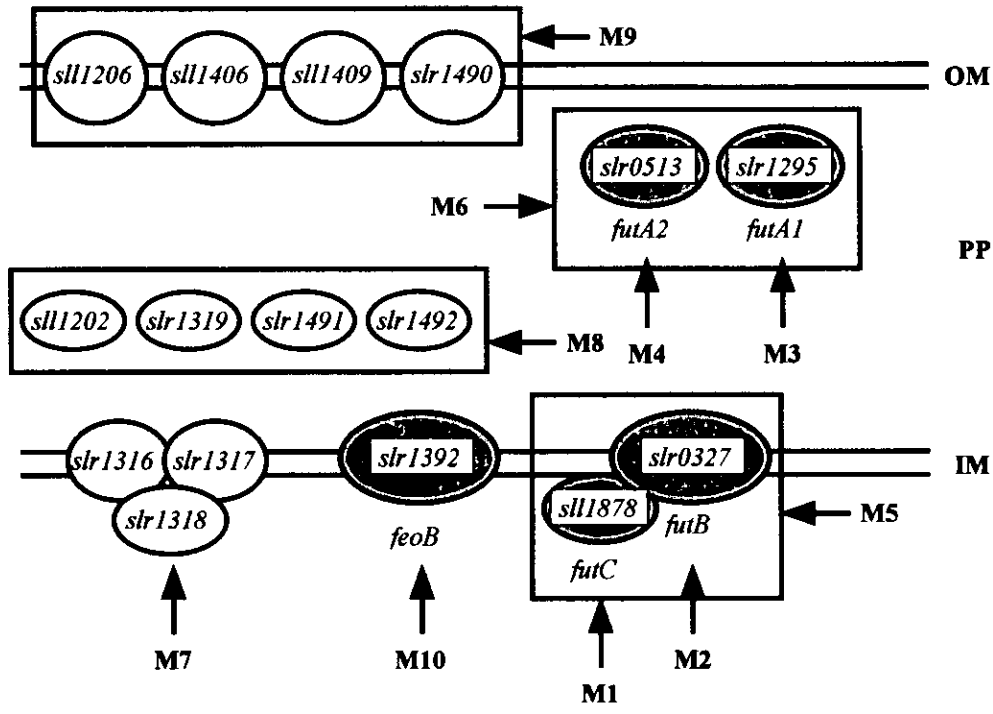

Fig. 3-2. Mutants constructed by inactivating genes presumably involved in iron acquisition and the possible localization of the gene products that are positioned based on the localization of their homologues in nonphotosynthetic bacteria; shaded ovals, putative proteins that were experimentally shown to function in iron transport in *Synechocystis* sp. strain PCC 6803. For details see text. Vertical arrows, genes that were individually inactivated; horizontal arrows, groups of genes (boxed) that were inactivated in a single strain. M1: Δ*sll1878* single mutant, M2: Δ*slr0327* single mutant, M3: Δ*slr1295* single mutant, M4: Δ*slr0513* single mutant, M5: Δ*sll1878*Δ*slr0327* double mutant, M6: Δ*slr0513*Δ*slr1295* double mutant, M7: Δ*slr1318* single mutant, M8: Δ*sll1202*Δ*slr1319*Δ*slr1491*Δ*slr1492* quadruplicate mutant, M9: Δ*sll1206*Δ*sll1406*Δ*slr1409*Δ*slr1490* quadruplicate mutant, M10: Δ*slr1392* single mutant. OM, outer membrane; PP, periplasmic space; IM, inner membrane.

Table 3-1. Regions of ORFs amplified by the RT-PCR method or replaced by drug resistance cassettes in the mutant strains.

	Positions[c] of:			
ORF	RT-PCR product[a]	Deleted region[b]	Drug[d]	Mutant Strain
sll1206	28 - 368	444 - 458	Kanamycin	M9
sll1406	24 - 387	533 - 583	Chloramphenicol	M9
sll1409	73 - 439	581 - 719	Hygromycin	M9
slr1490	55 - 418	418 - 563	Spectinomycin	M9
sll1202	84 - 480	454 - 500	Hygromycin	M8
slr0513	60 - 483	448 - 530	Kanamycin	M4 or M6
slr1295	20 - 427	317 - 373	Chloramphenicol	M3 or M6
slr1319	66 - 441	473 - 477	Kanamycin	M8
slr1491	81 - 435	481 - 511	Chloramphenicol	M8
slr1492	15 - 395	166[e]	Spectinomycin	M8
sll1878	32 - 400	134 - 479	Kanamycin	M1 or M5
slr0327	75 - 434	538 - 573	Spectinomycin	M2 or M5
slr1318	69 - 422	70 - 518	Spectinomycin	M7
slr1392	79 - 430	485 - 553	Hygromycin	M10

[a] Regions amplified by RT-PCR (from Fig. 3-3).

[b] Regions replaced by drug resistance cassettes.

[c] Positions of nucleotides are counted from the first nucleotide of the initiation codon.

[d] Drug to which the cassette confers resistance.

[e] Position at which cassette was inserted.

鉄輸送体相同体遺伝子 mRNA の発現パターンの解析

PCC 6803 の 13 個の鉄輸送体相同体遺伝子と第 2 章で同定した鉄輸送体遺伝子 *sll1878* について、通常の BG-11 培地で培養した野生株細胞と、鉄欠乏処理した野生株細胞からそれぞれ全 RNA を抽出し、RT-PCR 法 (Chelly and Kahn, 1994) により各遺伝子の mRNA の発現レベルを測定した (Fig. 3-3)。各遺伝子において RT-PCR により増幅される領域は Table 3-1 に示した。外膜レセプターをコードすると考えられる 4 つの遺伝子、*sll1206*, *sll1406*, *sll1409*, *slr1490* は BG-11 培養条件下で発現が低く、鉄欠乏処理により発現量が上昇することが示された。同様な傾向は、基質結合タンパク質をコードすると考えられる *sll1202*, *slr1491*, *slr1492* において、また ATP 結合タンパク質をコードすると推定される *slr1318*、内膜貫通タンパク質をコードすると予測される *slr1392* において観察された。一方で、基質結合タンパク質をコードすると考えられる *slr0513*, *slr1295*, *slr1319*、膜貫通タンパク質をコードすると考えられる *slr0327*、ATP 結合タンパク質をコードすると考えられる *sll1878*、の 5 つの遺伝子は BG-11 培養条件下で既にある程度 mRNA の蓄積が確認され、鉄欠乏処理することにより蓄積量が増加することが示された。以上の結果から、前者の遺伝子群は細胞の鉄欠乏ストレスに応答して発現するのに対し、後者の遺伝子群は通常の BG-11 培養条件下でも機能を果たしている可能性が示唆された。

鉄輸送体相同体遺伝子破壊株の生育特性

第 2 章で Δ*sll1878* 株は鉄欠乏培地上で生育が遅くなることが示された。細胞の生育における鉄の要求性をさらに厳密に解析するため、野生株と、Fig. 3-2 に示した 10 変異株の細胞を鉄欠乏処理し、段階的に希釈して鉄欠乏 BG-11 固形培地上にスポットし、生育状況を比較した (Fig. 3-4)。遺伝子破壊株 M3, M4, M7, M8, M9, M10 は野生株とほぼ同程度に生育したのに対し、M2 (Δ*slr0327*), M5 (Δ*sll1878*Δ*slr0327*), M6 (Δ*slr0513*Δ*slr1295*) 株は M1 (Δ*sll1878*) 株と同様に鉄欠乏培地上で著しく生育が遅かった。これらの結果から、*slr0327* (M2) は鉄輸送体の膜貫通タンパク質サブユニットをコードしている可能性が示唆された。また、PCC 6803 鉄輸送体の基質結合タンパク質は *slr0513* と *slr1295* の 2 つの遺伝子によりそれぞれコードされており、両方が破壊されることで初めて鉄欠乏

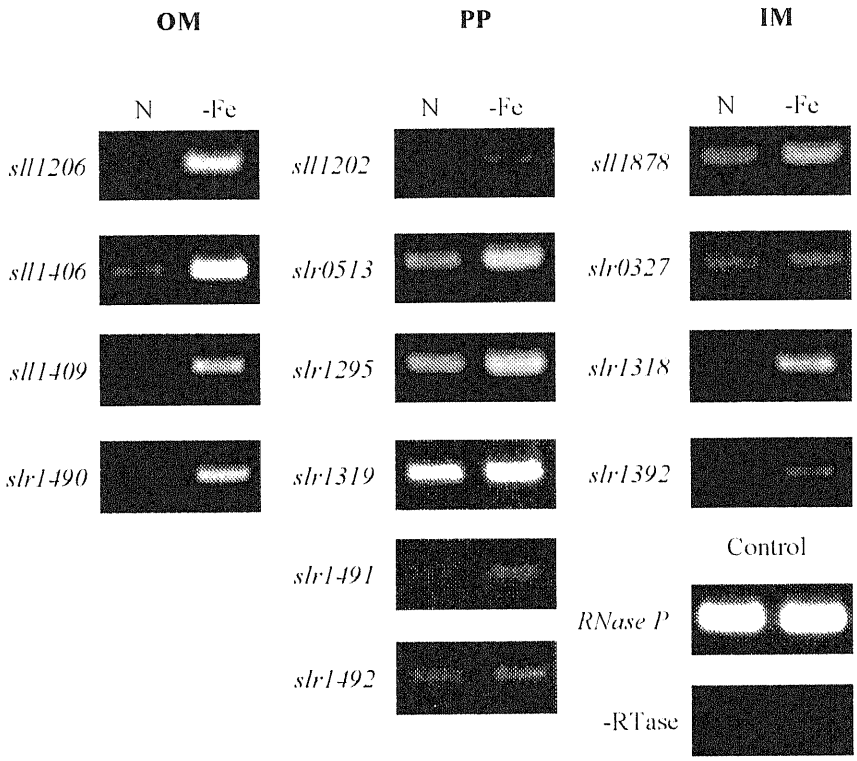

Fig. 3-3. Expression profiles of putative iron transporter genes in *Synechocystis*. The amounts of transcripts in cells grown in normal BG-11 medium (lanes N) or in iron-deficient BG-11 medium (lanes –Fe) were determined by the RT-PCR method. The regions of the genes amplified are summarized in Table 3-1. OM, PP, and IM are as indicated in Fig. 3-2. Absence of contamination of DNA was confirmed by performing the RT reaction without reverse transcriptase (-RT ase) followed by PCR.

培地上で生育が遅くなり (M6)、どちらかひとつが残っていればほぼ正常に生育できることが示された (M3, M4)。さらに *sll1878* と *slr0327* を同時に破壊した株 (M5) において、それぞれ単一に破壊した場合と生育特性が変わらなかったことから、この 2 つの遺伝子がそれぞれ同一の鉄輸送体の膜貫通タンパク質サブユニットと ATP 結合タンパク質サブユニットをコードしている可能性が示唆された。M7, M8, M9, M10 株は鉄欠乏培地で野生株並みの生育をしたことから、*slr1318*, *sll1202*, *slr1319*, *slr1491*, *slr1492*, *sll1206*, *sll1406*, *sll1409*, *slr1490* の遺伝子産物は今回の実験に用いた鉄欠乏培地での生育にとって重要なものではないことが示された。

鉄輸送体相同体遺伝子破壊株の三価鉄取り込み活性

生育特性の検定に用いた M1 – M10 変異株について、実際に三価鉄の輸送活性を野生株と比較した。Fig. 3-5, A は通常の BG-11 培地で培養した細胞、Fig. 3-5, B は鉄欠乏処理した細胞の三価の鉄の輸送活性を示している。Fig. 3-5, A において M2 (Δ*slr0327*), M5 (Δ*sll1878*Δ*slr0327*), M6 (Δ*slr0513*Δ*slr1295*) 株は M1 (Δ*sll1878*) 株と同程度の低い鉄取り込み活性を示した。その他の株は野生株と同程度の取り込み活性を持っていた。Fig. 3-5, B において、M2, M5, M6 はやはり M1 と同様に低い鉄取り込み活性を示した。生育特性と同様に *sll1878* と *slr0327* を同時に破壊した株 (M5) において、それぞれ単一に破壊した株 (M1, M2) よりも活性が低くなることはなかった。これらの結果からも、*sll1878*, *slr0327*, *slr0513*, *slr1295* 遺伝子が PCC 6803 の単一の三価鉄輸送体のサブユニットをそれぞれコードしていることが考えられた。M4 (Δ*slr0513*) は野生株と同程度の取り込み活性を示したが、M3 (Δ*slr1295*) は鉄欠乏処理した場合、三価鉄輸送活性が野生株の 1/2 程度であったことから、*slr1295* が三価鉄輸送体の主要な基質結合タンパク質サブユニットをコードしており、*slr0513* は細胞の鉄輸送において *slr1295* と重複した機能を持つが、活性は若干低いものであることが示唆された。

鉄輸送体相同体遺伝子破壊株の二価鉄取り込み活性

次に M1 – M10 株の二価鉄輸送活性を野生株と比較した。Fig. 3-6, A は通常の BG-11 培地で培養した細胞、Fig. 3-6, B は鉄欠乏処理した細胞の二価の

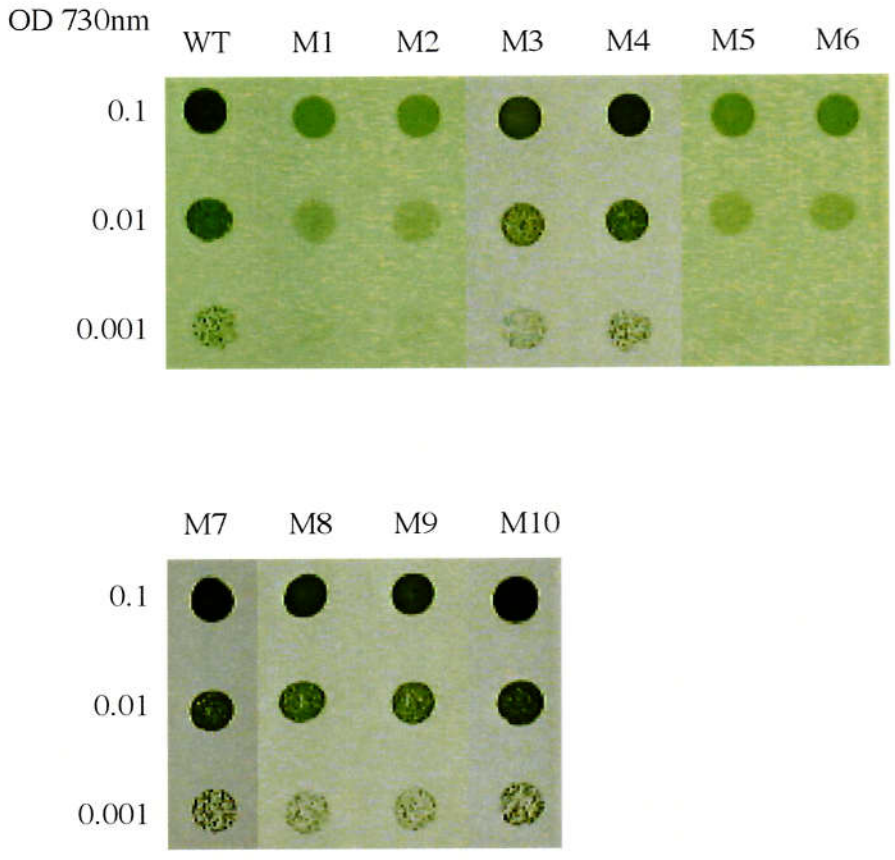

Fig. 3-4. Growth of the wild-type and mutants on solid iron-deficient BG-11 medium. Wild-type (WT) and mutant (M1 to M10 [Fig. 3-2]) cells of *Synechocystis* were pelleted by centrifugation and resuspended in iron-deficient BG-11 medium at pH 8.0. Two microliters each of cell suspensions, with OD 730 nm values of 0.1, 0.01, and 0.001 were spotted on agar plates containing iron-deficient BG-11 medium buffered at pH 8.0, and the plates were incubated under 3% (vol/vol) CO_2 in air for 7 days.

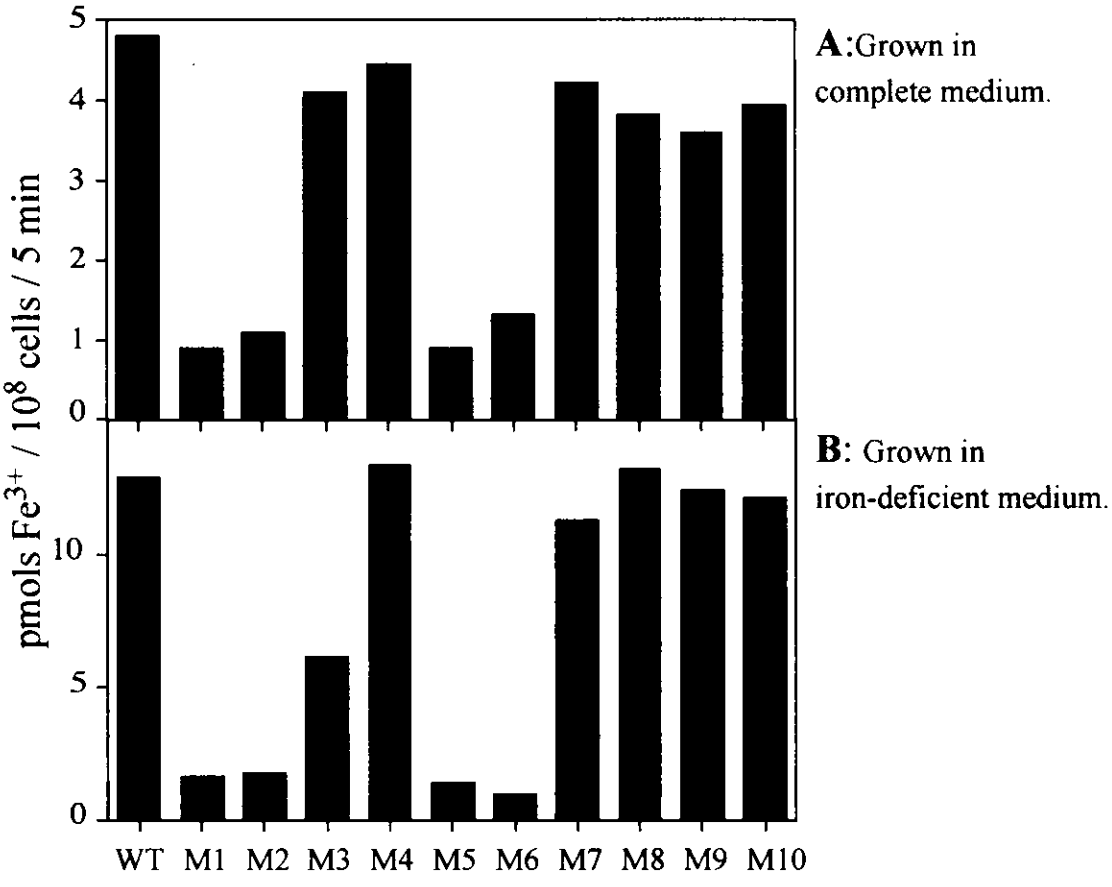

Fig. 3-5. Amounts of $^{59}Fe^{3+}$ taken up by wild-type (WT) and mutant (M1 to M10 [Fig. 3-2]) cells. Cells grown in complete medium (A) and in iron-deficient medium (B) were incubated with 10 μM $^{59}FeCl_3$ for 5 min in the light in the presence of 1 mM ferrozine.

鉄の輸送活性を示している。野生株において、通常の BG-11 で培養した場合の活性が 11 pmols $Fe^{2+}/10^8$ cells/5 min 程度であったのに対し、鉄欠乏処理することで活性が 8 倍程度上昇した。これは鉄欠乏ストレスにより二価鉄輸送系が誘導されてくることを示している。ところが、三価鉄輸送活性が低かった 4 つの変異株 (M1, M2, M5, M6) では通常の BG-11 で培養した場合、野生株の 4 倍程度活性が高く、鉄欠乏処理しても活性の上昇はほとんど認められなかった。このことから、これら 4 つの変異株は二価の鉄輸送活性は正常であり、かつ通常の培養条件下においても三価鉄輸送活性が低いために鉄欠乏ストレスを感じており、二価鉄輸送系の発現が誘導されているものと考えられた。 M3, M4, M7, M8, M9 株の二価鉄輸送活性は野生株と変わらなかった。しかし M10 (Δ*slr1392*) 株では鉄欠乏処理しても野生株で見られたような輸送活性の上昇が見られなかった。このことから、*slr1392* 遺伝子が PCC 6803 の二価鉄輸送体サブユニットをコードしており、鉄欠乏ストレスによって発現が誘導されることが示された。これは Fig. 3-3 で示した *slr1392* mRNA の発現パターンとも一致した。

ラン藻細胞の鉄輸送活性の解析

野生株における三価の鉄輸送活性の濃度依存性に関しては第 2 章で測定した。ここではさらにアスコルビン酸で化学的に還元した二価鉄の輸送活性の濃度依存性を調べ、三価及び二価鉄輸送活性の速度論的解析を行った。Fig. 3-7 は光照射下における野生株 (●, ○) と Δ*slr1392* (M10) 株 (▼, ▽) の二価鉄輸送活性の濃度依存性を示している。●, ▼ は鉄欠乏処理した細胞、○, ▽ は通常の BG-11 培地で培養した細胞における二価鉄輸送活性を示している。鉄欠乏処理した Δ*slr1392* (M10) 株においては、取り込み活性測定溶液中の鉄濃度を高くしても野生株で見られるような取り込み活性の上昇は認められなかった。この結果からも、*slr1392* が鉄欠乏ストレスにより発現が誘導される二価鉄輸送体の遺伝子であると考えられる。なお、両株とも暗所でも光照射下とほぼ同様の取り込み活性を示した (結果省略)。これと第 2 章で得た三価鉄輸送活性のデータをもとに逆数プロット法によりそれぞれの鉄取り込み反応の野生株における K_m (μM) 値と V_{max} (pmols Fe/10^8 cells/5 min) 値を求めた (Table 3-2)。三価の鉄の輸送活性の V_{max} 値は鉄欠乏処理することで 5 倍上昇したが、基質

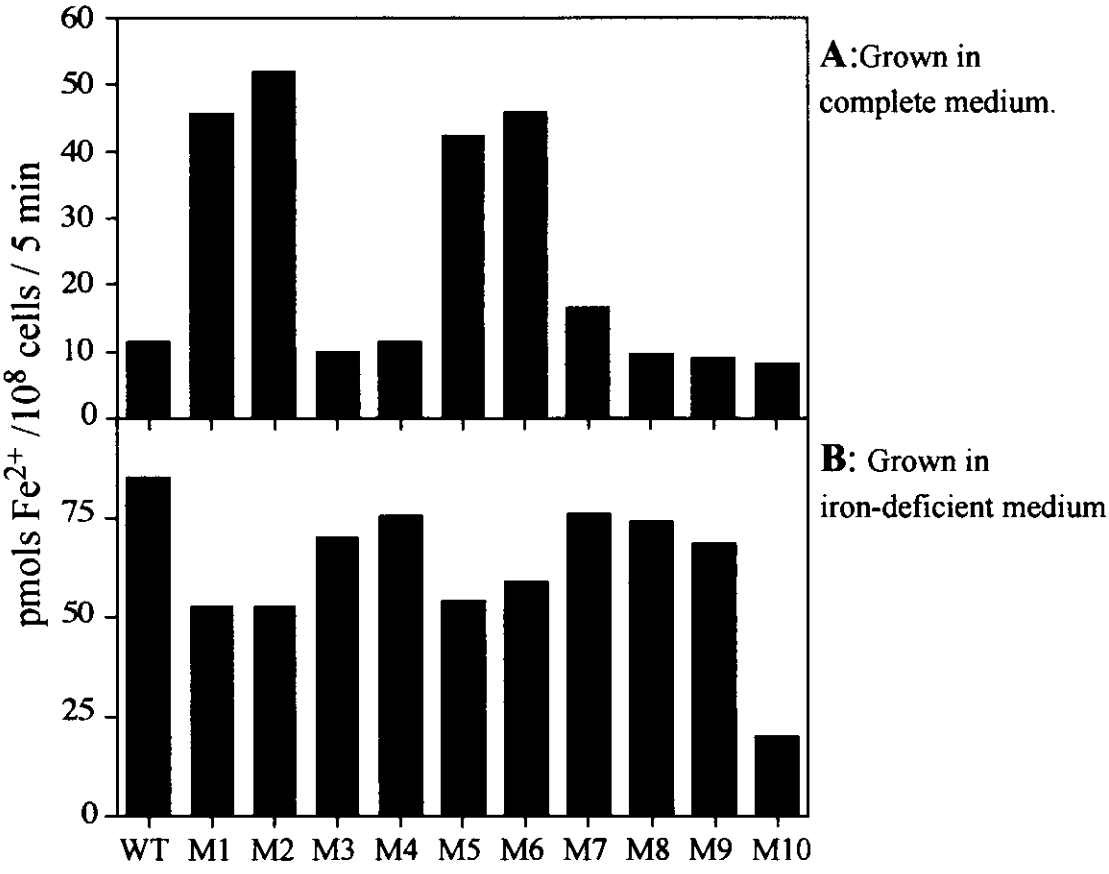

Fig. 3-6. Amounts of $^{59}Fe^{2+}$ taken up by wild-type (WT) and mutant (M1 to M10 [Fig. 3-2]) cells. Cells grown in complete medium (A) and in iron-deficient medium (B) were incubated with 10 μM $^{59}FeCl_3$ for 5 min in the light in the presence of 5 mM ascorbate.

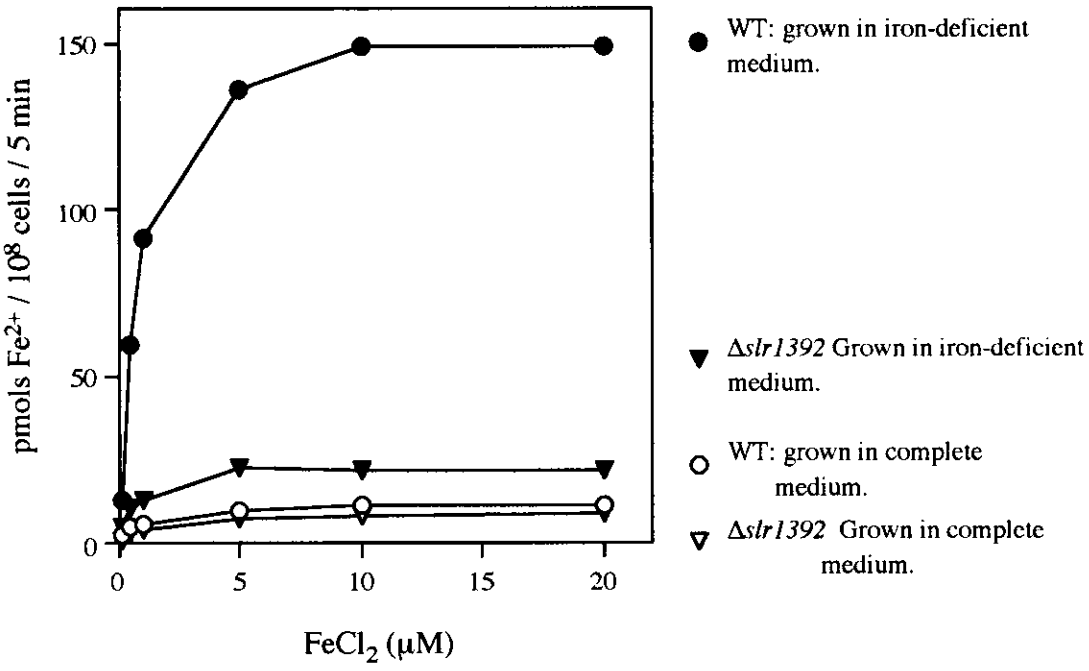

Fig. 3-7. Concentration-dependent uptake of $^{59}Fe^{2+}$ by wild-type (○, ●) and Δ*slr1392* (▽, ▼) cells grown in complete medium (open symbols) or in iron-deficient BG-11 medium (filled symbols) during 5 min incubation in the light.

に対する親和性は若干低下した。同様に二価鉄輸送活性の V_{max} 値は約 13 倍上昇し、親和性は半分程度に低下した。

次に鉄取り込み反応のエネルギー供給機構を調べるため、プロトノフォアである FCCP、ATP 合成阻害剤である DCCD、呼吸阻害剤である KCN を野生株細胞に添加し、鉄取り込み活性を測定した (Table 3-3)。 FCCP あるいは DCCD を添加することで三価鉄及び二価鉄の輸送活性は何も添加しない場合の 35%～60% 程度に低下した。これから、どちらの鉄輸送系も ATP の加水分解によるエネルギーの供給を必要とすることが示された。

最後に、鉄以外の金属により野生株細胞の鉄輸送活性がどの程度阻害されるか調べるため、亜鉛、マンガン、銅、コバルト、ニッケル、カドミウム、クロムをそれぞれ取り込み反応液中に鉄の 100 倍量添加して鉄の輸送活性を測定した (Fig. 3-8, A, B)。100 倍濃度の亜鉛存在下で三価鉄の取り込み活性が 23% に低下し、二価鉄取り込み活性はそれほど低下しなかった。また 100 倍濃度の銅存在下で二価鉄取り込み活性が 4% 程度にまで低下したが、三価鉄取り込み活性に影響はなかった。また亜鉛、銅ともに鉄と同濃度では取り込み阻害は認められなかった (結果省略)。100 倍濃度のコバルトとカドミウムは三価及び二価鉄取り込み活性ともに 60% あるいは 15% 程度までそれぞれ低下させた。これら 2 つの金属元素は細胞毒性を示すため、鉄輸送活性における阻害効果は基質の競合によるものではないと考えられた。

二価鉄輸送体遺伝子 *slr1392* と共転写される遺伝子の同定

PCC 6803 は三価の鉄特異的な輸送体と二価鉄特異的な輸送体を持っていることが示された。Δ*slr1392* (M10) 株の表現型と推定アミノ酸配列から、*slr1392* が二価の鉄輸送体の ATP 結合領域を含む膜タンパク質をコードしていることが推測された。しかし *E. coli* の二価鉄輸送体のもうひとつのサブユニットをコードする *feoA* 遺伝子に相当するような ORF は今のところ PCC 6803 ゲノム上で特定されていない (Kaneko, et al., 1996)。PCC 6803 には *slr1392* のすぐ上流に 79 アミノ酸から成るタンパク質をコードすると推定される ORF *ssr2333* が存在する。これは *E. coli* の *feoA* 遺伝子と僅かながらの相同性があり、推定される翻訳産物のアミノ酸残基数も同程度である (Kammler, et al., 1993)。そこで、この *ssr2333* 遺伝子が *slr1392* と共転写されているかどうかを

Table 3-2. The K_m and V_{max} values for ferric and ferrous iron transport in wild-type cells.

	ferric iron transport		ferrous iron transport	
Culture condition	Normal	-Iron	Normal	-Iron
K_m (μM)	0.7	2	0.6	1.1
V_{max} (pmols Fe/10^8 cells/5 min)	5	25	11	147

Table 3-3. Effects of metabolic inhibitors on ferric and ferrous iron uptake.

Addition	Fe^{3+} uptake (% activity)	Fe^{2+} uptake (% activity)
None	100	100
FCCP (10 μM)	61.6	41.1
DCCD (100 μM)	56.2	35.5

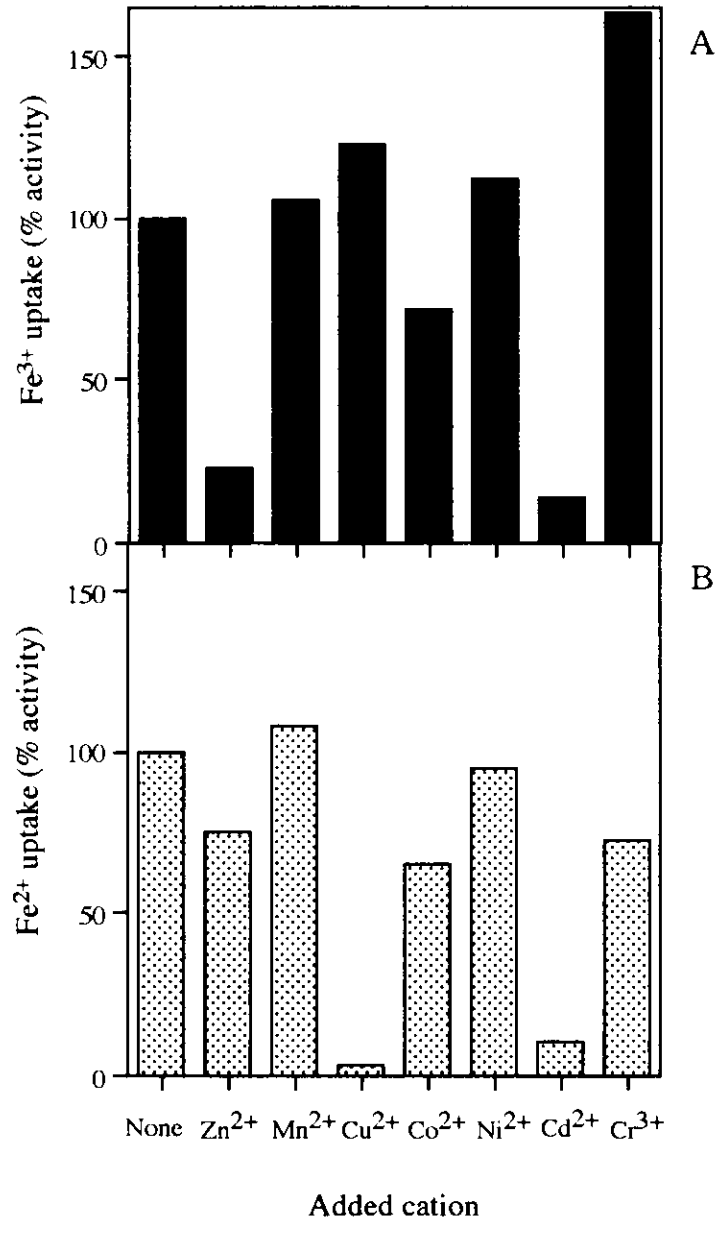

Fig. 3-8. Effect of transition metals on ferric (A) and ferrous (B) iron transport in *Synechocystis*. The amounts of iron taken up by the wild-type cells in the presence of 100 μM of transition metals are shown in percentages of the control. The cells were incubated with 1 μM Fe^{3+} or Fe^{2+} for 5 min in the light in the presence or absence of the metals.

RT-PCR 法で調べた。鉄欠乏処理した野生株細胞から全 RNA を抽出し、*slr1392* 遺伝子に特異的な配列を持つリバースプライマーで第 1 鎖 cDNA を合成し、これを鋳型にして *ssr2333* 遺伝子に特異的な配列を持つフォワードプライマーと先の *slr1392* リバースプライマーを用いて PCR 反応を行ったところ、予想される大きさ (647 bp) を持つPCR 産物が検出された (Fig. 3-9)。これは *ssr2333* と *slr1392* が共転写されていることを示している。このことから *ssr2333* 遺伝子が *E. coli* の *feoA* 遺伝子の相同体である可能性が示唆された。

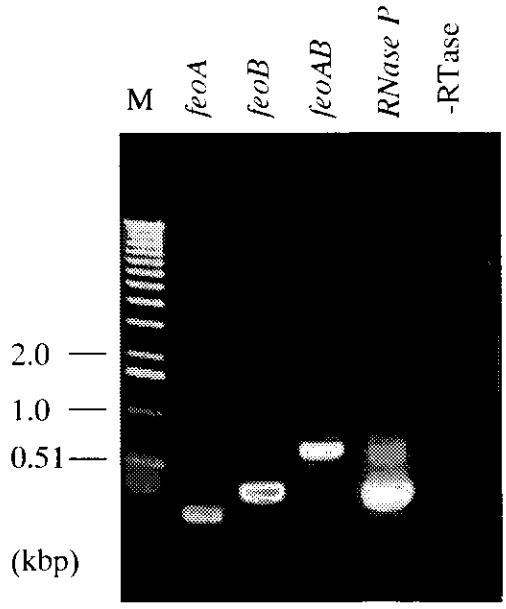

Fig. 3-9. Identification of mRNA of *feoAB* by using RT-PCR method. Total RNA was extracted from wild-type cells cultured in iron-deficient BG-11 medium. First strand cDNAs were synthesized by using reverse primers for *ssr2333* (lane *feoA*) or for *slr1392* (lane *feoB* and lane *feoAB*). The gene products were amplified by using each reverse primer and forward primers for *ssr2333* (lane *feoA* and lane *feoAB*) or for *slr1392* (lane *feoB*). lane M, molecular weight marker; lane *RNase P*, positive control; lane –RTase, negative control, see materials and methods 3-3.

考察

本章において、ラン藻 *Synechocystis* sp. strain PCC6803 の主要な鉄輸送体遺伝子、*sll1878*, *slr0327*, *slr1295*, *slr0513* を同定することができた。Slr1295 と Slr0513 は *S. marcescens* あるいは *H. influenzae* の鉄輸送体のペリプラズム基質結合タンパク質 SfuA/HitA と相同性が高く (Angerer, et al., 1990, Sanders, et al., 1994)、これら 2 つの遺伝子を同時に破壊することで鉄欠乏培地上での生育が遅くなり、かつ細胞の三価鉄輸送活性が低下した。このことから、*slr1295* と *slr0513* が PCC 6803 の三価の鉄輸送体の基質結合タンパク質サブユニットをコードしていることが示された。また、*slr0513* のみを破壊しただけでは生育および三価鉄輸送活性ともに野生株と同等であり、*slr1295* のみを破壊した場合、生育特性は野生株とほぼ同等であったが、鉄輸送活性については鉄欠乏処理した場合にのみ野生株よりも低い三価鉄輸送活性を示した。これは PCC 6803 の三価鉄輸送体にはどちらかひとつの基質結合タンパク質が存在すれば機能するが、Slr0513 の方が Slr1295 よりも活性が低いことを示唆している。Δ*slr1295*Δ*slr0513* 二重破壊株と同様の表現型が Δ*sll1878*, Δ*slr0327* 単一破壊株および Δ*sll1878*Δ*slr0327* 二重破壊株においても観察された。Sll1878 は分子内に ATP 結合モチーフが存在する。Slr0327 は分子内に結合タンパク質依存性輸送体の内膜タンパク質シグニチャーが存在し、かつ疎水性領域予測から 12 回の膜貫通領域の存在が予想される（結果省略）ため、それぞれ PCC 6803 の三価鉄輸送体の ATP 結合タンパク質サブユニットと膜貫通タンパク質サブユニットをコードしていると考えられた。またこれら 4 つの遺伝子は通常の BG-11 培地で培養した場合でもある程度発現しており、鉄欠乏処理することで mRNA の蓄積量が増加した。さらに Δ*slr1295*Δ*slr0513* 二重破壊株、Δ*sll1878*, Δ*slr0327* 単一破壊株および Δ*sll1878*Δ*slr0327* 二重破壊株は鉄欠乏処理をしなくても二価の鉄の輸送活性が高かった。これは、どの遺伝子も通常の BG-11 培地での生育において三価鉄輸送体 (のサブユニット) として機能しており、また、これらの遺伝子の機能を破壊すると、細胞は通常の BG-11 培地での生育においても鉄欠乏ストレスを感じ、これに応答して二価鉄輸送系の発現が誘導されることを示している。以上の結果からこれら 4 つの遺伝子の翻訳産物が PCC 6803 における単一の三価鉄輸送体を構成していると考えられた。そこで以後 Slr1295,

Slr0513, Slr0327, Sll1878 から成る三価鉄輸送体を Fut (ferric iron uptake) 輸送体と呼び、それぞれの遺伝子を *futA1*, *futA2*, *futB*, *futC* と呼ぶことにする。

PCC 6803 は三価の鉄輸送系だけでなく、アスコルビン酸で化学的に還元した二価鉄を輸送する系を持っていることが明らかとなった。二価鉄輸送系は野生株を通常の BG-11 (約 20 μM Fe) 培地上で生育させた場合には発現していないかあるいは発現レベルが非常に低く抑えられており、鉄欠乏処理することで発現誘導が起こる。Δ*slr1392* はこの二価鉄輸送系を持っておらず、また Slr1392 は *E. coli* の二価鉄輸送体サブユニット FeoB と相同性があり (Kammler, et al., 1993)、かつ ATP 結合モチーフを持っていることから、*slr1392* が PCC 6803 における二価鉄輸送体の ATP 結合タンパク質サブユニットをコードしていると考えられた。さらに RT-PCR 解析の結果から *slr1392* の直上に存在する ORF *ssr2333* が *slr1392* と共転写されていることも示された。これらの結果から、PCC 6803 における二価鉄輸送体遺伝子は *E. coli.* と同じようにゲノム上でオペロンを形成していることが明らかになった。そこで、Ssr2333, Slr1392 を構成要素として持つ二価鉄輸送体を Feo 輸送体と呼び、それぞれの遺伝子を *feoA*, *feoB* と呼ぶことにする。ところで、Fut 輸送体の機能を持たない変異株 (M1, M2, M5, M6) は鉄欠乏処理した場合の細胞あたりの二価鉄輸送活性が野生株の 7 割程度となっていた。これは二価鉄輸送体自体の活性が低下したわけではなく、鉄欠乏のため細胞の大きさが小さくなり、あるいは細胞のクロロフィル含量が低下した結果であると考えられた (Sherman and Sherman, 1983)。この場合、二価鉄輸送活性をクロロフィル当たりの取り込み量で表せば、Fut 変異株の活性は野生株と同程度となった (結果省略)。

本実験で破壊株を作製した *fut* および *feo* 以外の遺伝子について、細胞の鉄輸送における遺伝子産物の役割を特定することはできなかった。これらの遺伝子はその推定アミノ酸配列の相同性から、おそらくシデロフォア-鉄輸送体あるいはクエン酸鉄輸送体をコードしているものと予測できる (OM: *sll1206*, *sll1406*, *sll1409*, *slr1490*, PP: *sll1202*, *slr1319*, *slr1491*, *slr1492*, IM: *slr1316*, *slr1317*, *slr1318*)。多くのラン藻種は培地中の鉄濃度が低下するとシデロフォアを合成することが報告されているが、 PCC 6803 がシデロフォアを合成するかどうかは今のところ確かめられていない (Mahasneh, 1991, Trick and Kerry, 1992)。また、病原性バクテリア *Morganella morganii* は菌類が分泌したシデロフォアを利用して鉄を

輸送することが知られている (Kuhn, et al., 1996)。本実験に用いた生育検定条件や鉄輸送活性測定条件下では、フェリクロムやエンテロバクチンといったシデロフォアあるいはクエン酸等の鉄キレート化合物を加えていないため、各遺伝子産物の機能が認められなかったのかもしれない。少なくとも本章で用いた実験条件下ではこれらの遺伝子の機能は PCC 6803 の生育および鉄輸送において必須ではないことが示された。

野生株細胞の三価鉄輸送活性および二価鉄輸送活性の速度論的解析から、いずれの系も鉄に対して非常に高い親和性を持っていることが明らかになった。また、細胞を鉄欠乏処理することで鉄輸送活性の最大反応速度は上昇した。この上昇の大部分はそれぞれ Fut あるいは Feo 輸送体を破壊することで見られなくなることから、三価鉄輸送系においては Fut 輸送体が、二価鉄輸送系においては Feo 輸送体が担っているものと考えられる。これは、両輸送体遺伝子の各 mRNA の蓄積量が鉄欠乏ストレス下で増加することからも支持される。どちらの輸送系も ATP 合成を阻害すると活性が低下することから、ATP の加水分解によるエネルギーに依存的な取り込み反応であることが示された。これは FutC あるいは FeoB が ATP 結合モチーフを持っていることとよく一致する。野生株細胞の三価および二価鉄輸送活性は、例外的に高濃度の亜鉛で三価鉄輸送活性が、高濃度の銅で二価鉄輸送活性が阻害を受けたが、他の種々の二価または三価のカチオンの存在下ではほとんど阻害されなかった。すなわち Fut 輸送体と Feo 輸送体は非常に高い基質特異性を持っていると考えられる。これはそれぞれの輸送体の基質結合タンパク質サブユニットの基質特異性によるところが大きいものと考えられる。

第 4 章 鉄輸送体タンパク質 FutA1 の鉄結合活性の解析

序論

バクテリアの ABC 型輸送体は、その基質と特異的に結合する基質結合タンパク質サブユニットを必要とする (Higgins, et al., 1990, Tam and Saier, 1993)。前章までに、*Synechocystis* sp. strain PCC 6803 における三価鉄輸送体 (Fut 輸送体) と二価鉄輸送体 (Feo 輸送体) を同定したが、これらはその推定アミノ酸一次配列と ATP 加水分解エネルギー依存性から ABC 型輸送体であることが示された。三価の鉄輸送には Slr1295 (FutA1) と Slr0513 (FutA2) が高い基質特異性を持つ三価鉄結合タンパク質に相当するものと推定されたが、実際にこれらの遺伝子翻訳産物が鉄と結合するのか、あるいは結合する鉄の化学形が何なのか、生化学的な実験による証明はされていなかった。

FutA1/A2 は、*Neisseria gonorrhoeae* や *Haemophilus influenzae* においてペリプラスムに存在しフリーの三価鉄イオンと結合する FbpA/HitA と相同性を持っている (Berish, et al., 1990, Sanders, et al., 1994)。最近これらの基質結合タンパク質が大腸菌で大量発現され、その鉄結合活性がタンパク質溶液を用いた分光学的な実験や結晶タンパク質の X 線回折像による 3 次元構造に基づいて解析された (Chen, et al., 1993, Nowalk, et al., 1994, Adhikari, et al., 1995, Bruns, et al., 1997)。鉄イオンと結合した FbpA (以後 Fe^{3+}-FbpA と記す、他のタンパク質についても同様) 溶液は波長 481 nm にピークを持つ特徴的な可視吸収スペクトルを示し、同様に Fe^{3+}-HitA 溶液も波長 483 nm に吸収のピークが存在する。これらの吸収は鉄と結合していないアポ型タンパク質においては認められない。またこれらの鉄結合タンパク質の鉄に対する親和性はクエン酸のそれの約 1,000～10,000 倍程度と推定され、鉄との会合定数は実験条件下でおよそ $1\times10^{20\sim21}$ と見積もられている。さらに HitA については結晶構造解析からタンパク質分子内で鉄を配位する 4 つのアミノ酸残基が決定されている (Bruns, et al., 1997)。そこで、本章において Fut 輸送体における FutA1/A2 の鉄結合タンパク質サブユニットとしての役割を証明するため、まず大腸菌にそれぞれのリコンビナントタンパク質を大量発現させることを試みた。リコンビナント FutA1 (以下 rFutA1 と記す) は水溶性タンパク質として回収されたため、精製してタ

ンパク質溶液の分光学的な解析を行った。リコンビナント FutA2 は水溶性タンパク質として回収できなかったため、それ以上の解析は行わなかった。

PCC 6803 は *Escherichia coli* のクエン酸鉄輸送体の相同体遺伝子 *fecBCDE* を持っているが (Staudenmaier, et al., 1989)、本研究ではこれまで意図的に活性測定用培地にクエン酸を入れないことで細胞の鉄輸送経路を簡素化してきた。本章では鉄キレーターであるクエン酸が PCC 6803 細胞の鉄輸送活性にどのような影響を及ぼすのか検証するため、取り込み活性測定反応液中にクエン酸を添加して活性を測定する実験を行った。また同様にクエン酸が PCC 6803 細胞の生育にどのような影響を与えるかについても解析を行い、三価鉄輸送活性と二価鉄輸送活性との関わり合いについて考察した。

材料及び方法

4-1. リコンビナント FutA1 (rFutA) タンパク質の大量発現と精製

リコンビナント FutA1 タンパク質はグルタチオン S-トランスフェラーゼ (GST) との融合タンパク質として精製した。*futA1* 遺伝子の開始コドンの最初のヌクレオチドから 111 番目のヌクレオチドまでを持たない DNA 断片を、末端に制限酵素 *Eco*R I サイトを持った *futA1* 配列特異的プライマーを用いて PCR 法により増幅した。得られた DNA 断片を *Eco*R I で消化し、pGEX-2T 発現ベクター (Amersham Pharmacia Biotech) に翻訳枠が一致するように挿入した。このプラスミド (p*futA1-gst*) を用いて大腸菌 DH5α 株を形質転換した。得られた形質転換大腸菌を 100 μg/mL のアンピシリンを含む 2 L の 2×YT-G 培地中で 37°C で培養し、細胞懸濁液の OD 600 nm が 0.6 前後になった時点で IPTG を終濃度 1 mM となるように添加し、rFutA1 の発現を誘導した。2 時間培養を続けた後、大腸菌を遠心 (4,500×g, 4°C, 10 分間) して集め、氷冷した 1×PBS に懸濁した。細胞を、直径 10 - 5 mm のコニカルホーンを装備した超音波細胞破砕機 (No. 5202, 大岳製作所) で出力 20 W で破砕した。この操作は試料を氷上で冷却しながら行った。細胞破砕液に、終濃度 1% となるように 20% Triton X-100 を添加し、氷上で 30 分間穏やかに撹拌した。試料を遠心 (12,000×g, 4°C, 10 分間) し、上清を新しいチューブに移した (水溶性画分)。上清に 1/50 量の Glutathione-Sepharose 4B (50% スラリー) を添加し、室温で 30 分間穏やかに撹拌した後、遠心 (500×g, 4°C, 5 分間) して上清を取り除いた。ペレットを 10 倍容量の 1×PBS で 3 回洗浄した。支持体を 1 容量のグルタチオン溶出緩衝液 (10 mM 還元型グルタチオン, 50 mM Tris-HCl [pH 8.0]) に懸濁し、室温で 1 時間緩やかに撹拌した後、遠心 (500×g, 4°C, 5 分間) して上清を回収した。

4-2. rFutA1 タンパク質の鉄除去および鉄飽和

rFutA1 タンパク質の鉄除去および鉄付加は、Nowalk ら (1994) の方法に若干の改変を加えて以下のように行った。精製した rFutA1 溶液 (6 mg/mL) に 1/10 容量の 0.1% 酢酸を添加して溶液を酸性化し、そこに rFutA1 タンパク質の 2,000 倍濃度のクエン酸ナトリウム (pH 8.0) を加えて 4°C で 1 晩緩やか

に撹拌した。試料中の過剰量のクエン酸あるいはクエン酸鉄を Econo-10DG マイクロバイオスピンカラム (Bio-Rad) を用いて除去し、アポ rFutA1 タンパク質を 1 N HCl で洗浄した新しいチューブに回収した。アポ rFutA1 タンパク質を 20 mM Tris-HCl (pH 8.0)/200 mM NaCl 緩衝液中で 4.5 mg/mL (75 μM) となるように調製し、そこへ直接 2 倍濃度の塩化鉄溶液を加えることでアポ rFutA1 に鉄を付加した。

4-3. rFutA1 タンパク質の鉄結合活性の化学量論的解析と競合阻害検定

4.2 mg/mL (70 μM) のアポ rFutA1 タンパク質溶液に、鉄終濃度が 0 – 150 μM となるように段階的にそれぞれ塩化鉄溶液を添加し、室温で 15 分間緩やかに撹拌後、タンパク質溶液の OD 453 nm (A 453 nm) を測定して Fe^{3+}-rFutA1 の量を推定した。競合阻害実験はクエン酸ナトリウムを用いて以下のように行った (Chen, et al., 1993)。3.9 mg/mL (65 μM) の Fe^{3+}-rFutA1 (20 mMTris-HCl [pH 8.0]/200 mM NaCl 緩衝液中) にクエン酸ナトリウム (pH 8.0) を 0 – 130 mM となるように段階的にそれぞれ添加し、室温で 15 分間緩やかに撹拌後、タンパク質溶液の A 453 nm を測定した。

4-4. クエン酸存在下での細胞の鉄輸送活性の測定

ラン藻細胞の鉄輸送活性の測定は材料及び方法 2-6, 3-6 に従い行った。前培養の条件としては、鉄欠乏処理後、新たに鉄欠乏 BG-11 培地に終濃度 1 μM になるように塩化鉄を添加し (これを 1 μM Fe BG-11 培地と記す)、さらに必要に応じてクエン酸ナトリウム (終濃度 100 μM) を含んだ液体培地中で細胞を約 20 時間培養した。鉄取り込み反応測定溶液中の $^{59}FeCl_3$ の濃度は 1 μM に固定し、さらにクエン酸ナトリウム (pH8.0) を終濃度が 0 – 2 mM となるようにそれぞれ段階的に添加した。取り込み反応は光照射下で行った。

4-5. クエン酸存在下での液体培地中におけるラン藻の生育特性

鉄欠乏処理した野生株および変異株を、OD 730 nm の吸光度が 0.05 になるように 1 μM Fe BG-11 培地に再懸濁し、種々の濃度のクエン酸ナトリウム (pH 8.0) をそれぞれ添加 (終濃度 0 – 2 mM) して 60 $\mu Em^{-2}s^{-1}$ 連続光照射下、3% CO_2 通気条件で 72 時間培養を続けた。12 時間毎に細胞懸濁液の OD 730 nm

を測定した。細胞の生育速度 μ ($hour^{-1}$) および倍加時間 g は以下の計算式より求めた。

$$\mu = [\ln (N/N_0)]/t$$

$$g = 0.693/\mu$$

ここで、

N_0 ; t_0 時の OD 730 nm

N ; t 時間後の OD 730 nm

4-6. その他の方法

タンパク質試料の電気泳動は以下のようにして行った。大腸菌破砕液、水溶性画分、精製タンパク質それぞれに 3×SDS サンプル緩衝液 (200 mM Tris-HCl (pH 6.8), 9% (w/v) SDS, 15% (v/v) glycerol, 6% (v/v) 2-mercaptoethanol, 0.009% (w/v) bromophenol blue) を 1×濃度になるように添加し、95°C で 5 分間加熱した後、Laemmli の方法 (1970) に従い SDS-PAGE を行った。ゲル中のタンパク質は CBB により染色した。精製した rFutA1 溶液の濃度は OD 280 nm の値から推定した。rFutA1 の吸光係数 ($E^{1M}_{280\ nm}$) は、ポリペプチド中のチロシンとトリプトファンの残基数から、以下の式より求めた (Yin, et al., 1988)。

$E^{1M}_{280\ nm}$ = チロシン残基数×1390 + トリプトファン残基数×5800

タンパク質アミノ酸配列のアライメントには DNASIS (日立ソフトウェア) を、FutA1 のシグナル配列の予測には PSORT プログラム (Nakai and Kanehisa, 1991) を使用した。

rFutA1 溶液の可視吸収スペクトルおよび OD 453 nm, OD 280 nm、またラン藻細胞の OD 730 nm の測定には紫外/可視分光光度計 V-550 (Jasco, Tokyo, Japan) を使用した。

rFutA1 発現用のプラスミド *pfutA1-gst* の挿入塩基配列の確認のため、形質転換した大腸菌からアルカリ SDS 法により 2 本鎖プラスミド DNA を単離した。PEG 沈殿法によりプラスミド DNA を精製し、DNA Sequencing Kit (Applied Biosystems) によりシークエンス反応を行った。蛍光標識された DNA 断片の電気泳動と結果の解析には同社の自動 DNA 解析装置 Model 373A DNA Sequencing Systems を使用した。

鉄取り込み活性測定時においてクエン酸存在下での溶液中のフリーの鉄イオ

ンの濃度は以下の式から推定した。

$$[Fe^{3+}]_{Free} = [Fe^{3+}]_{TOTAL}\alpha / K_1([Citrate^{3-}]_{TOTAL} - [Fe^{3+}]_{TOTAL})$$

$$[Fe^{2+}]_{Free} = [Fe^{2+}]_{TOTAL}\alpha / K^{Fe}_{FeHCitrate}([HCitrate^{2-}]_{TOTAL} - [Fe^{2+}]_{TOTAL})$$

ここで、

$$\log \alpha = pK_a - pH$$

$$pK_{a1} = 3.1$$

$$pK_{a2} = 4.7$$

$$\log K_1 = 4.4$$

$$\log K^{Fe}_{FeHCitrate} = 2.7$$

である。

その他、特に言及していない試薬及び実験操作は材料及び方法 2-7 に従った。

結果

rFutA1 タンパク質の大腸菌での発現と精製

rFutA1 タンパク質発現用ベクターで形質転換した大腸菌からプラスミド DNA を単離し、その挿入塩基配列を決定したところ、目的とする領域での野生株の *futA1* 遺伝子と同一の配列を持った PCR 産物が挿入されたプラスミドであることが確認された (結果省略)。この大腸菌を IPTG 添加後 2 時間培養することで、分子量約 60 kDa のタンパク質の新たな発現が認められた (Fig. 4-1, レーン 1)。これは N 末端から 37 個のアミノ酸残基を持たない FutA1 タンパク質が GST と融合したおおよその分子量と一致する。このタンパク質バンドは IPTG による誘導前にはその存在が認められなかった (結果省略)。以上の結果からこれを rFutA1 とした。rFutA1 は水溶性画分中に存在し (Fig. 4-1, レーン 2)、水溶性画分を Glutathione Sepharose 4B レジンで処理することにより、ほぼ単一のタンパク質として精製された (Fig. 4-1, レーン 3)。

アポおよび鉄飽和 rFutA1 タンパク質の可視吸収スペクトル

Fig. 4-2 は rFutA1 タンパク質溶液の可視吸収スペクトルを示している。過剰量のクエン酸で処理した rFutA1 タンパク質溶液は可視波長 340 nm – 600 nm の範囲で吸収のピークを示さなかった。これに rFutA1 の 2 倍量の鉄を添加すると、波長 453 nm にピークを持つ特徴的な吸収帯が認められた。rFutA1 を含まない鉄溶液ではこのような吸収が見られないことから、波長 453 nm にピークを持つ吸収帯は、rFutA1 タンパク質が鉄と結合した状態を反映しているものと推測された。

化学量論的解析と rFutA1 の鉄に対する親和性

Fig. 4-3 は 70 μM のアポ rFutA1 タンパク質溶液に段階的に高濃度になるように塩化鉄を添加してそれぞれの溶液の A 453 nm を測定しプロットしたものである。A 453 nm の値は添加した鉄濃度がおよそ 70 μM になるまで直線的に上昇し、それ以上鉄を添加してもほぼ一定であった。これは鉄一分子が rFutA1 一分子と結合することを示しており、かつ A 453 nm が溶液中の Fe^{3+}-rFutA1 の量の推定に適していることを表している。

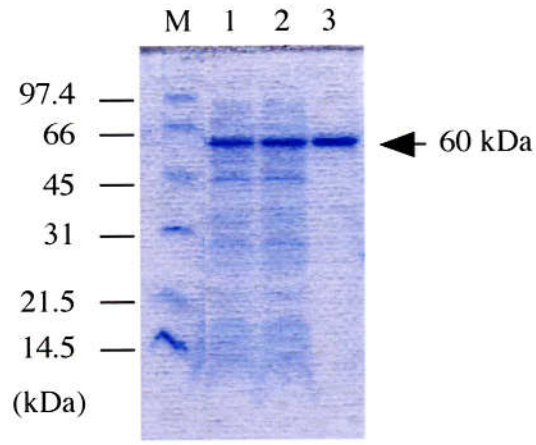

Fig. 4-1. SDS-PAGE patterns of rFutA1 expressed in *E. coli*. Truncated rFutA1 lacking the presumed signal peptide (37 amino acids on the N-terminal) was expressed in *E. coli* as a protein fused to glutathione S-transferase and purified on Glutathione Sepharose 4B resin. Proteins were separated on a 12.5 % SDS-polyacrylamide gel and stained with Coomassie Brilliant Blue. Lane 1, lysate of *E. coli* carrying p*futA1-gst* 2 h after addition of IPTG; lane 2, soluble fraction of the lysate; lane 3, rFutA1 purified on Glutathione Sepharose 4B resin; M, molecular mass markers (masses are indicated in kilodaltons). The amounts of proteins loaded were 20 μg in lane 1 and lane 2 and 5 μg in lane 3.

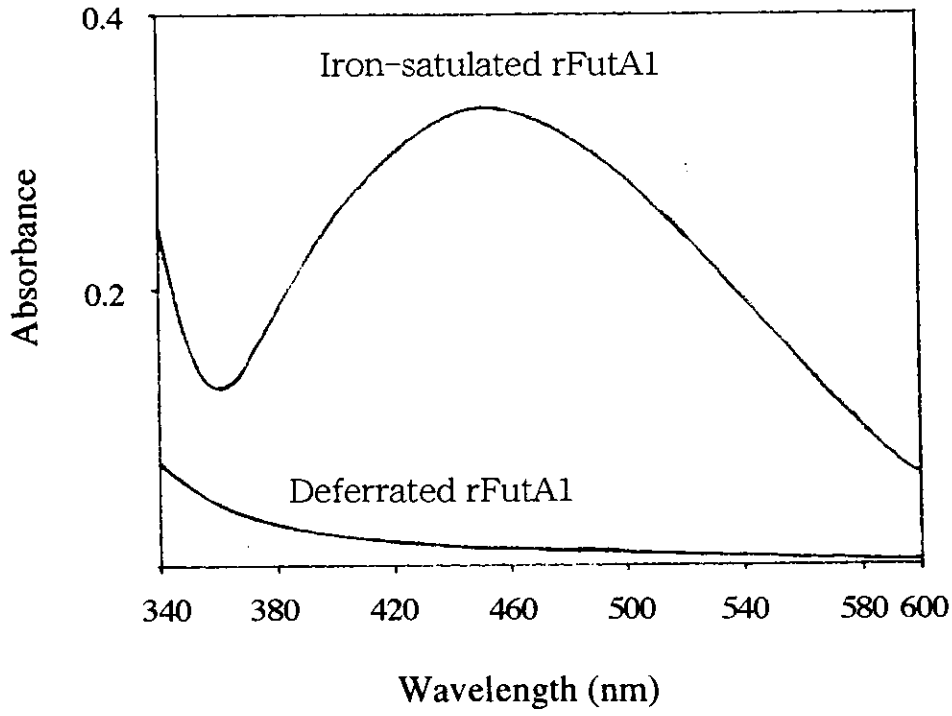

Fig. 4-2. Absorption spectra of deferrated and iron-saturated rFutA1. The sample solution contained 75 μM rFutA1 protein and 200 mM NaCl in 20 mM Tris-HCl buffer, pH 8.0.

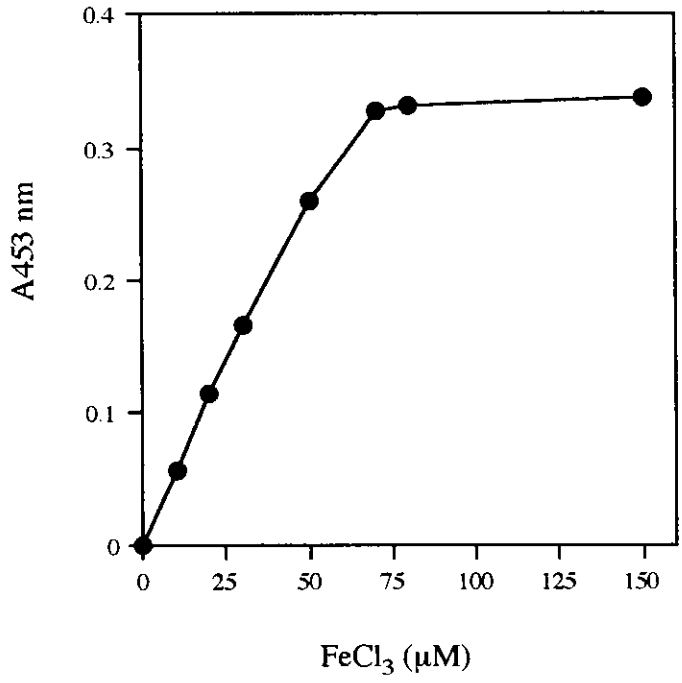

Fig. 4-3. Referration of rFutA1. Ferric chloride was added stepwise to the solution containing 70 μM deferrated rFutA1 to give the final concentrations of 0 to 150 μM and the absorbance was monitored at 453 nm.

この波長 453 nm における吸光度を用いて、rFutA1 の相対的な鉄に対する親和性を推定した。比較対照として、鉄キレーターであるクエン酸を使用した。Fig. 4-4 は 65 μM の Fe^{3+}-rFutA1 タンパク質溶液に段階的に高濃度になるようにクエン酸を添加して溶液の A 453 nm を測定しプロットしたものである。溶液中のクエン酸濃度が高くなるに従い、A 453 nm の値すなわち溶液中の Fe^{3+}-rFutA1 の量が減少した。これはクエン酸が rFutA1 タンパク質と鉄を競合していることを示している。また、rFutA1 の 2,000 倍量のクエン酸が存在すると rFutA1 はほとんどすべてアポ型になっていることが示された。競合阻害のため溶液中の Fe^{3+}-rFutA1 の量がクエン酸を加えない場合の 1/2 になるときのクエン酸の濃度は 6.5 mM、すなわち rFutA1 の約 100 倍の濃度であった。クエン酸の鉄に対する会合定数は pH 8.0 付近でおよそ 1×10^{17} (Crichton, 1990) と報告されていることから、rFutA1 の鉄に対する会合定数はおよそ 1×10^{19} と推定された。

FutA1 において鉄を配位するアミノ酸残基の推定

Fe^{3+}-rFutA1 に見られた特徴的な可視吸収スペクトルは、*N. gonorrhoeae* や *H. influenzae* の鉄結合タンパク質 FbpA/HitA においても同様に観察されている (Nowalk, et al., 1994, Adhikari, et al., 1995)。特に HitA は結晶構造が解析され、鉄を配位する 4 つのアミノ酸残基が同定されている (Bruns, et al., 1997)。そこで、FutA1 のアミノ酸一次配列を HitA のそれと比較することにより、FutA1 において鉄を配位するアミノ酸残基の推定を試みた (Fig. 3-5)。なお、FutA2 についても FutA1 と細胞の鉄輸送において同様な機能を持っている (第 3 章) ことから、推定アミノ酸配列を使用して比較した。その結果、HitA において鉄を配位するアミノ酸残基、ヒスチジン 9、グルタミン酸 57、チロシン 195、チロシン 196 の 4 つの残基のうち、ヒスチジンと 2 つのチロシン残基に相当する残基の存在が FutA1/A2 両タンパク質中に確認された。FutA1/A2 ともに 57 位のグルタミン酸に相当すると推定されるアミノ酸残基はバリンであった。これらの結果から、FutA1/A2 は HitA と比較して全体的な配列の相同性はそれほど高くないものの、鉄イオンを配位する機構は非常に良く似ているだろうと考えられた。以上の結果から、PCC 6803 の Fut 輸送体は病原性バクテリアに広く見られる Hit/Fbp 型の三価鉄イオン輸送体ファミリーに属するもの

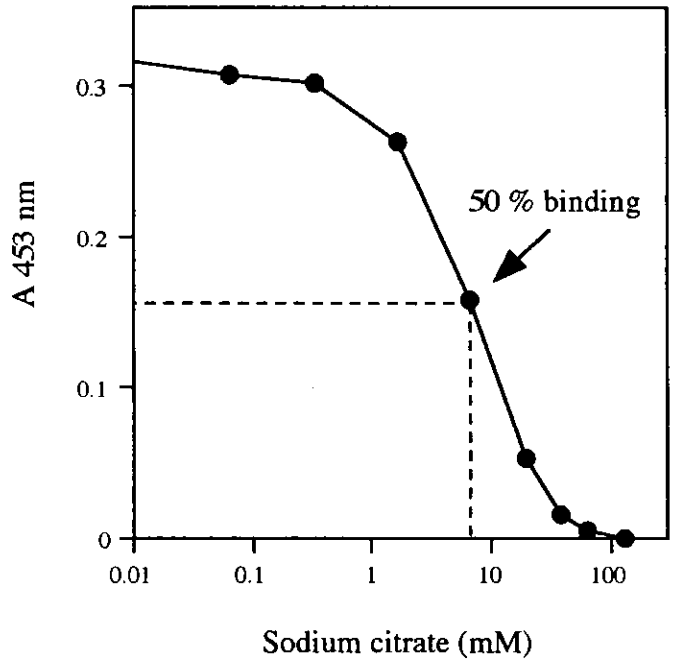

Fig. 4-4. Competition for rFutA1-bound iron by citrate. Sodium citrate was added stepwise to the solution containing 65 μM Fe^{3+}-rFutA1 and 200 mM NaCl in 20 mM Tris-HCl buffer, pH8.0 to give the final concentrations of 0 to 130 mM. The absorbance was monitored at 453 nm at each citrate concentration after incubation of the mixture at room temperature for 15 min.

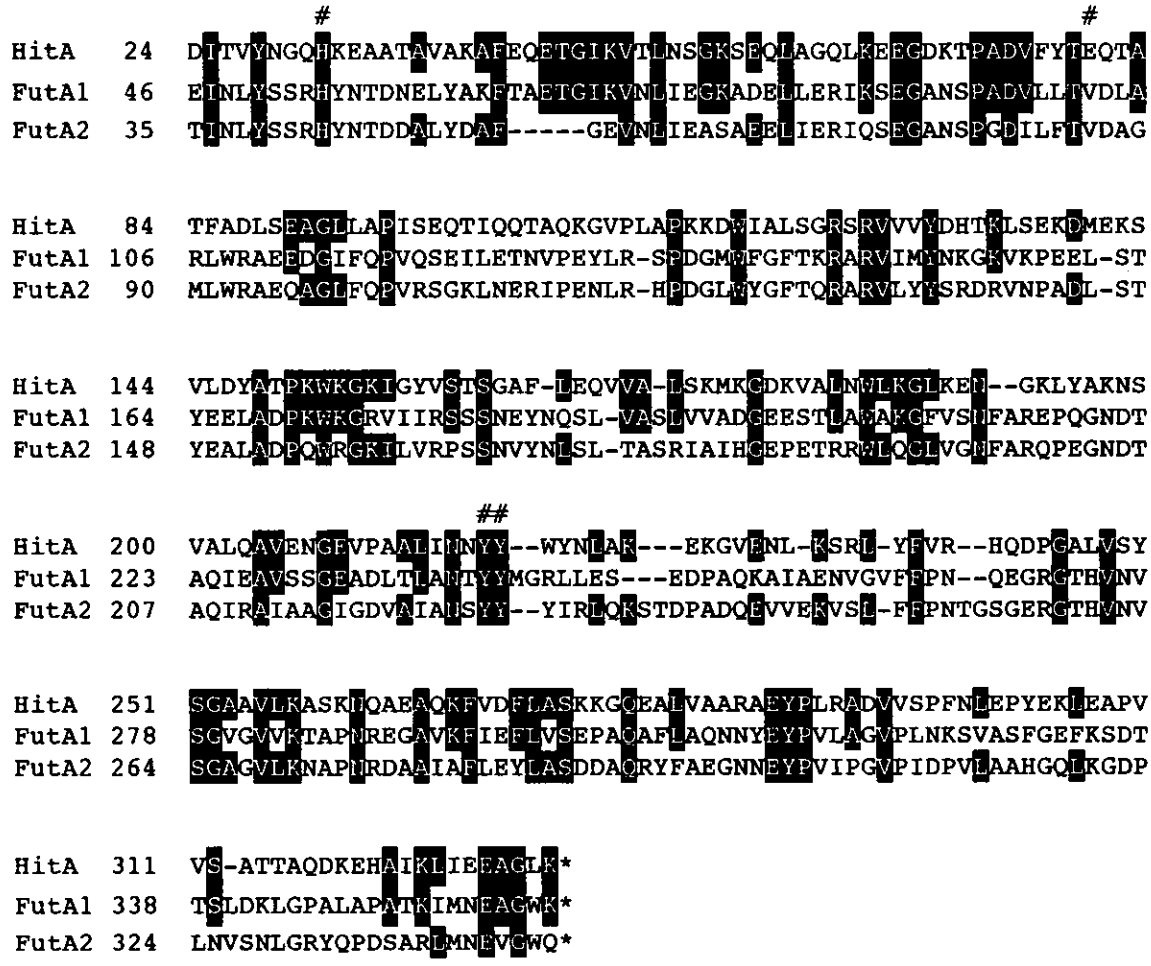

Fig. 4-5. Alignment of the amino acid sequences of FutA1, FutA2 and HitA. FutA1, deduced FutA2 of *Synechocystis*, and HitA of *H. influenzae* were aligned. Residues identical to those in HitA are shown in reverse type. Four residues (H9, E57, Y195, and Y196) involved in iron binding in HitA are represented by sharp symbols above the sequence (Bruns, et al., 1997).

であることが明らかになった。

ラン藻細胞の鉄輸送におけるクエン酸の影響

E. coli がクエン酸鉄輸送体を持っていることは既に第 3 章で述べた。この鉄輸送系は鉄欠乏下で培地中にクエン酸が存在するときに限って発現する (Frost and Rosenberg, 1973)。PCC 6803 ゲノム中には *fecBCDE* 相同体遺伝子 *slr1319*, *slr1316*, *slr1317*, *slr1318* が存在している (第 3 章)。これらが本当にクエン酸鉄輸送体遺伝子として機能しているのか、また PCC 6803 がクエン酸鉄輸送系をもっているかどうか調べるため、野生株と Δ*futA1*Δ*futA2* 二重破壊株のクエン酸存在下での鉄輸送活性を測定した。また、クエン酸鉄輸送系の発現に培地中のクエン酸の存在が必要である可能性も考えられることから、クエン酸を含む 1 μM Fe BG-11 培地で前培養した細胞とそうでない細胞を使用した。Fig. 4-6 は 100 μM クエン酸を含む 1 μM Fe BG-11 培地で培養した細胞 (●, ○; 野生株、▲, △; Δ*futA1*Δ*futA2* 株) の三価鉄輸送活性 (○, △) および二価鉄輸送活性 (●, ▲) に対する反応測定溶液中のクエン酸の影響を示している。野生株における三価の鉄の輸送活性は測定溶液中のクエン酸濃度が高くなるに従い急激に低下し、100 μM 以上のクエン酸存在下ではほとんど三価の鉄として取り込めないことが示された。二重破壊株ではもともと三価鉄輸送活性は非常に低いが、クエン酸の存在によりさらに活性が低下した。野生株の二価鉄輸送活性は、クエン酸濃度 100 μM 以下ではほぼ一定であり、それ以上の濃度から活性が急激に低下した。二重破壊株においてもこれと同様の傾向が観察された。二重破壊株において二価鉄輸送活性が野生株と比べて多少低いのは第 3 章で見た通りである。本実験において前培養の条件により細胞の鉄輸送活性が変わることは無かった (結果省略)。以上の結果、高濃度のクエン酸は細胞の鉄輸送活性に対し、阻害的な影響を及ぼすことが明らかになった。鉄に対するクエン酸の安定度定数 K_1, $K^{Fe}_{FeHCitrate}$ と pK_a (材料及び方法 4-6 参照) に基づいて各クエン酸濃度での溶液中のフリーの三価鉄および二価鉄イオンの濃度を推定すると、フリーの三価鉄イオンはフリー二価鉄イオンのおよそ千分の一程度しか存在していないことが分かった (Table 4-1.)。さらにフリー鉄イオン濃度に対する鉄輸送活性の K_m 値を逆数プロット法により推定したところ、フリー三価鉄イオン輸送の K_m 値は 100 pM 以上、これに対しフリー二価鉄イオン輸送の K_m

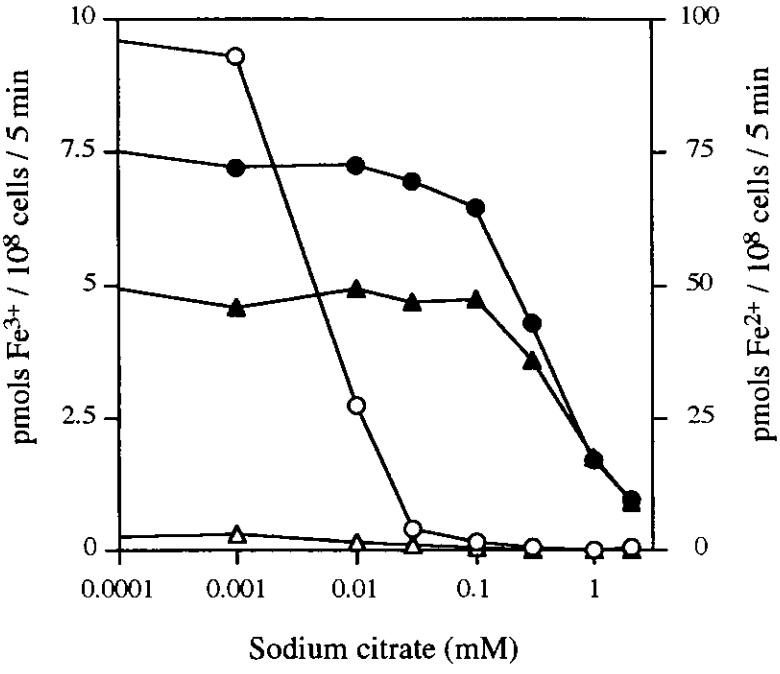

Fig. 4-6. Inhibition of iron uptake by citrate. Uptake reaction was initiated by adding 1 μM $^{59}FeCl_3$ to the suspension of cells containing various amounts of citrate (0 to 2 mM, final concentration) either with 500 μM ferrozine (○, △) or ascorbate (●, ▲). The reaction was terminated by transferring the reaction mixture on ice, followed by centrifugation at 4°C. The pellet was washed twice with 20 mM TES-KOH (pH 8.0) containing 10 mM EDTA. circles: wild-type, triangles: Δ*futA1*Δ*futA2*.

Table 4-1. Free iron concentrations and uptake of iron when the citrate is present.

$[Fe^{3+}]_{TOTAL}$	$[Citrate^{3-}]_{TOTAL}$	[free Fe^{3+}]	Fe^{3+} uptake (pmols Fe/10^8 cells/5 min), K_m >100 pM
1 μM	10 μM	56 pM	2.76
1 μM	30 μM	17 pM	0.42
1 μM	100 μM	5.1 pM	0.131
1 μM	300 μM	1.7 pM	0.039
1 μM	1 mM	0.5 pM	0.015
1 μM	2 mM	0.25 pM	0.039
$[Fe^{2+}]_{TOTAL}$	$[HCitrate^{2-}]_{TOTAL}$	[free Fe^{2+}]	Fe^{2+} uptake (pmols Fe/10^8 cells/5 min), K_m =3 nM
1 μM	10 μM	111 nM	72.6
1 μM	30 μM	34 nM	69.5
1 μM	100 μM	10 nM	64.7
1 μM	300 μM	3.3 nM	42.8
1 μM	1 mM	1 nM	17
1 μM	2 mM	0.5 nM	9.4

値はおよそ 3 nM であった。すなわち二価鉄輸送活性が三価鉄輸送活性よりもクエン酸の阻害に対する感受性が低いのは、 100 μM クエン酸存在下で還元状態ではフリー二価鉄イオンが K_m 値 (3 nM) よりも高濃度 (10 nM) で存在できるのに対し、同クエン酸濃度で酸化的な条件ではフリー三価鉄イオンが K_m 値 (>100 pM) よりもはるかに少ない濃度 (5.1 pM) であるためと考えられた。

液体培地中での生育におけるクエン酸の影響

Fig. 4-7 は、1 μM Fe BG-11 液体培地中での野生株 (○, ●)、Δ*futA1*Δ*futA2* 二重破壊株 (△, ▲)、Δ*feoB* 単一破壊株 (▽) の生育に対するクエン酸の影響を示している。野生株および二価鉄輸送活性の低下した Δ*feoB* 株は、鉄濃度の 10 倍程度のクエン酸存在下で全く添加していない場合よりも若干生育速度の上昇が認められたものの、高濃度のクエン酸 (100 μM 以上) 存在下では明らかに生育速度が低下した。これらの結果から PCC 6803 においてはクエン酸鉄輸送系が機能しておらず、鉄輸送は主に三価鉄イオン輸送体である Fut 輸送体が担っていると考えられる。この推定に基づけば、Δ*futA1*Δ*futA2* はクエン酸濃度によらず 1 μM Fe BG-11 培地中で常に低い生育速度を示すことが予想される。ところが予想に反し、クエン酸が 30 μM 程度存在する場合は野生株と同程度の生育速度を示した。この生育は二価鉄キレーターであるフェロジンを培地中に添加することで抑制された (Fig. 4-7, ▲)。一方この条件下で、野生株においてフェロジンの効果は認められなかった (Fig. 4-7, ●)。これらの結果から、Δ*futA1*Δ*futA2* 株はクエン酸が鉄の 30 倍程度存在している場合に二価鉄の形で鉄を取り込んで生育しているのに対し、野生株では三価鉄の形で取り込んで生育しているものと考えられた。

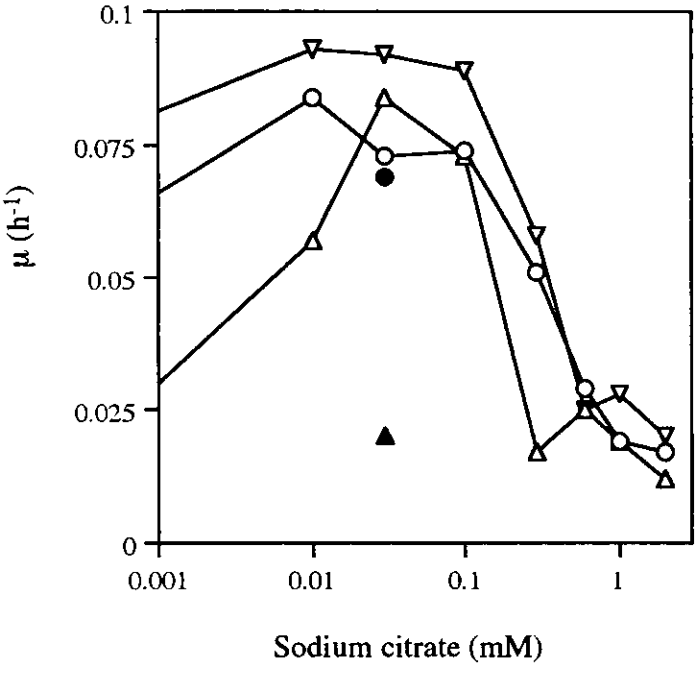

Fig. 4-7. Growth rates (μ) of wild-type (○), Δ*feoB* (▽), and Δ*futA1*Δ*futA2* (△) mutant cells as a function of citrate concentration in BG-11 liquid medium containing 1 μM $FeCl_3$. Cultures were aerated with 3% (vol/vol) CO_2 in air. ●, ▲: Ferrozine (500 μM) was added to the culture medium to inhibit ferrous iron uptake.

考察

rFutA1 タンパク質溶液の分光学的解析から、Fe^{3+}-rFutA1 が波長 453 nm に吸収のピークを持つ特徴的な可視吸収スペクトルを示すことが明らかになった。このような吸収スペクトルは Fe^{3+}-FbpA や Fe^{3+}-HitA 溶液でも観察され、タンパク質と結合した鉄イオンによるものであることが報告されている (Nowalk, et al., 1994, Adhikari, et al., 1995)。化学量論的解析から鉄イオンと rFutA1 がモル比 1 : 1 で結合することが明らかとなり、また鉄イオンと rFutA1 の会合定数はおおよそ 1×10^{19} 程度と見積もられた。HitA/FbpA も同じように鉄イオンとモル比 1 : 1 で結合するが、その会合定数はおよそ 1×10^{20} ～ 1×10^{21} 程度と報告されており、rFutA1 のそれよりも高い。また Fe^{3+}-HitA/Fe^{3+}-FbpA の可視吸収のピーク波長はそれぞれ 483/481 nm であり、Fe^{3+}-rFutA1 の 453 nm と比べて約 30 nm ほど長波長側になっている。アミノ酸一次配列の解析から、FutA1 には HitA において鉄イオンを配位するアミノ酸残基 4 つのうち 3 つまでが保存されていた。このことから、FutA1 の鉄結合アミノ酸残基が形成する配位子場の状態は HitA とよく似ているが全く同じではないだろうと考えられる。本章の実験で観察された rFutA1 と HitA/FbpA との間の吸収スペクトル特性や鉄に対する親和性の違いは、配位子場の電子状態の違いを反映しているのかもしれない。このように、タンパク質の鉄イオン結合活性に若干の差異は認められるものの、FutA1 タンパク質がシデロフォアやクエン酸などの鉄キレーターを介さず直接鉄と結合することは明らかである。これは光合成微生物において病原性バクテリアに広く存在する高親和性 Fbp/Hit 型鉄輸送体の存在を初めて証明したものである。

E. coli のクエン酸鉄輸送活性は培地中にクエン酸を必要とし、高濃度条件下 (～10 mM) でも機能する (Frost and Rosenberg, 1973)。本章で用いた条件下では 100 μM 以上のクエン酸存在下で二価鉄および三価鉄輸送活性、生育ともに阻害された。これらの結果から、PCC 6803 は *E. coli* のクエン酸鉄輸送系のような鉄輸送経路を持っていないと考えられた。特に三価の鉄輸送活性に関しては、*in vitro* でクエン酸が Fut 輸送体の基質結合タンパク質である FutA1 と鉄との結合を阻害することと良く一致している。また、Fut 輸送体は *in vivo* でクエン酸鉄を輸送しないことも明らかになった。このようなクエン酸による細胞の

鉄輸送活性の阻害効果は、*Salmonella typhimurium* においてエンテロバクチン合成経路を破壊した *enb* 変異株においても観察されている (Pollack, et al., 1970)。

ところで、Fut 輸送系の機能を持たない *ΔfutA1ΔfutA2* 株は鉄/クエン酸比が 1/30 程度では野生株並みの生育を示した。この程度の鉄/クエン酸比の範囲内で *ΔfutA1ΔfutA2* 株は十分な二価鉄輸送活性を持ち、またフェロジン存在下でこの生育は抑えられた。一方野生株ではフェロジンによる生育の阻害効果は無かった。この現象の解釈のひとつとして、*ΔfutA1ΔfutA2* 株が培地中の三価の鉄を二価鉄に還元し、Feo 輸送体を介して二価鉄を細胞内へ輸送していると考えることができる。さらに野生株、*ΔfeoB* 株および *ΔfutA1/ΔfutA2* 株は培地中に鉄が 1 μM 含まれていればクエン酸が 100 μM 程度存在しても正常に生育できた。この程度の鉄/クエン酸濃度比 (～1/100) の範囲ではフリーの三価鉄イオンは非常に低濃度であり、Fut 輸送体による鉄の取り込みは期待できないにも関わらず細胞は正常に生育し、しかも比較的多量に存在すると考えられるフリー二価鉄を輸送する Feo 輸送体の欠損株でも生育が可能である。これらの結果は、実験に適用した条件下で、細胞の鉄輸送活性測定において生育時の鉄輸送活性をそのまま反映しているものではないことを示唆している。野生株および *ΔfeoB* の生育がシデロフォア様化合物や有機酸などの鉄キレート化合物を介した第三の鉄輸送体によるものか、あるいは細胞の生育の過程で培地中あるいは細胞表面に鉄を還元するフェリレダクターゼ様酵素等が存在しており、細胞周辺を還元状態にすることでフリーの二価鉄をペリプラズムに取り込んだ後、再酸化された鉄を Fut 輸送体で輸送しているのか現段階では明らかでない。いずれにしても輸送活性測定の前に細胞を鉄欠乏緩衝液で洗浄することでこれらの物質あるいは酵素等が細胞表面や培地中から除去されてしまうものと考えられる。

第 5 章　総合討論

酸化的な現在の地球環境下で水中の鉄は生物が利用しにくい水酸化鉄として沈殿するため、海洋あるいは淡水に生息する光合成プランクトンは頻繁に鉄欠乏ストレスに遭遇する (Boyer, et al., 1987, Straue, 1994)。従って水界における一次生産の大部分を担う光合成プランクトンの光合成は鉄により律速されていると考えられている (Bultler, 1998)。光合成微生物の鉄欠乏ストレスに対する応答機構は、これまで種々の生物種を用い、様々な側面から研究されてきた。鉄欠乏ストレスはラン藻細胞の形態的変化を引き起こす。Sherman らは *Synechococcus* sp. strain PCC 7942 を用い、鉄が充分なコントロール細胞とそうでない細胞の電子顕微鏡観察を行った (Sherman and Sherman, 1983)。鉄欠乏ストレスのかかった細胞はコントロール細胞と同じ速度で分裂したが、細胞の長さは 2/3 から半分程度になっていた。さらに鉄欠乏ストレスによって細胞内のチラコイド膜、フィコビリソーム、カルボキシソームの数が減少し、逆にグリコーゲン貯蔵顆粒は増加することが報告された。鉄欠乏ストレスはまた、ラン藻細胞の光合成生理に影響を与える。*Synechococcus* sp. strain PCC 6301 や *Synechococcus* sp. strain PCC 6908 で、鉄欠乏ストレスにより細胞の低温吸収スペクトルの変化が観察された。これは PS I あるいは PS II のクロロフィル組成の変化によるものと考えられた (Oquist, 1974, Guikema and Sherman, 1983, Guikema, 1985)。鉄欠乏ストレスにより細胞が合成する新たなタンパク質の解析も行われてきた。光合成電子伝達鎖の構成要素フェレドキシンは鉄含有タンパク質であるが、*Nostoc* や *Anabaena*、*Synechococcus* など多くのラン藻種は鉄欠乏ストレスによりフェレドキシンの合成を停止し、代わりに鉄を含まない電子伝達タンパク質フラボドキシンを合成する (Hutber, et al., 1977, Laudenbach et al., 1988, Sandmann, et al., 1990)。このフラボドキシンが光合成におけるフェレドキシンの機能を代替するため、鉄ストレス下でも光合成活性はそれほど低下しないことが報告されている (Sandmann, et al., 1990)。また、*Synechococcus* sp. strain PCC 7942 や *Synechococcus* sp. strain PCC 7002 においてフラボドキシン遺伝子と共転写される *isiA* は CP43 と類似性の高い CPVI-4 をコードしており、これは PS II において鉄欠乏ストレス下における光捕集タンパク複合体の補助因子の役割を持っていると考えられている (Pakrasi, et al., 1985, Riethman and

Sherman, 1988)。さらに、ラン藻は鉄欠乏ストレスにより鉄輸送活性が上昇すること、また細胞質膜や細胞外膜に新たなタンパク質が蓄積されることが報告されており、これらのうちの幾つかは鉄輸送体であろうと考えられている (Scanlan, et al., 1989, Mahasneh, 1991)。このようにラン藻の鉄輸送機構に関してこれまで詳細な研究がなされてきたにも関わらず、鉄輸送体遺伝子の同定には至らなかった。

本研究は、ゲノム解析の結果その存在が明らかとなった多数の輸送体遺伝子に着目し、網羅的に遺伝子破壊株を作製して表現型を解析することにより、単細胞性ラン藻 *Synechocystis* sp. strain PCC 6803 の鉄輸送機構を分子レベルで解明したものである。PCC 6803 は三価鉄輸送体と二価鉄輸送体を持っており、どちらも基質の輸送に際して ATP 加水分解のエネルギーを必要とする ABC 型輸送体であった。通常の BG-11 培地での生育には鉄を主として三価の形で取り込んでおり、培地中の鉄濃度が低くなるかあるいは三価鉄輸送系が充分に機能しなくなることで細胞が鉄欠乏ストレスを感知すると、二価鉄輸送体の発現が誘導される。

PCC 6803 の三価鉄輸送体は *fut* 遺伝子群 (*futA1*, *futA2*, *futB*, *futC*) によりコードされている。各遺伝子の推定アミノ酸配列から、Fut 輸送体において *futA1/A2* は基質結合タンパク質を、*futB* は膜貫通タンパク質を、*futC* は ATP 結合タンパク質をコードしていると考えられた (Fig. 3-2)。FutB と FutC はホモロジー検索の結果、病原性バクテリア *H. influenzae* の HitB 、HitC と弱い相同性を示した。*hitB* 、*hitC* は三価鉄輸送体のそれぞれ膜貫通タンパク質と ATP 結合タンパク質をコードしていると考えられている (Sanders, et al., 1994)。このことからも PCC 6803 の *futB* は膜貫通タンパク質をコードしているであろうと推定されたが、モチーフ検索の結果 FutB には内膜タンパク質シグニチャーの他に ATP 結合モチーフも存在することが示された (AARSLGKS, 458–465 位)。一般的なバクテリアの ABC 型輸送体は膜貫通領域と ABC 領域をそれぞれ 2 つづつ持っており、これら 4 つの領域が別々のポリペプチドとしてコードされていたり、あるいは色々な組み合わせを持ったポリペプチドとしてコードされている (Higgins, 1992, Linton and Higgins, 1998)。FutB は推定アミノ酸配列を用いた疎水性プロファイルの予測から 12 回膜貫通タンパク質と考えられる (結果省略)。現段階では FutB と FutC から一つづつ ATP 結合領域を提供

しているのか、あるいは FutC がホモまたはヘテロダイマーで ABC タンパク質として機能するのか明らかではない。Fut 輸送系のドメイン構成を詳しく議論するためには、鉄イオン輸送に際し FutB の ATP 結合領域において実際に ATP が結合し加水分解を受けるかどうか実験的に確かめる必要がある。FutA1、FutA2 は病原性バクテリア *S. marcescens* の SfuA とある程度の相同性を示した。SfuA は三価鉄輸送体 Sfu の鉄結合タンパク質であり、Sfu 輸送体は Hit/Fbp 輸送体ファミリーに属している (Angerer, et al., 1990)。このことからも、PCC 6803 の *futA1*、*futA2* は Fut 輸送体の鉄結合タンパク質であることが推定された。しかし、Hit/Fbp 輸送体ファミリーにおいて別々の遺伝子にコードされた 2 種類の基質結合タンパク質を持っている生物は報告されていない。従って、主要な基質結合タンパク質遺伝子 *futA1* に加えて、これと重複した機能を持つ *futA2* 遺伝子が存在することは PCC 6803 の Fut 輸送体の大きな特徴と言える。PCC 6803 の二価鉄輸送体は *feoAB* 遺伝子にコードされている。*feoAB* は大腸菌 *E. coli* の *feoAB* 遺伝子と同じようにオペロン構造をとっていた (Fig. 3-9)。 PCC 6803 の FeoB は分子内に ABC 領域を持つと同時に全体にわたって疎水性が高かったことから、膜貫通領域と ABC 領域が融合したタンパク質であろうと考えられた。FeoA は分子内に特徴的なモチーフの存在は認められなかったが、疎水性領域を持たないため、ペリプラスムに存在して基質と結合する役割をもっているのではないかと考えられる。以上のことをふまえて Fig. 5-1 に PCC 6803 における鉄輸送機構のモデルを示す。

PCC 6803 の鉄輸送系の活性は他の金属によってほとんど阻害されなかった (Fig. 3-8)。これは両輸送体の基質結合タンパク質がそれぞれ基質である三価鉄あるいは二価鉄に対して親和性が高いことを示している。リコンビナントタンパク質 rFutA1 を用いた実験から、FutA1 が鉄キレート有機化合物を介さず、直接高い親和性を持って三価鉄イオンと結合することが証明された (Fig. 4-2, 4-3)。これによって、Fut 輸送体の基質が鉄イオンであり、病原性のグラム陰性バクテリアに広く存在する Hit/Fbp 型の高親和性鉄輸送体が光合成微生物に存在し、PCC 6803 細胞の鉄輸送に重要な役割を果たしていることが明らかになった。ところで、PCC 6803 において細胞外膜における鉄透過機構はどうなっているのであろうか？。*Neisseria* においては細胞外膜に宿主由来のトランスフェリンと結合するレセプタータンパク質 TbpA の存在が報告されている

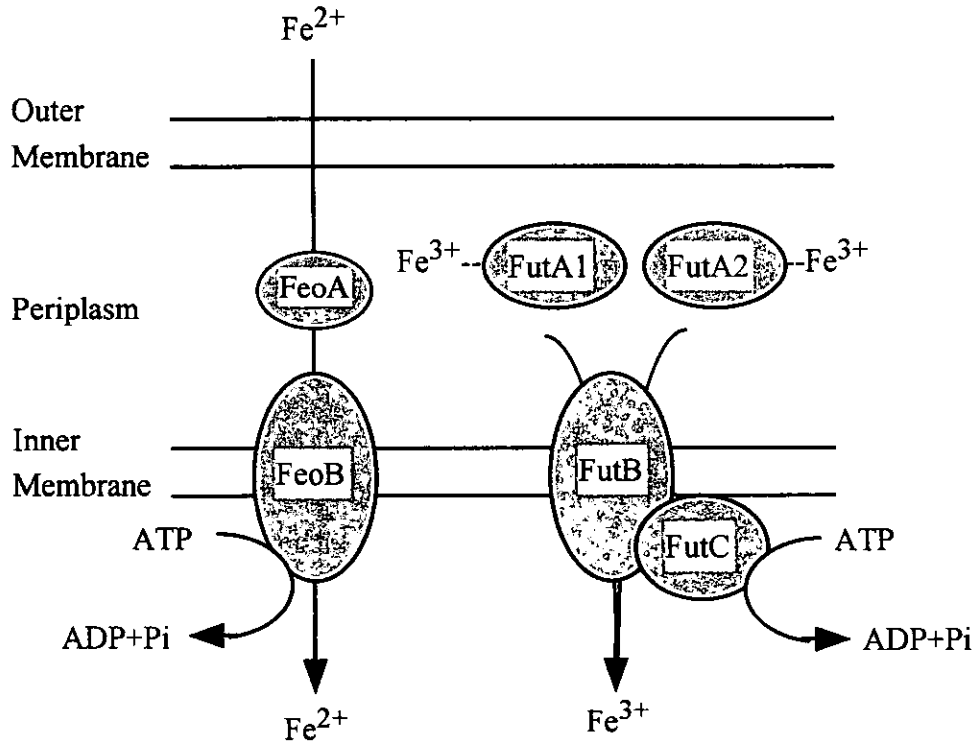

Fig. 5-1. A model for iron uptake in *Synechocystis*. Fut system transports ferric iron across inner membrane depending on the energy produced by ATP hydrolysis. The Fut system composes of FutA1/A2/B/C. The *futA1/A2* encode periplasmic iron-binding protein. The *futB* encodes transmembrane component of ferric iron transporter. The *futC* encodes ABC protein of ferric iron transporter. Feo system transports ferric iron across inner membrane depending on the energy produced by ATP hydrolysis. The Feo system is encoded by *feoAB* operon, in which the *feoA* encodes substrate-binding protein and the *feoB* encodes transmembrane component with ABC domain. Domain organization of these transport systems, however, should be certified. The molecular mechanism that how iron is transported through outermembrane is unclear.

(Irwin, et al., 1993, Anderson, et al., 1994)。TbpA のアミノ酸一次配列は他の微生物のシデロフォア-鉄レセプタータンパク質とある程度の類似性を持っており、結合したトランスフェリンから鉄を奪ってペリプラスムへ輸送すると考えられている。ペリプラスムにおいてこのフリー鉄が鉄結合タンパク質 FbpA と結合し、ABC 型の Fbp 輸送体により細胞質膜の内側へと輸送されるというモデルが提唱されている (Chen, et al., 1993)。しかし PCC 6803 には *tbpA* の相同体遺伝子は同定されておらず、またシデロフォア-鉄レセプタータンパク質をコードすると推定される 4 つ (*sll1206*, *sll1406*, *sll1409*, *slr1490*) の遺伝子を破壊しても、調べた条件下では何ら表現型を見い出せなかった (Fig. 3-4, 3-5, 3-6)。また *E. coli* はシデロフォア-鉄レセプターを介した外膜透過機構に加えて、細胞外膜にクエン酸鉄レセプター FecA を持ち、外膜を横切ってクエン酸鉄 (Fe^{3+}-dicitrate) をペリプラスムへ輸送した後クエン酸鉄輸送体 FecBCDE を用いて鉄を細胞質側へ輸送することが報告されている (Horst, et al., 1988, Staudenmaier, et al., 1989)。しかし PCC 6803 には *fecBCDE* 相同遺伝子 (*slr1319*, *slr1316*, *slr1317*, *slr1318*) の存在は認められるものの、*fecA* 相同体遺伝子の存在は報告されていない。従って、PCC 6803 における鉄の外膜透過機構を解明することは今後の重要な課題である。

培地中にクエン酸が鉄の 100 倍以上存在すると、野生株の生育は抑えられた。クエン酸の生育に与える影響は二価鉄輸送体を持たない Δ*feoB* 株においても同様であった。しかし Δ*futA1*Δ*futA2* 二重破壊株では低濃度鉄培地中でクエン酸が存在しない場合はほとんど生育できないにも関わらず、鉄/クエン酸比が 1/10～1/100 程度であれば二価鉄の形で取り込み、ほぼ正常に生育できることが示された (Fig. 4-7)。これらの結果から、PCC 6803 の鉄輸送における Fut 輸送体と Feo 輸送体の関係について次のようなモデルが考えられる。(1) 低濃度鉄培地中の鉄がクエン酸で可溶化されていない条件下では Fut 輸送体が細胞の鉄輸送のほとんど全てを担っているため、Fut 輸送系を破壊すると生育できなくなる。(2) 培地中の鉄が適度な条件 (鉄/クエン酸比 1/10～1/100) で可溶化されていれば、Fut 輸送体および Feo 輸送体の両方が鉄を輸送し、このうちの片方が機能しなくても細胞は正常に生育できる。(3) 鉄/クエン酸比が 1/100 以上の条件下では Fut および Feo 両輸送体が機能しなくなるため、細胞は生育できない。次に細胞の鉄輸送活性におけるクエン酸の影響を考えてみよう。

Δ*futA1*Δ*futA2* 株はクエン酸を含まない培地中で、アスコルビン酸で還元された二価鉄を輸送することができた (Fig. 4-6)。これは二価鉄の形であればクエン酸によって可溶化されていなくても輸送できることを示している。すなわち、Δ*futA1*Δ*futA2* 株がクエン酸を含まない培地中で生育できなかったのは、三価の鉄を二価に還元できなかったためと考えることができる。通常の酸化的な培養条件下では二価鉄は速やかに三価鉄に酸化されるため、培地中の鉄はほとんど三価の形になっていると考えられる。ところが Δ*futA1*Δ*futA2* 株が生育の過程で二価鉄を輸送しているということは PCC 6803 が三価の鉄を二価の鉄に還元するフェリレダクターゼ様活性を持っていることを示唆している。このフェリレダクターゼ様活性が働くためには鉄がクエン酸等のキレーターで適度に可溶化されている必要があるのかもしれない。真核微生物である酵母 *Saccharomyces cerevisiae* は、原形質膜において三価の鉄を二価の鉄に還元する FRE1 タンパク質が存在し、還元された二価鉄を二価鉄輸送体により細胞内へ輸送している (Dancis, et al., 1990)。また、グラム陰性細菌の *Helicobactor pylori* は三価クエン酸鉄 (Fe^{3+}-dicitrate) を二価クエン酸鉄 (Fe^{2+}-dicitrate) に還元した後、FeoB を含む二価鉄輸送系を用いて細胞内へ鉄を輸送している (Velaudhan, et al., 2000)。PCC 6803 の鉄輸送においてもこのような鉄還元機構が関与している可能性が考えられるため、細胞のフェリレダクターゼ活性についてさらに解析が必要である。

本研究により、PCC 6803 の三価鉄および二価鉄輸送体遺伝子が同定された。これらの遺伝子は細胞を鉄欠乏処理することで各 mRNA の発現の増加が認められた (Fig. 3-3)。また、鉄欠乏処理により三価鉄および二価鉄輸送活性が増大することから、Fut および Feo 輸送体タンパク質の発現量も増加していることが示唆された (Fig. 2-3, Fig. 3-7)。各 *fut* 遺伝子はゲノム上に散在しているのに対し、*feoAB* 遺伝子はオペロン構造をとっていた。これらの遺伝子およびタンパク質の発現がどのように調節されているのかは、非常に興味のある問題である。今後は鉄欠乏ストレスに応答する遺伝子の発現調節に関わっている遺伝子の探索が重要となる。*E. coli* においては Fur タンパク質が鉄欠乏ストレス応答性遺伝子の発現を調節している (Schaffer, et al., 1985, De Lorenzo, et al., 1988)。Fur は細胞内に鉄が充分ある場合は鉄と結合した形で標的遺伝子のプロモーター領域に結合し、標的遺伝子が転写されることを抑制している。細胞内の鉄が

不足してくると Fur と結合していた鉄は Fur から離れ、それによって Fur は標的遺伝子のプロモーター領域に結合できなくなり、標的遺伝子の転写が起こる。また、細胞外の鉄濃度の低下を感知しその情報を細胞内に伝えるタンパク質の存在も予想されるため、このような機能を持つタンパク質の遺伝子を同定することにより、 *Synechocystis* sp. strain PCC 6803 の鉄輸送機構の詳細を解明していくことができるものと考えられる。

要旨

鉄は生体に必須の元素であり地球上で豊富に存在するが、その化学的性質のため生物は常に十分な鉄を利用できるわけではない。そこで生物は様々な方法で微量の鉄を有効に利用し、また鉄欠乏条件下でも生存できるようにその形態や生理を変化させる能力を発達させてきた。光合成微生物の鉄欠乏ストレスに対する応答機構は古くから研究されてきたが、鉄輸送体遺伝子の同定はされていなかった。本研究はゲノムの全塩基配列が決定された単細胞性ラン藻 *Synechocystis* sp. strain PCC 6803 を用いて、逆遺伝学的手法により光合成微生物において初めて鉄輸送体遺伝子を同定し、また PCC 6803 の鉄輸送機構を分子レベルで解析したものである。

1. *Synechocystis* sp. strain PCC 6803 の輸送体遺伝子の機能解析

推定アミノ酸配列内に ATP 結合モチーフを持つ 32 個の輸送体遺伝子に着目し、各遺伝子の破壊株を作製してそれらの表現型の解析を試みた。種々の栄養素欠乏培地上での生育実験の結果から、*sll1878* (*futC*) を含む 4 つの遺伝子について機能を推定することができた。特に Δ*sll1878* 株は鉄欠乏培地上で生育が非常に抑えられたことから、この株を用いて野生株と三価鉄の輸送活性を比較したところ、明らかに三価鉄輸送活性が低下していた。以上の結果から *sll1878* (*futC*) が ABC 型の三価鉄輸送体の ATP 結合タンパク質サブユニットをコードしているであろうと考えられた。野生株において細胞を鉄欠乏処理することにより三価の鉄輸送活性が上昇することも示された。また、PCC 6803 の三価鉄輸送において光は必要でないことが示された。

2. *Synechocystis* sp. strain PCC 6803 の鉄輸送体遺伝子と鉄輸送機構

本ラン藻には、非光合成生物で同定された鉄輸送体の相同体遺伝子が多数存在する。PCC 6803 の鉄輸送機構においてこれら相同体遺伝子がどのような役割を持っているか解析するために、各遺伝子の破壊株を作製して、細胞の生育特性と鉄輸送活性を調べた。第 2 章で得られた Δ*sll1878* (Δ*futC*; M1) 株と同様な生育特性及び鉄輸送活性を示した変異株は、Δ*slr0327* (*futB*; M2)、Δ*sll1878*Δ*slr0327* (Δ*futC*Δ*futB*; M5)、Δ*slr1295*Δ*slr0513* (Δ*futA1*Δ*futA2*; M6) であった。この結果と推定アミノ酸配列の解析結果から、これら 4 つの遺伝子が単

一の三価鉄輸送体をコードしていると推定された。また、Δ*slr1392* (*feoB*; M10) 株は、生育特性は野生株と同じだがアスコルビン酸で化学的に還元した二価鉄の輸送活性が明らかに低下していることが示された。したがって PCC 6803 は二価鉄輸送体を持っており、*slr1392* (*feoB*) が膜貫通領域と ABC 領域を持つサブユニットをコードしていることが示された。また、*ssr2333* が *slr1392* (*feoB*) と共転写されることから、*E. coli* の *feoA* 遺伝子の相同体であろうと考えられた。これらの結果と RT-PCR 法による mRNA 発現パターンの解析から、本ラン藻は三価鉄輸送体 (Fut 輸送体) に加えて二価鉄輸送体 (Feo 輸送体) を持ち、Fut 輸送体は通常の BG-11 培地上で発現し、鉄欠乏ストレスによって発現量が増加すること、また Feo 輸送体は鉄欠乏ストレスに応答して発現することが示された。 さらに ATP 合成阻害剤を用いた実験から、どちらの鉄輸送体も ATP 加水分解エネルギーを必要とする ABC 型輸送体であることが示された。また、各種金属による輸送活性阻害実験から両輸送体はそれぞれ三価鉄あるいは二価鉄に対する親和性が高いことが示された。

3. 鉄輸送体タンパク質 FutA1 の鉄結合活性の解析

バクテリアの ABC 型輸送体は一般に基質結合タンパク質を必要とする。推定アミノ酸配列から *futA1/A2* が Fut 輸送体の鉄結合タンパク質サブユニットをコードすると推定された。そこで、リコンビナント FutA1 タンパク質 (rFutA1) を作製して分光学的手法により FutA1 の鉄結合活性を解析した。溶液中で鉄と結合した rFutA1 は波長 453 nm に吸収のピークを持つスペクトルを示し、鉄イオンと rFutA1 タンパク質がモル比 1 : 1 で結合することが示された。rFutA1 の鉄に対する会合定数はクエン酸を競合剤として用いた実験条件下でおよそ 1×10^{19} 程度と見積もられた。アミノ酸一次配列の比較から FutA1 および FutA2 は *H. influenzae* の鉄結合タンパク質 HitA とよく似た機構で鉄イオンを配位することが推定された。これらの結果から Fut 輸送体は Hit/Fbp ファミリーに属する高親和性のフリー鉄イオン輸送体であることが明らかになった。

培地中のクエン酸は細胞の鉄輸送活性および生育に複雑な影響を与えることが示された。これは PCC 6803 の鉄輸送機構において Fut 及び Feo 輸送体以外の他の因子の関与を示唆するものであり、更なる解析が必要とされた。

参考文献

Adams, M. D., and Oxender, D. L. (1989) Bacterial periiplasmic protein tertiary structures. J. Biol. Chem. **264**: 15739-15742.

Adhikari, P., Kirby, S. D., Nowalk, A. J., Veraldi, K. L., Schryvers, A. B., and Mietzner, T. A. (1995) Biochemical characterization of a *Haemophilus influenzae* periplasmic iron transport operon. J. Biol. Chem. **270**: 25142-25149.

Adhikari, P., Berish, S. A., Nowalk, A. J., Veraldi, K. L., Morse, S. A., and Mietzner, T. A. (1996) The *fbpABC* locus of *Neisseria gonorrhoeae* functions in the periplasm-to-cytosol transport of iron. J. Bacteriol. **178**: 2145-2149.

Agustin, V. (1992) Analysis of the gene encoding the RNA subunit of ribonuclease P from cyanobacteria. Nucleic Acids Res. **20**: 6331-6337.

Aiba, H., Adhya, S., and de Crombrugghe, B. (1981) Evidence for two functional gal promoters in intact *Escherichia coli* cells. J. Biol. Chem. **256**: 11905-11910.

Ames, G. F.-L. (1986) Bacterial periplasmic transport system: structure, mechanism, and evolution. Ann. Rev. Biochem. **55**: 397-425.

Ames, G. F.-L., and Lever, J. (1970) Components of histidine transport: Histidine-binding proteins and hisP protein. Proc. Natl. Acad. Sci. USA **66**: 1096-1103.

Anderson J. E., Sparling P. F., and Cornelissen C. N. (1994) Gonococcal transferrin-binding protein 2 facilitates but is not essential for transferrin utilization. J. Bacteriol. **176**: 3162-3170.

Angerer, A., Gaisser, S., and Braun, V. (1990) Nucleotide sequence of the *sfuA*, *sfuB*, and *sfuC* genes of *Serratia marcescens* suggest a periplasmic-binding-protein-dependent iron transport mechanism. J. Bacteriol. **172**: 572-578.

Badger, M. R., and Price, G. D. (1990) Carbon oxysulfide is an inhibitor of both CO_2 and HCO_3^- uptake in the cyanobacterium *Synechococcus* PCC7942. Plant Physiol. **94**: 35-39.

Bartsevich, V. V., and Pakrasi, H. B. (1995) Molecular identification of an ABC transporter complex for manganese: analysis of a cyanobacterial mutant strain impaired in the phtosynthetic oxygen evolution process. EMBO J. **14**: 1845-1853.

Bartsevich, V. V., and Pakrasi, H. B. (1996) Manganese transport in the

cyanobacterium *Synechocystis* sp. PCC 6803. J. Biol. Chem. **271**: 26057-26061.

Bartsevich, V. V., and Pakrasi, H. B. (1999) Membrane topology of MntB, the transmembrane protein component of an ABC transporter system for manganese in the cyanobacterium *Synechocystis* sp. strain PCC 6803. J. Bacteriol. **181**: 3591-3593.

Berger, E. A. (1973) Different mechanisms of energy coupling for the active transport of proline and glutamine in *Escherichia coli*. Proc. Natl. Acad. Sci. USA **70**: 1514-1518.

Berger, E. A., and Heppel, L. A. (1974) Different mechanisms of energy coupling for shock-sensitive and shock-resistant aminoacid permeases of *Escherichia coli*. J. Biol. Chem. **249**: 7747-7755.

Berish, S. A., Mietzner, T. A., Mayer, L. W., Genco, C. A., Holloway, B. P., and Morse, S. A. (1990) Molecular cloning and characterization of the structual gene for the major iron-regulated protein expressed by *Neisseria gonorrhoeae*. J. Exp. Med. **171**: 1535-1546.

Bishop, L., Agbayani, R., Ambudkar, S. V., Maloney, P. C., and Ames, G. F.-L. (1989) Reconstitution of a bacterial periplasmic permease in proteoliposomes and demonstration of ATP hydrolysis concomitant with transport. Proc. Natl. Acad. Sci. USA **86**: 6953-6957.

Bottin, H., and Lagoutte, B. (1992) Ferredoxin and flavodoxin from the cyanobacterium *Synechocystis* sp. strain PCC 6803. Biochim. Biophys. Acta **1101**: 48-56.

Boyer, G. L., Gillam, A. H., and Trick, C. (1987) Iron chelation and uptake, *In* The cyanobacteria (Fay, P., and Van Baalen, C., Eds.), pp.415-436, Elsevier, Amsterdam, The Netherlands.

Braun,,V., Gross, R., Koester, W., and Zimmermann, L. (1983) Plasmid and chromosomal mutants in the iron (III)-aerobactin transport system of *Escherichia coli*. Use of streptonigrin for selection. Mol. Gen. Genet. **192**: 131-139.

Brawn, V., Hantke, K., and Koester, W. (1998) Bacterial iron transport: mechanisms, genetics, and regulation. Metal ions in Biol. Sys. **35**: 67-145.

Briggs, L. M., Pecoraro, V. L., and McIntosh, L. (1990) Copper-induced expression,

cloning, and regulatory studies of the plastocyanin gene from the cyanobacterium *Synechocystis* sp. PCC 6803. Plant Mol. Biol. **15**: 633-642.

Bruns, C. M., Nowalk, A. J., Arvai, A. S., Mctigue, M. A., Vaughan, K. G., Mietzner, T. A., and McRee, D. E. (1997) Structure of *Haemophilus influenzae* Fe^{+3}-binding protein reveals convergent evolution within a superfamily. Nature Structural Biol. **4**: 919-924.

Butler, A. (1998) Acquisition and utilization of transition metal ions by marine organism. Science **281**: 207-210.

Chelly, J., and Kahn, A. (1994) RT-PCR and mRNA quantitation. *In* The polymerase chain reaction. (Mullis, K. B., Ferre', F., and Gibbs, R. A. Eds.), pp.97-109. Birkhauser, Boston.

Chen, C. Y., Berish, S. A., Morse, S. A., and Mietzner, T. A. (1993) The ferric iron-binding protein of pathogenic *Neisseria* spp. functions as a periplasmic transport protein in iron acquisition from human transferrin. Mol. Microbiol. **10**: 311-318.

Coulton, J. W., Mason,,P., and Allatt, D. D. (1987) *fhuC* and *fhuD* genes for iron (III)-ferrichrome transport into *Escherichia coli* K-12. J. Bacteriol. **169**: 3844-3849.

Coulton, J. W., Mason, P., and Dubow, M. S. (1983) Molecular cloning of the ferrichrome-iron receptor of *Escherichia coli* K-12. J. Bacteriol. **156**: 1315-1321.

Crichton, R. R. (1990) Proteins of iron storage and transport. Adv. Protein Chem. **40**: 281-365.

Crosa, J. H. (1989) Genetics and molecular biology of siderophore-mediated iron transport in bacteria. Microbiol. Rev. **53**: 517-530.

Dancis, A., Klausner, R. D., Hinnebusch, A. G., and Barriocanal, J. G. (1990) Genetic evidence that ferric reductase is required for iron uptake in *Saccharomyces cerevisiae*. Mol. Cell. Biol. **10**: 2294-2301.

Dean, D. A., Fikes, J. D., Gehring, K., Bassford, P. J., and Nikaido, H. (1989) Active transport of maltose in membrane vesicles obtained from *Escherichia coli* cells producing tethered maltose-binding protein. J. Bacteriol. **171**: 503-510.

De Lorenzo, V., Herrero, M., Giovannini, F., and Neillands, J. B. (1988) Fur (ferric uptake regulation) protein and CAP (catabolite-activator protein) modulate transcription of *fur* gene in *Escherichia coli*. Eur. J. Biochem. **173**: 537-546.

Ecker, D. J., and Emery, T. (1983) Iron uptake from ferrichrome A and iron citrate in *Ustilago sphaerogena*. J. Bacteriol. **155**: 616-622.

Elhai, J., and Wolk, C. P. (1988) A versatile class of positive-selection vectors based on the nonviability of palindrome-containing plasmid that allows cloning into long polylinkers. Gene **68**: 119-138.

Elkins, M. F., and Earhart, C. F. (1989) Nucleotide sequence and regulation of the *Escherichia coli* gene for ferrienterobactin transport protein FepB. J. Bacteriol. **171**: 5443-5451.

Flores, E., and Herrero, A. (1994) Assimilatory nitrogen metabolism and its regulation. *In* The molecular biology of cyanobacteria (Bryant, D. A. Ed.) pp.487-517. Kluwer, The Netherlands.

Frost, G. E., and Rosenberg, H. (1973) The inducible citrate-dependent iron transport system in *Escherichia coli* K12. Biochim. Biophys. Acta **330**: 90-101.

Gilis, A., Khan, M. A., Cornelis, P., Meyer, J. M., Mergeay, M., and van der Lelie, D. (1996) Siderophore-mediated iron uptake in *Alcaligenes eutrophus* CH34 and identification of *aleB* encoding the ferric iron-alcaligin E receptor. J. Bacteriol. **178**: 5499-5507.

Green, L. S., laudenbach, D. E., and Grossman, A. R. (1989) A region of a cyanobacterial genome required for sulfate transport. Proc. Natl. Acad. Sci. USA **86**: 1949-1953.

Grillo, J. F., and Gibson, J. (1979) Regulation of phosphate accumulation in the cyanobacterium *Synechococcus*. J. Bacteriol. **140**: 508-517.

Grossman, A. R., Schaefer, M. R., Chiang, G. G., and Collier, J. L. (1994) The response of cyanobacteria to enviromental condition: light and nutrients. *In* The molecular biology of cyanobacteria (Bryant, D. A. Ed.) pp.641-675. Kluwer, The Netherlands.

Guerinot, M. L., and Yi, Y. (1994) Iron: nutritious, noxious, and not readily available. Plant Physiol. **104**: 815-820.

Guikema, J. A., and Sherman, L. A. (1983) Organization and function of chlorophyll in membranes of cyanobacteria during iron starvation. Plant Physiol. **73**: 250-256.

Guikema, J. A. (1985) Fluorescence induction characteristics of *Ancystis nidulans*

during recovery from iron deficiency. J. Plant Nutr. **8**: 891-908.

Hantke, K. (1987) Ferrous iron transport mutants in *Escherichia coli* K12. FEMS Microbiol. Lett. **44**: 53-57.

Hegge, R., and Boos, W. (1983) Maltose and lactose transport in *Escherichia coli*. Examples of two different types of concentrative transport systems. Biochem. Biophys. Acta. **737**: 443-478.

Higgins, C. F. (1992) ABC transporeters; from microorganisms to man. Annu. Rev. Cell Biol. **8**: 67-113.

Higgins, C. F., Hiles, I. D., Whalley, K., and Jamieson, D. K. (1985) Nucleotide binding by membrane components of bacterial periplasmic binding protein-dependent transport systems. EMBO J. **4**: 1033-1040.

Higgins, C. F., Hyde, S. C., Mimmack, M. M., Gileadi, U., Gill, D. R., and Gallagher, M. P. (1990) Binding protein-dependent transport systems. J. Bioenerg. Biomemb. **22**: 571-592.

Hobson, A. C., Weatherwax, R., and Ames, G. F.-L. (1984) ATP-binding site in the membrane components of histidine permease, a periplasmic transport system. Proc. Natl. Acad. Sci. USA **81**: 7333-7337.

Holland, I. B., and Blight, M. A. (1999) ABC-ATPases, adaptable energy generators fuelling transmembrane movement of a variety of molecules in organisms from bacteria to humans. J. Mol. Biol. **293**: 381-399.

Hutber, G. N., Hutson, K. G., and Rogers, L. J. (1977) Effect of iron deficiency on levels of two ferredoxins and flavodoxins in a cyanobacterium. FEMS Microbiol. Lett. **1**: 193-196.

Irwin S. W., Averil, N., Cheng C. Y., Schryvers, A. B. (1993) Preparation and analysis of isogenic mutants in the transferrin receptor protein genes, *tbpA* and *tbpB*, from *Neisseria meningitidis*. Mol. Microbiol. **8**: 1125-1133.

Jeanjean, R., and Broda, E. (1977) Dependence of sulfate uptake by *Anacystis nidulans* on energy, on osmotic shock and on sulfate starvation. Arch. Microbiol. **114**: 19-23.

Kammler, M., Schon, C., and Hantke, K. (1993) Characterization of the ferrous iron uptake system of *Escherichia coli*. J. Bacteriol. **175**: 6212-6219.

Kaneko, T., Sato, S., Kotani, H., Tanaka, A., Asamizu, E., Nakamura, Y., Miyajima, N., Hirosawa, M., Sugiura, M., Sasamoto, S., Kimura, T., Hosouchi, T., Matsuno, A., Muraki, A., Nakazaki, N., Naruo, K., Okumura, S., Shimpo, S., Takeuchi, C., Wada, T., Watanabe, A., Yamada, M., Yasuda, M. and Tabata. S. (1996) Sequence analysis of the genome of the unicellular cyanobacterium *Synechocystis* sp. strain PCC6803. II. Sequence determination of the entire genome and assignment of potential protein-coding regions. DNA Res. **3**: 109-136.

Kaplan, A., Schwarz, R., Lieman-Hurwitz, J., and Reinhold, L. (1991) Physiological and molecular aspects of the inorganic carbon concentrating systems in unicellular cyanobacteria. Plant Physiol. **97**: 851-855.

Kuhn, S., Braun, V., and Koster, W. (1996) Ferric rhizoferrin uptake into *Morganella morganii*: characterization of genes involved in the uptake of a polyhydroxycarboxylate siderophore. J. Bacteriol. **178**: 496-504.

Laemmli, U. K. (1970) Cleavage of structural proteins during the assembly of the head of bacteriophage T4. Nature **227**: 680-685.

Laudenbach, D. E., Reith, M. E., and Straus, N. A. (1988) Isolation, sequence analysis, and transcriptional studies of the flavodoxin gene from *Anacystis nidulans* R2. J. Bacteriol. **170**: 258-264.

Laudenbach, D. E., and Grossman, A. R. (1991) Characterization and mutagenesis of sulfer-regulated genes in a cyanobacterium: evidence for function in sulfate transport. J. Bacterol. **173**: 2739-2750.

Lengeler, J. W., Titgemeyer, F., Vogler, A. P., and Wohrl, B. M. (1990) Structures and homologies of carbohydrate: phosphotransferase system (PTS) proteins. Philos. Trans. R. Soc. London Ser. B **326**: 489-504.

Linton, K. J., and Higgins, C. F. (1998) The *Escherichia coli* ATP-binding cassette (ABC) proteins. Mol. Microbiol. **28**: 5-13.

Mahasneh, I. A. (1991) Siderophore production in the Rivulariaceae, blue-green algae (cyanobacteria). Microbios. **65**: 97-103.

Montesinos, M. L., Herrero, A., and Flores, E. (1997) Amino acid transport in taxonomically diverse cyanobacteria and identification of two genes encoding

elements of a neutral amino acid permease putatively involved in recapture of leaked hydrophobic amino acids. J. Bacteriol. **179**: 853-862.

Nakai, K., and Kanehisa, M. (1991) Expert system for predicting protein localization sites in gram-negative bacteria. Proteins **11**: 95-110.

Neilands, J. B. (1995) Siderophores: structure and function of microbial iron transport compounds. J. Biol. Chem. **270**: 26723-26726.

Nowalk, A. J., Tencza, S. B., and Mietzner, T. A. (1994) Coordination of iron by the ferric iron-binding protein of pathogenic *Neisseria* is homologous to the transferrins. Biochemistry **33**: 12769-12775.

Ogawa, T., Miyano, A., and Inoue, Y. (1985) Photosystem-I-driven inorganic carbon transport in the cyanobacterium, *Anacystis nidulans*. Biochim. Biophys. Acta **808**: 77-84.

Omata, T. (1991) Cloning and characterization of the *nrtA* gene that encodes a 45 kDa protein involved in nitrate transport in the cyanobacterium *Synechococcus* PCC 7942. Plant Cell Physiol. **32**: 151-157.

Omata T., and Ogawa, T. (1986) Biosynthesis of a 42-kD polypeptide in the cytoplasmic membrane of the cyanobacterium *Anacystis nidulans* strain R2 during adaptation to low CO_2 concentration. Plant Physiol. **80**: 525-530.

Omata, T., Ogawa, T., Marcus, Y., Friedberg, D., and Kaplan, A. (1987) Adaptation to low CO_2 level in a mutant of *Anacystis nidulans* R_2 which requires high CO_2 for growth. Plant Physiol. **83**: 892-894.

Omata, T., Ohmori, M., Arai, N., and Ogawa, T. (1989) Genetically engineered mutant of the cyanobacterium *Synechococcus* PCC 7942 defective in nitrate transport. Proc. Natl. Acad. Sci. USA **86**: 6612-6616.

Omata, T., Andriesse, X., and Hirano, A. (1993) Identification and characterization of a gene cluster involved in nitrate transport in the cyanobacterium *Synechococcus* sp. PCC 7942. Mol. Gen. Genet. **236**: 193-202.

Omata, T., Price, G. D., Badger, M. R., Okamura, M., Gohta, S., and Ogawa, T. (1999) Identification of an ATP-binding cassette transporter involved in bicarbonate uptake in the cyanobacterium *Synechocystis* sp. strain PCC 7942. Proc. Natl. Acad. Sci. USA **96**: 13571-13576.

Oquist, G. (1974) Iron deficiency in the blue-green alga *Anacystis nidulans*: fluorescence and absorption spectra recorded at 77 K. Physiol. Plant **31**: 55-58.

Pakrasi, H. B., Riethman, H. C., and Sherman, L. A. (1985) Organization of pigment proteins in the Photosystem II complex of the cyanobacterium *Anacystis nidulans* R2. Proc. Natl. Acad. Sci. USA **82**: 6903-6907.

Pakrasi, H. B. (2000) personal communication.

Pollack, J. R., Ames, B. N., and Neilands, J. B. (1970) Iron transport in *Salmonella typhimurium*: mutants blocked in the biosynthesis of enterobactin. J. Bacteriol. **104**: 635-639.

Pressler, U., Staudenmaier, H., Zimmermann, L., and Braun, V. (1988) Genetics of the iron dicitrate transport system of *Escherichia coli*. J. Bacteriol. **170**: 2716-2724.

Rech, S., Deppenmeier, U., and Gunsalus, R. P. (1995) Regulation of the molybdate transport operon, *modABCD*, of *Escherichia coli* in response to molybdate availability. J. Bacteriol. **177**: 1023-1029.

Riethman, H. C., and Sherman, L. A. (1988) Purification and characterization of an iron stress-induced chlorophyll-protein from the cyanobacterium *Anacystis nidulans* R2. Biochim. Biophys. Acta **935**: 141-151.

Sambrook, J., Fritsch, E. F., and Maniatis, T. (1989) Molecular cloning: a laboratory manual, 2nd Ed., Cold Spring Harbor Laboratory, Cold Spring Harbor, NY.

Sanders, J. D., Cope, L. D., and Hansen, E. J. (1994) Identification of a locus involved in the utilization of iron by *Haemophilus influenzae*. Infect. Immun. **62**: 4515-4525.

Sandmann, G., Peleato, M. L., Fillat, M. F., Lazaro, M. C., and Gomez-Moreno, C. (1990) Consequences of iron-dependent formation of ferredoxin and flavodoxin on photosynthesis and nitrogen fixation on *Anabaena* strains. Photosynth. Res. **26**: 119-126.

Sauer, M., Hantke, K., and Braun, V. (1987) Ferric-coprogen receptor FhuE of *Escherichia coli*: processing and sequence common to all TonB-dependent outer membrane receptor proteins. J. Bacteriol. **169**: 2044-2049.

Scanlan, D. J., Mann, N. H., and Carr, N. G. (1989) Effect of iron and other nutrient

limitations in the cyanobacterium *Synechococcus* PCC 7942. Arch. Microbiol. **152**: 224-228.

Schaffer, S., Hantk, K., and Braun, V. (1985) Nucleotide sequence of the iron regulatory gene *fur*. Mol. Gen. Genet. **200**: 110-113.

Schmetterer, G. R. (1990) Sequence conservation among the glucose transporter from the cyanobacterium *Synechocystis* sp. PCC 6803 and mammalian glucose transporters. Plant Mol. Biol. **14**: 697-706

Schmidt, A., Erdle, I., and Koest, H.-P. (1982) Changes of c-phycocyanin in *Synechococcus* 6301 in relation to growth on various sulfur compounds. Z. Naturforsch **37c**: 870-876.

Sherman, D. M., and Sherman, L. A. (1983) Effect of iron deficiency and iron restoration on ultrastructure of *Anacystis nidulans*. J. Bacteriol. **156**: 393-401.

Silver, S., Nucifora, G., Chu, L., and Misra, T. K. (1989) Bacterial resistance ATPases: primary pumps for exporting toxic cations and anions. Trends Biochem. Sci. **14**: 76-80

Stanier, R. Y., Kunisawa, R., Mandel, M., and Cohen-Bazire, G. (1971) Purification and properties of unicellular blue-green algae (Order *Chroococcales*). Bacteriol. Rev. **35**: 171-205.

Staudenmaier, H., Van Hove, B., Yaraghi, Z., and Braun, V. (1989) Nucleotide sequences of the *fecBCDE* genes and locations of the proteins suggest a periplasmic-binding-protein-dependent transport mechanism for iron (III) dicitrate in *Escherichia coli*. J. Bacteriol. **171**: 2626-2633.

Straus, N. A. (1994) Iron deprivation: physiology and gene regulation. *In* The molecular biology of cyanobacteria. (Bryant, D. A. Ed.), pp.731-750. Kluwer, Dordrecht, The Netherlands.

Suzuki, I., Omata, T., and Sugiyama, T. (1992) Gene expression and regulation of nitrate assimilating enzymes in *Synechococcus* PCC7942. *In* Research in Photosynthesis, Vol. IV (Murata, N. Ed.) pp75-78. Kluwer, Dordrecht.

Tam, R., and Saier, J. M. H. (1993) Structural, functional, and evolutionary relationships among extracellular solute-binding receptors of bacteria. Microbiol. Rev. **57**: 320-346.

Thompson, J. D., Gibson, T. J., Plewniak, F., Jeanmougin, F., and Higgins, D. G. (1997) The CLUSTAL X windows interface: flexible strategies for multiple sequence alignment aided by quality analysis tolls. Nucleic Acids Res. **25**: 4876-4882.

Trick, C. G., and Kerry, A. (1992) Isolation and purification of siderophores produced by cyanobacteria, *Synechococcus* sp. strain PCC 7942 and *Anabaena variabilis* ATCC 29413. Curr. Microbiol. **24**: 241-245.

Utkilen, H. C., Heldal, M., and Knutsen, G. (1976) Characterization of sulfate uptake in *Anacystis nidulans*. Physiol. Plant **38**: 217-220.

Velayudhan, J., Hughes, N. J., McColm, A. A., Bagshaw, J., Clayton, C. L., Andrews, S. C., and Kelly, D. J. (2000) Iron acquisition and virulence in *Helicobactor pylori*: a major role for FeoB, a high-affinity ferrous iron transport. Mol. Microbiol. **37**: 274-286.

Walker, J. E., Saraste, M., Runswick, M. J., and Gay, N. J. (1982) Distantly related sequences in the alpha- and beta-subunits of ATP synthase, myosin, kinases and other ATP-requiring enzymes and a common nucleotide binding fold. EMBO J. **1**: 945-951.

Williams, J. G. K., and Szalay, A. A. (1983) Stable integration of foreign DNA into the chromosome of the cyanobacterium *Synechococcus* R2. Gene **24**: 37-51.

Yin, H. L., Iida, K., and Janmey, P. A. (1988) Identification of a polyphosphoinositide-modulated domain in gelsolin which binds to the sides of actin filaments. J. Cell Biol. **106**: 805-812.

謝辞

本研究を遂行するにあたり、終始御指導御鞭撻を賜りました名古屋大学生物分子応答研究センターの小川晃男教授に心より感謝致します。また、研究の過程で常に適切なご助言を頂きましたスタンフォード大学カーネギー研究所のArthur Grossman 博士、名古屋大学生物分子応答研究センターの上口智治助教授に厚く感謝致します。本論文を親しく御高覧頂きました岡崎国立共同研究機構基礎生物学研究所の村田紀夫教授に深くお礼申し上げます。個々の実験において御助力、御助言を頂きました園田雅俊博士、大河浩博士、多数のラン藻変異株を作製して頂いた萩野奈津氏に深く感謝致します。最後になりましたが生物分子応答研究センターでの職務を有意義なものにしてくれた環境応答統御講座の皆様、御理解を頂いた名古屋大学農学部技術部の皆様に心よりお礼申し上げます。

報文目録

1) Katoh, H., Grossman, A. R., Hagino, N., and Ogawa, T. (2000)

A Gene of *Synechocystis* sp. Strain PCC 6803 Encoding a Novel Iron Transporter.

J. Bacteriol. 182: 6523-6524.

2) Katoh, H., Hagino, N., Grossman, A. R., and Ogawa, T. (2001)

Genes Essential to Iron Transport in the Cyanobacterium *Synechocystis* sp. Strain PCC 6803.

J. Bacteriol. 183: 2779-2784.

3) Katoh, H., Hagino, N., and Ogawa, T. (2001)

Iron-Binding Activity of FutA1 Subunit of an ABC-type Iron Transporter in the Cyanobacterium *Synechocystis* sp. Strain PCC 6803.

Plant Cell Physiol. 42: 823-827.

参考論文目録

1) Katoh, A., Sonoda, M., Katoh, H., and Ogawa, T. (1996)

Absence of Light-Induced Proton Extrusion in a *cotA*-Less Mutant of *Synechocystis* sp. Strain PCC6803.

J. Bacteriol. 178: 5452-5455.

2) Sonoda, M., Kitano, K., Katoh, A., Katoh, H., Ohkawa, H., and Ogawa, T. (1997)

Size of *cotA* and Identification of the Gene Product in *Synechocystis* sp. Strain PCC6803.

J. Bacteriol. 179: 3845-3850.

3) Sonoda, M., Katoh, H., Ohkawa, H., and Ogawa, T. (1997)

Cloning of the *cotA* gene of *Synechococcus* PCC7942 and complementation of a *cotA*-less mutant of *Synechocystis* PCC6803 with chimeric genes of the two strains.

Photosynth. Res. 54: 99-105.

4) Sonoda, M., Katoh, H., Vermaas, V., and Ogawa, T. (1998)

CEMA HOMOLOGUE IN CYANOBACTERIA (PXCA) INVOLVED IN PROTON EXCHANGE.

Photosynthesis: Mechanisms and Effects, Vol. V, (Garab, G. Ed.) 3675-3678. Kluwer, The Netherlands.

5) Sonoda, M., Katoh, H., Vermaas, V., Schmetterer, G., and Ogawa, T. (1998)

Photosynthetic Electron Transport Involved in PxcA-Dependent Proton Extrusion in *Synechocystis* sp. strain PCC6803: Effect of *pxcA* Inactivation on CO_2, HCO_3^-, and NO_3^- Uptake.

J. Bacteriol. 180: 3799-3803.

6) Ohkawa, H., Sonoda, M., Katoh, H., and Ogawa, T. (1998)

The use of mutants in the analysis of the CO_2-concentrating mechanism in cyanobacteria.

Can. J. Bot. 76: 1035-1042.

7) Sonoda, M., Katoh, H., Ohkawa, H., Vermaas, W., and Ogawa, T. (1999)

STRUCTURE AND FUNCTION OF CEMA HOMOLOGUE (PXCA) IN CYANOBACTERIA.

The Chloroplast: From Molecular Biology to Biotechnology, (Argyroudi-Akoyunoglou, J. H., and Senger, H., Eds.) 149-154. Kluwer, The Netherlands.

JOURNAL OF BACTERIOLOGY, Nov. 2000, p. 6523–6524 Vol. 182, No. 22
0021-9193/00/$04.00+0

A Gene of *Synechocystis* sp. Strain PCC 6803 Encoding a Novel Iron Transporter

HIROKAZU KATOH,[1] ARTHUR R. GROSSMAN,[2] NATSU HAGINO,[1] AND TERUO OGAWA[1]*

Bioscience Center, Nagoya University, Chikusa, Nagoya 464-8601, Japan,[1] and Department of Plant Biology, Carnegie Institution of Washington, Stanford, California 94305[2]

Received 15 May 2000/Accepted 24 August 2000

A mutant of *Synechocystis* sp. strain PCC 6803 disrupted for *sll1878* exhibited greatly reduced Fe^{3+} transport activity. The K_m value of *sll1878*-dependent Fe^{3+} transport in cells grown in iron-replete medium was 0.5 μM. Both the maximal rate and K_m value were increased in iron-starved cells.

While the iron concentration in terrestrial environments is high, the biological availability of this element can be very low, since under aqueous, oxygenic conditions, iron is present as Fe^{3+} (ferric iron), which forms insoluble hydroxides. To promote the acquisition of this element, many bacteria produce extracellular, iron-specific chelators known as siderophores (2, 3, 5, 8). Iron chelation and uptake by cyanobacteria have been reviewed by Boyer et al. (2). The *Synechocystis* sp. strain PCC 6803 genome contains 32 genes that potentially code for nucleotide-binding components of ATP-binding cassette transporters that have no other strong similarity to functionally identified transport polypeptides (6). To determine which of these genes is involved in iron transport, we have analyzed the growth and iron uptake of *Synechocystis* strains in which these putative transport genes have been disrupted. The results suggest that the protein encoded by *sll1878* is a novel iron transporter.

Cells were grown in BG-11 medium (7) buffered by 20 mM *N*-Tris(hydroxymethyl) methyl-2-aminoethanesulfonic acid (TES)–KOH at pH 8.0 under 3% CO_2 in air (vol/vol). To make iron-free BG-11, $MgSO_4$ was replaced by K_2SO_4 and the citric acid, ferric ammonium dicitrate, $CaCl_2$, and trace elements were not initially added to the medium. The medium was treated with Chelex 100 resin (Bio-Rad, Hercules, Calif.) and then supplemented with trace elements and ultrapure $MgCl_2$ and $CaCl_2$ (Ultrapure Chemicals Co., Saitama, Japan). To starve *Synechocystis* for iron, cells were grown in normal BG-11 medium, washed by 20 mM TES-KOH (pH 8.0), and then grown in fresh iron-free BG-11 overnight under continuous illumination with fluorescent lamps at 60 $\mu E\ m^{-2}s^{-1}$.

The mutant lacking *sll1878* (designated M-1) constructed in this study has been deposited in the web site "CyanoMutants" (http://www.kazusa.or.jp/ cyano/mutants/), where the site of insertion of the kanamycin resistance cassette is shown. The wild-type and mutant cells before and after iron starvation were washed with 20 mM TES–KOH buffer and resuspended in fresh iron-free BG-11 at 2×10^9 cells/ml. $^{59}FeCl_3$ solution was added to iron-free BG-11 medium supplemented with various concentrations of cold $FeCl_3$. An aliquot (250 μl) of this solution was mixed with an equal volume of cell suspension in the presence of 1 mM ferrozine (Sigma Chemical Co., St. Louis, Mo.) and incubated at 30°C, either in the dark or light (at 700 $\mu E\ m^{-2}\ s^{-1}$). Uptake was terminated by centrifugation, and the pellet was washed twice with 20 mM Tes–KOH containing 10 mM EDTA before being analyzed for the incorporation of $^{59}FeCl_3$.

Out of 32 *Synechocystis* genes encoding nucleotide binding components of ATP-binding cassette transporters that have not been ascribed any function, we were able to construct 24 separate mutants by inactivating the transporter genes but were unable to attain complete disruption of the remaining 8 genes (*sll0759*, *sll0912*, *sll1276*, *sll1623*, *slr0075*, *slr0251*, *slr0354*, and *slr1735*). All of the mutants except for the one lacking *sll1878* (M-1) grew as well as the wild type on solid, iron-free BG-11 medium, probably utilizing iron that contaminates the iron-free medium or that is carried over from the cell cultures used for the initial inoculum. Wild-type cells grew at a maximal rate at 1 μM Fe^{3+}, while the M-1 mutant grew more slowly at this Fe^{3+} concentration.

The slow growth of the M-1 mutant in iron-free medium was ascribed to a defect in iron acquisition. We assayed the wild-type and mutant strains for the rate of Fe^{3+} transport using $^{59}FeCl_3$ in the presence of ferrozine (inhibits Fe^{2+} transport) (4). Figure 1A shows time courses of $^{59}Fe^{3+}$ accumulation by iron-deprived wild-type and M-1 mutant cells incubated with 10 μM $^{59}FeCl_3$ in the light or dark. The Fe^{3+} uptake proceeded in the dark; light did not have a stimulatory effect on the accumulation of iron over at least a 30-min period. Hence, respiration and other dark metabolic reactions must generate a sufficient supply of ATP to energize Fe^{3+} transport. This is in contrast to the transport of other ions such as Mn^{2+} that is light dependent (1). Since the amount of Mn^{2+} taken up by *Synechocystis* strain PCC 6803 cells is not more than that of Fe^{3+}, it might be expected that ATP produced in the dark would be sufficient to drive Mn^{2+} uptake. However, Mn^{2+} uptake may be linked to immediate incorporation of the cation into protein(s), a process that might be light dependent.

Figure 1B shows uptake of Fe^{3+} by wild-type and M-1 mutant cells grown in nutrient-replete medium (upper panel) or by iron-deprived cells (lower panel). The cells were incubated for 5 min in the dark with various concentrations of $FeCl_3$ in the presence of 1 mM ferrozine. Fe^{3+} uptake by the M-1 strain was about one-fifth that of wild-type cells. Fe^{3+} transport activity increased more than fivefold in wild-type cells and two to three times in the M-1 mutant following iron deprivation. The low-level Fe^{3+} transport activity retained in the M-1 mutant suggests the presence of additional Fe^{3+} transporter(s). The difference between the two curves a-b and c-d approximates the activity of the *sll1878*-dependent Fe^{3+} transport. The K_m and V_{max} values for *sll1878*-dependent Fe^{3+} transport, deter-

* Corresponding author. Mailing address: Bioscience Center, Nagoya University, Chikusa, Nagoya 464-8601, Japan. Phone: 81-52-789-5215. Fax: 81-52-789-5214. E-mail: h44975a@nucc.cc.nagoya-u.ac.jp.

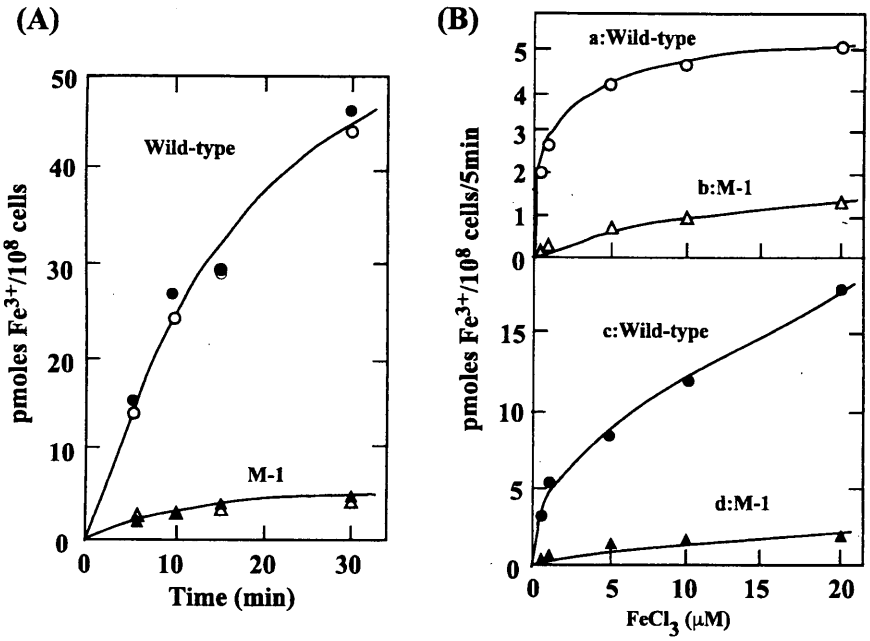

FIG. 1. (A) Time course of $^{59}Fe^{3+}$ uptake by iron-deprived wild-type and M-1 cells, either in the dark (filled symbols) or in the light (open symbols). The concentration of $^{59}FeCl_3$ was 10 μM. (B) Concentration-dependent uptake of $^{59}Fe^{3+}$ by wild-type and M-1 cells grown in complete medium (curves a and b in upper panel) or by iron-deprived cells (curves c and d in lower panel) during a 5-min incubation in the dark.

mined by plotting the reciprocals of curve a-b and curve c-d against the reciprocals of the substrate concentration were 0.5 μM and 3.9 pmol/10^8 cells/5 min, respectively, in the cells grown in nutrient-replete medium and 2.5 μM and 25 pmol/10^8 cells/5 min, respectively, in the iron-deprived cells. Thus, the activity of the *sll1878*-dependent Fe^{3+} transport increased about sixfold after iron deprivation treatment. The affinity of the transporter for the substrate decreased fivefold in the iron-deprived cells.

The product of *sll1878* appears to be a peripheral membrane protein. No citrate is required for *sll1878*-dependent Fe^{3+} uptake, demonstrating that the citrate-iron chelate is not the substrate for this transporter. However, the substrate may be a complex between ferric iron and siderophores produced by *Synechocystis* in response to iron deprivation.

This work was supported by a grant, JPSP-RFTF96L00105, from the Japan Society for the Promotion of Science and a grant from the Human Frontier Science Program to T.O. and by National Science Foundation grant MCB 9727836 to A.R.G.

REFERENCES

1. **Bartsevich, V. V., and H. B. Pakrasi.** 1996. Manganese transport in the cyanobacterium *Synechocystis* sp. PCC 6803. J. Biol. Chem. **271:**26057–26061.
2. **Boyer, G. L., A. H. Gillam, and C. Trick.** 1987. Iron chelation and uptake, p. 415–436. *In* P. Fay and C. Van Baalen (ed.), The cyanobacteria. Elsevier, Amsterdam, The Netherlands.
3. **Braun, V., K. Hantke, and W. Koester.** 1998. Bacterial iron transport: mechanisms, genetics, and regulation. Metal Ions Biol. Sys. **35:**67–145.
4. **Ecker, D. J., and T. Emery.** 1983. Iron uptake from ferrichrome A and iron citrate in *Ustilago sphaerogena*. J. Bacteriol. **155:**616–622.
5. **Guerinot, M. L.** 1994. Microbial iron transport, Annu. Rev. Microbiol. **48:** 743–772.
6. **Kaneko, T., S. Sato, H. Kotani, A. Tanaka, E. Asamizu, Y. Nakamura, N. Miyajima, M. Hirosawa, M. Sugiura, S. Sasamoto, T. Kimura, T. Hosouchi, A. Matsuno, A. Muraki, N. Nakazaki, K. Naruo, S. Okumura, S. Shimpo, C. Takeuchi, T. Wada, A. Watanabe, M. Yamada, M. Yasuda, and S. Tabata.** 1996. Sequence analysis of the genome of the unicellular cyanobacterium *Synechocystis* sp. strain PCC6803. II. Sequence determination of the entire genome and assignment of potential protein-coding regions. DNA Res. **3:**109–136.
7. **Stanier, R. Y., R. Kunisawa, M. Mandel, and G. Cohen-Bazire.** 1971. Purification and properties of unicellular blue-green algae (order *Chroococcales*). Bacteriol. Rev. **35:**171–205.
8. **Straus, N. A.** 1994. Iron deprivation: physiology and gene regulation, p. 731–750. *In* D. A. Bryant (ed.), The molecular biology of cyanobacteria. Kluwer, Dordrecht, The Netherlands.

JOURNAL OF BACTERIOLOGY, May. 2001, p. 2779–2784
0021-9193/01/$04.00+0 DOI: 10.1128/JB.183.9.2779–2784.2001

Vol. 183, No. 9

Genes Essential to Iron Transport in the Cyanobacterium *Synechocystis* sp. Strain PCC 6803

HIROKAZU KATOH,[1] NATSU HAGINO,[1] ARTHUR R. GROSSMAN,[2] AND TERUO OGAWA[1]*

Bioscience Center, Nagoya University, Chikusa, Nagoya 464-8601, Japan,[1] and Department of Plant Biology, Carnegie Institution of Washington, Stanford, California 94305[2]

Received 4 December 2000/Accepted 1 February 2001

Genes encoding polypeptides of an ATP binding cassette (ABC)-type ferric iron transporter that plays a major role in iron acquisition in *Synechocystis* sp. strain PCC 6803 were identified. These genes are *slr1295*, *slr0513*, *slr0327*, and recently reported *sll1878* (Katoh et al., J. Bacteriol. 182:6523–6524, 2000) and were designated *futA1*, *futA2*, *futB*, and *futC*, respectively, for their involvement in ferric iron uptake. Inactivation of these genes individually or *futA1* and *futA2* together greatly reduced the activity of ferric iron uptake in cells grown in complete medium or iron-deprived medium. All the *fut* genes are expressed in cells grown in complete medium, and expression was enhanced by iron starvation. The *futA1* and *futA2* genes appear to encode periplasmic proteins that play a redundant role in iron binding. The deduced products of *futB* and *futC* genes contain nucleotide-binding motifs and belong to the ABC transporter family of inner-membrane-bound and membrane-associated proteins, respectively. These results and sequence similarities among the four genes suggest that the Fut system is related to the Sfu/Fbp family of iron transporters. Inactivation of *slr1392*, a homologue of *feoB* in *Escherichia coli*, greatly reduced the activity of ferrous iron transport. This system is induced by intracellular low iron concentrations that are achieved in cells exposed to iron-free medium or in the *fut*-less mutants grown in complete medium.

Iron serves as an essential component of heme and iron sulfur centers integrated into a variety of proteins that function in basic physiological processes such as photosynthesis, respiration, and nitrogen metabolism (23). In the Earth's crust, iron is the fourth-most-abundant element. However, the biological availability of iron is severely reduced since in an aqueous oxygenic environment ferrous iron is quickly oxidized to ferric iron, which forms insoluble hydroxides at physiological pH (5, 6). Organisms have developed mainly two sophisticated systems for iron acquisition. One involves utilization of iron-chelating compounds including various siderophores and transport of chelated iron. The other system involves reduction of ferric iron to ferrous iron by a plasma membrane redox system, followed by uptake using specific transporters (11, 18).

Molecular analysis of iron transport systems has been carried out mostly on nonphotosynthetic bacteria (6). *Escherichia coli* has specific receptor proteins in the outer membrane that bind ferrichrome (FhuA), ferric aerobactin (IutA), ferric coprogen or ferric rhodotorulate (FhuE), and ferric dicitrate (FecA). FhuA, FhuE, and IutA are components of siderophore-mediated iron transport systems that involve typical ATP binding cassette (ABC)-type transporters consisting of a periplasmic iron-binding protein (FhuD) and cytoplasmic membrane proteins (FhuB and FhuC) (7). Ferric dicitrate is taken up via an ABC transporter system that consists of FecA to -E (22). *E. coli* also has a ferrous iron transport system consisting of polypeptides encoded by the *feoA*, *-B*, and *-C* genes. The product of the *feoB* gene has a typical ATP-binding motif at the N-terminal end. Mutants defective in *feoA* or *feoB* showed strongly reduced ferrous iron uptake activity (12). Transport systems for iron delivered as transferrin and lactoferrin, such as Sfu and Fbp systems in *Serratia marcescens* (3) and *Neisseria gonorrhoeae* (4), have been found in other bacteria. In these systems, ferric ion is transported across the inner membrane. The Sfu proteins constitute a typical ABC transporter in which SfuA is localized in the periplasm, SfuB is a cytoplasmic membrane protein, and SfuC is a membrane-bound protein carrying a nucleotide-binding motif.

In spite of these studies on nonphotosynthetic bacteria, little is known about the molecular mechanism of iron transport in photoautotrophic bacteria. We have recently demonstrated that one gene, registered as *sll1878* in CyanoBase (http://www.kazusa.or.jp/cyano/), plays an important role in iron uptake in the cyanobacterium *Synechocystis* sp. strain PCC 6803 (14). The whole-genome sequence revealed that *Synechocystis* has 15 open reading frames (ORFs) whose putative products show high similarity with components of iron transporters identified in other bacteria (13). In order to understand the molecular mechanism of iron acquisition in *Synechocystis*, we have constructed mutants by disrupting these ORFs. Analysis of the mutants for growth and iron uptake both in nutrient-sufficient and iron-deprived conditions enabled us to identify the genes essential to ferric and ferrous iron transport.

MATERIALS AND METHODS

Growth conditions. Wild-type and mutant cells of *Synechocystis* sp. strain PCC 6803 were grown at 30°C in BG-11 medium (21) buffered with 20 mM *N*-tris(hydroxymethyl)methyl-2-aminoethanesulfonic acid (TES)–KOH at pH 8.0. Cultures were aerated with 3% (vol/vol) CO_2 in air. Iron-free BG-11 medium was prepared as described previously (14). In order to simplify the assay system, sodium citrate, the ferric iron chelator, was omitted in iron-free BG-11 medium. To starve *Synechocystis* cells for iron, wild-type and mutant strains were grown in BG-11 medium, collected by centrifugation (1,600 × *g*, 8 min), and washed by resuspension in 20 mM TES-KOH buffer treated with Chelex 100 resin (Bio-

* Corresponding author. Mailing address: Bioscience Center, Nagoya University, Chikusa, Nagoya 464-8601, Japan. Phone: 81-52 789-5215. Fax: 81-52-789-5214. E-mail: h44975a@nucc.cc.nagoya-u.ac.jp.

TABLE 1. Regions of ORFs amplified by the RT-PCR method or replaced by drug resistance cassettes in the mutant strains

ORF	Position[c] of:		Drug[d]	Mutant strain
	RT-PCR product[a]	Deleted region[b]		
sll1206	28–368	444–458	Kanamycin	M9
sll1406	24–387	533–583	Chloramphenicol	M9
sll1409	73–439	581–719	Hygromycin	M9
slr1490	55–418	418–563	Spectinomycin	M9
sll1202	84–480	454–500	Hygromycin	M8
slr0513	60–483	448–530	Kanamycin	M4 or M6
slr1295	20–427	317–373	Chloramphenicol	M3 or M6
slr1319	66–441	473–477	Kanamycin	M8
slr1491	81–435	481–511	Chloramphenicol	M8
slr1492	15–395	166[e]	Spectinomycin	M8
sll1878	32–400	134–479	Kanamycin	M1 or M5
slr0327	75–434	538–573	Spectinomycin	M2 or M5
slr1318	69–422	70–518	Spectinomycin	M7
slr1392	79–430	485–553	Hygromycin	M10

[a] Regions amplified by RT-PCR (from Fig. 2).
[b] Regions replaced by drug resistance cassettes.
[c] Positions of nucleotides are counted from the first nucleotide of the initiation codon.
[d] Drug to which the cassette confers resistance.
[e] Position at which cassette was inserted.

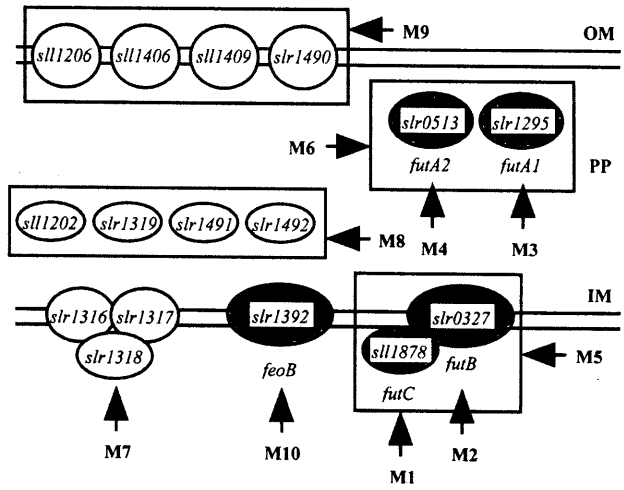

FIG. 1. Mutants constructed by inactivating genes presumably involved in iron acquisition and the possible localization of the gene products. Open ovals, gene products that are positioned based on the localization of their homologues in nonphotosynthetic bacteria; shaded ovals, putative proteins that were experimentally shown to function in iron transport. For details see the text. Vertical arrows, genes that were individually inactivated; horizontal arrows, groups of genes (boxed) that were inactivated in a single strain. OM, outer membrane; PP, periplasmic space; IM, inner membrane.

Rad, Hercules, Calif.) at pH 8.0. After a second wash, cells were resuspended in fresh iron-free BG-11 medium. In order to deplete trace iron in the medium and in the cells (iron deprivation treatment), culture was continued for 18 h under continuous illumination of photosynthetically active radiation at 60 μmol of photons m^{-2} s^{-1} (400 to 700 nm).

Analysis of gene expression. The amount of transcripts was evaluated by the reverse transcription-PCR (RT-PCR) method (8). RNAs were extracted from *Synechocystis* sp. strain PCC 6803 cells cultured in normal or iron-free BG-11 medium by the method of Aiba et al. (2), treated with RNase-free DNase I (Boehringer Mannheim), and then purified by phenol-chloroform extraction and ethanol precipitation. The RT reaction was performed using Superscript II (Gibco BRL) and reverse primers. The products were amplified by PCR and then analyzed by electrophoresis on a 0.8% agarose gel. Primers were designed so that the amplified products would be internal to the coding region of the gene. All the forward primers were designed for the sequences downstream of the translation initiation codon, and the reverse primers were designed to obtain PCR products of about 350 bp. The regions amplified by RT-PCR are summarized in Table 1 as base numbers counted from the initiation codons. The RNase P gene was used as a control template (1).

Construction of mutants. Two DNA fragments from different regions in a given *Synechocystis* sp. strain PCC 6803 gene, each containing 500- to 700-bp nucleotides, were amplified by PCR. The primers used for the amplification contained different restriction endonuclease sites and an additional three nucleotides at their proximal ends for recognition of specific endonucleases. These sites were chosen based on sites present at both ends of the drug resistance marker gene used for constructing the gene disruption. Following digestion of the PCR products with appropriate endonucleases, the products were ligated to a cartridge carrying the drug resistance marker gene and to the pGEM-T vector (Promega, Madison, Wis.). The vector harboring the drug resistance cassette flanked by the PCR products on each side was amplified in *E. coli* and then transformed (26) into wild-type *Synechocystis* sp. strain PCC 6803 cells. The mutants constructed in this study have been deposited in website CyanoMutants (http://www.kazusa.or.jp/cyano/mutants/). The drug resistance cassette used for each inactivation and the sites of insertion into the target gene are shown in Table 1. The disrupted target gene in the transformants was segregated to homogeneity by successive streak purifications as determined by PCR amplification.

Determination of growth characteristics. Iron-deprived wild-type and mutant cells were collected by centrifugation and resuspended in fresh iron-free BG-11 medium to optical densities at 730 nm (OD_{730}) of 0.1, 0.01, and 0.001. The OD_{730} of the cell culture was determined using a recording spectrophotometer (model UV2200; Shimadzu Co., Kyoto, Japan). Two microliters of each of the cell suspensions was spotted onto normal or iron-free BG-11 agar plates. The plates were incubated in 3% (vol/vol) CO_2 in air for 7 days with continuous illumination by fluorescent lamps providing photosynthetically active radiation at 60 μmol of photons m^{-2} s^{-1}.

Measurements of ferric and ferrous iron uptake. The amounts of iron taken up by wild-type and mutant cells were measured using radioactive tracer $^{59}FeCl_3$ (Amersham Pharmacia Biotech, Buckinghamshire, United Kingdom) as previously described (14). Ferric iron uptake was measured in the presence of 1 mM Ferrozine, which inhibits ferrous iron uptake (9). Uptake of ferrous iron was measured in the presence of 5 mM ascorbate, which reduces Fe^{3+} to Fe^{2+} (12). The uptake reaction was terminated by transferring the reaction mixture on ice, followed by centrifugation at 4°C. The pellet was washed twice with 20 mM TES-KOH (pH 8.0) containing 10 mM EDTA before being analyzed for the incorporation of ^{59}Fe. The gamma emission from ^{59}Fe in the cells was measured by the Auto Well gamma system (model ARC-380; Aloka, Tokyo, Japan). Cells at the late logarithmic stage of growth (OD_{730} = 1.0 to 1.3) were used for the iron uptake measurements. The concentration of $FeCl_3$ in the uptake reaction solution was fixed at 10 μM, and the uptake reaction was performed with continuous light illumination. The light source was from a 600-W halogen lamp (Cabin Co., Tokyo, Japan), and the intensity of photosynthetically active radiation was 700 μmol of photons m^{-2} s^{-1} (400 to 700 nm)

Other methods. Unless otherwise stated, standard techniques were used for DNA manipulation (19).

RESULTS

Location of gene products and genes inactivated in the mutants. The whole-genome sequence of *Synechocystis* sp. strain PCC 6803 revealed the presence of 15 genes that are homologous to iron transporter genes identified in various nonphotosynthetic organisms (13). In addition, we have recently demonstrated that *sll1878*, whose putative product shows sequence similarity to HitC of an Sfu/Fbp-type ferric ion transporter in *Haemophilus influenzae*, plays an essential role in ferric iron transport (14, 20). Figure 1 depicts the possible locations of the products of these genes in cells, as predicted from the locations of their homologues. Sll1406, Sll1409, Slr1490, and Sll1206 are homologous to FhuA of *E. coli* (7) and IutA of *Alcaligenes eutrophus* (10), which are located in the outer membrane.

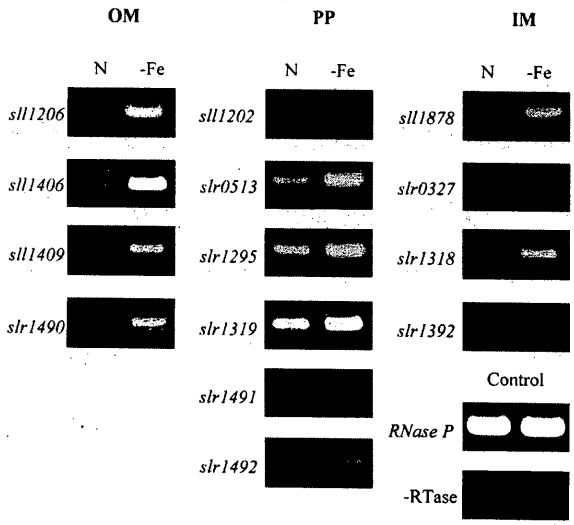

FIG. 2. Expression profiles of putative iron transporter genes in *Synechocystis* sp. strain PCC 6803. The amounts of transcripts in cells grown in normal BG-11 medium (lanes N) or in iron-free BG-11 medium (lanes -Fe) were determined by the RT-PCR method. The regions of the genes amplified are summarized in Table 1. OM, PP, and IM are as indicated in Fig. 1. Absence of contamination of DNA was confirmed by performing the RT reaction without reverse transcriptase (-RTase) followed by PCR.

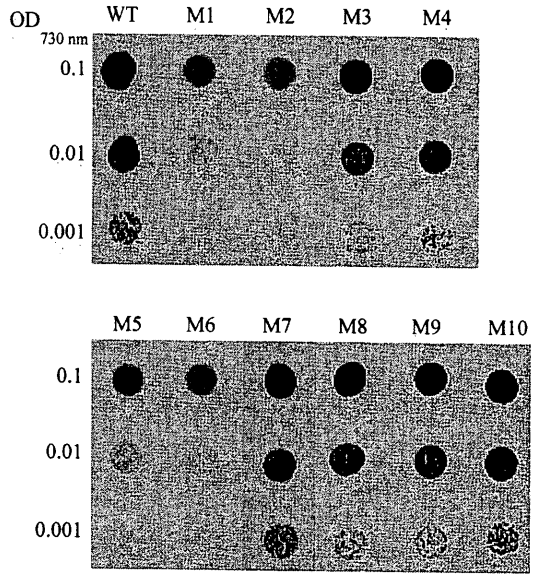

FIG. 3. Growth of the wild type and mutants on solid iron-free BG-11 medium. Wild-type (WT) and mutant (M1 to M10 [Fig. 1]) cells of *Synechocystis* were pelleted by centrifugation and resuspended in iron-free BG-11 medium at pH 8.0. Two microliters each of cell suspensions, with OD_{730} values of 0.1, 0.01, and 0.001, were spotted on agar plates containing iron-free BG-11 buffered at pH 8.0, and the plates were incubated under 3% (vol/vol) CO_2 in air for 7 days.

Sll1202, Slr1491, Slr1492, and Slr1319 showed similarities with FhuD and FecB of *E. coli* (7, 22). Slr0513 (FutA2) and Slr1295 (FutA1) are homologous to SfuA of *S. marcescens* (3). These homologues are the substrate-binding proteins located in the periplasmic space. Slr1316 and Slr1317 showed similarities with FecC and FecD (22). Slr0327 (FutB) is homologous to HitB of *H. influenzae* (20). FecC and FecD are the inner membrane subunits of an ABC transporter that moves iron(III) dicitrate across the cytoplasmic membrane, and HitB is the inner membrane subunit of an Sfu/Fbp-type ferric ion transporter. Slr1392 showed similarity with FeoB of *E. coli*, which functions in ferrous iron transport (12). Figure 1 shows genes that were individually inactivated and groups of genes that were inactivated in a single strain. In all, 10 mutant strains (M1 to M10) were analyzed for their growth and iron uptake characteristics.

In this paper, *slr1295, sl0513, slr0327*, and *sll1878* are designated *futA1, futA2, futB*, and *futC*, respectively, for ferric iron uptake based on their functions as demonstrated below.

Expression of genes putatively involved in iron acquisition. Figure 2 shows the levels of transcripts of 14 genes listed in Table 1 in wild-type cells grown in normal BG-11 medium and in iron deprived medium, as determined by the RT-PCR method. All four genes (*sll1206, sll1406, sll1409*, and *slr1490*) presumed to encode outer membrane receptor proteins were strongly expressed in iron-deprived cells. The *slr1295* (*futA1*), *slr0513* (*futA2*), and *slr1319* genes encoding putative substrate-binding proteins were expressed at high levels in both iron-replete and iron-deprived cells, with the levels of transcripts higher in iron-deprived cells. The *sll1878* (*futC*) and *slr0327* (*futB*) genes were also expressed constitutively in iron-replete cells. The amounts of transcripts of *sll1202, slr1491*, and *slr1492* were small, even in iron-deprived cells. The transcripts of *slr1318* and *slr1392* (*feoB*) were detected only in iron-deprived cells.

Growth characteristics. In a previous report, we showed that the *futC*-inactivated mutant (M1) grew much slower than the wild type on iron-free BG-11 agar plates (14). This was confirmed in this study (lanes M1 and WT in Fig. 3). The M2, M5, and M6 mutants showed growth characteristics similar to those of M1 and grew very poorly on iron-free plates, while all other mutants grew as well as the wild type under these conditions (Fig. 3). The growth of the M1, M2, M5, and M6 mutants appeared to be slower than that of the wild type on normal BG-11 plates, but the difference was not significant (not shown). The growth of the double mutant lacking *futB* and *futC* (M5) was similar to that of the single mutants (M1 and M2) in which these genes were individually inactivated. This suggested that *futB* and *futC* encode subunit polypeptides of a single transporter. The double mutant (M6), in which both *futA1* and *futA2* encoding putative substrate-binding proteins were inactivated, showed growth characteristics like those of the M1 strain, while single mutants M3 and M4, in which either of these genes was inactivated, grew as well as the wild type on the same iron-free medium. These results suggest that FutA1 and FutA2 are subunit proteins of an ABC transporter essential to iron acquisition in *Synechocystis* and that they have redundant or overlapping substrate-binding functions. These putative periplasmic iron-binding proteins may function in conjunction with FutB and FutC in the iron transporter complex. The M7, M8, M9, and M10 mutants showed wild-type growth characteristics under both normal and iron-free conditions. Thus, none of the genes inactivated in these mutants play a significant role in iron acquisition in wild-type cells under these conditions.

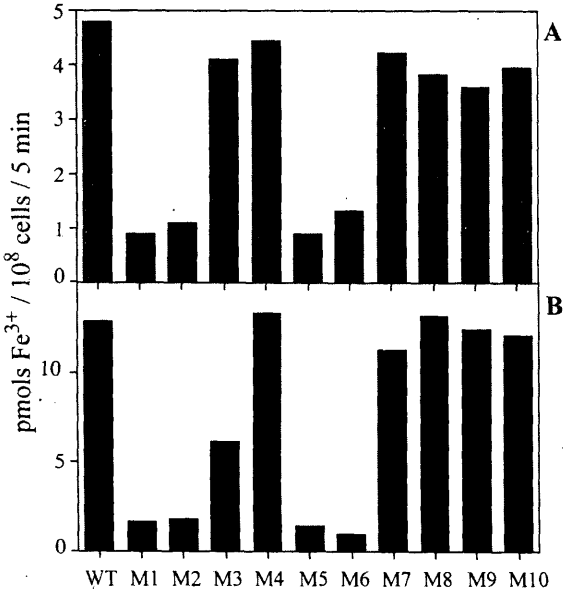

FIG. 4. Amounts of $^{59}Fe^{3+}$ taken up by wild-type (WT) and mutant (M1 to M10 [Fig. 1]) cells. Cells grown in complete medium (A) and iron-deprived cells (B) were incubated with 10 μM $^{59}FeCl_3$ for 5 min in the light in the presence of 1 mM Ferrozine.

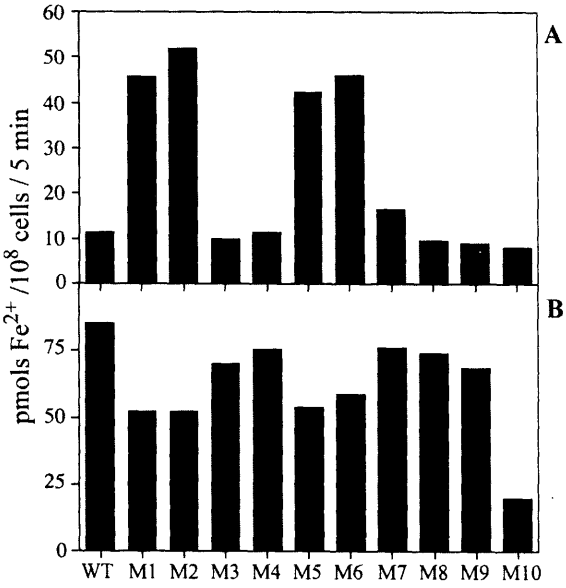

FIG. 5. Amounts of $^{59}Fe^{2+}$ taken up by wild-type (WT) and mutant (M1 to M10 [Fig. 1]) cells. Cells grown in complete medium (A) and iron-deprived cells (B) were incubated with 10 μM $^{59}FeCl_3$ for 5 min in the light in the presence of 5 mM ascorbate.

Uptake of ferric iron. Figure 4 shows the amounts of Fe^{3+} taken up by the wild-type and mutant strains grown in nutrient-replete medium (A) or by iron-deprived cells (B) during 5 min of incubation in the light with 10 μM $FeCl_3$ in the presence of 1 mM Ferrozine. The Fe^{3+} uptake activities of the M1, M2, M5, and M6 mutants, either maintained in nutrient-replete medium or starved for iron, were much lower than those of wild-type cells and of the other mutants. The activity of M5 was similar to that of M1 or M2. These results support the view that the *fut* genes disrupted in the mutants encode the subunits of a single Fe^{3+} transporter. These mutants still retained low levels of Fe^{3+} transport activity, suggesting the presence of an Fe^{3+} transporter(s) other than the *fut*-dependent system. The Fe^{3+} transport activity in the iron-deprived M3 cells was about half the activity of the M4 mutant (B), suggesting that FutA1 is a major iron-binding protein involved in *fut*-dependent Fe^{3+} transport.

Uptake of ferrous iron. Figure 5 shows the amounts of Fe^{2+} taken up by the wild-type and mutant strains grown in nutrient-replete medium (A) and by iron-deprived cells (B) during 5 min of incubation in the light with 10 μM $FeCl_3$ in the presence of 5 mM ascorbate (12). The activity of Fe^{2+} uptake was low in wild-type cells cultured in normal BG-11 medium and was increased about eightfold after iron deprivation. Thus, *Synechocystis* sp. strain PCC 6803 has an Fe^{2+} transporter that is induced by iron deprivation. The M3, M4, M7, M8, and M9 strains were similar to the wild type in that their activities were low in cells grown in normal medium and were increased six- to eightfold after iron deprivation. In contrast, the M1, M2, M5, and M6 mutants grown in nutrient-replete medium showed much higher activity of Fe^{2+} transport than wild-type cells, indicating that the Fe^{2+} transport system is induced in these mutants during growth in the complete medium. The activities in iron-deprived cells of these mutants were not significantly different from those in iron-replete cells and were two-thirds the activity in iron-deprived wild-type cells. The lower levels of Fe^{2+} uptake in the mutants may be due to changes in cell size or cellular composition. In fact, the chlorophyll contents of these four mutants were 2.7 to 3.1 μg/10^8 cells, while those in the wild-type cells and other mutant cells were 3.7 to 4.0 μg/10^8 cells. Therefore, the Fe^{2+} uptake activities in the iron-deprived cells of the mutants were similar to the wild-type activity when the values are expressed on a chlorophyll basis.

The Fe^{2+} uptake activity of the M10 mutant was similar to the wild-type activity when cells were grown in normal medium but was much lower, about one-fourth of the wild-type activity, after iron deprivation. Thus, *slr1392* (*feoB*) encodes a protein that is induced under iron deprivation and functions to transport ferrous iron.

DISCUSSION

In this study, we identified four genes that play a major role in iron acquisition in *Synechocystis* sp. strain PCC 6803, both in iron-replete and iron-deficient conditions. These four genes appear to encode subunits of a single Fe^{3+} transporter. The *Synechocystis* genome contains many genes that are homologous to the genes involved in iron acquisition in nonphotosynthetic bacteria. Ten mutants were constructed by inactivating single or multiple genes putatively involved in iron uptake (Fig. 1). Out of these mutants, only four mutants, with *slr1295* (*futA1*), *slr0513* (*futA2*), *slr0327* (*futB*), and/or *sll1878* (*futC*) in-activated, exhibited a mutant phenotype. Computer analysis indicated that all of these genes possess an ABC transporter gene family signature. The following results strongly suggest that these genes may encode subunit proteins of a single Fe^{3+} transporter. (i) The M1, M2, M5, and M6 mutants all exhibited the same growth characteristics (Fig. 3) and showed a marked

reduction in their ability to take up Fe^{3+} (Fig. 4). All of these mutants showed high Fe^{2+} uptake activity when grown in normal BG-11 medium, indicating that the intracellular iron concentrations were low enough to induce the expression of the *feoB* gene even when the cells were grown in iron-replete medium (Fig. 5A). (ii) Inactivation of *futB* against the background of *futC* mutation did not further decrease the Fe^{3+} uptake activity (M1 versus M5 in Fig. 4), which strongly suggested that FutB and FutC are the subunit polypeptides of a single transporter. An ATP/GTP-binding motif (consensus: [AG]-x(4)-G-K-[ST] [25]) was identified in FutB (AARSL GKS: positions 458 to 465) as well as in FutC (GPSGCGKT; positions 53 to 60). It is well known that the archetypal ABC transporter consists of two ABC domains and two transmembrane domains. In many bacterial ABC transporters, each of these four domains is encoded as an independent polypeptide, although in other transporters the domains can be fused in any one of a number of ways into multidomain polypeptides (17). However, association of one subunit carrying the membrane domain and the ABC domain fused on one polypeptide, with a second peripheral subunit carrying only the ABC domain, has not been reported. The present results for M1, M2, and M5 strains imply the presence of such a unique combination in the ABC transporter family. (iii) Both *futA1* and *futA2* are homologous to *sfuA* in *S. marcescens*, which encodes a substrate-binding protein (Fig. 1). The M3 and M4 strains, in which these genes were inactivated individually, showed growth characteristics similar to those of the wild type (Fig. 3). Inactivation of other genes that encode putative substrate-binding proteins had no effect on growth and Fe^{3+} uptake activity (lanes M8 in Fig. 3 and 4). Only the M6 strain, lacking both *futA1* and *futA2*, showed a mutant phenotype similar to those of the M1 and M2 strains. These results suggest that FutA1 and FutA2 have redundant or overlapping Fe^{3+} binding activities that function in the ABC transporter containing FutB and FutC as the inner membrane and membrane-associated subunits, respectively. (iv) All the *fut* genes were expressed constitutively in cells grown in normal medium (Fig. 2). This is consistent with the observation that inactivation of these genes significantly lowered the activity of Fe^{3+} uptake in cells grown in iron-replete medium (Fig. 4A). The form of iron transported across the inner membrane by the Fut system is most probably the ferric ion since this system is related to the Sfu/Fbp family, which transports ferric ion (3, 4). Our preliminary result for recombinant FutA1 expressed in *E. coli* indicated that the protein binds ferric ion directly.

The possibility of polar effects of the inactivation of *fut* genes is ruled out for the following reasons. Such polar effects may happen for the genes that constitute an operon structure. The insertion of a kanamycin resistance cassette does not suppress the expression of the gene(s) downstream of the cassette. As a result, the only possible gene whose inactivation causes a polar effect is *slr0327* (*futB*). *slr0328* and *slr0329* are downstream of *slr0327* on the genome. These genes are supposed to encode protein phosphatase and the xylose repressor, and it is unlikely that these proteins are involved in iron transport.

Inactivation of putative iron transporter genes other than *fut* genes did not have a significant effect on growth and Fe^{3+} uptake activity, suggesting that the contribution of these genes, if any, to iron acquisition is small. *Synechococcus* sp. strain PCC 7942 and *Anabaena variabilis* are known to produce unique hydroxamate-type siderophores (24). *Morganella morganii* takes up iron chelated to the fungal siderophore rhizoferrin (15). It is possible that the above putative iron transporter genes are involved in the transport of iron siderophores. The transport of iron in the form of complexes with siderophores may not be essential for iron acquisition under laboratory conditions, but it may give great advantage to *Synechocystis* cells in the natural environment. The low activities of Fe^{3+} uptake in M1, M2, M5, and M6 indicate the presence of another Fe^{3+} transporter(s), which could be encoded by the above putative iron transporter genes.

The mechanism by which ferric iron moves across the outer membrane to the periplasmic space is not known. Since the M9 strain did not show a mutant phenotype, a gene(s) other than those inactivated in this mutant may be involved in this process.

Synechocystis showed very high ability to take up ferrous iron when iron in the medium was reduced (Fig. 5). However, in the absence of ascorbate in the medium, the activity was much smaller. Since the activity in the absence of ascorbate fluctuates so much, depending on the growth conditions and stage of the growth, we did not include the results in this paper. The M10 strain grew as well as the wild type under iron-replete and iron-deficient conditions (Fig. 3), suggesting that the transport of Fe^{2+} is not essential for iron acquisition in the wild type. However, it is possible that FeoB-dependent Fe^{2+} uptake is essential for iron acquisition when Fut-dependent Fe^{3+} transport was impaired. In fact, we were unable to inactivate *sll1392* (*feoB*) against the background of mutations of *fut* genes. The low Fe^{2+} transport activity in wild-type and M10 cells grown in normal medium and in iron-deprived M10 cells indicates that a second Fe^{2+} transporter is present constitutively in iron-replete cells of wild-type and mutant strains used in this study (16).

ACKNOWLEDGMENTS

This work was supported by grants for the Research for the Future program (JSPS-RFTF97R16001 and JPSP-RFTF96L00105), a grant-in aid for scientific research (B) (2)(12440228), and a grant from the Human Frontier Science Program (RG0051/1997M) to T.O. and National Science Foundation grant MCB 9727836 to A.R.G.

REFERENCES

1. **Agustin, V.** 1992. Analysis of the gene encoding the RNA subunit of ribonuclease P from cyanobacteria. Nucleic Acids Res. **20**:6331–6337.
2. **Aiba, H., S. Adhya, and B. de Crombrugghe.** 1981. Evidence for two functional gal promoters in intact *Escherichia coli* cells. J. Biol. Chem. **256**:11905–11910.
3. **Angerer, A., S. Gaisser, and V. Braun.** 1990. Nucleotide sequences of the *sfuA*, *sfuB*, and *sfuC* genes of *Serratia marcescens* suggest a periplasmic-binding-protein-dependent iron transport mechanism. J. Bacteriol. **172**:572–578.
4. **Berish, S. A., T. A. Mietzner, L. W. Mayer, C. A. Genco, B. P. Holloway, and S. A. Morse.** 1990. Molecular cloning and characterization of the structual gene for the major iron-regulated protein expressed by *Neisseria gonorrhoeae*. J. Exp. Med. **171**:1535–1546.
5. **Boyer, G. L., A. H. Gillam, and C. Trick.** 1987. Iron chelation and uptake, p. 415–436. *In* P. Fay and C. van Baalen (ed.), The cyanobacteria. Elsevier, Amsterdam, The Netherlands.
6. **Braun, V., K. Hantke, and W. Koster.** 1998. Bacterial iron transport: mechanisms, genetics, and regulation. Met. Ions Biol. Syst. **35**:67–145.
7. **Braun, V., R. Gross, W. Koester, and L. Zimmermann.** 1983. Plasmid and chromosomal mutants in the iron(III)-aerobactin transport system of *Escherichia coli*. Use of streptonigrin for selection. Mol. Gen. Genet. **192**:131–139.
8. **Chelly, J., and A. Kahn.** 1994. RT-PCR and mRNA quantitation, p. 97–109.

In K. B. Mullis, F. Ferré, and R. A. Gibbs (ed.), The polymerase chain reaction. Birkhauser, Boston, Mass.
9. **Ecker, D. J., and T. Emery.** 1983. Iron uptake from ferrichrome A and iron citrate in *Ustilago sphaerogena*. J. Bacteriol. **155:**616–622.
10. **Gilis, A., M. A. Khan, P. Cornelis, J. M. Meyer, M. Mergeay, and D. van der Lelie.** 1996. Siderophore-mediated iron uptake in *Alcaligenes eutrophus* CH34 and identification of *aleB* encoding the ferric iron-alcaligin E receptor. J. Bacteriol. **178:**5499–5507.
11. **Guerinot, M. L., and Y. Yi.** 1994. Iron: nutritious, noxious, and not readily available. Plant Physiol. **104:**815–820.
12. **Kammler, M., C. Schon, and K. Hantke.** 1993. Characterization of the ferrous iron uptake system of *Escherichia coli*. J. Bacteriol. **175:**6212–6219.
13. **Kaneko, T., S. Sato, H. Kotani, A. Tanaka, E. Asamizu, Y. Nakamura, N. Miyajima, M. Hirosawa, M. Sugiura, S. Sasamoto, T. Kimura, T. Hosouchi, A. Matsuno, A. Muraki, N. Nakazaki, K. Naruo, S. Okumura, S. Shimpo, C. Takeuchi, T. Wada, A. Watanabe, M. Yamada, M. Yasuda, and S. Tabata.** 1996. Sequence analysis of the genome of the unicellular cyanobacterium *Synechocystis* sp. strain PCC6803. II. Sequence determination of the entire genome and assignment of potential protein-coding regions. DNA Res. **3:**109–136.
14. **Katoh, H., A. R. Grossman, N. Hagino, and T. Ogawa.** 2000. A gene of *Synechocystis* sp. strain PCC 6803 encoding a novel iron transporter. J. Bacteriol. **182:**6523–6524.
15. **Kuhn, A., V. Braun, and W. Koester.** 1996. Ferric rhizoferrin uptake into *Morganella morganii*: characterization of genes involved in the uptake of a polyhydroxycarboxylate siderophore. J. Bacteriol. **178:**496–504.
16. **Lesuisse, E., F. Raguzzi, and R. R. Crichton.** 1987. Iron uptake by the yeast *Saccharomyces cerevisiae*: involvement of a reduction step. J. Gen. Microbiol. **133:**3229–3236.
17. **Linton, K. J., and C. F. Higgins.** 1998. The *Escherichia coli* ATP-binding cassette (ABC) proteins. Mol. Microbiol. **28:**5–13.
18. **Marschner, H., and V. Römheld.** 1994. Strategies of plants for acquisition of iron. Plant Soil **165:**261–274.
19. **Sambrook, J., E. F. Fritsch, and T. Maniatis.** 1989. Molecular cloning: a laboratory manual, 2nd ed., Cold Spring Harbor Laboratory, Cold Spring Harbor, N.Y.
20. **Sanders, J. D., L. D. Cope, and E. J. Hansen.** 1994. Identification of a locus involved in the utilization of iron by *Haemophilus influenzae*. Infect. Immun. **62:**4515–4525.
21. **Stanier, R. Y., R. Kunisawa, M. Mandel, and G. Cohen-Bazire.** 1971. Purification and properties of unicellular blue-green algae (order *Chroococcales*). Bacteriol. Rev. **35:**171–205.
22. **Staudenmaier, H., B. van Hove. Z. Yaraghi, and V. Braun.** 1989. Nucleotide sequences of the *fecBCDE* genes and locations of the proteins suggest a periplasmic-binding-protein-dependent transport mechanism for iron(III) dicitrate in *Escherichia coli*. J. Bacteriol. **171:**2626–2633.
23. **Straus, N. A.** 1994. Iron deprivation: physiology and gene regulation, p. 731–750. *In* D. A. Bryant (ed.), The molecular biology of Cyanobacteria. Kluwer, Dordrecht, The Netherlands.
24. **Trick, C. G., and A. Kerry.** 1992. Isolation and purification of siderophores produced by cyanobacteria, *Synechococcus* sp. strain PCC7942 and *Anabaena variabilis* ATCC29413. Curr. Microbiol. **24:**241–245.
25. **Walker, J. E., M. Saraste, M. J. Runswick, and N. J. Gay.** 1982. Distantly related sequences in the alpha- and beta-subunits of ATP synthase, myosin, kinases and other ATP-requiring enzymes and a common nucleotide binding fold. EMBO J. **1:**945–951.
26. **Williams, J. G. K., and A. A. Szalay.** 1983. Stable integration of foreign DNA into the chromosome of the cyanobacterium *Synechococcus* R2. Gene **24:** 37–51.

Plant Cell Physiol. 42(8): 823–827 (2001)

Iron-Binding Activity of FutA1 Subunit of an ABC-type Iron Transporter in the Cyanobacterium *Synechocystis* sp. Strain PCC 6803

Hirokazu Katoh [1], Natsu Hagino and Teruo Ogawa

Bioscience Center, Nagoya University, Chikusa, Nagoya, 464-8601 Japan

The *futA1* (*slr1295*) and *futA2* (*slr0513*) genes encode periplasmic binding proteins of an ATP-binding cassette (ABC)-type iron transporter in *Synechocystis* sp. PCC 6803. FutA1 was expressed in *Escherichia coli* as a GST-tagged recombinant protein (rFutA1). Solution containing purified rFutA1 and ferric chloride showed an absorption spectrum with a peak at 453 nm. The absorbance at this wavelength rose linearly as the amount of iron bound to rFutA1 increased to reach a plateau when the molar ratio of iron to rFutA1 became unity. The association constant of rFutA1 for iron in vitro was about 1×10^{19}. These results demonstrate that the FutA1 binds the ferric ion with high affinity. The activity of iron uptake in the Δ*futA1* and Δ*futA2* mutants was 37 and 84%, respectively, of that in the wild-type and the activity was less than 5% in the Δ*futA1*/Δ*futA2* double mutant, suggesting their redundant role for binding iron. High concentrations of citrate inhibited ferric iron uptake. These results suggest that the natural iron source transported by the Fut system is not ferric citrate.

Key words: Cyanobacterium — FutA1 — Iron transporter — Periplasmic binding protein — *Synechocystis* sp. PCC 6803.

Abbreviations: ABC, ATP-binding cassette; GST, Glutathione *S*-transferase; rFutA1, recombinant FutA1; IPTG, isopropyl-1-thio-β-D-galactopyranoside; PBS, phosphate-buffered saline.

Introduction

Low levels of iron accessible by microorganisms are recurring nutrient stress conditions in both marine and fresh water oxic ecosystems and limit the primary production of phytoplankton in vast regions of the world's ocean (Straus 1994, Butler 1998). Iron deficiency causes a variety of physiological and morphological changes in cyanobacteria. These include a loss of light-harvesting phycobilisomes (Guikema and Sherman 1983), changes in the spectral characteristics of chlorophyll (Guikema and Sherman 1983, Pakrasi et al. 1985), decrease of thylakoids (Sherman and Sherman 1983), and replacement of iron-containing cofactors with non-iron cofactors such as ferredoxin with flavodoxin (Laudenbach et al. 1988).

In the cyanobacterium *Synechocystis* sp. strain PCC 6803, the acquisition of ferric iron occurs mainly by an ABC-type iron transporter composed of subunit proteins encoded by four *fut* genes, *futA1* (*slr1295*), *futA2* (*slr0513*), *futB* (*slr0327*), and *futC* (*sll1878*) (Katoh et al. 2000, Katoh et al. 2001). Based on the sequence homology, the Fut system is related to the Sfu, Hit and Fbp systems in *Serratia* (Angerer et al. 1990), *Haemophilus* (Sanders et al. 1994) and *Neisseria* (Chen et al. 1993, Nowalk et al. 1994), respectively. Mutants inactivated for *futB* or *futC*, which encode inner membrane-bound or membrane-associated subunits, respectively, showed poor growth in iron-free BG-11 medium and low activity of ferric iron transport. The double mutant lacking both *futA1* and *futA2*, which encode periplasmic binding proteins, showed the same phenotype as Δ*futB* and Δ*futC* single mutants. However, single mutants, Δ*futA1* and Δ*futA2* did not show the phenotype similar to that of Δ*futB* and Δ*futC* mutants. Thus the Fut system has an unusual composition of having two kinds of periplasmic binding proteins, FutA1 and FutA2. The iron-binding properties of these proteins and the form of iron transported by the Fut system have not been clarified. In order to solve these problems, we attempted to express *futA1* and *futA2* in *Escherichia coli*, and obtained soluble recombinant FutA1 fused to GST (rFutA1). We report in this paper the iron-binding properties of rFutA1 and the form of iron transported by the Fut system.

Results

Expression and purification of a recombinant FutA1 (rFutA1) protein

The region of signal peptide (37 amino acids in the N-terminal) in the FutA1 polypeptide was predicted using the PSORT program (Nakai and Kanehisa 1991). Truncated FutA1 lacking the predicted signal peptide was expressed in *E. coli* as a 60-kDa protein fused to GST by addition of IPTG (Fig. 1, lane 1). The protein was collected in the soluble fractions (lane 2) and was purified by Glutathione Sepharose 4B resin (lane 3). Trials to obtain recombinant FutA2 protein in soluble fractions by the same method were unsuccessful. The rFutA2 protein was unsolubilized even in the presence of 1% Triton. Therefore, further analysis was abandoned.

Absorption spectra of deferreted and iron-saturated rFutA1 protein

The absorption spectrum of deferrated rFutA1 protein did not show any peak in the visible region between 340 and

[1] Corresponding author: E-mail, L46611A@nucc.cc.nagoya-u.ac.jp; Fax, +81-52-789-5214.

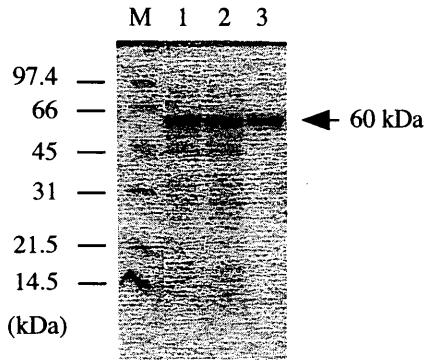

Fig. 1 SDS-PAGE patterns of rFutA1 expressed in *E. coli*. Truncated rFutA1 lacking the presumed signal peptide (37 amino acids on the N-terminal) was expressed in *E. coli* as a protein fused to glutathione *S*-transferase and purified on Glutathione Sepharose 4B resin. Proteins were separated on a 12.5% SDS-polyacrylamide gel and stained with Coomassie Brilliant Blue. Lane 1, lysate of *E. coli* carrying p*futA1-gst* 2 h after addition of IPTG; lane 2, soluble fraction of the lysate; lane 3, rFutA1 purified on Glutathione Sepharose 4B resin; M, molecular mass markers (masses are indicated in kilodaltons). The amounts of proteins loaded were 20 μg in lane 1 and lane 2 and 5 μg in lane 3.

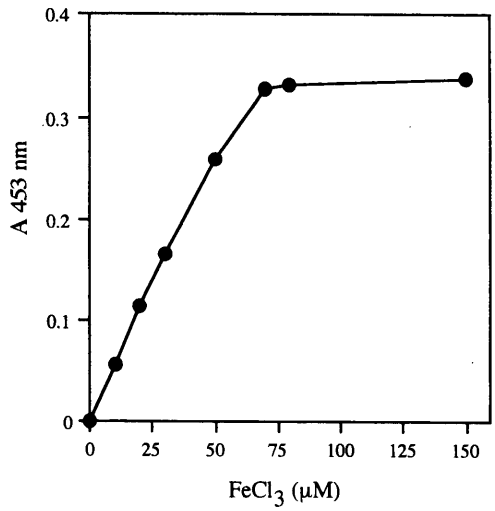

Fig. 3 Referration of rFutA1. Ferric chloride was added stepwise to the solution containing 70 μM deferrated rFutA1 to give the final concentrations of 0 to 150 μM and the absorbance was monitored at 453 nm.

600 nm (Fig. 2). A broad band with a peak at 453 nm appeared when $FeCl_3$ (2-fold molar excess over rFutA1) was added to the solution containing deferrated rFutA1. A similar absorption band has been observed with the Fbp protein and attributed to the absorption by the coordinated Fe^{3+} atom (Nowalk et al. 1994). Based on these results, we attributed this band to the absorption by the iron associated with rFutA1. The absorption maximum of Fe^{3+}-rFutA1 was about 30 nm lower than the peak positions of Fe^{3+} bound to Fbp and HitA (Nowalk et al. 1994, Adhikari et al. 1995). One possible reason for this difference might be due to extra GST region in rFutA1 protein and another one will be described in the discussion section.

Iron-binding properties of rFutA1

There was a linear relationship between the amount of iron added to the solution containing deferrated rFutA1 and the absorbance at 453 nm until the molar ratio of ferric chloride to deferrated rFutA1 became unity (Fig. 3). This indicates that absorbance at this wavelength is an accurate measure of the ferration state of this protein and that 1 molecule of rFutA1 is capable of incorporating 1 molecule of ferric ion. The iron chelator citrate effectively removed iron from ferrated rFutA1 (Fig. 4). The concentration of citrate required to remove 50%

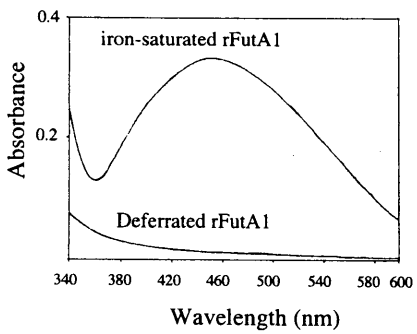

Fig. 2 Absorption spectra of deferrated and iron-saturated rFutA1. The sample solution contained 75 μM protein and 200 mM NaCl in 20 mM Tris-HCl buffer, pH 8.0.

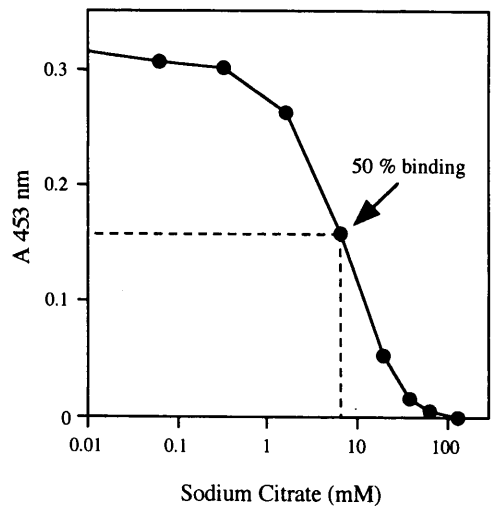

Fig. 4 Competition for rFutA1-bound iron by citrate. Sodium citrate was added stepwise to the solution containing 65 μM Fe^{3+}-rFutA1 and 200 mM NaCl in 20 mM Tris-HCl buffer, pH 8.0 to give the final concentrations of 0 to 130 mM. The absorbance was monitored at 453 nm at each citrate concentration after incubation of the mixture at room temperature for 15 min.

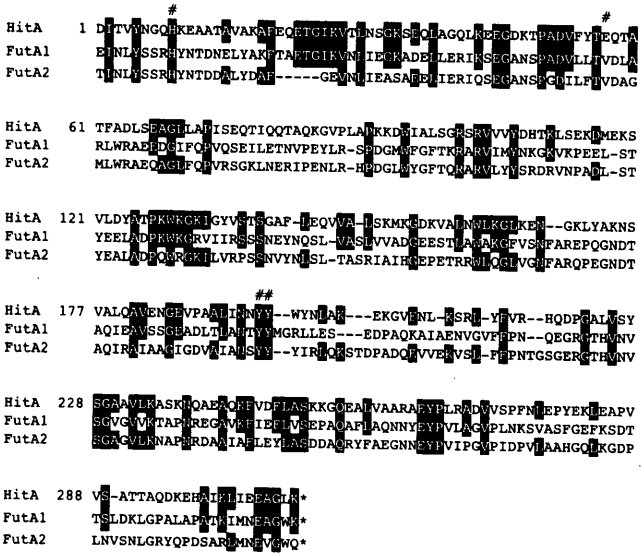

Fig. 5 Alignment of the amino acid sequences of FutA1, FutA2 and HitA. Deduced amino acid sequences of FutA1 and FutA2 of *Synechocystis* and HitA of *H. influenzae* were aligned. Residues identical to those in HitA are shown in reverse type. Four residues (H9, E57, Y195, and Y196) involved in iron binding in HitA are represented by sharp symbols above the sequence (Bruns et al. 1997).

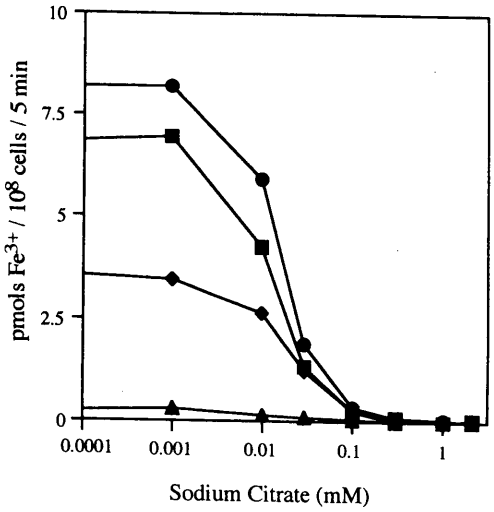

Fig. 6 Inhibition of $^{59}Fe^{3+}$ uptake by citrate. Uptake reaction was initiated by adding 1 μM $^{59}FeCl_3$ to the suspension of cells containing various amounts of citrate (0 to 2 mM, final concentration) and 500 μM ferrozine. The reaction was terminated by transferring the reaction mixture on ice, followed by centrifugation at 4°C. The pellet was washed twice with 20 mM TES-KOH (pH 8.0) containing 10 mM EDTA. Closed circle; wild-type, closed square; Δ*futA2*, closed diamond; Δ*futA1*, closed triangle; Δ*futA1*/Δ*futA2*.

of the iron from ferrated rFutA1 was 6.5 mM, which represents a 100-fold molar excess of citrate over rFutA1. The relative affinity of rFutA1 for iron estimated by using the association constant of citrate for iron (1×10^{17}, Crichton 1990) was about 1×10^{19}. Thus, ferric ion is the ligand that FutA1 protein binds to, supporting the role of this protein as a periplasmic binding subunit of the ABC-type ferric ion transporter in *Synechocystis* PCC 6803. There remains a possibility that additional GST region in rFutA1 affects the relative affinity of FutA1 protein for iron.

Fig. 5 shows protein sequence alignment of FutA1/A2 with HitA of *Haemophilus influenzae*. Sequence homology between HitA and FutA1/FutA2 was not so high. However, three amino acid residues out of four residues (His 9, Glu 57, Tyr 195, Tyr 196) binding iron in HitA were conserved in both FutA1 and FutA2 (Bruns et al. 1997). The residue at Glu 57 in HitA was Val in these Fut proteins (Fig. 5). The highly conserved iron-binding residues in HitA and two Fut proteins suggest that they have the same function in iron acquisition.

Effect of citrate on iron uptake

Citrate inhibited the activity of iron uptake in wild-type cells grown either in the presence (Fig. 6, circles) or absence (data not shown) of citrate, indicating that *Synechocystis* was unable to transport ferric citrate and that the natural iron source for Fut transport system was not ferric citrate. In the absence of citrate, the single mutants, Δ*futA2* and Δ*futA1*, showed 84 and 37% of the wild-type activity of Fe^{3+} uptake, respectively, whereas the activity was nearly zero in the Δ*futA1*/Δ*futA2* double mutant. Citrate inhibited the uptake of ferric iron by Δ*futA1* and Δ*futA2* single mutants (Fig. 6). This may support the view that FutA1 and FutA2 play a redundant role in iron binding in the Fut system.

Discussion

Bacterial ABC transporter possesses a periplasmic binding protein that has high affinity to its specific ligand (Higgins et al. 1990, Tam and Saier 1993). The ABC-type iron transporter encoded by the *fut* genes possesses two periplasmic binding proteins, FutA1 and FutA2 (Katoh et al. 2001). We demonstrated in this study that FutA1 binds iron without organic iron chelator such as siderophore or citrate. This is the first finding of the presence of high affinity Hit/Fbp-type iron-acquisition system in photosynthetic microorganisms. A recombinant FutA1 (rFutA1) was successfully obtained as a soluble protein. Ferric ion bound to this protein gave a typical absorption spectrum with a peak at 453 nm, which was about 30 nm lower than the peak position of Fe^{3+} bound to HitA. Structural analysis of HitA suggested that four amino acid residues, His 9, Glu 57, Tyr 195, Tyr 196 are involved in binding iron to the protein (Bruns et al. 1997). Sequence comparison revealed that these residues except Glu 57 are conserved in FutA1 and FutA2, suggesting that those are also involved in binding iron in the FutA proteins. The difference in absorption maxima between Fe^{3+}-HitA and Fe^{3+}-rFutA1 may be attributed to the substitution of

Glu 57 in HitA to Val in FutA1 or to the presence of GST region in rFutA1.

The natural iron source for the Fut system is unclear. In the case of Fbp system, free ferric iron is passed across the outer membrane through the transferrin receptor protein (TbpA), which shows similar characteristics to the siderophore receptors (Irwin et al. 1993, Anderson et al. 1994). However, *Synechocystis* PCC 6803 does not possess a homologue of *tbpA*. Furthermore, our previous results indicated that simultaneous inactivation of four genes homologous to siderophore receptor genes had no effect on the uptake of iron and there has been no report on the production of siderophore by *Synechocystis* PCC 6803. In *E. coli*, citrate strongly enhanced the uptake of iron because this organism possesses an inducible ferric dicitrate transporter encoded by *fecA*, *B*, *C*, *D*, and *E* (Frost and Rosenberg 1973, Staudenmaier et al. 1989). Ferric citrate passes across the outer membrane through the FecA protein localized in the outer membrane. *Synechocystis* does not possess a homologue of *fecA*, although the homologues of *fecB*, *C*, *D*, and *E* have been identified in its genome (Kaneko et al. 1996). Inactivation of *fecB* or *fecE* did not decrease the activity of ferric iron uptake (Katoh et al. 2001). Furthermore, citrate competitively inhibited the binding of iron to rFutA1 in vitro and the uptake of ferric iron in vivo regardless of culture conditions of the cells (Fig. 4, 6). Taken together, *Synechocystis* is unable to take up iron in the form of Fe^{3+}-citrate under the experimental conditions used in this study. The negative effects of citrate on iron uptake were also observed on *enb* mutants of *Salmonella typhimurium* which were blocked in the biosynthesis of enterobactin, an iron chelator that was secreted by the wild-type bacteria when they were grown on low iron media (Pollack et al. 1970). The inhibitory effect of citrate on iron uptake in *Synechocystis* suggests that ferric citrate transport system is not functioning, presumably due to the absence of *fecA*. Alternatively, *fecBCDE* genes might encode a transporter for another molecule.

The FutA2 protein plays an essential role in ferric iron acquisition by Δ*futA1* mutant. Citrate inhibited the uptake of ferric iron by this mutant, suggesting that the form of iron bound to FutA2 is not ferric citrate. The deduced protein sequence of FutA2 is very similar to FutA1 and three amino acid residues of HitA functioning to bind ferric ion are conserved in these FutA proteins. These results imply that the ligand for FutA2 is also ferric ion, although this assumption should be confirmed by spectral analyses of FutA2 protein.

Materials and Methods

Preparation of recombinant FutA1

A DNA fragment, carrying a truncated *futA1* (*slr1295* on "CyanoBase", http://www.kazusa.or.jp/cyano/) lacking 111 bases from the initiation codon, was amplified by PCR using primers containing *Eco*RI sites at their proximal ends. After digesting with *Eco*RI, the PCR product was cloned into the *Eco*RI site of the pGEX-2T expression vector (Amersham Pharmacia Biotech, U.K.). The resulting plasmid (*pfutA1-gst*) carried a chimeric gene which encodes a truncated FutA1 lacking the N-terminal 37 amino acids fused to glutathione *S*-transferase (GST). This plasmid was used to transform *E. coli* DH5α. Expression of the chimeric gene in the transformant was induced by 1 mM isopropyl-1-thio-β-D-galactopyranoside (IPTG). After a 2 h induction, *E. coli* carrying *pfutA1-gst* were harvested and re-suspended with ice-cold PBS. GST-FutA1 recombinant protein was isolated from the cells using GST purification Kit (Amersham Pharmacia Biotech, U.K.) according to the instruction manual. Briefly, cells were lysed using a sonic oscillator equipped with a conical horn of 10–5 mm diameter (Ohtake Co., Tokyo, Japan) at 20 W. Triton X-100 (20%) was added to the disrupted cells to a final concentration of 1%. After incubation for 30 min on ice with gentle agitation, the sample was centrifuged (12,000×*g*, 4°C, 10 min). The supernatant was transferred to a fresh tube, to which 1/50 volume of 50% slurry of Glutathione Sepharose 4B was added. The mixture was incubated at room temperature for 30 min with gentle agitation, then centrifuged and the supernatant was removed. After washing the Glutathione Sepharose 4B pellet with PBS, the GST-FutA1 fusion protein was eluted from the matrix by incubating with Glutathione Elution Buffer at room temperature for 1 h.

Deferration/referration of rFutA1

Deferration and referration of rFutA1 were done according to the method used for Fbp in *Neisseria* (Nowalk et al. 1994). Solution containing purified rFutA1 (6 mg ml^{-1}) was acidified by adding 0.1 volume of 0.1% acetic acid, and iron was chelated by adding 2,000-fold molar excess of sodium citrate (pH 8.0) over rFutA1. Excess citrate and iron-citrate were removed by using an Econo-10DG microbiospin column (Bio-Rad) and fractions containing deferrated rFutA1 were collected in acid-washed tubes. Referration was accomplished by adding two-fold molar excess of $FeCl_3$ to the solution containing 4.5 mg ml^{-1} (75 μM) apo-rFutA1 and 200 mM NaCl in 20 mM Tris-HCl (pH 8.0). Absorption spectra of solutions containing apo- and Fe^{3+}-rFutA1 were measured using a UV/VIS spectrophotometer V-550 (Jasco, Tokyo, Japan).

Measurement of iron binding properties of rFutA1

$FeCl_3$ (final concentrations between 0 and 150 μM) was added to a solution containing 4.2 mg ml^{-1} (70 μM) of deferrated rFutA1 and the mixture was incubated at room temperature for 15 min. Relative affinity of rFutA1 for iron in vitro, was estimated by the method employed for rFbp (Chen et al. 1993). Solution containing 3.9 mg ml^{-1} (65 μM) Fe^{3+}-rFutA1 and 200 mM NaCl in 20 mM Tris-HCl buffer (pH 8.0) was mixed with sodium citrate (final concentrations between 0 and 130 mM) and was incubated at room temperature for 15 min. The amount of Fe^{3+}-rFutA1 in the mixture was estimated from the absorbance at 453 nm.

Measurements of iron uptake

Uptake of iron by wild-type and mutant cells of *Synechocystis* sp. strain PCC 6803 was measured using the radioactive tracer $^{59}FeCl_3$ (Amersham Pharmacia Biotech, U.K.) as described previously (Katoh et al. 2000, Katoh et al. 2001). Cells were pre-cultured in modified BG-11 medium (Stanier et al. 1971, Katoh et al. 2000) containing 1 μM $FeCl_3$ with or without 100 μM sodium citrate. The reaction solution contained 1 μM $^{59}FeCl_3$ and various concentrations of sodium citrate between 0 and 2 mM. Ferrozine (500 μM) was added to the reaction solution to inhibit ferrous iron uptake. Reaction was performed in the light at 700 μmol photons m^{-2} s^{-1} (400–700 nm). The light source was a 600 W halogen lump (Cabin Co., Tokyo). The gamma emission from ^{59}Fe in the cells was measured by the Auto Well gamma system (model ARC-380; Aloka, Tokyo, Japan).

Protein analyses

Lysates of *E. coli* cells and proteins were suspended in the sample buffer used for SDS-PAGE and were heated at 95°C for 5 min. After gel electrophoresis in the buffer system of Laemmli (1970), polypeptides in the gel were stained with Coomassie Brilliant Blue. Concentration of rFutA1 was calculated from the absorbance at 280 nm. The extinction coefficient of rFutA1 was determined based on the number of tyrosine and tryptophan residues in the protein (Yin et al. 1988). Protein sequences were aligned using the DNASIS program (Hitachi Software, Yokohama, Japan).

Acknowledgements

This work was supported by a grant, JPSP-RFTF96L00105, from the Japan Society for the Promotion of Science and a grant on Human Frontier Science Program to T.O.

References

Adhikari, P., Kirby, S.D., Nowalk, A.J., Veraldi, K.L., Schryvers, A.B. and Mietzner, T.A. (1995) Biochemical characterization of a *Haemophilus influenzae* periplasmic iron transport operon. *J. Biol. Chem.* 270: 25142–25149.

Anderson, J.E., Sparling, P.F. and Cornelissen, C.N. (1994) Gonococcal transferrin-binding protein 2 facilitates but is not essential for transferrin utilization. *J. Bacteriol.* 176: 3162–3170.

Angerer, A., Gaisser, S. and Braun, V. (1990) Nucleotide sequences of the *sfuA*, *sfuB*, and *sfuC* genes of *Serratia marcescens* suggest a periplasmic-binding protein-dependent iron transport mechanism. *J. Bacteriol.* 172: 572–578.

Bruns, C.M., Nowalk, A.J., Arvai, A.S., Mctigue, M.A., Vaughan, K.G, Mietzner, T.A. and McRee, D.E. (1997) Structure of *Haemophilus influenzae* Fe^{+3}-binding protein reveals convergent evolution within a superfamily. *Nat. Struct. Biol.* 4: 919–924.

Butler, A. (1998) Acquisition and utilization of transition metal ions by marine organism. *Science* 281: 207–210.

Chen, C.Y., Berish, S.A., Morse, S.A. and Mietzner, T.A. (1993) The ferric iron-binding protein of pathogenic *Neisseria* spp. functions as a periplasmic transport protein in iron acquisition from human transferrin. *Mol. Microbiol.* 10: 311–318.

Crichton, R.R. (1990) Proteins of iron storage and transport. *Adv. Protein Chem.* 40: 281–365.

Frost, G.E. and Rosenberg, H. (1973) The inducible citrate-dependent iron transport system in *Escherichia coli* K12. *Biochim. Biophys. Acta* 330: 90–101.

Guikema, J.A. and Sherman, L.A. (1983) Organization and function of chlorophyll in membranes of cyanobacteria during iron starvation. *Plant Physiol.* 73: 250–256.

Higgins, C.F., Hyde, S.C., Mimmack, M.M., Gileadi, U., Gill, D.R. and Gallagher, M.P. (1990) Binding protein-dependent transport systems. *J. Bioenerg. Biomembr.* 22: 571–592.

Irwin, S.W., Averil, N., Cheng, C.Y. and Schryvers, A.B. (1993) Preparation and analysis of isogenic mutants in the transferrin receptor protein genes, *tbpA* and *tbpB*, from *Neisseria meningitidis*. *Mol. Microbiol.* 8: 1125–1133.

Kaneko, T., Sato, S., Kotani, H., Tanaka, A., Asamizu, E., Nakamura, Y., Miyajima, N., Hirosawa, M., Sugiura, M., Sasamoto, S., Kimura, T., Hosouchi, T., Matsuno, A., Muraki, A., Nakazaki, N., Naruo, K., Okumura, S., Shimpo, S., Takeuchi, C., Wada, T., Watanabe, A., Yamada, M., Yasuda, M. and Tabata, S. (1996) Sequence analysis of the genome of the unicellular cyanobacterium *Synechocystis* sp. strain PCC 6803. II. Sequence determination of the entire genome and assignment of potential protein-coding regions. *DNA Res.* 3: 109–136.

Katoh, H., Grossman, A.R., Hagino, N. and Ogawa, T. (2000) A gene of *Synechocystis* sp. PCC 6803 encoding a novel iron transporter. *J. Bacteriol.* 182: 6523–6524.

Katoh, H., Hagino, N., Grossman, A.R. and Ogawa, T. (2001) Genes essential to iron transport in the Cyanobacterium *Synechocystis* sp. strain PCC 6803. *J. Bacteriol.* 183: 2779–2784.

Laemmli, U.K. (1970) Cleavage of structural proteins during the assembly of the head of bacteriophage T4. *Nature* 227: 680–685.

Laudenbach, D.E., Reith, M.E. and Straus, N.A. (1988) Isolation, sequence analysis, and transcriptional studies of the flavodoxin gene from *Anacystis nidulans* R2. *J. Bacteriol.* 170: 258–265.

Nakai, K. and Kanehisa, M. (1991) Expert system for predicting protein localization sites in Gram-negative bacteria. *Proteins* 11: 95–110.

Nowalk, A.J., Tencza, S.B. and Mietzner, T.A. (1994) Coordination of iron by the ferric iron-binding protein of pathogenic *Neisseria* is homologous to the transferrins. *Biochemistry* 33: 12769–12775.

Pakrasi, H.B., Goldenberg, A. and Sherman, L.A. (1985) Membrane development in the cyanobacterium, *Anacystis nidulans*, during recovery from iron starvation. *Plant Physiol.* 79: 290–295.

Pollack, J.R., Ames, B.N. and Neilands, J.B. (1970) Iron transport in *Salmonella typhimurium*: Mutants blocked in the biosynthesis of Enterobactin. *J. Bacteriol.* 104: 635–639.

Sanders, J.D., Cope, L.D. and Hansen, E.J. (1994) Identification of a locus involved in the utilization of iron by *Haemophilus influenzae*. *Infect. Immun.* 62: 4515–4525.

Sherman, D.M. and Sherman, L.A. (1983) Effect of iron deficiency and iron restoration on ultrastructure of *Anacystis nidulans*. *J. Bacteriol.* 156: 393–401.

Stanier, R.Y., Kunisawa, R., Mandel, M. and Cohen-Bazire, Z. (1971) Purification and properties of unicellular blue-green algae (Order *Chroococcales*). *Bacteriol. Rev.* 35: 171–205.

Staudenmaier, H., Hove, B.V., Yaraghi, Z. and Braun, V. (1989) Nucleotide sequences of the *fecBCDE* genes and locations of the proteins suggest a periplasmic-binding-protein-dependent transport mechanism for iron (III) dicitrate in *Escherichia coli*. *J. Bacteriol.* 171: 2626–2633.

Straus, N.A. (1994) Iron deprivation: Physiology and gene regulation. *In* The Molecular Biology of Cyanobacteria. Edited by Bryant, D.A. pp. 731–750. Kluwer, Dordrecht.

Tam, R. and Saier, J.M.H. (1993) Structural, functional, and evolutionary relationships among extracellular solute-binding receptors of bacteria. *Microbiol. Rev.* 57: 320–346.

Yin, H.L., Iida, K. and Janmey, P.A. (1988) Identification of a polyphosphoinositide-modulated domain in gelsolin which binds to the sides of actin filaments. *J. Cell Biol.* 106: 805–812.

(Received March 8, 2001; Accepted May 21, 2001)

JOURNAL OF BACTERIOLOGY, Sept. 1996, p. 5452–5455
0021-9193/96/$04.00+0

Vol. 178, No. 18

Absence of Light-Induced Proton Extrusion in a *cotA*-Less Mutant of *Synechocystis* sp. Strain PCC6803

AKIRA KATOH,[1] MASATOSHI SONODA,[1] HIROKAZU KATOH,[2] AND TERUO OGAWA[1,2]

Biochemical Regulation, School of Agriculture,[1] and Bioscience Center,[2] Nagoya University, Nagoya 464-01, Japan

Received 22 March 1996/Accepted 17 July 1996

***cotA* of *Synechocystis* sp. strain PCC6803 was isolated as a gene that complemented a mutant defective in CO_2 transport and is homologous to *cemA* that encodes a chloroplast envelope membrane protein (A. Katoh, K. S. Lee, H. Fukuzawa, K. Ohyama, and T. Ogawa, Proc. Natl. Acad. Sci. USA 93:4006–4010, 1996). A mutant (M29) constructed by replacing *cotA* in the wild-type (WT) *Synechocystis* strain with the omega fragment was unable to grow in BG11 medium (~17 mM Na^+) at pH 6.4 or at any pH in a low-sodium medium (100 μM Na^+) under aeration with 3% (vol/vol) CO_2 in air. The WT cells grew well in the pH range between 6.4 and 8.5 in BG11 medium but only at alkaline pH in the low-sodium medium. Illumination of the WT cells resulted in an extrusion followed by an uptake of protons. In contrast, only proton uptake was observed for the M29 mutant in the light without proton extrusion. There was no difference in sodium uptake activity between the WT and mutant. The mutant still possessed 51% of the WT CO_2 transport activity in the presence of 15 mM NaCl. On the basis of these results we concluded that *cotA* has a role in light-induced proton extrusion and that the inhibition of CO_2 transport in the M29 mutant is a secondary effect of the inhibition of proton extrusion.**

The *cotA* gene of *Synechocystis* sp. strain PCC6803, a homolog of the *cemA* genes found in chloroplast genomes of higher plants, was cloned as a gene which complemented mutants defective in CO_2 transport (4). The gene encodes a hydrophobic protein of 247 amino acids (CotA). The exact function of CotA in CO_2 transport, however, remains unknown. The *cemA* genes in higher plants have been postulated to encode b-type heme-binding proteins (2, 9, 16, 20). Sasaki et al. have shown that the gene product in pea chloroplasts is localized in the inner envelope membrane (14). However, no data are available on the function of the *cemA* gene product (CemA). Both CemA and CotA contain four membrane-spanning domains, and their amino acid sequences are highly conserved, especially in the C-terminal regions (4). These results suggested that these chloroplast and cyanobacterial gene products may have a similar function, and elucidation of the role of CotA is an important step not only in the study of cyanobacterial physiology but also in clarifying the role of CemA in higher plants.

In this study, we constructed a mutant in which the *cotA* gene was completely deleted and demonstrated that the mutant does not extrude protons in the light. Light-induced proton extrusion has been found in a number of cyanobacterial strains. Kaplan et al. reported light-induced, sodium-dependent acidification of the medium by *Synechococcus* sp. and inferred that the acidification is mediated by H^+-ATPase (3). Scherer et al. (15) and Ogawa and Kaplan (7) observed a similar phenomenon for *Anabaena variabilis* and *Synechococcus* sp., respectively. They attributed the acidification to the efflux of protons produced as a result of CO_2 to HCO_3^- conversion during CO_2 transport. Lockau and Pfeffer (5) reported on a plasma membrane-located proton pump, the activity of which is light and sodium dependent. However, no data were available on a gene(s) involved in light-induced proton extrusion. Physiological studies of the *cotA*-less mutant suggest that inhibition of CO_2 transport in the mutant is a secondary effect of the inhibition of proton extrusion. A possible role of *cotA* in light-induced proton extrusion will be discussed.

* Corresponding author. Mailing address: Bioscience Center, Nagoya University, Chikusa-ku, Nagoya 464-01, Japan. Phone: 81-52-789-5215. Fax: 81-52-789-5214. Electronic mail address: h44975a@nucc.cc.nagoya-u.ac.jp.

MATERIALS AND METHODS

Growth conditions. Cells of *Synechocystis* sp. strain PCC6803 were grown at 30°C in BG11 medium (17) buffered with 20 mM 2-[4-(2-hydroxyethyl)-1-piperazinyl]ethanesulfonic acid (HEPES)–KOH (pH 7.0 to 8.0), *N,N*-bis(2-hydroxyethyl)glycine (bicine)–KOH (pH 8.5), or 2-(*N*-morpholino)ethanesulfonic acid (MES)–KOH (pH 6.4) during aeration with 3% (vol/vol) CO_2 in air. Low-sodium (low-Na^+) medium was prepared by adding NaCl (final concentration of 100 μM) to a modified BG11 medium in which all the sodium salts were replaced by potassium salts. Continuous illumination was provided by fluorescent lamps at 120 μmol of photosynthetically active radiation per m^2 per s (400 to 700 nm).

Transformation of *Synechocystis* sp. strain PCC6803. The *cotA* gene was replaced by the omega fragment (10), which confers spectinomycin and streptomycin resistance (the Sp^r/Sm^r cartridge). The plasmid containing the substituted gene was used to transform the wild-type (WT) cells of *Synechocystis* sp. strain PCC6803 into the Sp^r/Sm^r mutant, by the protocol of Williams and Szalay (21).

Silicone oil-filtering centrifugation. Time courses of uptake of $^{14}CO_2$ and $H^{14}CO_3^-$ into the intracellular inorganic carbon (C_i) pool of the WT and mutant cells were determined by the silicone oil-filtering centrifugation method (19). Cells were harvested by centrifugation and resuspended in 20 mM tris(hydroxymethyl)methyl-2-aminoethanesulfonic acid (TES)–KOH buffer (pH 8.0) containing 15 mM (or 100 μM) NaCl at a chlorophyll (Chl) concentration of 20 μg/ml. C_i uptake was initiated by the addition of $^{14}CO_2$ or $H^{14}CO_3^-$ (final concentrations of 25 and 120 μM, respectively; 2.0 MBq/μmol) in the light to the cell suspension layered on the silicone oil layer in a plastic tube (0.5 ml) and terminated by centrifugation. The sorbitol impermeable spaces of the WT and mutant cells and the pH of the cytoplasm were determined by the methods described by Heldt (1). The sorbitol impermeable spaces of the WT and mutant cells were 81 and 63 μl/mg of Chl, respectively. For the determination of the pH in the cytoplasm, the thylakoid space was assumed to be 10% of the sorbitol impermeable space.

Uptake of $^{22}Na^+$ into the WT and mutant cells was determined by the same method except that Na^+ uptake was initiated by the addition of $^{22}NaCl$ (final concentration of 100 μM or 15 mM; 4.7 or 0.47 MBq/μmol, respectively) in the light.

All the radioisotopes used in this study are the products of Dupont (Wilmington, Del.).

Measurements of proton exchange and O_2 evolution. The net proton exchange was measured at 30°C as described by Kaplan et al. (3). Cells were harvested by centrifugation and washed to achieve the required pH. Cells were suspended in the same buffer containing 100 μM NaCl, 15 mM KCl, or 15 mM NaCl at a Chl concentration of 14 μg/ml. Photosynthetic CO_2 fixation was inhibited by adding glyceraldehyde (11) to the cell suspension at a final concentration of 20 mM, and the pH of the external solution was monitored by a pH electrode with a meter (Inlar 423 and Delta 350; Mettler Toledo, Halstead Essex, United Kingdom) in a sample chamber used for the O_2 evolution measurement.

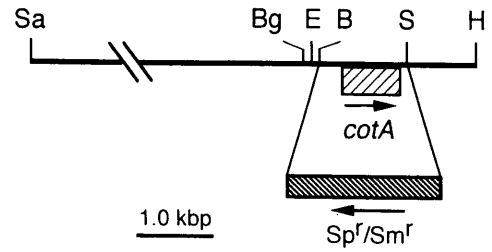

FIG. 1. Restriction map of a 6.9-kbp DNA insert in plasmid p*SC*. The 1.1-kbp *Bam*HI-*Spe*I fragment was replaced by the omega fragment (Sp^r/Sm^r cartridge) (10) in plasmid p*MSC*. The *cotA* gene (▨) and the omega fragment (▩) are indicated; the arrows show the directions of transcription. B, *Bam*HI; Bg, *Bgl*II; E, *Eco*RI; H, *Hpa*I; S, *Spe*I; Sa, *Sal*I.

The rate of photosynthetic O_2 evolution was measured at 30°C with an O_2 electrode (Rank Brothers, Cambridge, United Kingdom). The suspension buffer was 20 mM TES-KOH buffer (pH 8.0) containing various concentrations of NaCl.

For all these measurements, the cell suspension was illuminated with white light from a 150-W halogen lamp guided to the sample chamber (tube) by a glass fiber (MHF-150L; Kagaku Kyoeisha Ltd., Osaka, Japan). The light intensity at the surface of the chamber (tube) was 4.0 mmol of photosynthetically active radiation per m^2 per s.

Growth curves. Growth curves were determined from the rise in the optical density at 730 nm with a Shimadzu recording spectrophotometer (model UV-2200). The specific growth rates (μ) are expressed per day. (To convert the growth rates to doublings per day, divide ln 2 (0.693) by μ.)

Other methods. Unless otherwise stated, standard techniques were used for DNA manipulations (13). Pigments in the cells were extracted with methanol, and the Chl concentration in the extract was determined (8).

RESULTS

Construction of mutant (M29) lacking the *cotA* gene. The *cotA* gene in the p*SC* plasmid, constructed by inserting a 6.9-kbp *Sal*I-*Hpa*I fragment of *Synechocystis* sp. strain PCC6803 into the pKY184 vector (18), was replaced by the omega fragment (10) to produce the p*MSC* plasmid (Fig. 1). The p*MSC* plasmid was used to transform the WT cells of *Synechocystis* sp. strain PCC6803 to Sp^r/Sm^r resistance through homologous recombination. The transformant showed a mutant phenotype and was unable to grow in low-Na^+ medium. The segregation of the modified gene(s) in the mutant cells was complete, as confirmed by the PCR method (12) with genomic DNA of the mutant as a template (data not shown). The mutant thus constructed was named as M29.

Growth characteristics of WT and mutant cells. The growth rates of the WT and M29 cells were determined in standard (BG11) and low-Na^+ media buffered at various pHs during aeration with 3% (vol/vol) CO_2 in air and are plotted as a function of the pH of the growth media (Fig. 2). The WT cells showed 80% of the growth rate at pH 8.5 in the standard medium even at pH 6.4. In low-Na^+ medium, the WT cells were unable to grow at pH 6.4, and the growth rate at pH 7.2 was half the rate at pH 8.5. The M29 mutant grew well at pHs above 7.6 in standard medium but hardly grew at pHs below 7.2. In low-Na^+ medium, the mutant did not grow at any pH examined. With the CO_2 concentrations used in these experiments, the growth of cells was not limited by the supply of the carbon source. This finding was confirmed by the result obtained with the *ndhB*-less mutant, M55, which does not have C_i transport activity (6). The M55 mutant grew as fast as the WT in low-Na^+ medium at 3% (vol/vol) CO_2 in air but did not grow with air even in the standard medium (data not shown). Thus, the inability of M29 to grow under low-sodium conditions is not due to an insufficient supply of C_i.

The growth rates of the WT and mutant cells plotted as a function of the sodium concentration in the medium are shown in Fig. 3. The mutant required more than 5 mM sodium for growth (curve B) whereas the WT grew well at 100 μM NaCl (curve A). These results suggest that translocation of the ion(s) essential for growth of the cells is affected by the sodium concentration in the medium.

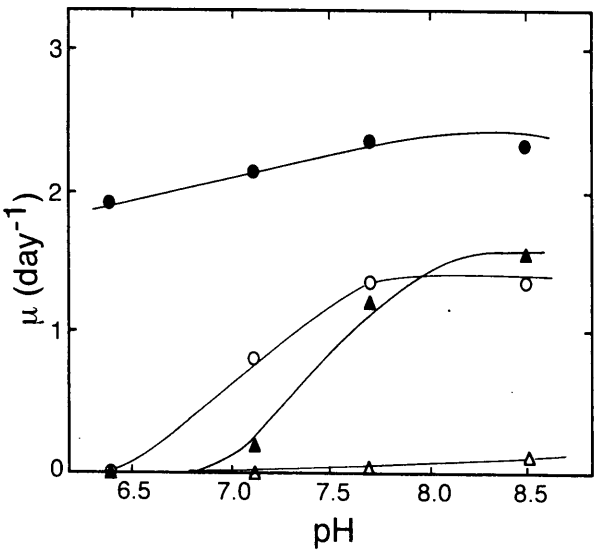

FIG. 2. Growth rates (μ) of WT (circles) and M29 (triangles) cells as a function of pH of the medium (closed symbols for BG11 medium and open symbols for low-Na^+ medium). Cultures were aerated with 3% (vol/vol) CO_2 in air.

O_2 evolution. O_2 evolution of the WT at 100 μM NaCl was as high as that at 15 mM NaCl (Fig. 4, curve A). In contrast, the level of activity in the M29 mutant was low at 100 μM NaCl and increased as the sodium concentration was raised to attain a maximum level above 1 mM NaCl (curve B). The results are consistent with the growth characteristics of the WT and mutant cells (Fig. 3), although growth of the mutant required higher concentrations of sodium.

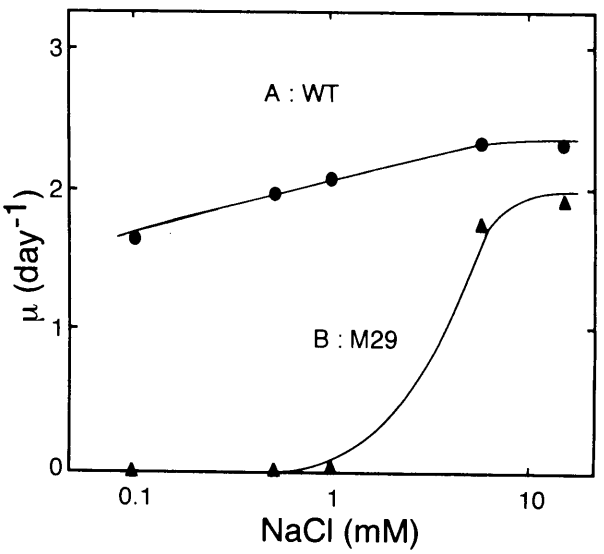

FIG. 3. Growth rates (μ) of WT (circles) and M29 (triangles) cells as a function of sodium concentration in BG11 medium (pH 8.0) in which all sodium salts were replaced by potassium salts. Cultures were aerated with 3% (vol/vol) CO_2 in air.

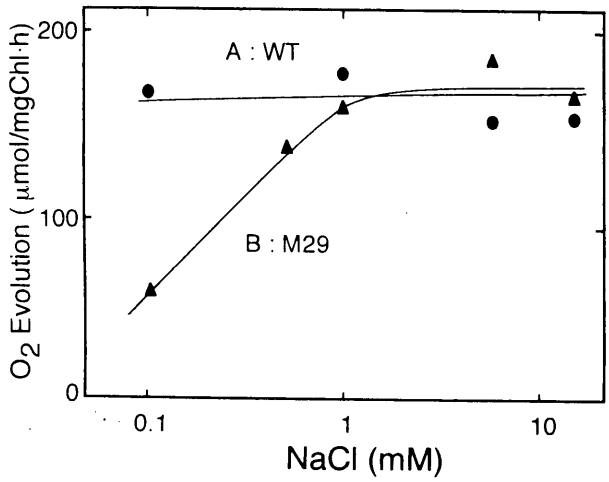

FIG. 4. Rates of O_2 evolution of WT (circles) and M29 (triangles) cells as a function of sodium concentration in the sample solution. Cells were suspended in 20 mM TES-KOH buffer (pH 8.0) containing various concentrations of NaCl.

^{22}Na uptake, C_i transport, and intracellular pH. Figure 5A shows the time courses of sodium uptake by the WT and M29 cells in light at the extracellular NaCl concentrations of 15 mM and 100 μM. There was no significant difference between sodium uptake in the WT and the mutant. Thus, the sodium uptake system is not impaired in the mutant. The rate of sodium uptake at 15 mM NaCl was about 60 times the rate at 100 μM NaCl.

Since *cotA* was cloned as a gene which complemented mutants defective in CO_2 transport, the gene product was postulated to encode a component of the CO_2 transport system (4). The deletion of the *cotA* gene, however, did not abolish CO_2 transport completely; M29 still possessed about 51 and 17% of the WT activity at 15 mM and 100 μM NaCl, respectively (Fig. 6B). The HCO_3^- transport was also reduced in the mutant and was 77 and 62% of the WT activity at 15 mM and 100 μM NaCl, respectively (Fig. 6B). On the basis of these results, we conclude that the observed inhibition of CO_2 transport (and HCO_3^- transport in M29) in the mutants described previously (4) and herein is a secondary effect which also affects the growth of the cells under low-sodium conditions.

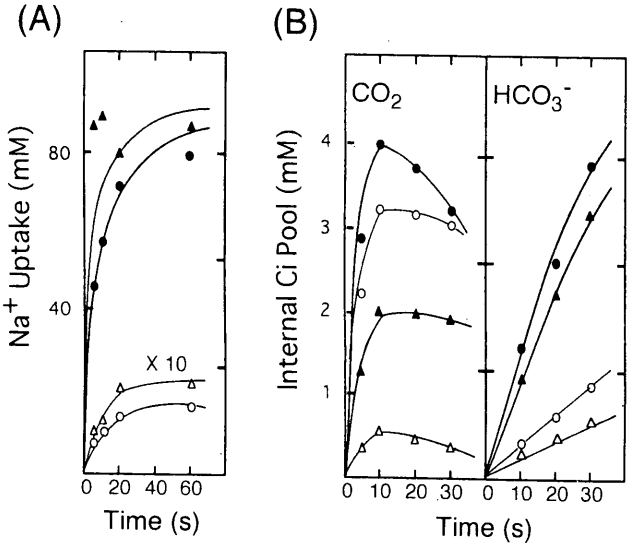

FIG. 5. (A) Time courses of $^{22}Na^+$ uptake by WT (circles) and M29 (triangles) cells in light. Cells were suspended in 20 mM TES-KOH buffer (pH 8.0) containing 100 μM (open symbols) or 15 mM (closed symbols) NaCl. The ^{22}NaCl solution was added to the cell suspension in the light in an amount to give the above concentrations of NaCl. (B) Time courses of uptake of CO_2 and HCO_3^- into the intracellular C_i pool of WT (circles) and M29 (triangles) cells. Cells were suspended in 20 mM TES-KOH buffer (pH 8.0) containing 100 μM (open symbols) or 15 mM (closed symbols) NaCl. The concentrations of CO_2 and HCO_3^- were 25 and 120 μM, respectively.

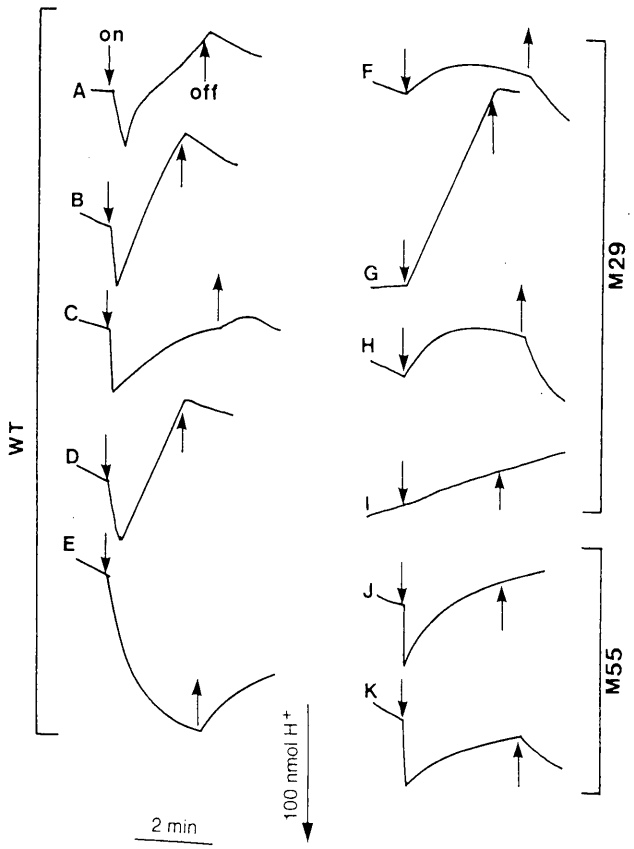

FIG. 6. Changes in pH of cell suspensions with (on) and without (off) light. WT (profiles A to E), M29 (profiles F to I), and M55 (profiles J and K) cells were suspended in 0.2 mM MES, HEPES, bicine-KOH buffer (pH 7.9 for profiles A to C, F to H, J and K; pH 6.5 for profiles D, E, and I) containing 15 mM KCl (profiles A and F) or 15 mM NaCl (profiles B to E, G to K). Photosynthetic CO_2 fixation of the cells was inhibited by 20 mM glyceraldehyde in profiles C, E, and K.

To test whether the inability of the mutant to grow under acidic conditions is due to a failure to control the intracellular pH, the uptake of ^{14}C-labeled 5,5-dimethyloxazolidine-2,4-dione was determined in WT and mutant cells suspended in BG11 medium buffered at pH 6.5. The pHs in the cytoplasm of the mutant were 6.9 in the dark and 7.5 in the light, which were essentially the same as pHs 6.8 and 7.5, respectively, obtained with the WT. Thus, the pH homeostasis is functioning normally in the mutant.

Net proton movements. The profiles of net proton movements determined in the WT and M29 cells are shown in Fig. 6. When the WT cells suspended in 0.2 mM MES, HEPES, bicine-KOH buffer (pH 7.9) containing 15 mM KCl (curve A) or NaCl (B) were illuminated, there was an acidification (H^+ extrusion or OH^- uptake) followed by an alkalization (H^+ uptake or OH^- extrusion) of the medium. In contrast, acidi-

fication was not observed for the M29 mutant with illumination under the same conditions, and only alkalization of the medium was observed (profiles F and G). Both acidification and alkalization were stimulated by 15 mM sodium (profiles A, B, F, and G), but the profiles obtained with 15 mM KCl and 100 μM NaCl were the same as those without NaCl (data not shown). Inhibition of photosynthetic CO_2 fixation by glyceraldehyde (11) significantly reduced the rate of alkalization (profiles C and H), indicating that the hydroxyl ion produced as a result of bicarbonate utilization is extruded in the light. Glyceraldehyde did not have any effect on light-induced acidification. The profile of net proton movement of the WT cells obtained at pH 6.5 (profile D) was the same as that obtained at pH 7.9 (profile B). However, the addition of glyceraldehyde completely abolished the alkalization at pH 6.5 (profile E). Proton movement was hardly observable for the M29 mutant at pH 6.5 in either the absence (profile I) or presence of glyceraldehyde. It is evident that M29 is a mutant which is unable to extrude protons in the light. The M55 mutant, which does not have C_i transport activity (6), showed profiles of proton movement similar to that of the WT (profiles J and K). These profiles indicate that the observed proton movement is not a phenomenon accompanied by C_i transport.

DISCUSSION

The present study clearly demonstrated that the mutant (M29) in which the *cotA* gene was completely deleted did not show light-induced proton extrusion (Fig. 6). Although light-induced acidification of the medium has been observed for a number of cyanobacterial strains, there were no data available on the gene(s) involved in this phenomenon. *cotA* is the first gene found to be involved in light-induced proton extrusion.

The extrusion of protons will produce $\Delta\psi$ and ΔpH across the cytoplasmic membrane to drive the transport of other ions. C_i transport was inhibited in the M29 mutant (Fig. 5B), indicating that transport is at least partially coupled with proton extrusion. However, we were not able to specify other transporting processes coupled with the observed light-induced proton extrusion. The growth characteristics of the mutant cannot be explained by the inhibition of C_i transport since 3% CO_2 in air (vol/vol) was bubbled during the growth rate determination. It is considered that the supply of the carbon source does not limit cell growth under these conditions. pH homeostasis was normal in the mutant at external pH 6.5, and there was no significant difference between sodium uptake in the WT and in the mutant (Fig. 5A). Therefore, at present we have to ascribe the inability of the mutant to grow in low-Na^+ medium or in standard medium below pH 7.0 to reduced activities of transport processes which are coupled to the light-induced proton extrusion in the WT. Some transport processes may be dependent on the pH and the sodium concentration.

The light-induced proton exchange was observed for the M55 mutant (Fig. 6, profiles J and K), which does not have active C_i transport and an NADPH-mediated photosystem-1 cyclic electron pathway (6). Thus, the acidification of the medium is not due to the efflux of protons produced during CO_2 uptake, and a cyclic electron flow of this type is not needed for energizing the proton exchange. The mechanism of proton extrusion dependent on the *cotA* gene product is not known. It is unlikely that the gene product is H^+-ATPase because of the absence of an ATP-binding motif in the deduced amino acid sequence. The gene product could be another type of H^+ transporter or a component involved in the energization or regulation of the transporting system.

ACKNOWLEDGMENTS

This study was supported by Grants-in-Aid for Scientific Research on Priority Areas (no. 0427103) from the Ministry of Education, Science and Culture, Tokyo, Japan, and the New Energy and Industrial Technology Development Organization (NEDO), Tokyo, Japan.

REFERENCES

1. **Heldt, H. W.** 1980. Measurement of metabolite movement across the envelope and of the pH in the stroma and the thylakoid space in intact chloroplast. Methods Enzymol. **69**:604–613.
2. **Hiratsuka, J., H. Shimada, R. Whittier, T. Ishibashi, M. Sakamoto, M. Mori, C. Kondo, Y. Honji, C. R. Sun, B. Y. Meng, Y. Q. Li, A. Kanno, Y. Nishizawa, A. Hirai, K. Shinozaki, and M. Sugiura.** 1989. The complete sequence of the rice (*Oryza sativa*) chloroplast genome: intermolecular recombination between distinct tRNA genes accounts for a major plastid DNA inversion during the evolution of the cereals. Mol. Gen. Genet. **217**:185–194.
3. **Kaplan, A., S. Scherer, and M. Lerner.** 1989. Nature of the light-induced H^+ efflux and Na^+ uptake in cyanobacteria. Plant Physiol. **89**:1220–1225.
4. **Katoh, A., K. S. Lee, H. Fukuzawa, K. Ohyama, and T. Ogawa.** 1996. *cemA* homologue essential to CO_2 transport in the cyanobacterium, *Synechocystis* PCC6803. Proc. Natl. Acad. Sci. USA **93**:4006–4010.
5. **Lockau, W., and S. Pfeffer.** 1982. A cyanobacterial ATPase distinct from the coupling factor of photophosphorylation. Z. Naturforsch. Teil C **37**:658–664.
6. **Ogawa, T.** 1991. A gene homologous to the subunit-2 gene of NADH dehydrogenase is essential to inorganic carbon transport of *Synechocystis* PCC6803. Proc. Natl. Acad. Sci. USA **88**:4275–4279.
7. **Ogawa, T., and A. Kaplan.** 1987. The stoichiometry between CO_2 and H^+ fluxes involved in the transport of inorganic carbon in cyanobacteria. Plant Physiol. **83**:888–891.
8. **Ogawa, T., and K. Shibata.** 1965. A sensitive method for determining chlorophyll b in plant extracts. Photochem. Photobiol. **4**:193–200.
9. **Ohyama, K., H. Fukuzawa, T. Kohchi, H. Shirai, T. Sano, S. Sano, K. Umesono, Y. Shiki, M. Takeuchi, Z. Chang, S. Aota, H. Inokuchi, and H. Ozeki.** 1986. Chloroplast gene organization deduced from complete sequence of liverwort *Marchantia polymorpha* chloroplast DNA. Nature (London) **322**:572–574.
10. **Prentki, P., and H. M. Krisch.** 1984. In vitro insertional mutagenesis with a selectable DNA fragment. Gene **29**:303–313.
11. **Romero, J. M., C. Lara, and M. G. Guerrero.** 1985. Dependence of nitrate utilization upon active CO_2 fixation in *Anacystis nidulans*: a regulatory aspect of the interaction between photosynthetic carbon and nitrogen metabolism. Arch. Biochem. Biophys. **237**:396–401.
12. **Saiki, R. K., D. H. Gelfand, S. Stoffel, S. J. Scharf, R. Higuchi, G. T. Horn, K. B. Mullis, and H. A. Erlich.** 1988. Primer-directed enzymatic amplification of DNA with a thermostable DNA polymerase. Science **239**:487–491.
13. **Sambrook, J., E. F. Fritsch, and T. Maniatis.** 1989. Molecular cloning: a laboratory manual, 2nd ed. Cold Spring Harbor Laboratory Press, Cold Spring Harbor, N.Y.
14. **Sasaki, Y., K. Sekiguchi, Y. Nagano, and R. Matsuno.** 1993. Chloroplast envelope protein encoded by chloroplast genome. FEBS Lett. **316**:93–98.
15. **Scherer, S., I. Hinrichs, and P. Boger.** 1988. Light-induced proton release by the cyanobacterium *Anabaena variabilis* dependence on CO_2 and Na^+. Plant Physiol. **86**:769–772.
16. **Shinozaki, K., M. Ohme, M. Tanaka, T. Wakasugi, N. Hayashida, T. Matsubayashi, N. Zaita, J. Chunwongse, J. Obokata, K. Yamaguchi-Shinozaki, C. Ohto, K. Torazawa, B. Y. Meng, M. Sugita, H. Deno, T. Kamogashira, K. Yamada, J. Kusuda, F. Takaiwa, A. Kato, N. Tohdoh, H. Shimada, and M. Sugiura.** 1986. The complete nucleotide sequence of the tobacco chloroplast genome: its gene organization and expression. EMBO J. **5**:2043–2049.
17. **Stanier, R. Y., R. Kunisawa, M. Mandel, and G. Cohen-Bazire.** 1971. Purification and properties of unicellular blue-green algae (order *Chroococcales*). Bacteriol. Rev. **35**:171–205.
18. **Ueguchi, C., and K. Itoh.** 1992. Multicopy suppression: an approach to understanding intracellular functioning of the protein export system. J. Bacteriol. **174**:1454–1461.
19. **Volokita, M., D. Zenvirth, A. Kaplan, and L. Reinhold.** 1984. Nature of the inorganic carbon species actively taken up by the cyanobacterium *Anabaena variabilis*. Plant Physiol. **76**:599–602.
20. **Willey, D. L., and J. C. Gray.** 1990. An open reading frame encoding a putative haem-binding polypeptide is cotranscribed with the pea chloroplast gene for apocytochrome f. Plant Mol. Biol. **15**:347–356.
21. **Williams, J. G., and A. A. Szalay.** 1983. Stable integration of foreign DNA into the chromosome of the cyanobacterium *Synechococcus* R2. Gene **24**: 37–51.

JOURNAL OF BACTERIOLOGY, June 1997, p. 3845–3850
0021-9193/97/$04.00+0

Vol. 179, No. 12

Size of *cotA* and Identification of the Gene Product in *Synechocystis* sp. Strain PCC6803

MASATOSHI SONODA,[1] KATSUHIKO KITANO,[1] AKIRA KATOH,[1] HIROKAZU KATOH,[2] HIROSHI OHKAWA,[1] AND TERUO OGAWA[1,2]*

Biochemical Regulation, School of Agriculture,[1] and Bioscience Center,[2] Nagoya University, Nagoya 464-01, Japan

Received 14 October 1996/Accepted 5 April 1997

***cotA* of *Synechocystis* sp. strain PCC6803 is a gene involved in light-induced proton extrusion (A. Katoh, M. Sonoda, H. Katoh, and T. Ogawa, J. Bacteriol. 178:5452–5455, 1996). There are two possible initiation codons in *cotA*, and either long (L-) or short (S-) *cotA* encoding a protein of 440 or 247 amino acids could be postulated. To determine the gene size, we inserted L-*cotA* and S-*cotA* into the genome of a *cotA*-less mutant (M29) to construct M29(L-*cotA*) and M29(S-*cotA*), respectively. M29(L-*cotA*) showed essentially the same net proton movement profile as the wild type, whereas no light-induced proton extrusion was observed with M29(S-*cotA*). Two kinds of antibodies were raised against partial gene products of the N- and C-terminal regions of L-*cotA*, respectively, fused to glutathione *S*-transferase expressed in *Escherichia coli*. Both antibodies cross-reacted with a band at 52 kDa in both cytoplasmic and thylakoid membrane fractions of the wild-type cells. The same cross-reacting band was present in the membranes of M29(L-*cotA*) but not in M29 or M29(S-*cotA*). These antibodies cross-reacted more strongly with the cytoplasmic membrane fraction than with the thylakoid membrane fraction. The antibody against NrtA, a nitrate transporter protein present only in the cytoplasmic membrane, also cross-reacted with the thylakoid membrane fraction strongly. Based on these results we concluded that CotA of 440 amino acids (51 kDa) is located in the cytoplasmic membrane. Whether CotA is absent in the thylakoid membrane remains to be solved.**

cotA of *Synechocystis* sp. strain PCC6803 is a homolog of *cemA* which has been found in chloroplast genomes of various plants (3, 6, 15, 24, 29, 30). *cemA* genes of higher plants encode proteins of 229 to 231 amino acids (3, 24, 29, 30), whereas those of liverwort (15) and *Chlamydomonas reinhardtii* spp. (EMBL Sequence Library, accession no. X90559; N. Rolland) encode much larger proteins, of 434 and 500 amino acids, respectively, as estimated from their DNA sequences. The *cemA* product has been found in the inner envelope membrane of pea chloroplasts as a band at 34 kDa during sodium docecyl sulfate-polyacrylamide gel electrophoresis (SDS-PAGE) (24), but the products of the liverwort and *Chlamydomonas* genes have not been identified. There are two possible initiation codons in *cotA* of *Synechocystis*. When the first ATG was postulated as the initiation codon, the gene product was a 51-kDa protein of 440 amino acids. We concluded in a previous paper that the translation started from the second ATG codon, giving a gene product of 29 kDa (247 amino acids), close in size to CemA of higher plant chloroplasts (6, 24). However, a preliminary experiment to identify the gene product suggested that it may be much larger. This led us to the present study to determine the size of *cotA* and to identify and locate the gene product.

A *cotA* deletion mutant of *Synechocystis* (M29) constructed in a previous study was used for this purpose. The mutant did not show light-induced proton extrusion and was unable to grow at pH 6.4 or in a low-sodium medium (7). We inserted long (L-) or short (S-) *cotA* into a neutral site of the genome of this mutant to see which *cotA* transforms the mutant to the wild phenotype. Measurements of growth characteristics and light-induced proton extrusion of these two kinds of *cotA*-inserted M29 mutants and Western analysis using antibodies raised against partial gene products enabled us to determine the size of *cotA* and to identify and locate the gene product.

* Corresponding author. Mailing address: Bioscience Center, Nagoya University, Chikusa-ku, Nagoya 464-01, Japan. Phone: 81-52-789-5215. Fax: 81-52-789-5214. E-mail: h44975a@nucc.cc.nagoya-u.ac.jp.

MATERIALS AND METHODS

Growth conditions. Wild-type (WT) and mutant cells of *Synechocystis* sp. strain PCC6803 were grown at 30°C in BG-11 medium (28) buffered with 20 mM *N*-tris(hydroxymethyl)methyl-2-aminoethanesulfonic acid (TES)–KOH at pH 8.0 during aeration with 3% (vol/vol) CO_2 in air. Continuous illumination was provided by fluorescent lamps at 120 μmol of photosynthetically active radiation/m^2s (400 to 700 nm).

Transformation of *Synechocystis*. An L-*cotA* or S-*cotA* gene was inserted into a neutral site of the genome of a *cotA*-less mutant (M29) of *Synechocystis* sp. strain PCC6803 (see Fig. 1 and 2). The plasmid containing L-*cotA* or S-*cotA* with the kanamycin resistance (Km^r) cartridge (16) was used to transform M29 cells into Km^r mutants, by the protocol of Williams and Szalay (31).

Measurements of proton exchange. Net proton exchange was measured at 30°C as described previously (5, 7). Cells were harvested by centrifugation, washed twice with 0.2 mM TES-KOH buffer (pH 8.0), and then suspended in the same buffer containing 15 mM NaCl and chlorophyll at a concentration of 14 μg/ml. The pH of the cell suspension was monitored by a pH electrode with a meter (Inlar 423 electrode and Delta 350 meter; Mettler Toledo, Halstead, Essex, United Kingdom). Light from a 150-W halogen lamp was guided by a glass fiber (catalog no. MHF-150L; Kagaku Kyoeisha Ltd., Osaka, Japan) to illuminate the sample in the chamber at an intensity of 4.0 mmol of photosynthetically active radiation/m^2s.

Preparation of antibodies. The DNA fragments encoding 191- and 38-amino-acid residues of the N- and C-terminal regions of *cotA* (see Fig. 2), amplified by PCR (22), were ligated to pGEX-2T (Pharmacia, Uppsala, Sweden) containing the glutathione *S*-transferase (GST) gene (*gst*). The fusion proteins (GST-191 and GST-38) were induced for 3 h at 37°C by adding 1 mM isopropyl-β-D-thiogalactopyranoside (IPTG) to *Escherichia coli* cells transformed with the chimeric plasmids. The GST protein was also expressed in *E. coli*. GST-38 formed inclusion bodies, while GST-191 and GST were recovered as soluble proteins. The inclusion bodies were isolated, solubilized with 5% SDS, and electrophoresed by SDS-PAGE (4, 9). A predominant GST-38 band at 31 kDa was cut out from the gel and was mashed with a mortar and pestle to be injected into rabbits. GST-191 and GST were purified on a glutathione-Sepharose 4B column (Pharmacia).

The antibodies against GST-191 and GST-38 fusion proteins were obtained from rabbits according to the standard procedure (2). The antibody against

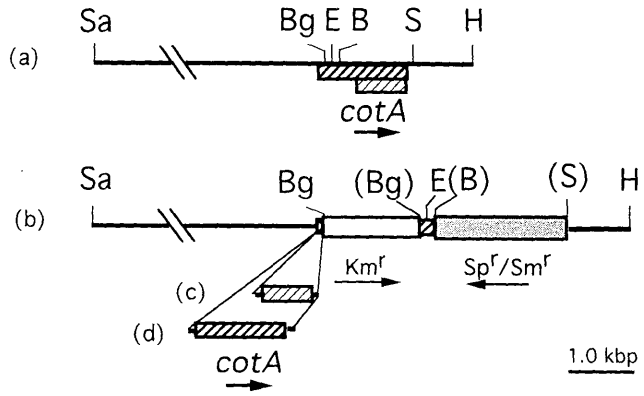

FIG. 1. (a) Restriction map of a 6.9-kbp DNA insert in plasmid p*SC*. L-*cotA* and S-*cotA* are indicated by the thickly and thinly hatched bars, respectively, with the arrow showing the direction of transcription. (b) The 1.1-kbp *Bam*HI/*Spe*I fragment was replaced with the omega fragment (Sp^r/Sm^r cartridge) (21) and the kanamycin resistance cartridge was inserted at the *Bgl*II site to produce plasmid p*KMSC*. DNA fragments containing S-*cotA* and L-*cotA* were inserted at the *Bgl*II site in the p*KMSC* plasmid to produce the p*KMSC*(S-*cotA*) (c) and p*KMSC*(L-*cotA*) (d) plasmids. The sites shown in parentheses are not present in the constructs. Abbreviations for restriction enzymes: B, *Bam*HI; Bg, *Bgl*II; E, *Eco*RI; H, *Hpa*I; S, *Spe*I; Sa, *Sal*I.

GST-38 was purified by the method reported by Kelly et al. (8). The fused protein in the gel was blotted onto a polyvinylidene difluoride membrane and reacted with the antibody. After washing, the antibody was eluted from the membrane with 0.2 M glycine-HCl solution (pH 2.8), containing 1 mM EGTA and bovine serum albumin (0.1 mg/ml). The antibody immunospecific to GST was similarly purified from the antibody against GST-38. The antiserum for GST-191 was used for Western analysis without further purification.

Preparation of membrane and soluble fractions. Cytoplasmic and thylakoid membranes and soluble fractions were prepared from the WT cells by modification (20) of the method of Omata and Murata (17). Cells were disrupted through a French pressure cell at 120 MPa. Total membrane fractions were prepared from the WT and mutant cells as described by Nilsson et al. (11).

Electrophoresis and Western analysis. SDS-PAGE was performed according to the system of Laemmli (9) as modified by Ikeuchi and Inoue (4). Polypeptides were electrotransferred to a nitrocellulose membrane and reacted with the antibodies. Goat anti-rabbit immunoglobulin G conjugated to peroxidase was used as the secondary antibody, and reacting bands were detected with an enhanced chemiluminescence kit (Amersham).

Northern blot analysis. To determine the size of transcript of the *cotA* gene, RNAs in the WT and mutant cells of *Synechocystis* were extracted by the method of Aiba et al. (1). The probes used for hybridization were PCR products containing S-*cotA* (see Fig. 1 and 2) and the carbonic anhydrase-like gene (open reading frame [ORF] slr0051 in the CyanoBase sequence bank of the Kazusa DNA Research Institute).

Other methods. Unless otherwise stated, standard techniques were used for DNA manipulation (23). Pigments in the cells were extracted by methanol, and the chlorophyll concentration in the extract was determined (14).

RESULTS

Insertion of different sizes of *cotA* into a *cotA*-less mutant. The p*SC* plasmid contains the *cotA* gene of *Synechocystis* sp. strain PCC6803 in a 6.9-kbp DNA insert (Fig. 1a) in the pKY184 vector (29). Two sizes of *cotA*, encoding proteins of 440 and 247 amino acids, are shown (Fig. 1a). The *Bam*HI/*Spe*I fragment containing *cotA* was replaced by the omega fragment (21) to produce plasmid p*MSC*, which was used to construct the *cotA*-less mutant of *Synechocystis*, M29 (not shown; see reference 7). A kanamycin resistance (Km^r) cartridge having the *Bgl*II and *Bam*HI sites at each end (synthesized by the PCR method with p*UC4K* as a template) was inserted at the *Bgl*II site of p*MSC* to produce plasmid p*KMSC* (Fig. 1b). The DNA

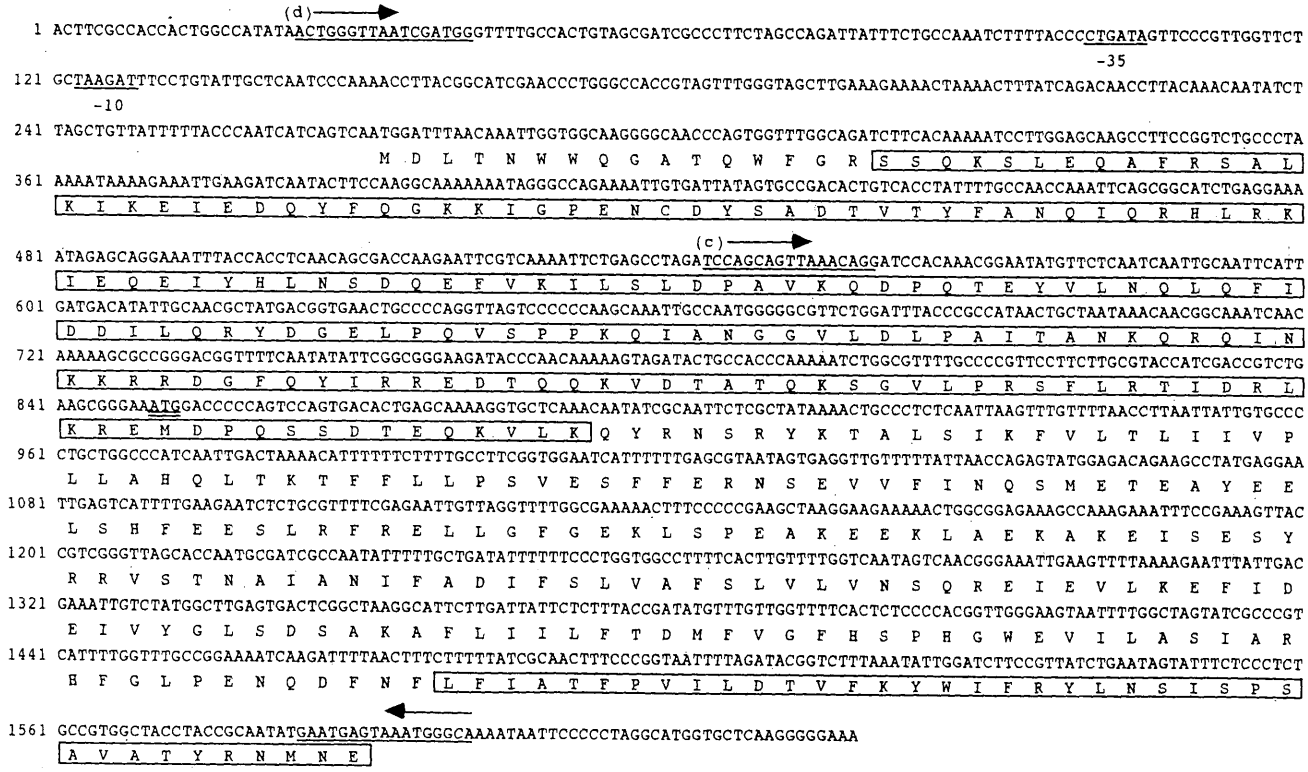

FIG. 2. Nucleotide sequence of DNA in the region of *cotA* and deduced amino acid sequence (single-letter code) of the protein encoded by *cotA*. The putative promoter sequences (−10 and −35) are underlined. Sequences of primers used for PCR to synthesize S-*cotA* (c) and L-*cotA* (d) are also underlined, and arrows above the sequence indicate the directions. An initiation codon postulated for S-*cotA* is double underlined.

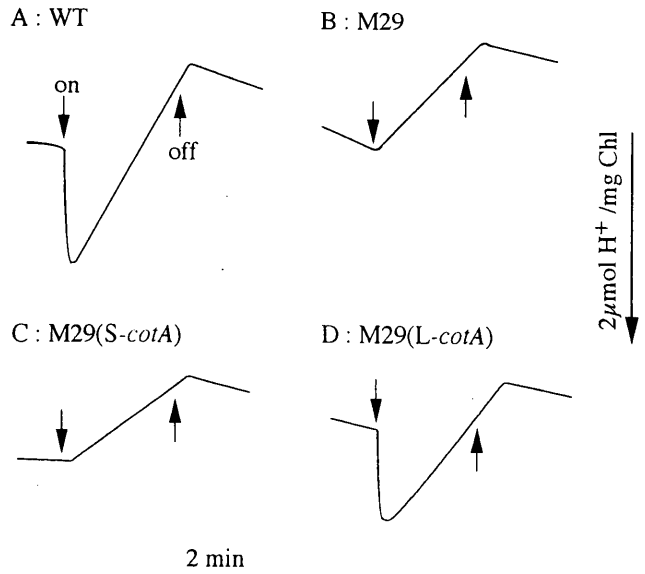

FIG. 3. Changes in pH of cell suspensions upon switching the light on and off. WT (A), M29 (B), M29(S-*cotA*) (C), and M29(L-*cotA*) (D) cells were suspended in 0.2 mM TES-KOH buffer (pH 8.0) containing 15 mM NaCl. Chl, chlorophyll.

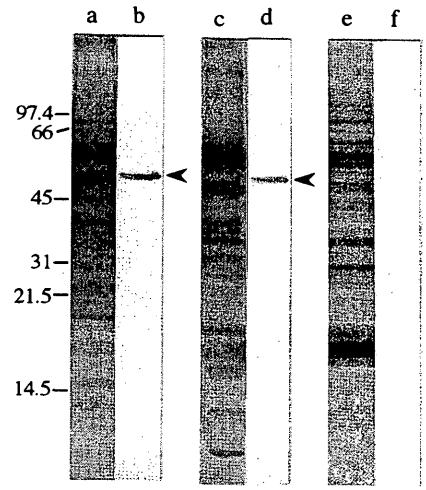

FIG. 4. Electrophoretic profiles showing CBB staining patterns of polypeptides (lanes a, c, and e) and immunoblots of CotA (b, d, and f) in the cytoplasmic membrane (a and b) and thylakoid membrane (c and d) fractions and soluble fraction (e and f) of *Synechocystis* sp. strain PCC6803. Samples (30 μg of proteins for CBB staining and 15 μg for immunoblotting) were solubilized at room temperature, boiled for a few minutes, and run in a 12% gel containing 7 M urea. The antibody against GST-191 was used for immunoblottings. The sizes of marker proteins are indicated (in kilodaltons) on the left.

fragments containing S-*cotA* and L-*cotA* were synthesized by the PCR method (using primers shown in Fig. 2) and were inserted into p*KMSC* to produce the p*KMSC*(S-*cotA*) and p*KMSC*(L-*cotA*) plasmids, respectively (Fig. 1c and d). These plasmids were used to transform M29 to Km^r through homologous recombination. The transformants are referred to in this work as M29(S-*cotA*) and M29(L-*cotA*), respectively.

Growth characteristics. M29(L-*cotA*) and M29(S-*cotA*) cells were grown in BG-11 medium buffered at pH 8.0 and then on agar plates buffered to pH 8.0 or 6.5. Kanamycin (10 μg/ml) was added to the medium, and 3% (vol/vol) CO_2 in air was supplied during the culture. Both M29(L-*cotA*) and M29(S-*cotA*) grew well on the plates buffered to pH 8.0, but M29(S-*cotA*) was unable to grow on the plates buffered to pH 6.5. Thus, M29(S-*cotA*) still showed the mutant phenotype whereas M29(L-*cotA*) formed many colonies even at pH 6.5.

Net proton movements. When the WT cells suspended in 0.2 mM TES-KOH buffer (pH 8.0) containing 15 mM NaCl were illuminated, there was an acidification followed by an alkalization of the medium (Fig. 3A). The light-induced acidification was not observed with the M29 mutant; only alkalization of the medium was observed (Fig. 3B). These characteristics of the WT and mutant were essentially the same as those reported previously (7). The M29(S-*cotA*) cells showed the same characteristics as M29 (Fig. 3C). In contrast, M29(L-*cotA*) showed the WT activity of light-induced proton extrusion (Fig. 3D). The results clearly demonstrated that L-*cotA* but not S-*cotA* is functional for light-induced proton extrusion.

Identification of CotA. Western analysis of the membrane and soluble fractions of the WT *Synechocystis* sp. strain PCC6803 indicated that a protein in the cytoplasmic and thylakoid membrane fractions with an apparent molecular mass of 52 kDa cross-reacted with the antibody raised against GST-191 (lanes b and d in Fig. 4). The same band cross-reacted with the antibody raised against GST-38. No reacting band was observed in the soluble fraction (lane f). The antibody immunospecific to the GST protein did not react with this band (data not shown), indicating that the protein cross-reacted with the antibodies immunospecific to the partial CotA in the fused proteins. To confirm that the 52-kDa cross-reacting band is the product of *cotA*, Western analysis was performed with the total membrane fractions prepared from the WT, M29, M29(L-*cotA*), and M29(S-*cotA*) cells, and the results are shown in Fig. 5. No cross-reacting band was observed at 52 kDa in the mem-

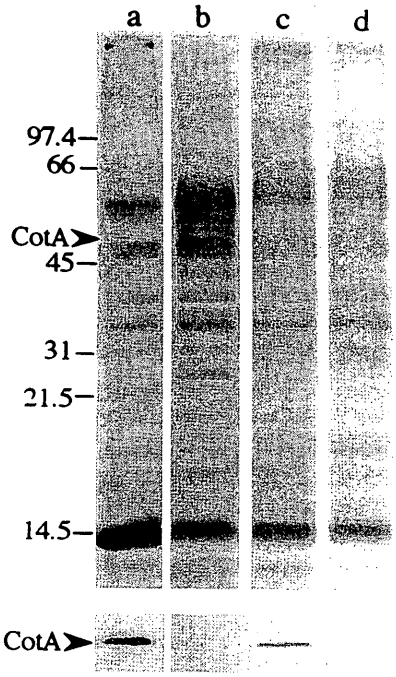

FIG. 5. Electrophoretic profiles showing CBB staining patterns of polypeptides (upper lanes) and immunoblots of CotA (lower lanes) of the membrane fractions of WT (lane a), M29 (lane b), M29(L-*cotA*) (lane c), and M29(S-*cotA*) (lane d). The conditions for SDS-PAGE and the indication of marker proteins are as described in the legend to Fig. 4. The antibody against GST-38 was used for immunoblottings.

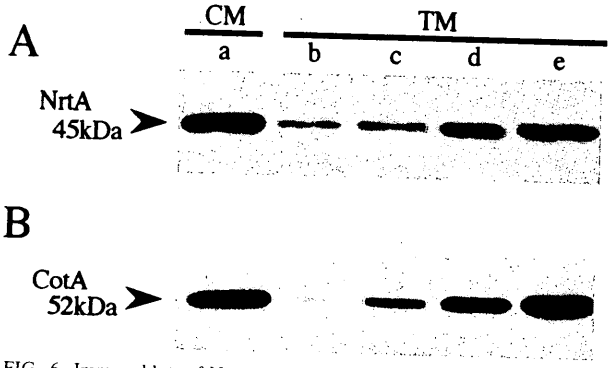

FIG. 6. Immunoblots of NrtA (upper column) and CotA (lower column) in the cytoplasmic membrane (CM [lane a]) and thylakoid membrane (TM [lanes b to e]) fractions of *Synechocystis* sp. strain PCC6803. The conditions used for SDS-PAGE are described in the legend to Fig. 3, and the amounts of proteins loaded were 15 μg (lane e), 7.5 μg (lanes a and d), 3 μg (lane c), and 1.5 μg (lane b).

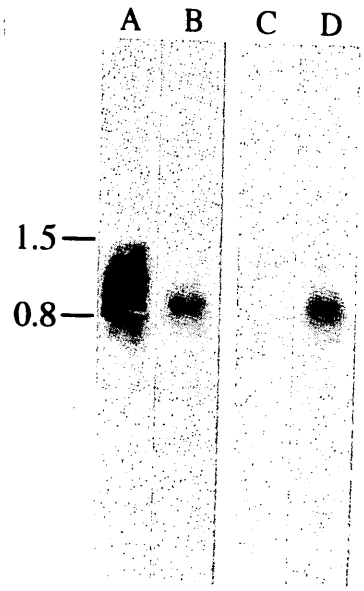

FIG. 7. Northern blot analysis of total RNA from WT (lanes A and B) and M29 (lanes C and D) cells of *Synechocystis* sp. strain PCC6803. RNA was denatured with formaldehyde, electrophoresed on a 1.2% agarose gel, transferred to a nylon membrane, and hybridized with the ^{32}P-labeled DNA fragment containing S-*cotA* (lanes A and C) or the carbonic anhydrase-like gene (lanes C and D). RNA sizes are shown to the left (in kilobases).

brane fractions of M29 or M29(S-*cotA*). As expected, the cross-reacting 52-kDa band was clearly observed with the WT membranes and the same cross-reacting band was found in the M29(L-*cotA*) membrane fraction. Evidently, the protein that cross-reacted with the antibodies is the product of *cotA* (CotA). The size of CotA estimated from SDS-PAGE agreed with that deduced from the nucleotide sequence of L-*cotA*. The 52-kDa band was not detected on the Coomassie brilliant blue R-250 (CBB) staining profiles of the membranes of WT or M29(L-*cotA*) (lanes a and c in Fig. 4 and lanes a and c in Fig. 5). The amount of CotA appears to be low.

Location of CotA. Both cytoplasmic and thylakoid membrane fractions of the WT contained CotA (Fig. 4). It was not possible to isolate these two types of membranes from *Synechocystis* sp. strain PCC6803 cells without cross-contamination. Therefore, the presence of CotA in the fractions of these two types of membranes do not necessarily mean that CotA is present in both membranes. As reported previously, about one-fourth of the proteins in the cytoplasmic membrane fraction originated from contaminated thylakoid membrane (12). In order to test whether the thylakoid membrane fraction is free from contaminated cytoplasmic membrane, we have tested the cross-reactivity of the thylakoid membrane fraction to the antibody against NrtA, which is a protein involved in nitrate transport and is localized only in the cytoplasmic membrane of *Synechococcus* sp. strain PCC7942 (18, 19). The antibody against NrtA strongly cross-reacted with the thylakoid membrane fraction of *Synechocystis*, with the cross-reactivity about half that with the cytoplasmic membrane fraction (Fig. 6A). This result, together with the 25% contamination of thylakoid membrane in the cytoplasmic membrane fraction (12), indicated that about 38% of the proteins in the thylakoid membrane fraction originated from contaminated cytoplasmic membrane. If CotA is localized only in the thylakoid membrane, the cross-reactivity of the thylakoid membrane fraction with the antibody against GST-191 must be about 2.5 times that of the cytoplasmic membrane fraction. The cross-reactivity of the antibody against GST-191 with the thylakoid membrane fraction was, however, about half that with the cytoplasmic membrane fraction (lanes b and d in Fig. 4, lanes a and d in Fig. 6B). The results clearly demonstrated that CotA is located in the cytoplasmic membrane. The cross-reactivities of the antibodies against GST-191 and NrtA with the thylakoid membrane fraction were similar, which suggested that the antibody against GST-191 cross-reacted predominantly, if not totally, with contaminated cytoplasmic membrane. It is, however, not possible at present to exclude the possibility that a small amount of CotA is present in the thylakoid membrane.

Northern analysis. Northern analysis with RNAs prepared from the WT in the previous study indicated that the *cotA* transcript is 0.8 kb (6), which is much smaller than the L-*cotA* transcript. The *Bam*HI/*Spe*I fragment used as a probe in the previous study, however, cross-reacted with the transcript for the ORF on the complementary strand downstream of *cotA*. This ORF was strongly expressed, and the size of the transcript was 0.8 kb (1a). To avoid this complexity, we used the PCR product containing S-*cotA* as a probe (Fig. 1 and 2) and performed Northern analysis with RNAs from the WT and M29. The transcript was found in the WT as a smear band starting at 1.4 to 1.5 kb, but no hybridizing band was detected with M29 (lanes A and C in Fig. 7). Thus, the probe specifically cross-reacted with the *cotA* transcript of the L-*cotA* size. When the carbonic anhydrase-like gene was used as a probe, both WT and mutant RNAs gave a single band at 950 bases (lanes B and D). Thus, the quality of these RNA preparations is sufficiently high.

***cotA* sequences.** The nucleotide sequence of L-*cotA* and the amino acid sequence deduced from the nucleotide sequence are shown in Fig. 2, where amino acid sequences in the fusion proteins, GST-191 and GST-38, are boxed. There was no Shine-Dalgarno (26) sequence upstream of the initiation codon. A possible promoter sequence can be found upstream of the initiation codon at bases 100 to 105 (CTGATA [−35 box]) and 123 to 128 (TAAGAT [−10 box]).

Comparison of CotA and CemA sequences. As reported in a previous paper (6), the amino acid sequence deduced from the nucleotide sequence of the *cotA* gene of *Synechocystis* sp. strain PCC6803 showed significant similarity to the sequences of *cemA* gene products of various plants (3, 15, 24, 27, 30). Figure 8 shows the homology in the amino acid sequences among CotA of *Synechocystis* and CemA of liverwort (15) and

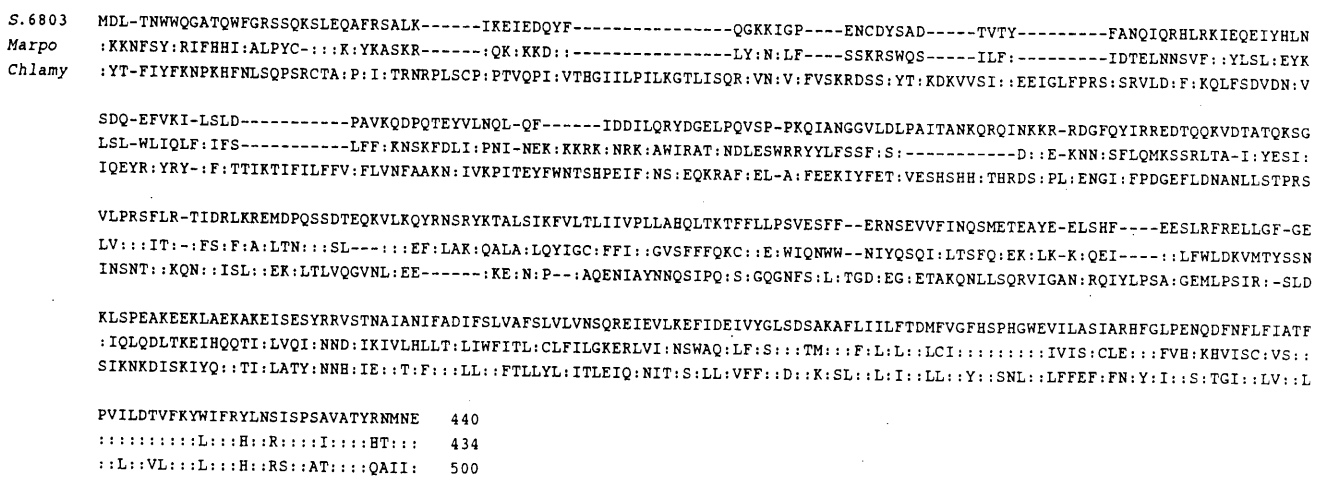

FIG. 8. Comparison of the deduced amino acid sequences for CotA of *Synechocystis* (*S.*6803), CemA of liverwort (*Marpo*), and *Chlamydomonas* (*Chlamy*). Residues in CemA identical to corresponding residues in CotA are indicated (:).

Chlamydomonas. The homology was high in the C-terminal regions but was low in the N-terminal regions.

DISCUSSION

The present study clearly demonstrated that *cotA* consists of 1,320 nucleotides and encodes a protein of 440 amino acids. Northern analysis using a probe specific to *cotA* (Fig. 7) and the strong cross-reactivity of the antibodies against GST-191 and GST-38 with a band at 52 kDa (Fig. 4 and 5) supported this result. Therefore, CotA has 200 additional amino acids differing from CemA of higher plants and is similar in size to CemA of liverwort (15) and *Chlamydomonas*. Although there was significant homology in the amino acid sequences in the C-terminal region among CotA of *Synechocystis* and CemA of various plants (3, 15, 24, 27, 30) and *Chlamydomonas*, the homology of the additional 200- to 250-amino-acid sequences in the N-terminal region was low among CotA and CemA of liverwort and *Chlamydomonas* (Fig. 8). These amino acids in the N-terminal regions might have been lost in the course of evolution.

The antibodies raised against GST-191 and GST-38 cross-reacted with the cytoplasmic and thylakoid membrane preparations. As described in Results, the stronger cross-reactivity of the antibodies with the cytoplasmic membrane fraction indicates that CotA is present in the cytoplasmic membrane. The thylakoid membrane fraction of *Synechocystis* sp. strain PCC7942 contains about 8% contaminated cytoplasmic membrane (18). The same fraction from *Synechocystis* was, however, contaminated with more cytoplasmic membrane. Although results in this study showed that the cross-reactivity of the antibodies with the thylakoid membrane fraction is predominantly, if not totally, due to contaminated cytoplasmic membrane, we were unable to exclude the possibility that thylakoid membrane contains a small amount of CotA. CemA, a homolog of CotA, is absent in the thylakoid membrane of pea chloroplasts (24). This strongly suggests that CotA is also absent in the thylakoid membrane of *Synechocystis*.

Light-induced proton extrusion has been observed with various cyanobacterial strains (5, 7, 10, 13, 25). The proton extrusion was abolished in a *cotA* deletion mutant (M29) (Fig. 3B and reference 7). The finding of the recovery of light-induced proton extrusion in M29(L-*cotA*) confirmed that the inhibition of this activity was not the result of a pleiotropic effect of *cotA* deletion. Thus, CotA in the cytoplasmic membrane has a role in the light-induced proton extrusion, although the exact function of CotA in this reaction is not known. The absence of an ATP-binding motif in *cotA* indicates that CotA is not an H^+-ATPase itself. It is possible that CotA plays a role in regulating or activating an H^+-ATPase or it could be another type(s) of proton pump. Further studies are in progress to answer these questions on the role of CotA.

ACKNOWLEDGMENTS

This study was supported by a Grant-in-Aid for Scientific Research on Priority Areas (no. 0427103) from the Ministry of Education, Science, and Culture, Japan, and by the New Energy and Industrial Technology Development Organization (NEDO), Japan.

We thank T. Omata (Nagoya University) for providing us with the antibody against NrtA.

REFERENCES

1. **Aiba, H., S. Adhya, and B. de Crombrugghe.** 1981. Evidence for two functional *gal* promoters in intact *Escherichia coli* cells. J. Biol. Chem. **256:**11905–11910.
1a. **Fukuzawa, H.** Personal communication.
2. **Harlow, E., and D. Lane (ed.).** 1988. Antibodies: a laboratory manual, p. 92–119. Cold Spring Harbor Laboratory Press, Cold Spring Harbor, N.Y.
3. **Hiratsuka, J., H. Shimada, R. Whittier, T. Ishibashi, M. Sakamoto, M. Mori, C. Kondo, Y. Honji, C. R. Sun, B. Y. Meng, Y. Q. Li, A. Kanno, Y. Nishizawa, A. Hirai, K. Shinozaki, and M. Sugiura.** 1989. The complete sequence of the rice (*Oryza sativa*) chloroplast genome: intermolecular recombination between distinct tRNA genes accounts for a major plastid DNA inversion during the evolution of the cereals. Mol. Gen. Genet. **217:**185–194.
4. **Ikeuchi, M., and Y. Inoue.** 1988. A new 4.8-kDa polypeptide intrinsic to the PSII reaction center, as revealed by modified SDS-PAGE with improved resolution of low-molecular-weight proteins. Plant Cell Physiol. **29:**1233–1239.
5. **Kaplan, A., S. Scherer, and M. Lerner.** 1989. Nature of the light-induced H^+ efflux and Na^+ uptake in cyanobacteria. Plant Physiol. **89:**1220–1225.
6. **Katoh, A., K. S. Lee, H. Fukuzawa, K. Ohyama, and T. Ogawa.** 1996. *cemA* homologue essential to CO_2 transport in the cyanobacterium, *Synechocystis* PCC6803. Proc. Natl. Acad. Sci. USA **93:**4006–4010.
7. **Katoh, A., M. Sonoda, H. Katoh, and T. Ogawa.** 1996. Absence of light-induced proton extrusion in a *cotA*-less mutant of *Synechocystis* sp. strain PCC6803. J. Bacteriol. **178:**5452–5455.
8. **Kelly, J. L., A. L. Greenleaf, and I. R. Lehman.** 1986. Isolation of the nuclear gene encoding a subunit of the yeast mitochondrial RNA polymerase. J. Biol. Chem. **261:**10348–10351.
9. **Laemmli, U. K.** 1970. Cleavage of structural proteins during the assembly of the head of bacteriophage T4. Nature (London) **227:**680–685.
10. **Lockau, W., and S. Pfeffer.** 1982. A cyanobacterial ATPase distinct from the coupling factor of photophosphorylation. Z. Naturforsch. Teil C **37:**658–664.
11. **Nilsson, F., D. J. Simpson, C. Jansson, and B. Andersson.** 1992. Ultrastructural and biochemical characterization of a *Synechocystis* 6803 mutant with

inactivated *psbA* genes. Arch. Biochem. Biophys. **295:**340–347.
12. **Ogawa, T.** 1992. Identification and characterization of the *ictA/ndhL* gene product essential to inorganic carbon transport of *Synechocystis* PCC6803. Plant Physiol. **99:**1604–1608.
13. **Ogawa, T., and A. Kaplan.** 1987. The stoichiometry between CO_2 and H^+ fluxes involved in the transport of inorganic carbon in cyanobacteria. Plant Physiol. **83:**888–891.
14. **Ogawa, T., and K. Shibata.** 1965. A sensitive method for determining chlorophyll b in plant extracts. Photochem. Photobiol. **4:**193–200.
15. **Ohyama, K., H. Fukuzawa, T. Kohchi, H. Shirai, T. Sano, S. Sano, K. Umesono, Y. Shiki, M. Takeuchi, Z. Chang, S. Aota, H. Inokuchi, and H. Ozeki.** 1986. Chloroplast gene organization deduced from complete sequence of liverwort *Marchantia polymorpha* chloroplast DNA. Nature (London) **322:**572–574.
16. **Oka, A., H. Sugisaki, and M. Takanami.** 1981. Nucleotide sequence of the kanamycin resistance transposon Tn903. J. Mol. Biol. **147:**217–226.
17. **Omata, T., and N. Murata.** 1983. Isolation and characterization of the cytoplasmic membranes from the blue-green alga (cyanobacterium) *Anacystis nidulans*. Plant Cell Physiol. **24:**1101–1112.
18. **Omata, T., and N. Murata.** 1986. Glycolipid synthesis activities in cytoplasmic and thylakoid membranes from the cyanobacterium, *Anacystis nidulans*. Plant Cell Physiol. **27:**485–490.
19. **Omata, T., M. Ohmori, N. Arai, and T. Ogawa.** 1989. Genetically engineered mutant of the cyanobacterium *Synechocystis* PCC7942 defective in nitrate transport. Proc. Natl. Acad. Sci. USA **86:**6612–6616.
20. **Omata, T., and T. Ogawa.** 1986. Biosynthesis of a 42-kD polypeptide in the cytoplasmic membrane of the cyanobacterium *Anacystis nidulans* strain R2 during adaptation to low CO_2 concentration. Plant Physiol. **80:**525–530.
21. **Prentki, P., and H. M. Krisch.** 1984. *In vitro* insertional mutagenesis with a selectable DNA fragment. Gene **29:**303–313.
22. **Saiki, R. K., D. H. Gelfand, S. Stoffel, S. J. Scharf, R. Higuchi, G. T. Horn, K. B. Mullis, and H. A. Erlich.** 1988. Primer-directed enzymatic amplification of DNA with a thermostable DNA polymerase. Science **239:**487–491.
23. **Sambrook, J., E. F. Fritsch, and T. Maniatis.** 1989. Molecular cloning: a laboratory manual, 2nd ed. Cold Spring Harbor Laboratory Press, Cold Spring Harbor, N.Y.
24. **Sasaki, Y., K. Sekiguchi, Y. Nagano, and R. Matsuno.** 1993. Chloroplast envelope protein encoded by chloroplast genome. FEBS Lett. **316:**93–98.
25. **Scherer, S., I. Hinrichs, and P. Böger.** 1988. Light-induced proton release by the cyanobacterium *Anabaena variabilis* dependence on CO_2 and Na^+. Plant Physiol. **86:**769–772.
26. **Shine, J., and L. Dalgarno.** 1975. Determination of cistron specificity in bacterial ribosomes. Nature (London) **254:**34–38.
27. **Shinozaki, K., M. Ohme, M. Tanaka, T. Wakasugi, N. Hayashida, T. Matsubayashi, N. Zaita, J. Chunwongse, J. Obokata, K. Yamaguchi-Shinozaki, C. Ohto, K. Torazawa, B. Y. Meng, M. Sugita, H. Deno, T. Kamogashira, K. Yamada, J. Kusuda, F. Takaiwa, A. Kato, N. Tohdoh, H. Shimada, and M. Sugiura.** 1986. The complete nucleotide sequence of the tobacco chloroplast genome: its gene organization and expression. EMBO J. **5:**2043–2049.
28. **Stanier, R. Y., R. Kunisawa, M. Mandel, and G. Cohen-Bazire.** 1971. Purification and properties of unicellular blue-green algae (order *Chroococcales*). Bacteriol. Rev. **35:**171–205.
29. **Ueguchi, C., and K. Itoh.** 1992. Multicopy suppression: an approach to understanding intracellular functioning of the protein export system. J. Bacteriol. **174:**1454–1461.
30. **Willey, D. L., and J. C. Gray.** 1990. An open reading frame encoding a putative haem-binding polypeptide is cotranscribed with the pea chloroplast gene for apocytochrome f. Plant Mol. Biol. **15:**347–356.
31. **Williams, J. G. K., and A. A. Szalay.** 1983. Stable integration of foreign DNA into the chromosome of the cyanobacterium *Synechocystis* R2. Gene **24:**37–51.

Photosynthesis Research **54:** 99–105, 1997.

Regular paper

Cloning of the *cotA* gene of *Synechococcus* PCC7942 and complementation of a *cotA*-less mutant of *Synechocystis* PCC6803 with chimeric genes of the two strains

Masatoshi Sonoda[1], Hirokazu Katoh[2], Hiroshi Ohkawa[1] & Teruo Ogawa[1,2]
[1]*Biochemical Regulation, School of Agriculture,* [2]*Bioscience Center, Nagoya University, Nagoya 464-01, Japan*

Received 25 February 1997; accepted in revised form 21 July 1997

Key words: cemA, chloroplast envelope, cytoplasmic membrane, mutant, proton extrusion

Abstract

cotA, a homologue of *cemA* that encodes a chloroplast envelope membrane protein, was cloned from *Synechococcus* PCC7942. The gene encodes a protein of 421 amino acids, which is similar in size to CotA of *Synechocystis* PCC6803 and CemA of liverwort and *Chlamydomonas*. There was significant sequence homology among these CotA and CemA in the C-terminal region but the homology was low in the N-terminal region. Sequencing of *Synechococcus* DNA in the *cotA* region revealed two other genes downstream of *cotA*, one of which is homologous to *cobP* and could be cotranscribed with *cotA*. A mutant (M48) was constructed by inactivating *cotA* in the wild-type (WT) *Synechococcus*. The mutant showed the same characteristics as the *cotA*-deletion mutant of *Synechocystis* (M29) and was unable to grow in a low sodium medium or at acidic pH under aeration with 3% CO_2 in air (v/v). *Synechococcus cotA* did not comple-ment M29. Three chimeric *cotA* genes of the two cyanobacterial strains were constructed. One of these chimeric genes strongly and the other two weakly complemented the mutant.

Abbreviations: kbp – kilobasepair; km^r – kanamycin resistant; ORF – open reading frame; PAR – photosynthetically active radiation; PCR – polymerase chain reaction; TES – N-Tris(hydroxy-methyl)methyl-2-aminoethanesulfonic acid; WT – wild type

Introduction

cemA is a gene found in chloroplast genomes of plants (Ohyama et al. 1986; Shinozaki et al. 1986; Hiratsuka et al. 1990; Willey and Gray 1990) and *Chlamydomonas* (N. Rolland, EMBL Sequence Library, Accession No. X90559) and encodes a functionally unknown protein localized in chloroplast envelope membrane (Sasaki et al. 1993). A *cemA* homologue has been cloned from *Synechocystis* PCC6803 as a gene that complemented the mutants defective in CO_2 transport and was named *cotA* (Katoh et al. 1996a). Both CemA and CotA contain 4 membrane spanning domains and their amino acid sequences are highly conserved in the C-terminal regions (Ohyama et al. 1986; Shinozaki et al. 1986; Hiratsuka et al. 1989; Willey and Gray 1990; Katoh et al. 1996a). We have once reported that *Synechocystis* CotA consists of 247 amino acids, being similar in size to CemA of higher plants. However, recently we concluded that *Synechocystis* CotA consists of 440 amino acids and is much larger than higher plant CemA (Sonoda et al. 1997). Deletion of *cotA* from the WT *Synechocystis* completely abolished proton extrusion activity in the light (Katoh et al. 1996b). The results indicated that *cotA* of *Synechocystis* has a role in the light-induced proton extrusion. In an attempt to see whether *cotA* is present in other cyanobacterial strains and whether it has a similar size and function to those of *Synechocystis cotA*, we have cloned and inactivated the *cotA* gene

of *Synechococcus* PCC7942. We have also tried to complement a *cotA*-deletion mutant of *Synechocystis* with *Synechococcus cotA* or with chimeric *cotA* genes of the two cyanobacterial strains. This paper describes isolation and characterization of the *Synechococcus cotA* gene, some physiological properties of a *cotA*-inactivated mutant and the ability of *Synechococcus cotA* or chimeric genes to complement the *Synechocystis* mutant.

Materials and methods

Growth conditions

Cells of *Synechococcus* PCC7942 were grown at 30 °C in BG-11 medium (Stanier et al. 1971) buffered with 20 mM of TES-KOH (pH 8.0) during aeration with 3% CO_2 in air (v/v) under illumination by fluorescent lamps (120 μmol PAR/m^2s), as described previously (Katoh et al. 1996a, b).

Cloning and inactivation of cotA

A fragment of *Synechocystis cotA* amplified by PCR method (Saiki et al. 1988) was used as a probe for heterologous hybridization to clone the corresponding gene from WT *Synechococcus*. A fraction containing 2 to 3-kbp *Bam*HI digests of *Synechococcus* DNA that hybridized with the probe was used to construct a partial genomic library in p*UC18*. A clone (p*UCB2.3*) containing *cotA* was isolated from the library by colony hybridization. A 17-kbp fragment containing the contiguous region was isolated from a λDASH II library of WT *Synechococcus* by plaque hybridization, using the insert DNA of p*UCB2.3* as a probe, and was digested by *Eco*RI. A 3.2-kbp band that hybridized to the probe was subcloned into p*UC18* (p*UCE3.2*). The *cotA* gene in p*UCB2.3* was inactivated by inserting the km^r cartridge (Oka et al. 1981). The plasmid containing the modified gene was used to transform the WT cells of *Synechococcus* PCC7942 into the km^r mutant, using the protocol of Williams and Szalay (1983).

Construction of chimeric cotA *genes*

Chimeric genes of *Synechococcus* and *Synechocystis cotA* were synthesized by the PCR method reported by Horton et al. (1989). Each chimeric gene was inserted into p*KMSC* plasmid (Sonoda et al. 1997) and was used to transform the *cotA*-deletion mutant of *Synechocystis* (M29) into kanamycin resistance.

Measurements of net proton exchange

Cells were harvested by centrifugation, washed twice with 0.2 mM of TES-KOH buffer (pH8.0) and suspended in the same buffer containing 15 mM NaCl at a chlorophyll concentration of 14 μg/ml. Changes in pH of the cell suspension (3 ml) were monitored by a pH electrode with a meter (Inlar 423 and Delta 350; Mettler Toledo, Halstead Essex, UK). After each measurement, the signal was calibrated by injecting 10 μl of 7.5 mM HCl to the cell suspension. Cells in a sample chamber kept at 30 °C were illuminated with white light from a 150 W halogen lamp guided to the sample chamber by a glass fiber (MHF-150L; Kagaku Kyoeisha Ltd., Osaka, Japan) at 4.0 mmol PAR/m^2s.

Other methods

Growth curves were determined from the rise in the OD at 730 nm using a Shimadzu recording spectrophotometer (Model UV-2200). Unless otherwise stated, standard techniques were used for DNA manipulation (Sambrook et al. 1989). Pigments in the cells were extracted by methanol and the chlorophyll concentration in the extract was determined (Ogawa and Shibata 1965).

Results

Cloning and sequence analysis of cotA *and genes in the neighboring region*

The restriction maps of the insert DNA in p*UCB2.3* and p*UCE3.2* are shown in Figure 1. Sequencing of the 2.3-kbp insert DNA revealed an ORF encoding a protein of 421 amino acids near the *Bam*HI site at the right end. This ORF was found to be *cotA* based on the strong sequence homology to *cotA* of *Synechocystis* PCC6803 (see Figure 2). A part of an ORF was found upstream of *cotA* in the complementary strand and four ORFs (ORF180, ORF164, ORF108 and the gene encoding Fur repressor protein) downstream of *cotA* on the same strand (Figure 1). The nucleotide sequence from the middle of the ORF in the complementary strand to the beginning of the Fur repressor gene, together with the amino-acid sequences deduced from the nucleotide sequences for *cotA*, ORF180 and

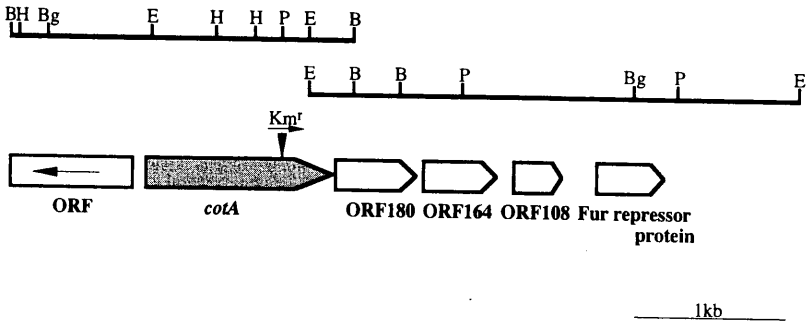

Figure 1. Restriction maps of a 2.3 kbp-DNA insert in p*UCB2.3* (left) and a 3.2-kbp DNA insert in p*UCE3.2* (right). Six ORFs and the direction of transcription are shown by the boxes with arrowheads. The *cotA* gene is shadowed and the site of insertion of the km^{r}cartridge is shown with the direction indicated by the arrow. B, *Bam*HI; Bg, *Bgl*II; E, *Eco*RI; H, *Hin*dIII; P, *Pst*I.

ORF164, have been deposited in the EMBL library (Accession No. AB004281). No SD sequence (Shine and Dalgarno 1975) was found upstream of the postulated initiation codon for *cotA*. There are only 9 bp nucleotides between the termination codon for *cotA* and the initiation codon for ORF180, which suggests that these two genes are cotranscribed.

Homologous genes

The *cotA* gene of *Synechococcus* PCC7942 encodes a protein of 421 amino acids that is close in size to CotA of *Synechocystis* PCC6803 (440 amino acids; Sonoda et al. 1997) and CemA of liverwort (434; Ohyama et al. 1986) and *Chlamydomonas* (500; N. Rolland, EMBL Sequence Library, Accession No. X90559) but much larger than CemA of higher plants (229-231; Shinozaki et al. 1986; Hiratsuka et al. 1989; Willey and Gray 1990). Figure 2 shows the homology in the amino-acid sequences among CotA of *Synechococcus* and *Synechocystis* and CemA of liverwort and *Chlamydomonas*. *Synechococcus* CotA showed higher homology with *Synechocystis* CotA than with CemA. The homology was high in the C-terminal regions but was low in the N-terminal regions. Comparison of the sequences of 230 amino acid residues in the C-terminal region revealed that 136 residues of *Synechococcus* CotA are identical in *Synechocystis* CotA (59%), 83 residues in *Chlamydomonas* CemA (36%) and 81 residues in liverwort CemA (35%). Comparison of the sequences of 200 amino-acid residues in the N-terminal region indicated that 28 residues of *Synechococcus* CotA are identical in *Synechocystis* CotA (14%), 37 residues in *Chlamydomonas* CemA (18.5%) and 17 residues in liverwort CemA (8.5%).

ORF180 encodes a hydrophilic protein of 180 amino acids and a homologous gene was found in *Synechocystis* PCC6803 (slr0216 in Cyanobase; Kaneko et al. 1996). These genes showed significant sequence homology to *cobP* or *cobU* of various organisms, where the ATP binding motif was highly conserved (Figure 3A). A gene homologous to ORF164 was also present in *Synechocystis* PCC6803 (slr0217 in Cyanobase) but no genes homologous to ORF164 were found in other organisms in the database (Figure 3B).

Insertional inactivation of the cotA *gene*

In *Synechocystis* PCC6803, deletion of *cotA* abolished the activity of light-induced proton extrusion and the deletion mutant was unable to grow in a low sodium medium or under acidic conditions (Katoh et al. 1996b). To see whether *cotA* of *Synechococcus* is also involved in light-induced proton extrusion, the gene was inactivated by inserting the km^r cartridge at the *Pst*I site within the *cotA* gene in p*UCB2.3* (see Figure 1). The km^r mutant (M48) thus constructed was unable to grow in a low sodium medium (curve D in Figure 4) or in normal BG-11 medium buffered at pH 6.5 (data not shown) while the WT cells grew in these media (curve B). Both WT and mutant grew well in BG-11 medium buffered at pH 8.0 (curves A and C). When the WT cells suspended in 0.2 mM Tes-KOH buffer (pH 8.0) containing 15 mM NaCl (curve E in Figure 4) were illuminated, there was an acidification (H^+ extrusion or OH^- uptake) of the medium, being consistent with the observations reported by Ogawa and Kaplan (1987) and Kaplan et al. (1989). The activity of light-induced proton extrusion of the mutant was only one tenth of the WT activity (curve F). Thus, these characteristics of the mutant were the same as those of

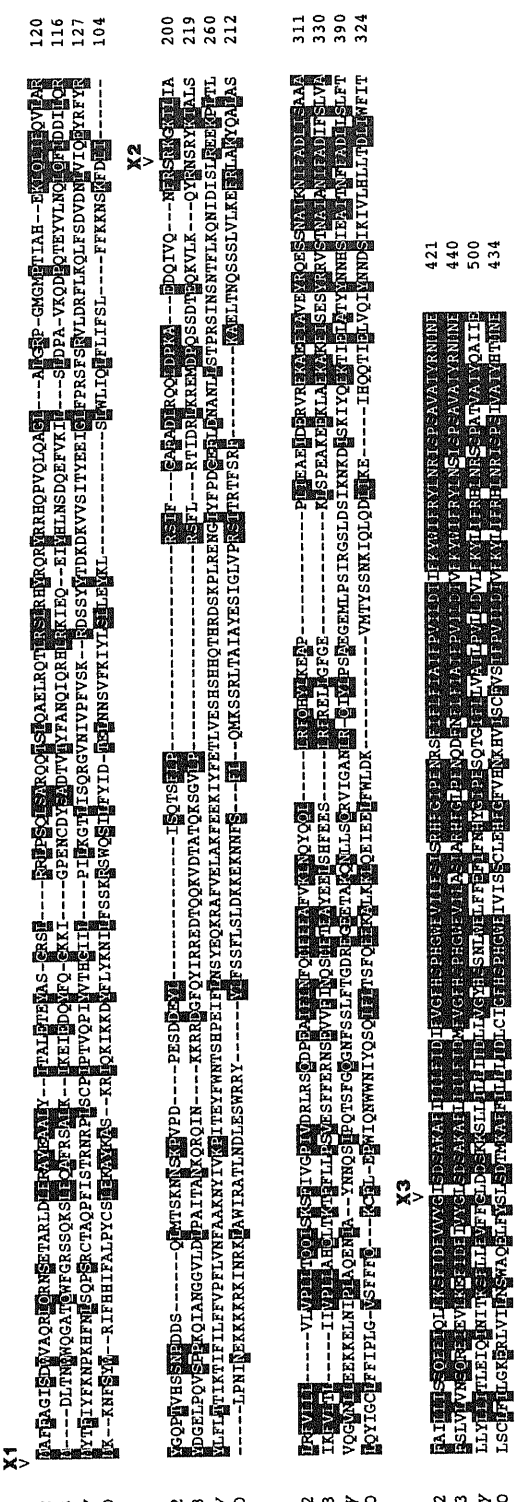

Figure 2. Comparison of the deduced amino-acid sequences for CotA of *Synechococcus* and *Synechocystis*, CemA of liverwort and *Chlamydomonas*. Residues in CotA of *Synechocystis* and CemA identical to corresponding residues in *Synechococcus* CotAare shown in black boxes. X1, X2 and X3 indicate the sites of fusion between CotA of *Synechococcus* and *Synechocystis* in the chimeric genes.

Figure 3. (A) Comparison of the deduced amino-acid sequences for the protein encoded by ORF180 with the slr0216 product of *Synechocystis* PCC6803, CobP of *P.denitrificans* (*P*), CobU of *S. typhimurium* (*S*) and *E. coli* (*E*) and (B) those for the protein encoded by ORF164 with the slr0217 product of *Synechocystis* PCC6803. Black boxes represent amino-acid residues identical to those in ORF180 or ORF164 of *Synechococcus* PCC7942. Asterisks indicate ATP-binding consensus sequences.

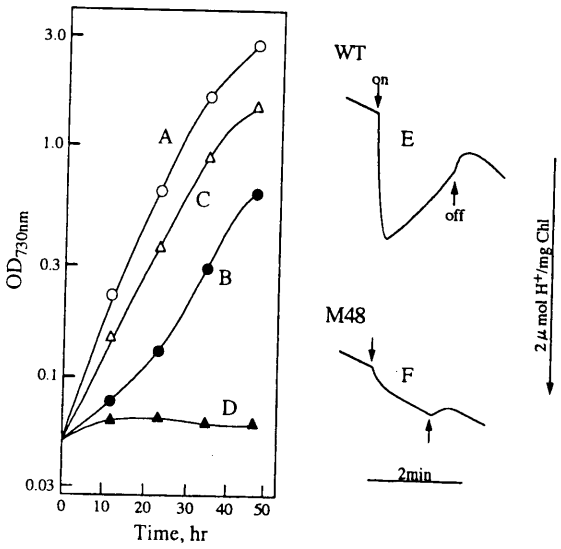

Figure 4. Left: growth curves of WT (curves A, B) and M48 (C, D) cells in BG-11 medium containing 17 mM Na^+ (A,C) or in a medium containing 100 μM Na^+ (B,D) during aeration with 3% CO_2 in air (v/v). Right: changes in pH of cell suspensions upon switching the light on and off. WT (curve E), M48 (F) cells were suspended in 0.2 mM TES-KOH buffer (pH 8.0) containing 15 mM NaCl.

the *cotA*-deletion mutant of *Synechocystis* PCC6803 (M29). The results clearly demonstrated that *cotA* has a role in the light-induced proton extrusion both in *Synechococcus* PCC7942 and *Synechocystis* PCC6803.

Complementation of the M29 mutant with chimeric henes of Synechococcus *and* Synechocystis cotA

cotA of *Synechococcus* with its own promoter did not complement the *Synechocystis* mutant, M29; the transformant did not grow at pH 6.5. Northern analysis suggested that the gene was not or only weakly expressed in *Synechocystis* (data not shown). Three kinds of chimeric genes of *Synechococcus* and *Synechocystis cotA* (X1, X2 and X3) were constructed. X1 is the *Synechococcus* gene fused to the promoter region of *Synechocystis*. X2 and X3 are the chimeric genes with the sequences of the promoter and N-terminal regions from *Synechocystis cotA* and those of C-terminal region from *Synechococcus cotA* (see Figure 2 for the sites of fusion). X3 transformed the M29 mutant completely to the WT phenotype; the transformant showed the WT activity of light-induced proton extrusion and grew as fast as the WT at pH 6.5 (curves A and B in Figure 5). The X2 transformant grew more slowly than the WT at pH 6.5 and showed only small activity of light-induced proton extrusion (C). X1 complemented the M29 mutant but very weakly, judging from the slow growth of the transformant at pH 6.5 (D) in contrast to the inability of the M29 mutant to grow under these conditions (E). However, the light-induced proton extrusion was not detectable in the X1 transformant (D).

Discussion

This paper clearly demonstrated that *Synechococcus* PCC7942 possesses *cemA* homologue (*cotA*) and that inactivation of the gene resulted in inhibition of proton extrusion in the light. Thus, the presence of *cotA* and its involvement in light-induced proton extrusion appear to be common in cyanobacteria. The significant homology of *cotA* with *cemA*, suggests that *cemA* in chloroplasts of plants and algae has the same function as *cotA* in cyanobacteria.

ORF180, which showed strong homology to *cobP* or *cobU* involved in cobalamin biosynthesis (Figure 3A), was located very close to *cotA* in the *Synechococcus* genome. This suggests that *cotA* and ORF180 are cotranscribed. Trials to inactivate ORF180 or *cobP/cobU* homologue in *Synechocystis* were unsuccessful. Inactivation of these genes might be lethal to the cells.

The light-induced proton extrusion has been observed with various strains of cyanobacteria but the physiological significance of this reaction remains unknown (Lockau and Pfeffer 1982; Ogawa and Kaplan 1987; Scherer et al. 1988; Kaplan et al. 1989). The extrusion of protons will produce $\Delta\psi$ and ΔpH across the cytoplasmic membrane to drive transport of other ions. The inability of the M48 mutant to grow in a low sodium medium could be ascribed to reduced activities of transport processes which are coupled either to the light-induced proton extrusion or to a reaction requiring a sodium concentration in the millimolar range. The latter reaction could be Na^+/H^+ antiport, which may complement the CotA-dependent reaction. The following scheme is possible as to the effect of these reactions on the growth of cells. The cells grow in normal BG-11 medium when either of these reactions is functioning but the *cotA*-less mutant is unable to grow when Na^+/H^+ antiport is not functioning efficiently in the low sodium medium. The growth at pH 6.5 may require functioning of both reactions. The transport of many ions may be coupled to or affected by these reactions. The transport of

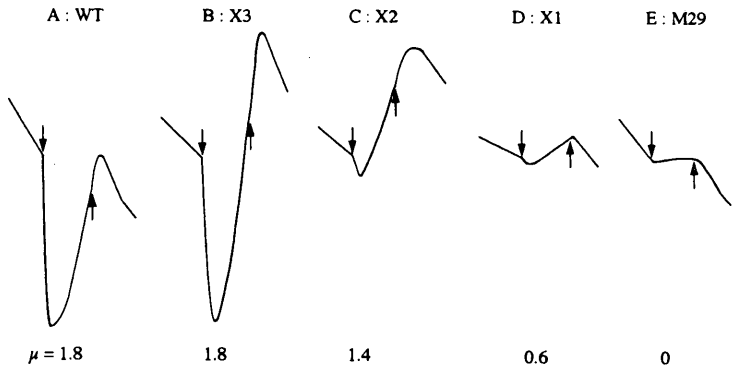

Figure 5. Changes in pH of cell suspensions upon switching the light on and off. WT of *Synechocystis* (curve A), X3 (B), X2 (C), X1 (D) transformants and M29 (E) were suspended in the same buffer as in Figure 4. Growth rates of these cells in BG-11 medium buffered at pH 6.5 are shown by the μ values. Doubling time (in days) = $0.693/\mu$. Cultures were aerated with 3% CO_2 in air (v/v).

CO_2 is strongly affected by the CotA-dependent reaction (Katoh et al. 1996b) and also probably by Na^+/H^+ antiport. Absence of an ATP-binding motif in the deduced amino-acid sequence of CotA may indicate that the gene product is not a H^+-ATPase but could be another type of H^+ transporter or a component involved in energization or regulation of a H^+-transporting system.

Although we were unable to observe any difference between the WT and *cotA*-less mutant of *Synechocystis* in their internal pH under the experimental conditions we applied (Katoh et al. 1996b), the possibility that *cotA* is involved in pH regulation during the cell growth can not be ruled out.

Synechococcus cotA with its own promoter did not complement the *cotA*-deletion mutant of *Synechocystis*, suggesting that the *Synechococcus* promoter was not functioning efficiently in *Synechocystis*. The chimeric genes (X1 and X2) which contain relatively less conserved regions of *Synechococcus* only weakly complemented the mutant (Figure 5). Such strain-specific stringency for the functioning of CotA suggests that CotA may form a complex with other protein(s) and may require high stringency for the complex formation.

Acknowledgments

This study was supported by Grants-in Aid for Scientific Research on Priority Areas (No. 0427103) from the Ministry of Education, Science, Sports and Culture, Japan, and the New Energy and Industrial Technology Development Organization (NEDO), Japan. We thank Prof. N. Murata (Natl. Inst. Basic Biol.) for the kind gift of *Synechococcus* DNA library in λDASH II.

References

Hiratsuka J, Shimada H, Whittier R, Ishibashi T, Sakamoto M, Mori M, Kondo C, Honji Y, Sun CR, Meng BY, Li YQ, Kanno A, Nishizawa Y, Hirai A, Shinozaki K and Sugiura M (1989) The complete sequence of the rice (*Oryza sativa*) chloroplast genome: Intermolecular recombination between distinct tRNA genes accounts for a major plastid DNA inversion during the evolution of the cereals. Mol Gen Genet 217: 185–194

Horton RM, Hunt HD, Ho SN, Pullen JK and Pease LR (1989) Engineering hybrid genes without the use of restriction enzymes: Gene splicing by overlap extension. Gene 77: 61–68

Kaneko T, Sato S, Kotani H, Tanaka A, Asamizu E, Nakamura Y, Miyajima N, Hirosawa M, Sugiura M, Sasamoto S, Kimura T, Hosouchi T, Matsuno A, Muraki A, Nakazaki N, Naruo K, Okumura S, Shimpo S, Takeuchi C, Wada T, Watanabe A, Yamada M, Yasuda M and Tabata S (1996) Sequence analysis of the genome of the unicellular cyanobacterium *Synechocystis* sp strain PCC6803. II. Sequence determination of the entire genome and assignment of potential protein-coding regions. DNA Res 3: 109–136

Kaplan A, Scherer S and Lerner M (1989) Nature of the light-induced H^+ efflux and Na^+ uptake in cyanobacteria. Plant Physiol 89: 1220–1225

Katoh A, Lee KS, Fukuzawa H, Ohyama K and Ogawa T (1996a) *cemA* homologue essential to CO_2 transport in the cyanobacterium, *Synechocystis* PCC6803. Proc Natl Acad Sci USA 93: 4006–4010

Katoh A, Sonoda M, Katoh H and Ogawa T (1996b) Absence of light-induced proton extrusion in *cotA*-less mutant of *Synechocystis* sp. strain PCC6803. J Bacteriol 178: 5452–5455

Lockau W and Pfeffer S (1982) A cyanobacterial ATPase distinct from the coupling factor of photophosphorylation. Z Naturforsch Teil 37C: 658–664

Ogawa T and Kaplan A (1987) The stoichiometry between CO_2 and H^+ fluxes involved in the transport of inorganic carbon in cyanobacteria. Plant Physiol 83: 888–891

Ogawa T and Shibata K (1965) A sensitive method for determining chlorophyll *b* in plant extracts. Photochem Photobiol 4: 193–200

Ohyama K, Fukuzawa H, Kohchi T, Shirai H, Sano T, Sano S, Umesono K, Shiki Y, Takeuchi M, Chang Z, Aota S, Inokuchi H and Ozeki H (1986) Chloroplast gene organization deduced from complete sequence of liverwort *Marchantia polymorpha* chloroplast DNA Nature 322: 572–574

Oka A, Sugisaki H and Takanami M (1981) Nucleotide sequence of the kanamycin resistance transposon Tn903. J Mol Biol 147: 217–226

Saiki RK, Gelfand DH, Stoffel S, Scharf SJ, Higuchi R, Horn GT, Mullis KB and Erlich HA (1988) Primer-directed enzymatic amplification of DNA with a thermostable DNA polymerase. Science 239: 487–491

Sambrook J, Fritsch EF and Maniatis T (1989) Molecular Cloning: A Laboratory Manual, 2nd Ed. Cold Spring Harbor Laboratory Press, Cold Spring Harbor, NY

Sasaki Y, Sekiguchi K, Nagano Y and Matsuno R (1993) Chloroplast envelope protein encoded by chloroplast genome. FEBS Lett 316: 93–98

Scherer S, Hinrichs I and Böger P (1988) Light-induced proton release by the cyanobacterium *Anabaena variabilis* dependence on CO_2 and Na^+. Plant Physiol 86: 769–772

Shine J and Dalgarno L (1975) Determination of cistron specificity in bacterial ribosomes. Nature (London) 254: 34–38

Shinozaki K, Ohme M, Tanaka M, Wakasugi T, Hayashida N, Matsubayashi T, Zaita N, Chunwongse J, Obokata J, Yamaguchi-Shinozaki K, Ohto C, Torazawa K, Meng BY, Sugita M, Deno H, Kamogashira T, Yamada K, Kusuda J, Takaiwa F, Kato A, Tohdoh N, Shimada H and Sugiura M (1986) The complete nucleotide sequence of the tobacco chloroplast genome: Its gene organization and expression. EMBO J 5: 2043–2049

Sonoda M, Kitano K, Katoh A, Katoh H, Ohkawa H and Ogawa T (1997) Size of *cotA* and identification of the gene product in *Synechocystis* sp. strain PCC6803. J Bacteriol 179: 3845–3850

Stanier RY, Kunisawa R, Mandel M and Cohen-Bazire G (1971) Purification and properties of unicellular blue-green algae (order *Chroococcales*). Bacteriol Rev 35: 171–205

Willey DL and Gray JC (1990) An open reading frame encoding a putative haem-binding polypeptide is cotranscribed with the pea chloroplast gene for apocytochrome *f*. Plant Mol Biol 15: 347–356

Williams JG and Szalay AA (1983) Stable integration of foreign DNA into the chromosome of the cyanobacterium *Synechococcus* R2. Gene 24: 37–51

CEMA HOMOLOGUE IN CYANOBACTERIA (PXCA) INVOLVED IN PROTON EXCHANGE

M. Sonoda[1], H. Katoh[1], W. Vermaas[2] and T. Ogawa[1]

[1]Bioscience Center, Nagoya University, Nagoya 464-8601, Japan, and
[2]Center for the Study of Early Events in Photosynthesis, Arizona State University, Tempe, AZ 85287-1601, USA

Key words: chloroplast genes, CO_2 uptake, electron transport, mutants, photosystem 2, proton transport

1. Introduction

When suspension of cyanobacterial cells are illuminated, there is an acidification of the medium followed by an alkalization [1-4]. Both acidification and alkalization are specifically stimulated by Na^+. The acidification was assumed to be due to a light-dependent uptake of CO_2 that is converted to HCO_3^- [2,3] and the alkalization due to extrusion of OH^- produced as a result of conversion of HCO_3^- to CO_2 that is fixed by photosynthesis [1]. Ambiguity, however, remains on the source of protons or hydroxyl ions extruded in the light and electron transport involved in the proton extrusion is not yet known.

pxcA (formerly known as *cotA*) is a cyanobacterial gene homologous to *cemA* or *ycf10* in chloroplast genomes and has been cloned from *Synechocystis* PCC6803 and *Synechococcus* PCC7942 [5-7]. Mutants with inactivated *pxcA* were unable to grow in low Na^+ medium or in acidic medium and did not show light-dependent proton extrusion [4,7]. Western analysis indicated that PxcA is located in the cytoplasmic membrane [8]. These results indicated that PxcA is involved in light-dependent proton extrusion and is essential to cell growth under acidic or low salt conditions. The present study aims to clarify which mode of electron transport is involved in the light-dependent proton extrusion and to see the effect of *pxcA* inactivation on the uptake of CO_2, HCO_3^- and NO_3^- .

2. Materials and Methods

Cells of wild-type (WT) and mutants (*pxcA*$^-$[4], *psaAB*$^-$[9] and *psbDIC*$^-$/*psbDII*$^-$[10]) of *Synechocystis* PCC6803 were grown at 30°C in BG-11 medium [11] buffered at pH 8.0 during aeration with 3% (vol/vol) CO_2 in air. Continuous illumination was provided at 40 μmol photosynthetically active radiation/m^2s (400-700 nm) for *psaAB*$^-$ cells and at 100 μmol /m^2s for the other strains. Glucose (5 mM) was added to the above medium for the growth of *psaAB*$^-$ and *psbDIC*$^-$/*psbDII*$^-$.

Changes in pH of the cell suspension (3 ml) kept at 30 °C were monitored by a pH electrode with a meter (Inlar 423 and Delta 350; Mettler Toledo, Halstead Essex, UK) [4].

G. Garab (ed.), Photosynthesis: Mechanisms and Effects, Vol. V, 3675–3678.

3. Results and Discussion

3.1. *Proton exchange by the WT and pxcA⁻ mutant.*
When cell suspension of WT *Synechocystis* was illuminated, there was an acidification followed by an alkalization of the medium (Fig. 1, curve A). In contrast, only alkalization was observed with the *pxcA*⁻ mutant in the light (D). The result indicates that *pxcA* is involved in light-dependent proton extrusion. In the presence of glyceraldehyde (GA; an inhibitor of CO_2 fixation) the alkalization was inhibited both in the WT and mutant (B and E), which supports the view that the alkalization is due to extrusion of OH^- produced as a result of HCO_3^- to CO_2 conversion [1]. The inhibition was not complete, indicating the presence of alkalization independent of this reaction. When WT cells were illuminated in the presence of 2,5-dimethyl-p-benzoquinone (DMBQ), an electron acceptor from photosystem(PS) II, the net proton extrusion ceased after a minute of illumination and a post-illumination influx of protons was observed (C). This suggests that in the light both extrusion and influx of protons occur, reaching a stationary level where there is no net proton exchange. After the light is turned off (causing proton extrusion to cease) proton influx continues for a short time until new steady-state level is attained. In the presence of DMBQ, inorganic carbon uptake does not occur [12] and the observed proton fluxes are independent of this reaction. Both light-dependent proton extrusion and postillumination proton influx were very small in the *pxcA*⁻ mutant in the presence of DMBQ (F).

3.2. *Net proton exchange in mutants defective in PS I or PS II.*
To clarify with which part(s) of photosynthetic electron transport proton extrusion may be associated, mutants lacking either PS I or PS II were investigated. The *psaAB*⁻ (PSI-less) strain showed light-dependent proton extrusion (curve A in Fig. 2). On a per-chlorophyll basis, the amplitude of proton extrusion was 2-3 fold larger than that in WT (compare with curve A in Fig. 1). The result indicates that PS II-mediated electron transfer can drive a significant amount of proton extrusion. No proton uptake was observed in the PS I-less mutant in the light, consistent with the lack of CO_2 fixation in this strain. In the presence of DMBQ, a more extensive acidification was observed with this mutant followed by proton uptake (Fig. 2 B). Thus, PS II-driven electron transport from water to DMBQ or, to a lesser extent, to oxygen can lead to proton extrusion. A small amount of light-induced

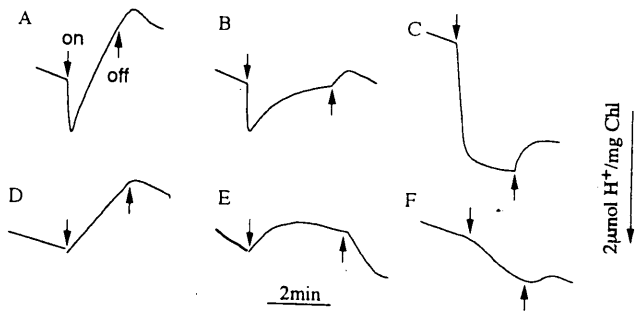

Figure 1. Net proton movements in suspensions of WT (curves A-C) and *pxcA*⁻ (D-F) cells of *Synechocystis* PCC6803 upon switching the light on and off. Cells were suspended in 0.2 mM Tes-KOH buffer (pH 8.0) containing 15 mM NaCl in the absence (A, D) and presence of 20 mM GA (B, E) or 1 mM DMBQ (C, F).

proton extrusion was observed when a cell suspension of the *psbDIC⁻/psbDII⁻* strain was illuminated in the absence of DMBQ (C) but not in its presence (D).

The above results indicate that the activity of proton extrusion is correlated with the activity of photosynthetic water splitting and electron transport through the cyt.b_6/f complex, both of which produce a proton gradient across the thylakoid membrane and thereby can lead to the generation of ATP. PxcA does not have an ATP-binding motif and is unable to hydrolyze ATP by itself. PxcA could be a regulator of an ATP-dependent proton extrusion pump, of which activity may be very low in the absence of PxcA.

3.3. *Effect of Na^+ and pH on the uptake of CO_2, HCO_3^- and NO_3^- in WT and pxcA⁻.*

Cells have a mechanism to maintain a homeostasis with respect to the intracellular pH and electroneutrality during transport of nutrients. To test whether the PxcA-dependent proton exchange is involved in maintaining this homeostasis, the uptake of CO_2, HCO_3^- and NO_3^- was monitored in the WT and *pxcA⁻* strain at pH 8.0 and 6.5 in the presence of normal concentration (15 mM) of NaCl (N-Na^+) or KCl with a contaminating concentration of Na^+ (L-Na^+; ~100μM Na^+). There was no difference between the WT and mutant in their HCO_3^- uptake at least at pH 8; the activity was high at N-Na^+ and low at L-Na^+ (Fig. 3, middle column). At L-Na^+, the activity of NO_3^- uptake was very low in *pxcA⁻* at pH 8.0

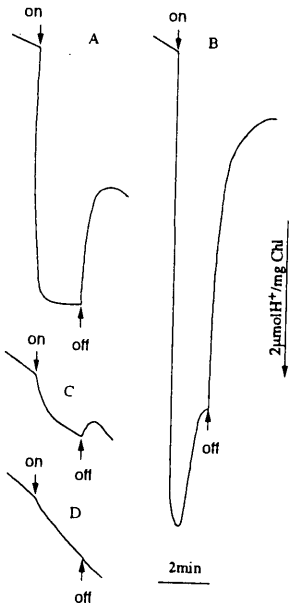

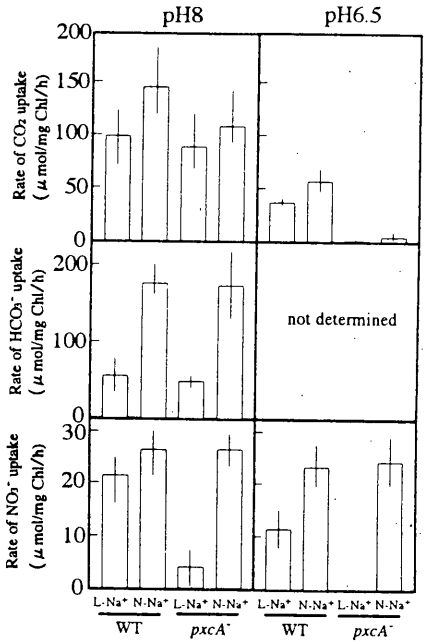

Figure 2. (left) Net proton movement in the suspensions of *psaAB⁻* (A, B) and *psbDIC⁻/psbDII⁻* (C, D,) cells upon switching the light on and off. DMBQ was added prior to illumination for curves B and D.

Figure 3. (right) The rates of CO_2, HCO_3^- and NO_3^- uptake in WT and *pxcA⁻* cells of *Synechocystis* at pH 8.0 and 6.5 at normal (N-) and low (L-) Na^+ concentrations.

and was zero at pH 6.5 (bottom columns). At N-Na^+, no significant effect of *pxcA* inactivation was observed on CO_2 and NO_3^- uptake at pH 8.0 but CO_2-uptake activity was reduced significantly at pH 6.5 (upper and bottom columns). No CO_2 uptake was observed in the mutant at pH 6.5 and L-Na^+. It is evident that the inactivation of *pxcA* strongly affected the CO_2 uptake under acidic conditions and the NO_3^- uptake at low Na^+ concentrations.

We propose a working hypothesis involving two complementary proton exchange systems, *i.e.* PxcA-dependent and PxcA-independent proton exchange systems, in maintaining homeostasis with respect to the intracellular pH and electroneutrality. The PxcA-independent system could be Na^+/H^+ antiport. The proton exchange catalyzed by these systems is stimulated by Na^+. Both systems are essential to CO_2 transport at pH 6.5 but PxcA-independent system alone is sufficient at pH 8 at N-Na^+. However, both systems are required at L-Na^+ even at this alkaline pH. At L-Na^+, NO_3^- uptake requires the PxcA-dependent system. When PxcA-independent proton exchange is active at N-Na^+, PxcA-dependent system is not required for NO_3^- uptake. Uptake of HCO_3^- requires high activity of PxcA-independent proton exchange at N-Na^+ either in the WT or in *pxcA*$^-$.

Proton exchange catalyzed by the PxcA-independent system should be observed as the pH changes of the suspension medium of *pxcA*$^-$ cells. The slow alkalization observed with *pxcA*$^-$ in the light and the slow acidification in the dark may be due to proton influx and efflux by the PxcA-independent system; it is also possible that rapid influx and efflux of protons *via* the PxcA-independent system system with a small net proton movement that can not be measured by the pH electrode used in this study.

References

1 Miller, A.G. and Colman, B. (1980) J. Bacteriol 143, 1253-1259.
2 Scherer, S., Riege, H. and Boger, P. (1988) Plant Physiol. 86, 769-772.
3 Ogawa, T. and Kaplan, A. (1987) Plant Physiol. 83: 888-891.
4 Katoh, A., Sonoda, M., Katoh, H. and Ogawa, T. (1996) J. Bacteriol. 178, 5452-5455.
5 Sasaki, Y., Sekiguchi, K., Nagano, Y. and Matsuno, R. (1993) FEBS Lett. 316, 93-98.
6 Katoh, A., Lee, K.S., Fukuzawa, H. Ohyama, K. and Ogawa, T. (1996) Proc. Natl. Acad. Sci. USA 93, 4006-4010.
7 Sonoda, M., Katoh, H. Ohkawa, H. and Ogawa, T. (1997) Photosynth. Res. 54, 99-105.
8 Sonoda, M., Kitano, K., Katoh, A., Katoh, H., Ohkawa, H. and Ogawa, T. (1997) J. Bacteriol. 179, 3845-3850.
9 Shen, G., Boussiba, S. and Vermaas, W.F.J. (1993) Plant Cell **5:** 1853-1863.
10 Vermaas, W.F.J., Charit, J. and Eggers, B. (1990) in Current Research in Photosynthesis (M. Baltscheffsky, ed.), Vol. 1, pp. 231-238, Kluwer, Dordrecht, The Netherlands.
11 Stanier, R.Y., Kunisawa, R., Mandel, M. and Cohen-Bazire, G. (1971) Bacteriol. Rev. 35, 171-205.
12 Ogawa, T., Miyano, A,. and Inoue, Y. (1985) Biochim Biophys Acta 808, 77-84.

JOURNAL OF BACTERIOLOGY, Aug. 1998, p. 3799–3803
0021-9193/98/$04.00+0

Vol. 180, No. 15

Photosynthetic Electron Transport Involved in PxcA-Dependent Proton Extrusion in *Synechocystis* sp. Strain PCC6803: Effect of *pxcA* Inactivation on CO_2, HCO_3^-, and NO_3^- Uptake

MASATOSHI SONODA,[1] HIROKAZU KATOH,[2] WIM VERMAAS,[3] GEORGE SCHMETTERER,[4] AND TERUO OGAWA[1,2]*

Graduate School of Bioagricultural Sciences[1] and Bioscience Center,[2] Nagoya University, Nagoya 464-01, Japan; Department of Plant Biology and Center for the Study of Early Events in Photosynthesis, Arizona State University, Tempe, AZ 85287-1601[3]; and Institute of Physical Chemistry, University of Vienna, A-1090 Vienna, Austria[4]

Received 9 February 1998/Accepted 20 May 1998

The product of *pxcA* (formerly known as *cotA*) is involved in light-induced Na^+-dependent proton extrusion. In the presence of 2,5-dimethyl-*p*-benzoquinone, net proton extrusion by *Synechocystis* sp. strain PCC6803 ceased after 1 min of illumination and a postillumination influx of protons was observed, suggesting that the PxcA-dependent, light-dependent proton extrusion equilibrates with a light-independent influx of protons. A photosystem I (PS I) deletion mutant extruded a large number of protons in the light. Thus, PS II-dependent electron transfer and proton translocation are major factors in light-driven proton extrusion, presumably mediated by ATP synthesis. Inhibition of CO_2 fixation by glyceraldehyde in a cytochrome *c* oxidase (COX) deletion mutant strongly inhibited the proton extrusion. Leakage of PS II-generated electrons to oxygen via COX appears to be required for proton extrusion when CO_2 fixation is inhibited. At pH 8.0, NO_3^- uptake activity was very low in the *pxcA* mutant at low [Na^+] (~100 μM). At pH 6.5, the *pxcA* strain did not take up CO_2 or NO_3^- at low [Na^+] and showed very low CO_2 uptake activity even at 15 mM Na^+. A possible role of PxcA-dependent proton exchange in charge and pH homeostasis during uptake of CO_2, HCO_3^-, and NO_3^- is discussed.

Light-induced extrusion of protons into the medium has been observed in various cyanobacterial strains (2, 3, 6, 8, 9, 12, 17, 18, 21, 22). Scherer et al. (17, 18) reported two phases of light-induced proton extrusion in *Anabaena variabilis*. The first phase is due to a light-dependent uptake of CO_2, which is converted to HCO_3^-, and the second phase was considered to be dependent on ATP and linear photosynthetic electron flow. Both phases of proton extrusion are specifically stimulated by Na^+. Similar Na^+-dependent light-induced proton extrusion has been observed with *Synechococcus* and *Plectonema* (2, 6, 12). The light-induced proton extrusion in *Plectonema* has been assumed to be due to a respiratory electron transport chain localized on the cytoplasmic membrane (2). The physiological significance of the light-induced proton extrusion is not yet known, and ambiguity remains whether photosynthetic or respiratory electron transport and whether cytoplasmic or thylakoid membranes are involved in this reaction.

pxcA (formerly known as *cotA*) is a homolog of *cemA* or *ycf10* in chloroplast genomes (7, 8, 21, 22). Light-induced proton extrusion activity was abolished when *pxcA* was inactivated in *Synechocystis* sp. strain PCC6803 (8, 21) or *Synechococcus* sp. strain PCC7942 (22). The *pxcA* mutants were unable to grow in low-Na^+ medium or in acidic medium. PxcA is located in the cytoplasmic membrane (21), and the *cemA* or *ycf10* gene in chloroplast genomes encodes a chloroplast envelope membrane protein (16). These results indicate that PxcA is involved in light-induced proton extrusion and that this protein is essential for cell growth under acidic or low-salt conditions.

* Corresponding author. Mailing address: Bioscience Center, Nagoya University, Chikusa-ku, Nagoya 464-8601, Japan. Phone: 81-52-789-5215. Fax: 81-52-789-5214. E-mail: h44975a@nucc.cc.nagoya-u.ac.jp.

The present study aims to clarify which mode of electron transport is involved in the light-induced proton extrusion and to determine the effect of *pxcA* inactivation on the uptake of CO_2, HCO_3^-, and NO_3^-. For this reason, *pxcA* mutants and strains carrying deletions of genes that code for photosynthetic or respiratory electron transport components in *Synechocystis* sp. strain PCC6803 were analyzed. Measurements of net proton exchange in the wild-type (WT) and mutant cells with or without electron acceptors or inhibitors enabled us to conclude that photosystem II (PS II)-driven electron transport was primarily involved in this reaction. We have also measured the uptake of CO_2, HCO_3^-, and NO_3^- in the WT and *pxcA* mutant. The results demonstrate that the PxcA-dependent proton exchange is essential for CO_2 uptake under acidic conditions and for NO_3^- uptake at low-Na^+ concentrations.

MATERIALS AND METHODS

Mutants and growth conditions. The following mutants were used in this study: *pxcA* (previously named M29) (8), *psaAB* (PS I-less) (20), *psbDIC/psbDII* (PS II-less) (24), and *coxAB* (cytochrome *c* oxidase-less) (19). WT, *pxcA*, and *coxAB* cells were grown at 30°C in BG-11 medium (23) buffered with 20 mM N-Tris(hydroxymethyl)methyl-2-aminoethanesulfonic acid (TES)–KOH at pH 8.0; the cultures were aerated with 3% (vol/vol) CO_2 in air. Glucose (5 mM) was added to the above medium for the growth of *psaAB* and *psbDIC/psbDII* mutants. Continuous illumination was provided by fluorescent lamps at 40-μmol photosynthetically active radiation/m^2/s (400 to 700 nm) for *psaAB* cells, which are sensitive to higher light intensity, and at 100 μmol/m^2/s for the other strains.

Measurements of proton exchange and uptake of CO_2, HCO_3^-, and NO_3^-. Cells harvested by centrifugation were washed twice with 0.2 mM TES-KOH buffer (pH 8.0) and then suspended in the same buffer at a chlorophyll concentration of 14 μg/ml (1.4 μg/ml for the *psaAB* mutant, which has about sevenfold less chlorophyll on a per-cell basis [20]). Changes in the pH of the cell suspension (3 ml) kept at 30°C were monitored by using a pH electrode with a meter (Inlar 423 and Delta 350; Mettler Toledo, Halstead, United Kingdom). After each measurement, the signal was calibrated by injecting 10 μl of 7.5 mM HCl into the cell suspension.

Uptake of CO_2 and HCO_3^- was measured by the silicone oil-filtering centrif-

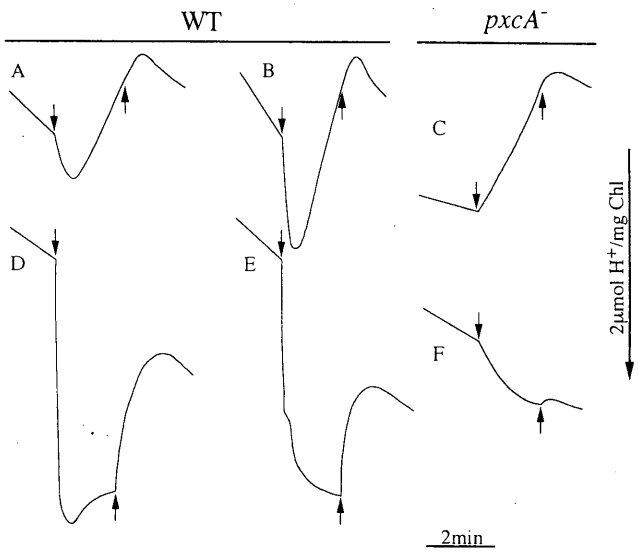

FIG. 1. Net proton movements in suspensions of WT (A, B, D, and E) and *pxcA* (C and F) cells upon switching the light on (arrow down) and off (arrow up). The cells were suspended in 0.2 mM TES-KOH buffer (pH 8.0) containing 15 mM KCl (A and D) or NaCl (B, C, E, and F) in the absence (A to C) and presence (D to F) of 1 mM DMBQ. The chlorophyll concentration in the cell suspension was 14 μg/ml.

ugation method (11, 25). Nitrate uptake was measured as described by Omata et al. (13). The cells were washed twice with nitrate-free medium (BG-11 medium minus $NaNO_3$, Na_2CO_3, and microelements) buffered with 5 mM MES-KOH at pH 6.5 or with 5 mM TES-KOH at pH 8.0 and then suspended in the same buffer supplemented with 5 mM $KHCO_3$ to a chlorophyll concentration of 7 μg/ml. NaCl (final concentration, 15 mM) was added to the cell suspension. The concentration of nitrate was determined with a Technicon autoanalyzer.

The light source for all the experiments was a 150-W halogen lamp (MHF-150L; Kagaku Kyoeisha Ltd., Osaka, Japan) equipped with a glass fiber. Cells in a sample chamber or in a 1.5-ml Eppendorf tube were illuminated by white light from the fiber at an intensity of 4.0 mmol of photosynthetically active radiation/m^2/s.

RESULTS

Effect of DMBQ on net proton exchange. The profiles of net proton exchange measured with the WT and *pxcA* cells are shown in Fig. 1. For these measurements, the cells were suspended in 0.2 mM TES-KOH buffer (pH 8.0) with (Fig. 1D to F) or without (Fig. 1A to C) 2,5-dimethyl-p-benzoquinone (DMBQ). When WT cells suspended in buffer containing 15 mM KCl (Fig. 1A) or NaCl (Fig. 1B) were illuminated, acidification followed by alkalization of the medium was observed. The acidification was stimulated by 15 mM Na^+. In contrast, for the *pxcA* mutant, only alkalization, not acidification, of the medium was observed upon illumination (Fig. 1C). It has been reported that alkalization of the medium is linked to photosynthetic fixation of CO_2 produced by dehydration of HCO_3^- (10). These results confirm that Na^+-stimulated light-induced proton extrusion occurs in the WT strain but not in the mutant (8).

Acidification of the medium was stimulated when WT cells were illuminated in the presence of DMBQ (Fig. 1D and E). DMBQ can oxidize the plastoquinone pool and may be reduced by PS I; hence, it is an electron acceptor in photosynthetic electron transport. Therefore, proton extrusion is linked to photosynthetic electron transfer. No net alkalization followed the acidification on illumination under these conditions, due to the absence of photosynthetic CO_2 fixation. The presence of Na^+ showed little effect on the extent of proton extrusion in the presence of DMBQ. Figure 1D and E indicates that the net proton extrusion does not proceed continuously in the light but ceases after 1 min of illumination. After the light was turned off, an influx of protons was observed. This suggests that in the light, both extrusion and influx of protons occur, reaching an equilibrium where there is no net proton exchange, whereas after the light is turned off (causing proton extrusion to cease), proton influx continues for a short time until a new steady-state level is attained. Both light-induced proton extrusion and postillumination proton influx were very low in *pxcA* cells in the presence of DMBQ (Fig. 1F).

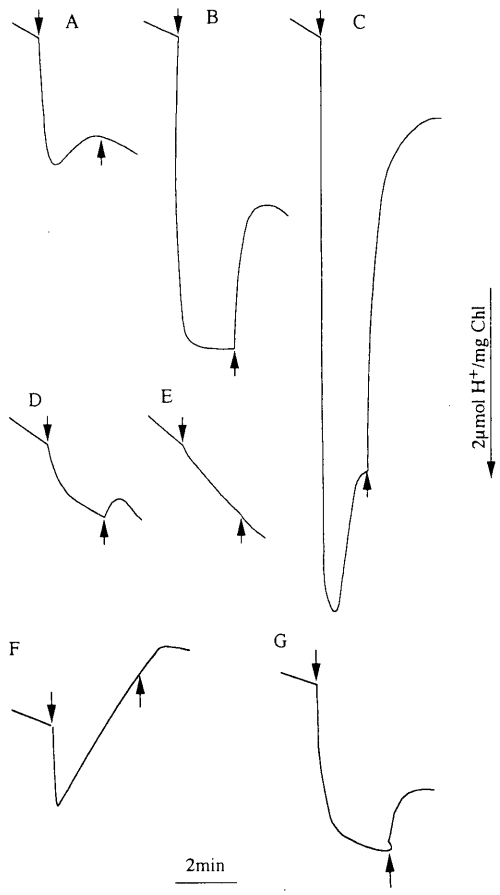

FIG. 2. Net proton movement in the suspensions of *psaAB* (A to C), *psbDIC/psbDII* (D and E), and *coxAB* (F and G) cells upon switching the light on (arrow down) and off (arrow up). The cells were suspended in 0.2 mM TES-KOH buffer containing 15 mM KCl (A) and NaCl (B to G). DMBQ was added prior to illumination in panels C, E, and F. The chlorophyll concentration in the cell suspension was 1.4 μg/ml for the *psaAB* mutant and 14 μg/ml for the *psbDIC/psbDII* and *coxAB* mutants.

Net proton exchange in mutants defective in PS I, PS II or cytochrome *c* oxidase. Now that a role of photosynthetic electron transfer in proton extrusion has been established, the next question involves the part(s) of photosynthetic electron transport proton with which extrusion is associated and whether respiratory electron transfer also plays a role. To address this question, mutants lacking either PS I, PS II, or cytochrome *c* oxidase were investigated. The *psaAB* (PS I-less) strain showed Na^+-stimulated light-induced proton extrusion (Fig. 2A and B). On a per-chlorophyll basis, the amplitude of proton extrusion was two- to threefold larger than that in WT cells (compare with Fig. 1A and B). Since about 85% of the chlorophyll in WT *Synechocystis* sp. strain PCC6803 is associated with PS I (20), this indicates that PS II-mediated electron transfer can

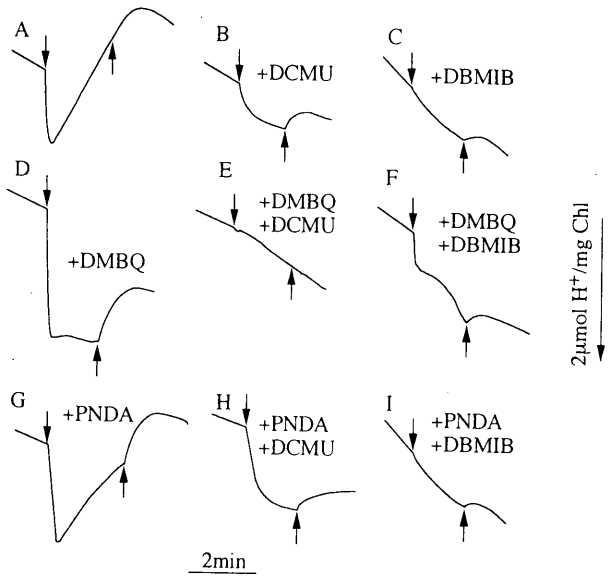

FIG. 3. Effect of DMBQ, PNDA, DCMU, and DBMIB on net proton movements in WT *Synechocystis* cells. The light was switched on (arrow down) and off (arrow up) as indicated. The cells were suspended in 0.2 mM TES-KOH buffer (pH 8.0) containing 15 mM NaCl. DMBQ (final concentration, 1 mM) (D to E), PNDA (3 mM) (G to I), DCMU (20 μM) (B, E, and H), and DBMIB (10 μM) (C, F, and I) were added as indicated. All additions were done prior to illumination.

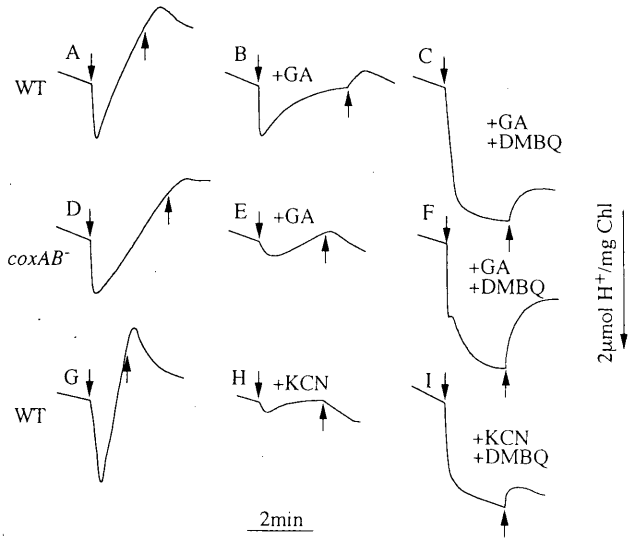

FIG. 4. Effect of GA, KCN, and DMBQ on net proton movements involving WT (A to C and G to I) and *coxAB* (D to F) cells of *Synechocystis*. The light was switched on (arrow down) and off (arrow up). The cells were suspended in 0.2 mM TES-KOH buffer (pH 8.0) containing 15 mM NaCl at a chlorophyll concentration of 14 μg/ml. GA (final concentration, 20 mM) (B, C, E, and F) and KCN (5 mM) (H and I) were added prior to illumination and DMBQ (1 mM) (C, F, and H) was added in the dark to the cell suspensions after the profiles in the presence of the inhibitors were obtained.

drive a significant amount of proton extrusion. No proton uptake was observed in the PS I-less mutant in the light, consistent with the lack of CO_2 fixation in this strain. In the presence of DMBQ, a more extensive acidification followed by proton uptake was observed (Fig. 2C), similar to what was seen in WT cells but again with a two- to threefold-higher amplitude on a per-chlorophyll basis. Thus, PS II-driven electron transport from water to DMBQ or, to a lesser extent, to oxygen (the latter involving oxidase[s]) can lead to proton extrusion.

A small amount of light-induced proton extrusion was observed when a cell suspension of the *psbDIC/psbDII* strain was illuminated in the absence of DMBQ (Fig. 2D) but not in its presence (Fig. 2E). The initial rate of light-induced proton extrusion in the *psbDIC/psbDII* strain was about 5% of that in the *psaAB* stain on a per-chlorophyll basis (the rates were 200 and 4,020 μmol/mg of chlorophyll/h in *psbDIC/psbDII* and *psaAB* strains, respectively, in the presence of 15 mM NaCl but in the absence of DMBQ).

The proton exchange profiles obtained for the *coxAB* mutant in the presence and absence of DMBQ were the same as those obtained for WT cells (Fig. 2F and G). Thus, cytochrome *c* oxidase is not essential to proton extrusion under these conditions.

Effect of electron transfer inhibitors and acceptors on proton exchange. The results presented thus far imply that electron transfer involving PS II is a major factor in light-driven proton extrusion. To further test this, proton extrusion was measured in WT cells after addition of 3-(3-4-dichlorophenyl)-1,1-dimethylurea (DCMU), a PS II electron transport inhibitor. Indeed, DCMU strongly inhibited the proton extrusion and created a pattern similar to that observed in the PS-II less mutant (compare Fig. 3B with Fig. 2D). The proton extrusion was more strongly inhibited by 2,5-dibromo-3-methyl-6-isopropyl-*p*-benzoquinone (DBMIB), an inhibitor of electron transport at the cytochrome b_6/f complex (Fig. 3C). The light-induced proton extrusion of WT cells in the presence of DMBQ was completely inhibited by DCMU (Fig. 3D and E); addition of DBMIB resulted in partial inhibition (Fig. 3F). Addition of DCMU during illumination in the presence of DMBQ caused influx of protons into the cells, and no postillumination proton influx was observed on subsequent removal of the light source (data not shown).

Addition of *p*-nitrosodimethylaniline (PNDA), a PS I electron acceptor (1), had little effect. However, if both PNDA and DCMU were added, the amount of proton extrusion was somewhat greater than when DCMU alone was added (Fig. 3B and H). DBMIB strongly inhibited the proton extrusion in the presence of PNDA (Fig. 3I). These results indicate that the extrusion of protons was abolished when both water splitting and the cytochrome b_6/f complex were inhibited. However, electron transport from water to DMBQ, and, to a lesser extent, from the intracellular reductants to electron acceptors via PS I and/or PS I-dependent cyclic electron flow energizes proton extrusion.

To test the hypothesis that alkalization is driven by HCO_3^- utilization, photosynthetic CO_2 fixation was inhibited by glyceraldehyde (GA) treatment. This treatment reduced the rate of alkalization in both the WT and *coxAB* cells (Fig. 4A, B, D, and E), indicating that OH^- produced as a result of bicarbonate utilization is extruded in the light. Interestingly, GA did not affect the light-induced proton extrusion in the WT strain (Fig. 4A and B) but had a strong inhibitory effect on proton extrusion in the *coxAB* strain (Fig. 4D and E). The GA inhibition was relieved by addition of DMBQ (Fig. 4F). A similar result was obtained with the WT strain when 5 mM KCN was added (Fig. 4G to I). At this concentration, KCN inhibits both photosynthetic CO_2 fixation and oxidase activity. Therefore, in the absence of photosynthetic CO_2 fixation, electron flow to oxygen via cytochrome *c* oxidase is essential for proton extrusion. If this electron flow cannot occur, the quinone pool may be overreduced and continuous electron transfer cannot occur.

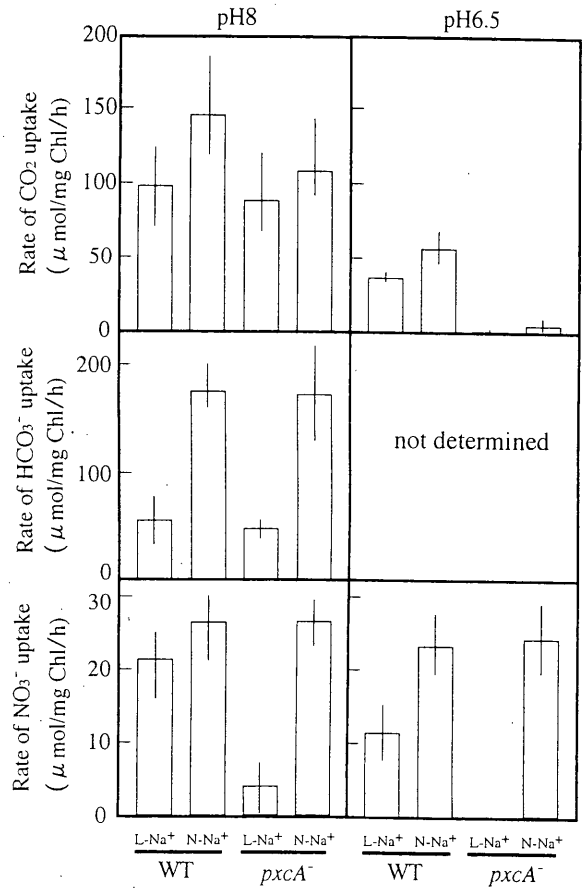

FIG. 5. Rates of CO_2, HCO_3^-, and NO_3^- uptake in WT and *pxcA* cells of *Synechocystis* at pH 8.0 and pH 6.5 in the presence of 15 mM NaCl (N-Na^+) or KCl (L-Na^+).

However, if DMBQ is added, PS II-mediated electron transfer can resume and proton extrusion is observed.

Effect of Na^+ and pH on the uptake of CO_2, HCO_3^-, and NO_3^- in WT and *pxcA* strains. Protons are produced during the transport of CO_2 and are consumed when NO_3^- is reduced to NH_4 via NO_2^- or when HCO_3^- is converted to CO_2. Cells have a mechanism to maintain homeostasis with respect to the intracellular pH and electroneutrality during these processes. To test whether the PxcA-dependent proton exchange is involved in maintaining this homeostasis, the uptake of CO_2, HCO_3^-, and NO_3^- was monitored as a function of the activity of proton exchange. For this purpose, the uptake of CO_2, HCO_3^-, and NO_3^- in the WT and the *pxcA* strains was measured at pH 8.0 and 6.5 in the presence of a normal concentration of NaCl (15 mM, close to the concentration in BG-11 medium) or KCl (15 mM) with a low contaminating concentration of Na^+ (~100 μM Na^+). As reported previously (5), HCO_3^- uptake was high at the normal Na^+ concentration and low at the low Na^+ concentration in the WT and the *pxcA* strains (Fig. 5, middle row). Thus, *pxcA* inactivation did not affect the HCO_3^- uptake. At the low Na^+ concentration, the NO_3^- uptake was very low in the *pxcA* strain at pH 8.0 and was zero at pH 6.5 (bottom rows). At the normal Na^+ concentration, no significant effect of *pxcA* inactivation was observed on CO_2 and NO_3^- uptake at pH 8.0 but CO_2 uptake activity was reduced significantly at pH 6.5 (top and bottom rows). No CO_2 uptake was observed in the mutant at pH 6.5 in the presence of a low Na^+ concentration. It is evident that the inactivation of *pxcA* strongly affected the CO_2 uptake under acidic conditions and the NO_3^- uptake at low Na^+ concentrations.

DISCUSSION

The results presented here demonstrate that proton extrusion is driven by PS II coupled to the cytochrome b_6/f complex (Fig. 1 to 3). Some proton extrusion can also be driven by PS I. PxcA is an important factor in mediating this proton extrusion. The question now is how this proton extrusion occurs. First, it is unlikely that protons produced by PS II and the cytochrome b_6/f complex are directly extruded into the medium, since the lumen and the periplasmic space are presumed to be two different compartments. In addition, protons pumped by these complexes should lead to ATP synthesis and should not be "wasted" by extrusion. Therefore, an energy carrier would be required. ATP seems to be the only candidate for such a carrier that energizes the proton extrusion system; NADPH is not a candidate, because the PS II electron transfer is effective in causing proton extrusion.

The activity of proton extrusion appears to be correlated with the activity of photosynthetic water splitting and electron transport through the cytochrome b_6/f complex; both of these processes produce a proton gradient across the thylakoid membrane and thereby can lead to the generation of ATP. This supports the view that the PxcA-dependent proton extrusion is energized by ATP. PxcA does not have an ATP-binding motif and therefore probably is unable to hydrolyze ATP by itself. PxcA may be a regulator of an ATP-dependent proton extrusion pump, and the pump activity is very low in the absence of PxcA.

Besides this PxcA-dependent proton exchange system, cyanobacterial cells possess a Na^+/H^+ antiport system (14). In fact, the genome of *Synechocystis* sp. strain PCC6803 contains five genes resembling those coding for Na^+/H^+ antiporters (4). Two of these gene products contain an ATP-binding motif. It is possible that these gene products are involved in PxcA-dependent proton exchange.

The results presented in Fig. 5 indicate that inactivation of *pxcA* affects the uptake of CO_2 and NO_3^-. Recently, Rolland et al. reported that inactivation of *cemA* affects the uptake of inorganic carbon in the chloroplast of *Chlamydomonas* (15). These results obtained with *Synechocystis* and *Chlamydomonas* strongly suggest that *cemA* and *pxcA* have the same function in chloroplasts and cyanobacterial cells, respectively.

Based on the results obtained, we propose a working hypothesis involving two complementary proton exchange systems, one of which depends on PxcA, to explain the growth characteristics and inorganic carbon and nitrate uptake of the WT and *pxcA* strains. This hypothesis has the following features. (i) PxcA-dependent and PxcA-independent proton exchange systems play essential roles in maintaining homeostasis with respect to the intracellular pH and electroneutrality. The proton exchange catalyzed by both systems is stimulated by Na^+. (ii) Both systems are essential to growth and CO_2 transport at pH 6.5, but the PxcA-independent system alone is sufficient at pH 8 when the activity is high at the normal Na^+ concentration. However, both systems are required even at this alkaline pH when the activity of each system is low at the low Na^+ concentration. (iii) At the low Na^+ concentration, NO_3^- uptake requires the PxcA-dependent system. However, when PxcA-independent proton exchange is active at the normal Na^+ concentration, the PxcA-dependent system is not required for NO_3^- uptake. (iv) Uptake of HCO_3^- requires a

high activity of PxcA-independent proton exchange at the normal Na^+ concentration in both WT and *pxcA* cells.

Proton exchange catalyzed by the PxcA-independent system should be observed as the pH of the suspension medium of *pxcA* cells changes. The slow alkalization observed with *pxcA* cells in the light may be due to proton influx by the PxcA-independent system; it is also possible that rapid influx and efflux of protons via the PxcA-independent system occur with a small net proton movement that cannot be measured by the pH electrode used in this study.

ACKNOWLEDGMENTS

This study was supported by a Grant-in-Aid for Scientific Research (grant 09640767) from the Ministry of Education, Science, Sports and Culture of Japan and by grants from the New Energy and Industrial Technology Development Organization (NEDO) of Japan and from the Human Frontier Science Program.

REFERENCES

1. **Elstner, E. F., and H. Zeller.** 1978. Bleaching of p-nitrosodimethylaniline by photosystem 1 of spinach lamellae. Plant Sci. Lett. **13**:15–20.
2. **Hawkesford, M. J., P. Rowell, and W. D. P. Stewart.** 1963. Energy transduction in cyanobacteria, p. 199–218. *In* G. C. Papageorgiou and L. Packer (ed.), Photosynthetic prokaryotes: cell differentiation and function. Elsevier, Amsterdam, The Netherlands.
3. **Hinrichs, I., S. Scherer, and P. Boger.** 1985. Two different mechanisms of light induced proton efflux in the blue-green alga *Anabaena variabilis*. Physiol. Veg. **23**:717–724.
4. **Kaneko, T., S. Sato, H. Kotani, A. Tanaka, E. Asamizu, Y. Nakamura, N. Miyajima, M. Hirosawa, M. Sugiura, S. Sasamoto, T. Kimura, T. Hosouchi, A. Matsuno, A. Muraki, N. Nakazaki, K. Naruo, S. Okumura, S. Shimpo, C. Takeuchi, T. Wada, A. Watanabe, M. Yamada, M. Yasuda, and S. Tabata.** 1996. Sequence analysis of the genome of the unicellular cyanobacterium *Synechocystis* sp. strain PCC6803. II. Sequence determination of the entire genome and assignment of potential protein-coding regions. DNA Res. **3**:109–136.
5. **Kaplan, A., R. Schwarz, J. Lieman-Hurwitz, M. Ronen-Tarazi, and L. Reinhold.** 1994. Physiological and molecular studies on the response of cyanobacteria to changes in the ambient inorganic carbon concentration, p. 469–485. *In* D. A. Bryant (ed.), The molecular biology of cyanobacteria. Kluwer Academic Publishers, Dordrecht, The Netherlands.
6. **Kaplan, A., S. Scherer, and M. Lerner.** 1989. Nature of the light-induced H^+ efflux and Na^+ uptake in cyanobacteria. Plant Physiol. **89**:1220–1225.
7. **Katoh, A., K. S. Lee, H. Fukuzawa, K. Ohyama, and T. Ogawa.** 1996. A *cemA* homologue essential to CO_2 transport in the cyanobacterium, *Synechocystis* PCC6803. Proc. Natl. Acad. Sci. USA **93**:4006–4010.
8. **Katoh, A., M. Sonoda, H. Katoh, and T. Ogawa.** 1996. Absence of light-induced proton extrusion in *cotA*-less mutant of *Synechocystis* sp. strain PCC6803. J. Bacteriol. **178**:5452–5455.
9. **Lockau, W., and S. Pfeffer.** 1982. A cyanobacterial ATPase distinct from the coupling factor of photophosphorylation. Z. Naturforsch. Sect. C **37**:658–664.
10. **Miller, A. G., and B. Colman.** 1980. Active transport and accumulation of bicarbonate by a unicellular cyanobacterium. J. Bacteriol. **143**:1253–1259.
11. **Ogawa, T.** 1991. A gene homologous to the subunit-2 gene of NADH dehydrogenase is essential to inorganic carbon transport of *Synechocystis* PCC6803. Proc. Natl. Acad. Sci. USA **88**:4275–4279.
12. **Ogawa, T., and A. Kaplan.** 1987. The stoichiometry between CO_2 and H^+ fluxes involved in the transport of inorganic carbon in cyanobacteria. Plant Physiol. **83**:888–891.
13. **Omata, T., M. Ohmori, N. Arai, and T. Ogawa.** 1989. Genetically engineered mutant of the cyanobacterium *Synechococcus* PCC7942 defective in nitrate transport. Proc. Natl. Acad. Sci. USA **86**:6612–6616.
14. **Ritchie, R. J.** 1992. Sodium transport and the origin of the membrane potential in the cyanobacterium *Synechococcus* R-2 (*Anacystis nidulans*) PCC7942. J. Plant Physiol. **139**:320–330.
15. **Rolland, N., A.-J. Dorne, G. Amoroso, D. F. Sultemeyer, J. Joyard, and J.-D. Rochaix.** 1997. Disruption of the plastid *ycf10* open reading frame affects uptake of inorganic carbon in the chloroplast of *Chlamydomonas*. EMBO J. **16**:6713–6726.
16. **Sasaki, Y., K. Sekiguchi, Y. Nagano, and R. Matsuno.** 1993. Chloroplast envelope protein encoded by chloroplast genome. FEBS Lett. **316**:93–98.
17. **Scherer, S., I. Hinrichs, and P. Boger.** 1986. Effect of monochromatic light on proton efflux of the blue-green alga *Anabaena variabilis*. Plant Physiol. **81**:939–941.
18. **Scherer, S., H. Riege, and P. Boger.** 1988. Light-induced proton release by the cyanobacterium *Anabaena variabilis*: dependence on CO_2 and Na^+. Plant Physiol. **86**:769–772.
19. **Schmetterer, G., D. Alge, and W. Gregor.** 1994. Deletion of cytochrome c oxidase genes from the cyanobacterium *Synechocystis* sp. PCC6803: evidence for alternative respiratory pathways. Photosynth. Res. **42**:43–50.
20. **Shen, G., S. Boussiba, and W. F. J. Vermaas.** 1993. *Synechocystis* sp. PCC6803 strains lacking photosystem I and phycobilisome function. Plant Cell **5**:1853–1863.
21. **Sonoda, M., K. Kitano, A. Katoh, H. Katoh, H. Ohkawa, and T. Ogawa.** 1997. Size of *cotA* and identification of the gene Product in *Synechocystis* sp. strain PCC6803. J. Bacteriol. **179**:3845–3850.
22. **Sonoda, M., H. Katoh, H. Ohkawa, and T. Ogawa.** 1997b. Cloning of *cotA* gene of *Synechococcus* PCC7942 and complementation of a *cotA*-less mutant of *Synechocystis* PCC6803 with chimeric genes of the two strains. Photosynth. Res. **54**:99–105.
23. **Stanier, R. Y., R. Kunisawa, M. Mandel, and G. Cohen-Bazire.** 1971. Purification and properties of unicellular blue-green algae (order *Chroococcales*). Bacteriol. Rev. **35**:171–205.
24. **Vermaas, W. F. J., J. Charit, and B. Eggers.** 1990. System for site-directed mutagenesis in the *psbD1/C* operon of *Synechocystis* sp. PCC6803, p. 231–238. *In* M. Baltscheffsky (ed.), Current research in photosynthesis, vol. 1. Kluwer Academic Publishers, Dordrecht, The Netherlands.
25. **Volokita, M., D. Zenvirth, A. Kaplan, and L. Reinhold.** 1984. Nature of the inorganic carbon species actively taken up by the cyanobacterium *Anabaena variabilis*. Plant Physiol. **76**:599–602.

The use of mutants in the analysis of the CO_2-concentrating mechanism in cyanobacteria[1]

Hiroshi Ohkawa, Masatoshi Sonoda, Hirokazu Katoh, and Teruo Ogawa

Abstract: Mutants of cyanobacteria defective in parts of the CO_2-concentrating mechanism are classified into three types. (*i*) Mutants defective in inorganic carbon transporters. One of these mutants was constructed by inactivating *cmpA* encoding 42 kDa protein in the cytoplasmic membrane. (*ii*) Mutants defective in NAD(P)H dehydrogenase(s). There are five *ndhD* genes in *Synechocystis* PCC6803, two of them expressed constitutively and three inducible by low CO_2. Two kinds of NAD(P)H dehydrogenase appear to be involved in energizing and inducing the high affinity inorganic carbon transport system. (*iii*) Mutants defective in carboxysome with impaired *ccm* or *icfA* genes. New type of mutants with impaired *cotA* (renamed as *pxcA*) have also been isolated. These mutants did not show light-induced proton extrusion and were unable to grow at acidic pHs. A mutant constructed by inactivating *cotA* (*pxcA*) in the wild-type *Synechocystis* was unable to transport CO_2 at pH 6.5. We concluded that *cotA* (*pxcA*) has a role in light-induced proton extrusion that is essential at acidic pHs to extrude protons produced during CO_2 transport.

Key words: CO_2-concentrating mechanism (CCM), CO_2 transport, NAD(P)H dehydrogenase, proton extrusion, carboxysome, mutant.

Résumé : On classifie en trois catégories les mutants cyanobactériens partiellement défectueux au niveau de parties du mécanisme de concentration du CO_2. (*i*) Des mutants défectueux au niveau des transporteurs de carbone inorganique. Un de ces mutants a été construit en inactivant le *cmpA* codant pour une protéine de 42 kDa localisée dans la membrane cytoplasmique. (*ii*) Des mutants défectueux au niveau de la (des) déshydrogénase(s) de la NAD(P)H. Il y a cinq gènes *ndhD* chez le *Synechocystis* PCC6803, dont deux s'expriment constitutivement et trois sont inductibles par la faible teneur en CO_2. Deux sortes de déshydrogénase de la NAD(P)H semblent être impliquées dans l'apport en énergie et dans l'induction du système de transport de carbone inorganique à haute affinité. (*iii*) Des mutants défectueux au niveau du carboxysome avec des gènes *ccm* et *icfA* déréglés. On a également isolé un nouveau type de mutant avec le gène *cotA* (renommé *pxcA*) déréglé. Ces mutants ne montrent pas d'expulsion de protons induite par la faible luminosité et sont incapables de croître aux pH acides. Un mutant construit par inactivation des *cotA* (*pxcA*) chez le type sauvage du *Synechocystis* s'est avéré incapable de transporter le CO_2 au pH 6,5. Les auteurs concluent que le *cotA* (*pxcA*) joue un rôle dans l'expulsion de protons sous l'influence de la lumière, lequel est esentiel aux pH acides pour expulser les protons produit au cours du transport du CO_2.

Mots clés : mécanisme de concentration du CO_2 (CCM), transport du CO_2, déshydrogénase de la NAD(P)H, expulsion de protons, carboxysome, mutant.

[Traduit par la rédaction]

Introduction

The use of mutants of transformable strains of cyanobacteria is a powerful technique to analyze the CO_2-concentrating mechanism (CCM). Kaplan's group first isolated the high CO_2 requiring (HCR) mutant of *Synechococcus* PCC7942 defective in the CCM (Marcus et al. 1986) and mapped the site of mutation at *ccmN* in the unstream region of *rbc* operon (Friedberg et al. 1989). Since their pioneering work, many mutants defective in parts of the CCM have been isolated and analyzed using transformable strains of cyanobacteria; *Synechococcus* PCC 7942, *Synechocystis* PCC6803, and *Synechococcus* PCC7002 (Ogawa et al. 1987; Abe et al. 1988; Price and Badger 1989*b*; Ogawa 1990; Yu et al. 1994; Sültemeyer et al. 1997; Ronen-Tarazi et al. 1997). Physiological and molecular analyses of these mutants reveal that the cyanobacterial CCM consists of three basic systems: (*i*) C_i transporters, (*ii*) a system for energizing C_i transport and (*iii*) the Rubisco-containing carboxysome system for CO_2 fixation. The *cmp* genes that encode a bicarbonate transporter are involved in the first system (T. Omata, T. Ogawa, G.D. Price, M.R. Badger, and M. Oka-

Received July 30, 1997.

H. Ohkawa and M. Sonoda. Biochemical Regulation Center, Nagoya University, Chikusa, Nagoya 464-8601, Japan.
H. Katoh. Bioscience Center, Nagoya University, Chikusa, Nagoya 464-8601, Japan.
T. Ogawa.[2] Biochemical Regulation and Bioscience Center, Nagoya University, Chikusa, Nagoya 464-8601, Japan.

[1] This paper arises from work presented at a conference on "The 3rd International Symposium on Inorganic Carbon Utilization by Aquatic Photosynthetic Organisms" held at The University of British Columbia, July 28 – August 1, 1997.

[2] Author to whom all correspondence should be addressed. e-mail: h44975a@nucc.cc.nagoya-u.ac.jp

mura, unpublished data), *ndh* genes encoding subunits of NAD(P)H dehydrogenase in the second system (Ogawa 1991*a*, 1991*b*; Marco et al. 1993) and *ccm* (Friedberg et al. 1989; Schwarz et al. 1988; Kaplan et al. 1994; Price et al. 1993; Ogawa et al. 1994*a*, 1994*b*) and *icfA* genes (Fukuzawa et al. 1992) encoding components of carboxysome in the third system. In addition to these CCM mutants, we have isolated a new type of mutants from *Synechocystis* PCC6803 that are defective in CO_2 transport (Katoh et al. 1996*a*). The gene (designated as *cotA* and renamed as *pxcA*) impaired in the mutants is a homologue of *cemA* in chloroplast genomes that encodes a protein localized in chloroplast envelope membrane (Katoh et al. 1996*a*; Sonoda et al. 1997*a*; Sasaki et al. 1993). Physiological analysis of a mutant constructed by deleting *cotA* (*pxcA*) revealed that the mutant did not extrude protons in the light and this resulted in an inhibition of the CO_2 transport (Katoh et al. 1996*b*). In this paper, we shall describe the use of these mutants in the analysis of the CCM in cyanobacteria while focusing on the physiological analysis of some of the mutants constructed in our laboratory.

Isolation of mutants

Most of the HCR mutants were isolated by the classical technique of mutagenizing the wild-type (WT) cells by a chemical mutagen, such as *N*-methyl-*N'*-nitro-*N*-nitrosoguanidine, and enriched using ampicillin (Ogawa 1990). After mutagenesis, cells were washed, grown under nonselective conditions (at 3% CO_2) and then grown under selective conditions (at low CO_2 concentrations where the WT cells grow normally but the HCR mutants are unable to grow) in the presence of ampicillin for few days. Cells were subsequently washed and plated on agar plates containing BG11 medium (Stanier et al. 1971) and incubated under 3% CO_2 conditions in the light until colonies appeared. Colonies are screened on duplicate plates under nonselective and selective conditions. Mutants defective in the CCM are recovered as colonies that do not grow or grow very slowly under the selective conditions.

The other method of generating HCR mutants is to mutagenize the cells by random "tagging" or through insertional inactivation or deletion of defined regions of DNA (Williams and Szalay 1983). The principle of this method is depicted by Vermaas (1993) and the isolation of mutants by tagging is shown by Dolganov and Grossman (1993). There is also a technique to express foreign genes on host specific plasmids or on the host genome (Price and Badger 1989*a*). These techniques have been used to create various specific mutants of the CCM.

Complementation test

The method of transformation reported by Dzelzkalns and Bogorad (1988) has been used for genetic complementation of mutants. Mutant cells at logarithmic phase of growth are plated in 0.8% top agar onto 1.5% agar plates. After solidification of the agar, each library (50–500 ng DNA/μL of water) is applied directly onto the surface of the plate. The transformants capable of growing under the selective conditions (low CO_2) are detected in 7 days. The complementation test is done with a fractionated library and then with clones obtained from a complementing fraction. Another method is complementation by tagging (Friedberg et al. 1989), which introduces WT gene tagged with a drug-resistant marker into the mutated gene. Once the mutated gene is tagged, it can be easily cloned and analyzed.

Mutants defective in C_i transporter(s)

Physiological analysis of C_i transport indicated that both CO_2 and HCO_3^- are transported into the cells and delivered to the interior of the cells as HCO_3^- (Volokita et al. 1984). There are several differences between the characteristics of CO_2 transport and HCO_3^- transport (Kaplan et al. 1994; Espie et al. 1991; Miller et al. 1991). CO_2 transport is constitutive and its activity is high even in high CO_2 grown cells (H-cells). In contrast HCO_3^- transport is inducible and its activity is low in H-cells and is increased during adaptation of the cells to low CO_2 conditions. Early studies by Omata and Ogawa (1986) have demonstrated that a protein with the molecular mass of 42 kDa was absent in the cytoplasmic membranes of H-cells of *Synechococcus* PCC7942 and was synthesized during adaptation of the cells to low CO_2 conditions. The gene (*cmpA*, *c*ytoplasmic *m*embrane *p*rotein *A*) encoding the 42-kDa protein was cloned and sequenced (Omata et al. 1990). A mutant (M42) constructed by inactivating this gene by inserting a kanamycin resistance cartridge still possessed the activity of HCO_3^- transport and grew under air levels of CO_2. Sequencing of the region downstream of *cmpA* however, revealed that the gene has the structure of an ABC transporter and Northern analysis indicated that *cmpA* is cotranscribed with *cmpB*, *cmpC*, and *cmpD* (Omata 1992). These results strongly suggested that *cmp* genes encode a HCO_3^- transporter. Cells deficit in *cmpA* can still grow on low CO_2 levels. However, the presence of multiple HCO_3^- transporters makes the phenotype of the M42 mutant not much different from that of the WT. Recently, Omata et al. analyzed the activity of HCO_3^- transport in the WT and the M42 mutant under various conditions and demonstrated that *cmp* genes encode subunits of a HCO_3^- transporter (T. Omata, T. Ogawa, G.D. Price, M.R. Badger, and M. Okamura, unpublished data). Homologues of *cmp* genes have been found in *Synechocystis* PCC6803 (Kaneko et al. 1996). These genes were expressed only under low-CO_2 conditions but inactivation of these genes had no effect on the activity of HCO_3^- transport under low-CO_2 conditions (unpublished). It is likely that the functioning of other HCO_3^- transporter(s) may compensate for the inactivation of the *cmp* genes. Recently, Ronen-Tarazi et al. (1997) have isolated mutants impaired in HCO_3^- uptake with the aid of an inactivation library and cloned the tagged genes in the mutants. These genes could encode another type of HCO_3^- transporter.

There are more than 150 transporter genes on the genome of *Synechocystis* PCC6803 (Cyanobase, Kazusa DNA Research Institute; Kaneko et al. 1996), but a few of them have been characterized and their pysiological role established. It might be possible to identify other HCO_3^- transporter genes of *Synechocystis* by studying the transporter genes that are expressed under low CO_2 conditions.

Regarding the transport of CO_2, several models have been proposed. The simplest model will be that CO_2 and HCO_3^- are transported by two separate systems (Espie et al. 1991; Miller et al. 1991). In another model CO_2 is hydrated to HCO_3^- as they are transported into the cells (Volokita et al. 1984). Mu-

Fig. 1. Changes in the level of the transcripts of five *ndhD* genes in *Synechocystis* PCC6803 during aeration of 50 ppm CO_2 in the light. Cells grown at 3% CO_2 were aerated with the low-CO_2 air for the periods indicated on the abscissas.

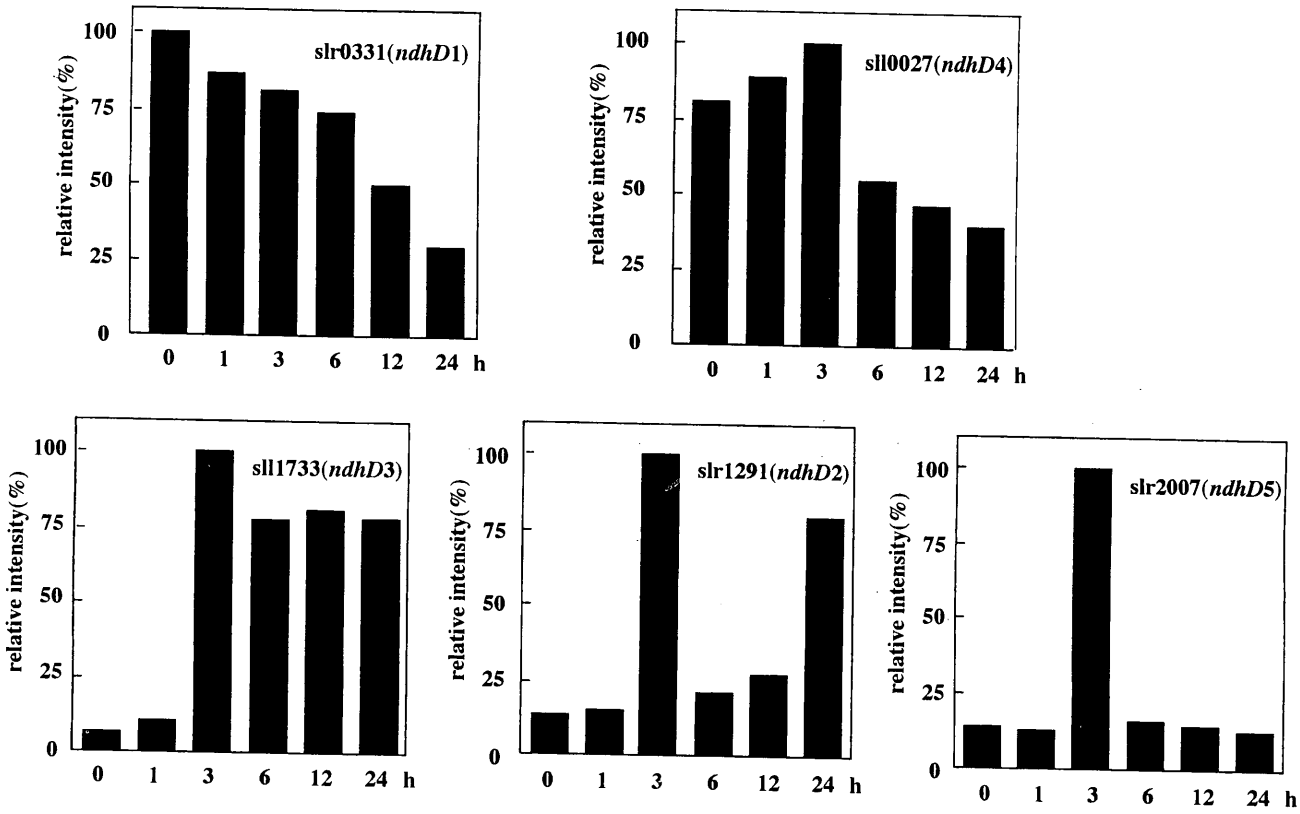

tants defective in CO_2 transport have been isolated. The gene that complemented these mutants was cloned and named *cotA* (CO_2 transport A; Katoh et al. 1996). However, a mutant constructed by deleting *cotA* (M29) still possessed the activity of CO_2 transport but had lost the activity of proton extrusion in the light (Katoh et al. 1996*b*). Based on this result, *cotA* was renamed *pxcA* (*p*roton e*x*change *A*). The possible role of *pxcA* in the transport of CO_2 and anions will be discussed in the latter part of this paper. Thus, the gene encoding a CO_2 transporter has as yet to be identified. Isolation of such gene will help to clarify the mechanism of CO_2 transport.

Mutants defective in NAD(P)H dehydrogenase

RKa and RKb are the HCR mutants of *Synechocystis* PCC6803 that do not have the ability to transport extracellular C_i into the cells (Ogawa 1990). Genes impaired in these mutants were cloned and identified to be *ndhB* and *ndhL*, respectively, both encoding hydrophobic subunits of NAD(P)H dehydrogenase (Ogawa 1991*a*, 1991*b*). An antibody raised against the *ndhL* gene product cross-reacted with a 6.7-kDa protein in the thylakoid membrane of the WT *Synechocystis* (Ogawa 1992). The immunoblot of the cytoplasmic membrane indicated that the 6.7-kDa band was poorly stained. Based on these results we concluded that the immunoreactive band in the cytoplasmic membrane preparation originated from contaminating thylakoid membranes. However, based on the Western analysis using the antibody raised against the products of *ndhJ* and *ndhK*, Berger et al. (1991) claimed that NAD(P)H dehydrogenase is present both in the thylakoid and cytoplasmic membranes. Preparation of cytoplasmic membranes free from contamination of thylakoid membrane is needed to conclusively determine the localization of NAD(P)H dehydrogenase.

Table 1. The growth rates of the WT and *ndhD*-inactivated mutants of *Synechocystis* PCC6803.

Cells	Growth rates (h)*	
	3% CO_2	50 ppm CO_2
WT	6.9	15.7
Δ*ndhD1*	6.9	15.0
Δ*ndhD2*	6.7	15.9
Δ*ndhD3*	10.5	52.0
Δ*ndhD4*	10.5	17.5
Δ*ndhD5*	11.1	17.2

*Growth rates at pH 6.5 expressed by doubling times in hours.

The C_i transport in cyanobacteria is driven by photosystem I (PS I) cyclic electron flow (Ogawa and Ogren 1985; Ogawa et al. 1985). After isolation of NAD(P)H dehydrogenase mutants deficient in the CCM, it was presumed that NAD(P)H dehydrogenase is involved in this process. This hypothesis was supported by Mi et al. (1994, 1995) who demonstrated that NADPH donates electrons to plastoquinone in the WT cells but not in *ndhB*-inactivated mutant of *Synechocystis* (M55). It was assumed that ATP produced by coupling to the cyclic

Fig. 2. A hypothetical model for the role of NAD(P)H dehydrogenase(s) in energization and induction of high-affinity C_i transport system.

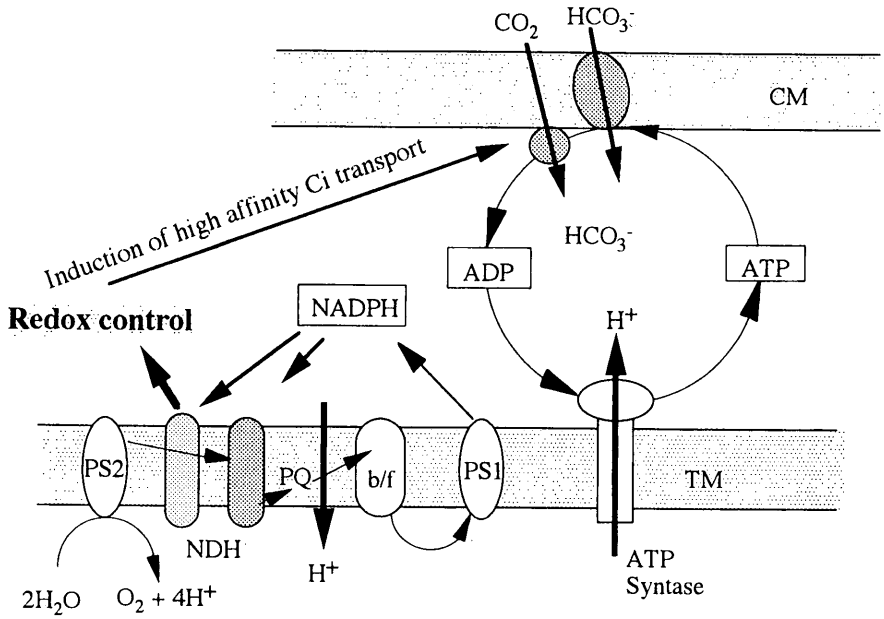

Fig. 3. The size and hydrophobic regions of CemA and PxcA. Shadowed boxes indicate potential hydrophobic membrane spanning domains.

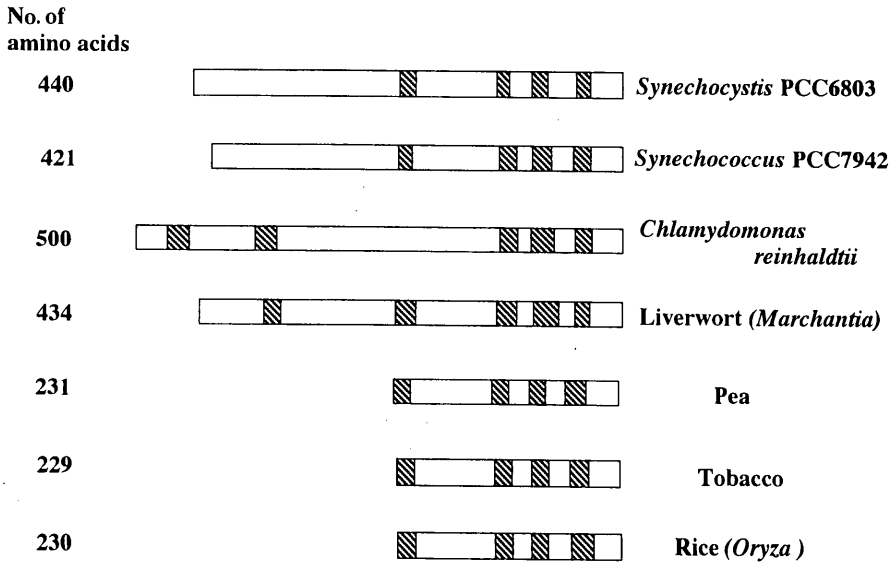

electron flow may be the direct energy source of the C_i transport. Inactivation of *ndhB* in the WT *Synechococcus* PCC7942 also produced a HCR mutant and indicated that NAD(P)H dehydrogenase is essential to C_i transport in this cyanobacterial strain (Marco et al. 1993).

The genome of *Synechocystis* PCC6803 ($\sim 3.6 \times 10^6$ bp DNA) contains one copy of *ndhA, ndhB, ndhC, ndhE, ndhG, ndhH, ndhJ, ndhK* (denoted as *psbG*), and *ndhL* (classified into the transporter gene group as *ictA* in the Cyanobase); two copies of *ndhI*; five copies of *ndhD*; and four copies of *ndhF* (the Cyanobase; Kaneko et al. 1996). There is another *psbG* gene in one of the plasmids. The presence of multiple copies of *ndhI*, *ndhD*, and *ndhF* raises the possibility of heterogeneity in the NAD(P)H dehydrogenase complexes.

Sültemeyer et al. (1997) have isolated mutants of *Synechococcus* PCC7002 that lack the ability to induce a high-affinity CO_2 transport system and do not grow at pH 6.5 during aeration of 30 ppm CO_2. The lesions in both mutants were mapped at *ndhD*, which is a homologue of sll1733 of *Synecocystis* PCC6803 in the Cyanobase and is named as *ndhD3*. slr0331, slr1291, sll0027, and slr2007 in the Cyanobase are named as *ndhD1*, *ndhD2*, *ndhD4*, and *ndhD5*, respectively. Northern analysis has been done using the *ndhD* genes of *Synecocystis* as probes and mutants have been constructed by inactivating

Fig. 4. Net proton movements in suspensions of WT (curves A–C and E) and MΔ*pxcA* (D) cells of *Synechocystis* upon switching the light on and off. Cells were suspended in 0.2 mM Tes-KOH buffer containing 15 mM NaCl (B, D, and E) or KCl (C) and pH of the external solution was monitored by a pH electrode with a meter (Inlar 423 and Delta 350; Mettler Toledo, Halstead Essex, U.K.). Curve E was obtained in the presence of 1 mM DMQ. DCMU was added as indicated. For details of the pH measurement, see Katoh et al. 1996*b*.

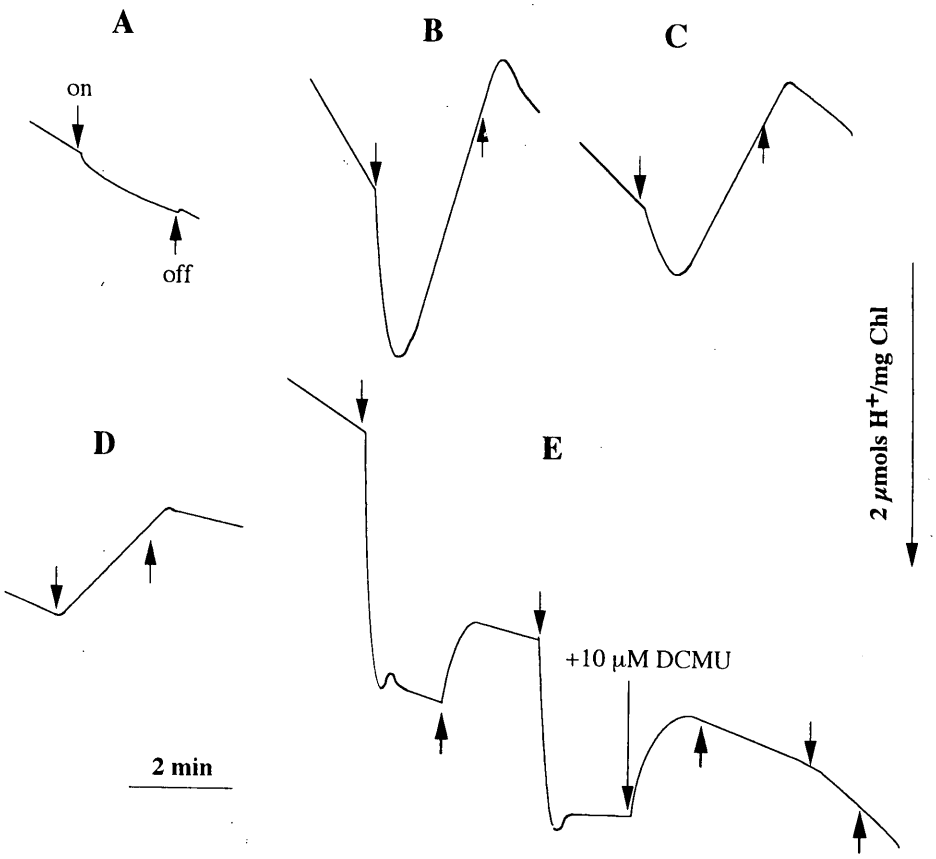

each of the *ndhD* genes. The Northern analysis indicated that there are two types of *ndhD* genes; *ndhD1* and *ndhD4* were constitutively expressed, whereas *ndhD2*, *ndhD3*, and *ndhD5* were induced by low CO_2 (Fig. 1). A mutant constructed by inactivating *ndhD3* grew very poorly at 50 ppm CO_2 on pH 6.5 media (Table 1), being consistent with the observation with the *Synechococcus* PCC7002 mutants (Sültemeyer et al. 1997). Inactivation of other *ndhD* genes did not have a significant effect on growth characteristics. These results suggested that there are at least two kinds of functionally different NAD(P)H dehydrogenases. The one that has *ndhD3* gene product as a subunit is involved in inducing high affinity CO_2 transport system, possibly by redox control of gene expression or protein phosphorylation, and the other is a component of PS I cyclic electron flow to energize the C_i transport (Fig. 2). The fact that inactivation of single *ndhD* gene did not produce a HCR mutant suggests that multiple *ndhD* genes encode the subunit of the latter type of NAD(P)H dehydrogenase.

Mutants defective in carboxysomes

The E1 mutant of *Synechococcus* PCC7942 isolated by Marcus et al. (1986) was the first cyanobacterial HCR mutant. Since then, many mutants of a similar phenotype have been isolated. These include C3P-O (Abe et al. 1988), O221 (Schwarz et al. 1988), RK1 (Ogawa et al. 1987), and types I and II mutants (Price and Badger 1989*b*) of *Synechococcus* PCC794 and RK11 (Ogawa 1990), G3 (Ogawa et al. 1994*a*), and G7 (Ogawa et al. 1994*b*) of *Synechocystis* PCC6803. All of these mutants accumulated high concentrations of intracellular C_i but were unable to fix it by photosynthesis. The lesions in the *Synechococcus* mutants were mapped in the *ccm* genes in the 5′-flanking region of *rbc* operon (Friedberg et al. 1989; Kaplan et al. 1994; Price et al. 1993) or in the gene (*icfA*) encoding carboxysomal CA that was mapped about 20 kilobase pairs downstream of the *rbc* operon (Fukuzawa et al. 1992). Five *ccm* genes were found in *Synechococcus* PCC7942 in the order of *ccmK–ccmL–ccmM–ccmN–ccmO*. In contrast, *ccm* genes in *Synechocystis* PCC6803 are not located in the vicinity of the *rbc* operon and showed a cluster in the order of *ccmK–ccmK–ccmL–ccmM–ccmN* (Kaneko et al. 1996). A homologue of *ccmO* is not present and five *ccmK* genes are found in this strain. These genes are considered to encode proteins essential to carboxysomal structure and function. The carboxysome contains most of the carboxylating enzyme, Rubisco, and defects in its structure lead to the decrease in the cell's activity to fix the intracellular C_i by photosynthesis.

Fig. 5. The rates of CO_2 transport and HCO_3^- transport in the WT and MΔ*pxcA* measured by the silicon oil filtering centrifugation method (Volokita et al. 1984) in the presence (right columns) and absence (left columns) of 15 mM NaCl. Cells were suspended in 20 mM Tes-KOH (pH 8.0) or in Mes-KOH (pH 6.5) and $^{14}CO_2$ and $H^{14}CO_3^-$ were added in the light at the final concentrations of 22 and 145 μM, respectively.

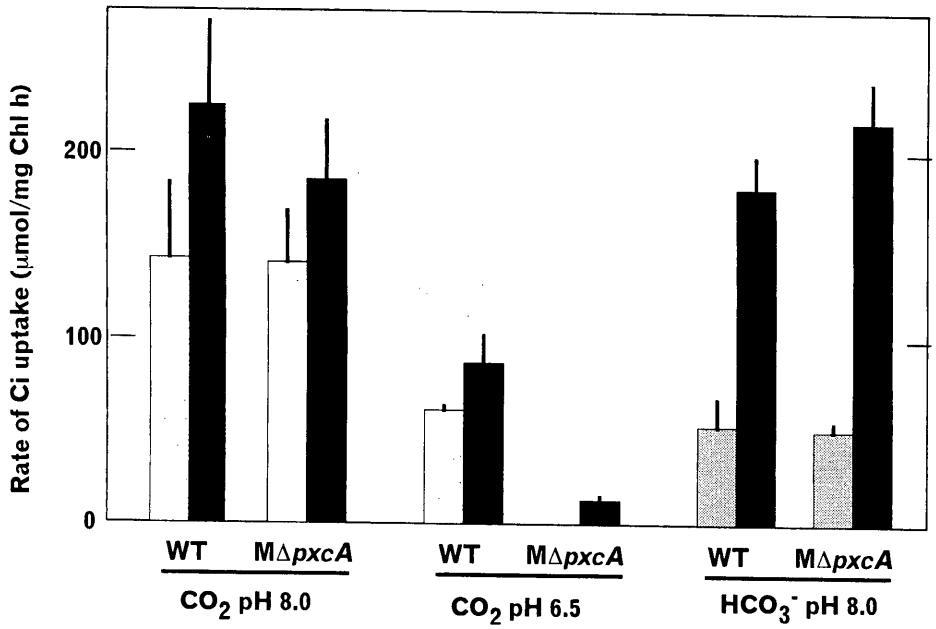

Fig. 6. Hypothetical model of the role of PxcA and Na^+/H^+ antiporters in regulating the transport of inorganic carbon and other anions. Failure to function both PxcA and Na^+/H^+ antiporter systems may be lethal to the cells. Functioning of either the PxcA system or the Na^+/H^+ antiporter system at alkaline pHs and of both systems at acidic pHs may be essential to keep the homeostasis of the intracellular ionic environment.

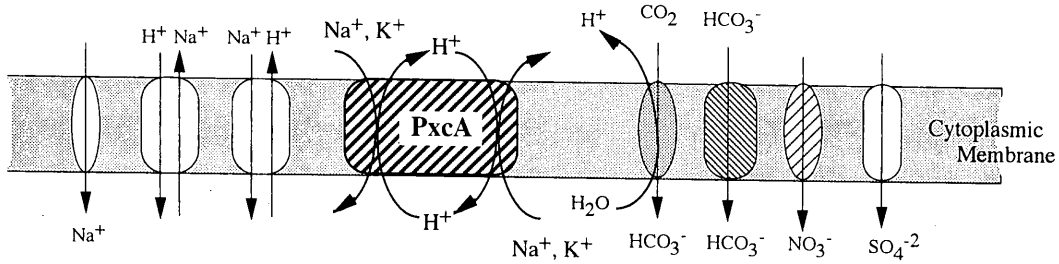

Mutants impaired in proton extrusion

Another type of mutants impaired in proton extrusion has recently been isolated. These mutants were first thought to be defective in CO_2 transport (Katoh et al. 1996*a*). Later the inhibition of CO_2 transport was found to be indirect (Katoh et al. 1996*b*). The gene, *cotA* (*pxcA*), impaired in the mutants of *Synechocystis* PCC6803 encodes a protein of 440 amino acids (Sonoda et al. 1997*a*). The same gene in *Synechococcus* PCC7942 encodes a protein of 427 amino acids (Sonoda et al. 1997*b*). These genes showed significant amino-acid sequence homology to *cemA* that encodes a protein found in the inner envelope membrane of chloroplasts in terrestrial plants (Katoh et al. 1996*a*; Sonoda et al. 1997*a*, 1997*b*; Sasaki et al. 1993). The homology was high in the C-terminal region and low in the N-terminal region. There are two types of CemA/PxcA. CemA in chloroplasts of higher plants consists of 229–231 amino acids, whereas CemA/PxcA in liverwort, *Chlamydomonas* (N. Rolland, EMBL Library, Accession No. X90559) and cyanobacteria are much larger and consist of 421–500 amino acids. Both the short-type and the long-type CemA/PxcA contain four membrane-spanning domains (Fig. 3).

Mutants were constructed by substituting *pxcA* in the WT cells of *Synechocystis* and *Synechococcus* with the spectinomycin resistance cartridge (omega fragment). These cells were unable to grow in BG11 medium (~17 mM Na^+) at pH 6.4 or at any pH in a low sodium medium (~100 μM Na^+) under aeration with 3% v/v CO_2 in air (Katoh et al. 1996*b*; Sonoda et al. 1997*b*). The WT cells grew well in the pH range between 6.4 and 8.5 in BG11 medium but only at alkaline pH in the low sodium medium. Illumination of WT cells suspended in 0.2 mM Tes-KOH buffer containing 15 mM NaCl resulted in an extrusion of protons followed by an uptake of protons (Fig. 4, curve B). However, only proton uptake was observed with the mutants under the same conditions (Fig. 4, curve D). The WT cells showed a lower rate of light-induced proton extrusion when sodium salt was replaced with potassium salt (curve C) and did not show the activity in the absence of the salts (curve A). These results indicated that *pxcA* is involved

in light-induced proton extrusion, presumably as a result of exchange of protons with Na^+ or K^+ ions.

Proton extrusion was observed in the presence of dimethylquinone (DMQ), an electron acceptor from photosystem II (PS II), and 3-(3,4-dichlorophenyl)-1,1-dimethylurea (DCMU) completely inhibited this reaction (Fig. 4, curve E). The result indicated that linear electron transport via PS II is essential for this reaction and that the proton extrusion proceeds without PS I reaction. When WT cells were illuminated in the presence of DMQ, protons were extruded but net proton movement was not observable after 10–20 s of illumination (curve E). Proton uptake occurred after turning the light off or when DCMU was added in the light. This indicates that proton extrusion and proton uptake proceed simultaneously in the light and proton uptake continues for a short period when proton extrusion was terminated after turning the light off or by adding DCMU. Probably, the ion gradients produced by proton extrusion (and uptake of Na^+ or K^+) are utilized for the uptake of protons and for the extrusion of Na^+ or K^+.

Measurements of the activity of CO_2 transport in the WT and *pxcA*-less mutant of Synechocystis (MΔ*pxcA*) revealed that the activity was very low at pH 6.5 and nearly zero in the absence of Na^+. At pH 8.0, there was no significant difference between the WT and mutant in their activity of CO_2 and HCO_3^- tansport (Fig. 5). We have also measured the activity of NO_3^- uptake in the WT and in the MΔ*pxcA* mutant. We found that NO_3^- uptake in the mutant was as high as the WT at pH 8.0 or 6.5 in the presence of 15 mM NaCl but was very low at pH 8.0 and was absent at pH 6.5 when NaCl was replaced by KCl (data not shown). These results indicate that PxcA has a role in controlling the transport of NO_3^- and possibly other anions in a low sodium medium.

The transport of anions is accompanied by an influx of negative charges and the transport of CO_2 is accompanied by the extrusion of protons as a result of CO_2 to HCO_3^- conversion that might occur in the cytoplasmic membrane (Fig. 6). Cells should have sophisticated mechanisms to keep their charge and pH homeostasis. PxcA may play a role in one of these mechanisms. Protons produced during CO_2 transport might be neutralized at alkaline pH but, at an acidic pH, extrusion of protons may be essentital for CO_2 transport. The functioning of the mechanism involving PxcA appears to be essential to the transport of NO_3^- at acidic pH or in a low sodium medium.

Acknowledgments

This study was supported by grants-in-aid for Scientific Research (No. 09640767) from the Ministry of Education, Science, Sports and Culture, Japan; the New Energy and Industrial Technology Development Organization (NEDO), Japan; and Human Frontier Science Program.

References

Berger, S., Ellersiek, U., and Steinmuller, K. 1991. Cyanobacteria contain a mitochondrial complex I-homologous NADH-dehydrogenase. FEBS Lett. **286**: 129–132.

Dolganov, N., and Grossman, A.R. 1993. Insertional inactivation of mutants of *Synechococcus* sp. strain PCC7942: isolation of filamentous strains. J. Bacteriol. **175**: 7644–7651.

Dzelzkalns, V.A., and Bogorad, L. 1988. Molecular analysis of a mutant defective in photosynthetic oxygen evolution and isolation of a complementing clone by a novel screening procedure. EMBO J. **7**: 333–338.

Espie, G.S., Miller, A.G., Kandasamy, R.A., and Canvin, D.T. 1991. Active HCO_3^- transport. Can. J. Bot. **69**: 936–944.

Friedberg, D., Kaplan, A., Ariel, R., Kessel, M., and Seijffers, J. 1989. The 5′-flanking region of the gene encoding the large subunit of ribulose-1,5-bisphosphate carboxylase–oxygenase is crucial for growth of the cyanobacterium *Synechococcus* sp. strain PCC 7942 at air levels of CO_2. J. Bacteriol. **171**: 6069–6076.

Fukuzawa, H., Suzuki, E., Komurai, Y., and Miyachi, S. 1992. A gene homologous to chloeoplast carbonic anhydrase (*icfA*) is essential to photosynthetic dioxide fixation by *Synechococcus* PCC7942. Proc. Natl. Acad. Sci. U.S.A. **89**: 4437–4440.

Kaneko, T., Sato, S., Kotani, H., Tanaka, A., Asamizu, E., Nakamura, Y., Miyajima, N., Hirosawa, M., Sugiura, M., Sasamoto, S., Kimura, T., Hosouchi, T., Matsuno, A., Muraki, A., Nakazaki, N., Naruo, K., Okumura, S., Shimpo, S., Takeuchi, C., Wada, T., Watanabe, A., Yamada, M., Yasuda, M., and Tabata, S. 1996. Sequence analysis of the genome of the unicellular cyanobacterium *Synechocystis* sp. strain PCC6803. II. Sequence determination of the entire genome and assignment of potential protein-coding regions. DNA Res. **3**: 109–136.

Kaplan, A., Schwarz, R., Lieman-Hurwitz, J., Ronen-Tarazi, M., and Reinhold, L. 1994. Physiological and molecular studies on the response of cyanobacteria to changes in the ambient inorganic carbon concentration. *In* The molecular biology of cyanobacteria. *Edited by* D.A. Bryant. Kluwer Academic Publishers, Dordrecht, The Netherlands. pp. 469–485.

Katoh, A., Lee, K.S., Fukuzawa, H., Ohyama, K., and Ogawa, T. 1996*a*. *cemA* homologue essential to CO_2 transport in the cyanobacterium, *Synechocystis* PCC6803. Proc. Natl. Acad. Sci. U.S.A. **93**: 4006–4010.

Katoh, A., Sonoda, M., Katoh, H., and Ogawa, T. 1996*b*. Absence of light-induced proton extrusion in *cotA*-less mutant of *Synechocystis* sp. Strain PCC6803. J. Bacteriol. **178**: 5452–5455.

Marco, M., Ohad, N., Schwarz, R., Lieman-Hurwitz, J., Gabay, C., and Kaplan, A. 1993 High CO_2 concentration alleviates the block in photosynthetic electron transport in an *ndhB*-inactivated mutant of *Synechococcus* sp. PCC7942. Plant Physiol. **101**: 1047–1053.

Marcus, Y., Schwarz, R., Friedberg, D., and Kaplan, A. 1986. High CO_2 requiring mutant of *Anacystis nidulans* R2. Plant Physiol. **82**: 610–612.

Mi, H., Endo, T., Schreiber, U., Ogawa, T., and Asada, K. 1994. NAD(P)H dehydrogenase-dependent cyclic electron flow around photosystem I in the cyanobacterium *Synechocystis* PCC6803: a study of dark-starved cells and spheroplasts. Plant Cell Physiol. **35**: 163–173.

Mi, H., Endo, T., Ogawa, T., and Asada, K. 1995. Thylakoid membrane-bound, NADPH-specific pyridine nucleotide dehydrogenase complex mediates cyclic electron transport in the cyanobacterium *Synechocystis* sp. PCC6803. Plant Cell Physiol. **36**: 661–668.

Miller, A.G., Espie, G.S., and Canvin, D.T. 1991. Active CO_2 transport in cyanobacteria. Can. J. Bot. **69**: 925–935.

Ogawa, T. 1990. Mutants of *Synechocystis* PCC6803 defective in inorganic carbon transport. Plant Physiol. **94**: 760–765.

Ogawa, T. 1991*a*. A gene homologous to the subunit-2 gene of NADH dehydrogenase is essential to inorganic carbon of *Synechocystis* PCC6803. Proc. Natl. Acad. Sci. U.S.A. **88**: 4275–4279.

Ogawa, T. 1991*b*. Cloning and inactivation of a gene essential to inorganic carbon transport of *Synechocystis* PCC6803. Plant Physiol. **96**: 280–284.

Ogawa, T. 1992. Identification and characterization of the *ictA/ndhL* gene product essential to inorganic carbon transport of *Synechocystis* PCC6803. Plant Physiol. **99**: 1604–1608.

Ogawa, T., and Ogren, W.L. 1985. Action spectra for accumulation

of inorganic carbon in the cyanobactyerium, *Anabaena variabilis*. Photochem. Photobiol. **41**: 583–587.

Ogawa, T., Miyano, A., and Inoue, Y. 1985. Photosystem-I-driven inorganic carbon transport in the cyanobacterium, *Anacystis nidulans*. Biochim. Biophys. Acta, **808**: 77–84

Ogawa, T., Kaneda, T., and Omata, T. 1987. A mutant of *Synechococcus* PCC7942 incapable of adapting to low CO_2 concentration. Plant Physiol. **84**: 711–715.

Ogawa, T., Amichay, D., and Gurevitz, M. 1994*a*. Isolation and characterization of the *ccmM* gene required by the cyanobacterium *Synechocystis* PCC6803 for inorganic carbon utilization. Photosynth. Res. **39**: 183–190.

Ogawa, T., Marco, E., and Orus, M.I. 1994*b*. A gene (*ccmA*) required for carboxysome formation in the cyanobacterium *Synechocystis* sp. strain PCC6803. J. Bacteriol. **176**: 2374–2378.

Omata, T. 1992. Characterization of the downstream region of *cmpA*: Identification of a gene cluster encoding a putative permease of the cyanobacterium *Synechococcus* PCC7942. *In* Research in Photosynthesis, Vol. III. Proceedings of the International Congress on Photosynthesis, 30 August – 4 September 1992, Nagoya, Japan. *Edited by* N. Murata. Kluwer Academic Publishers, Dordrecht, The Netherlands. pp. 807–810.

Omata, T., and Ogawa, T. 1986. Biosynthesis of a 42-kD polypeptide in the cytoplasmic membrane of the cyanobacterium *Anacystis nidulans* strain R2 during adaptation to low CO_2 concentration. Plant Physiol. **80**: 525–530.

Omata, T., Carlson, T.J., Ogawa, T., and Pierce, J. 1990. Sequencing and modification of the gene encoding the 42-kilodalton protein in the cytoplasmic membrane of *Synechocystis* PCC7942. Plant Physiol. **93**: 305–311.

Price, G.D., and Badger, M.R. 1989*a*. Expression of human carbonic anhydrase in the cyanobacterium *Synechococcus* PCC7942 create a high CO_2-requiring phenotype. Evidence for a central role for the carboxysome in the CO_2 concentrating mechanism. Plant Physiol. **91**: 505–513.

Price, G.D., and Badger, M.R. 1989*b*. Isolation and characterization of high CO_2-requiring-mutants of the cyanobacterium *Synechococcus* PCC7942. Two phenotypes that accumulate inorganic carbon but are apparently unable to generate CO_2 within the carboxysome. Plant Physiol **91**: 514–525.

Price, G.D., Howitt, S.M., Harrison, K., and Badger, M.R. 1993. Analysis of a genomic DNA region from the cyanobacterium *Synechococcus* sp. strain PCC7942 involved in carboxysome assembly and function. J. Bacteriol. **175**: 2871–2879.

Ronen-Tarazi, M., Bonfil, D.J., Schatz, D., and Kaplan, A. 1998. Cyanobacterial mutants impaired in bicarbonate uptake isolated with the aid of an inactivation library. Can. J. Bot. **76**: 942–948.

Sasaki, Y., Sekiguchi, K., Nagano, Y., and Matsuno, R. 1993. Chloroplast envelope protein encoded by chloroplast genome. FEBS Lett. **316**: 93–98.

Schwarz, R., Friedberg, D., and Kaplan, A. 1988. Is there a role for the 42kDa polypeptide in inorganic carbon uptake by cyanobacteria? Plant Physiol. **88:** 284–288.

Sonoda, M., Kitano, K., Katoh, A., Katoh, H., Ohkawa, H., and Ogawa, T. 1997*a*. Size of *cotA* and identification of the gene product in *Synechocystis* sp. strain PCC6803. J. Bacteriol. **179**: 3845–3850.

Sonoda, M., Katoh, H., Ohkawa, H., and Ogawa, T. 1997*b*. Cloning of *cotA* gene of *Synechococcus* PCC7942 and complementation of a *cotA*-less mutant of *Synechocystis* PCC6803 with chimeric genes of the two strains. Photosynth. Res. **54**: 99–105.

Stanier, R.Y., Kunisawa, R., Mandel, M., and Cohen-Bazire, G. 1971. Purification and properties of unicellular blue-green algae (order *Chroococcales*). Bacterial Rev. **35**: 171–205.

Sültemeyer, D., Klughammer, M., Ludwig, M., Badger, M.R., and Price, D.G. 1997. Random insertional mutagenesis used in the generation of mutants of the marine cyanobacterium *Synechochoccus* sp. strain PCC7002 with an impaired CO_2 concentrating mechanism. Aust. J. Plan Physiol. **24**: 317–327.

Vermaas, W. 1993. Molecular-biological approaches to analyze photosystem II structure and function. Annu. Rev. Plant Physiol. Plant Mol. Biol. **44**: 457–481.

Volokita, M., Zenvirth, D., Kaplan, A., and Reinhold, L. 1984. Nature of the inorganic carbon species actively taken up by the cyanobacterium *Anabaena variabilis*. Plant Physiol. **76**: 599–602.

Williams, J.G.K., and Szalay, A.A. 1983. Stable integration of foreign DNA into the chromosome of the cyanobacterium *Synechococcus* R2. Gene, **24**: 37–51.

Yu, J.-W., Price, G.D., and Badger, M.R. 1994. A mutant isolated from the cyanobacterium *Synechococcus* PCC7942 is unable to adapt to low inorganic carbon conditions. Plant Physiol. **104**: 605–611.

STRUCTURE AND FUNCTION OF CEMA HOMOLOGUE (PXCA) IN CYANOBACTERIA

M. Sonoda[1], H. Katoh[2], A. Katoh[3], H. Ohkawa[1], W. Vermaas[4] and T. Ogawa[1,2]
[1]*Graduate School of Bioagricultural Sciences and* [2]*Bioscience Center, Nagoya University, Nagoya 464-8601, Japan,* [3]*Bioscience Department, Tsukuba University, Tsukuba 305-8572, Japan and* [4]*Center for the Study of Early Events in Photosynthesis, Arizona State University, Tempe, AZ 85287-1601, USA*

1. Introduction

The *cemA* (*ycf10*) gene codes for a chloroplast envelope membrane protein [1] and is conserved in higher and lower plants and in algae [2-8]. CemA in higher plants consists of 229 to 231 amino-acids [2-4] whereas that in liverwort (*Marchantia*) [5] and *Chlamydomonas* [6] is much larger and consists of 434 and 500 amino-acids, respectively. Recent sequencing of whole chloroplast genomes of *Porphyra* [7] and *Chlorella* [8] revealed that *cemA* in these algae encodes proteins of 278 and 264 amino-acids, respectively. The function of CemA is not known. Rolland et al [6] have constructed mutants by disrupting *cemA* in *Chlamydomonas*. They showed that the disruption of the gene led to increased light sensitivity and affected CO_2-dependent photosynthesis and inorganic carbon uptake.

We have isolated a homologue of *cemA* from *Synechocystis* PCC6803 as the gene which complemented mutants defective in CO_2 transport [9]. The gene, *pxcA* (formerly known as *cotA*), was also isolated from *Synechococcus* PCC7942 [10]. Mutants were constructed by disrupting *pxcA* in these two strains. In this paper, we show that the primary effect of *pxcA* disruption is inactivation of light-dependent proton extrusion and that the proton extrusion is PSII-dependent and is accompanied by an influx of protons. A possible role of PxcA-dependent proton exchange in pH and charge homeostasis is discussed.

2. Materials and Methods

The wild-type (WT) cells and *pxcA*$^-$ mutants of *Synechocystis* PCC6803 and *Synechococcus* PCC7942 and *psaAB*$^-$(PS I-less) mutant [11] were grown at 30°C in BG-11 medium [12] buffered with 20 mM N-Tris(hydroxy-methyl)methyl-2-aminoethanesulfonic acid (TES)-KOH at pH 8.0 during aeration with 3% (vol/vol) CO_2 in air. Glucose (5 mM) was added to the above medium for the growth of *psaAB*$^-$. Continuous illumination was provided by fluorescent lamps at 40 μmol photosynthetically active radia-

J. H. Argyroudi-Akoyunoglou and H. Senger (eds.),
The Chloroplast: From Molecular Biology to Biotechnology, 149–154.

tion/m^2s (400-700 nm) for *psaAB*$^-$ cells which are sensitive to higher light intensity, and at 100 μmol/m^2s for the other strains.

Changes in pH of the cell suspension (3 ml) kept at 30 °C were monitored by a pH electrode with a meter (Inlar 423 and Delta 350; Mettler Toledo, Halstead Essex, UK). Details of this method and the methods for measuring uptake of CO_2 and nitrate have been described elsewhere [13, 14].

3. Results

3.1. PHYLOGENETIC TREE OF PXCA AND CEMA

The *pxcA* genes of *Synechocystis* PCC6803 and *Synechococcus* PCC7942 encode proteins of 440 and 427 amino-acids, respectively [9,10], which were close in size to CemA of *Marchantia* and *Chlamydomonas* (434 and 500 amino-acids, respectively) [5,6], but was much larger than CemA of higher plants (229-231 amino-acids) [2-4]. Although CemA proteins of *Porphyra* and *Chlorella* were smaller than PxcA and consists of 278 and 264 amino-acids, respectively [7,8], they showed higher homology to PxcA than CemA of *Marchantia* and *Chlamydomonas*. PxcA and CemA contain 4 membrane spanning domains in the C-terminal region [2-10]. The homology was high in this region but was low in the N-terminal region. Phylogenetic tree for PxcA of cyanobacteria and CemA of plants and algae, which was computed for the 230 amino-acid sequences in the C-terminal regions, suggested that PxcA and CemA have the same ancestor (Fig. 1).

In addition to *pxcA* (slr1596), another *cemA* homologue (sll1685) exists in *Synechocystis* genome [15]. This gene encodes a protein of 393 amino-acids which was less homologous to CemA than PxcA. The lower homology can be also seen from the phylogenetic tree in Fig. 1.

3.2. IDENTIFICATION AND LOCALIZATION OF PXCA

Western analysis using an antibody raised against *Synechocystis* PxcA (partial) fused to glutathione S-transferase indicated that a protein in the cytoplasmic membrane with an apparent molecular mass of 52 kDa cross-reacted with the antibody. No reacting band was

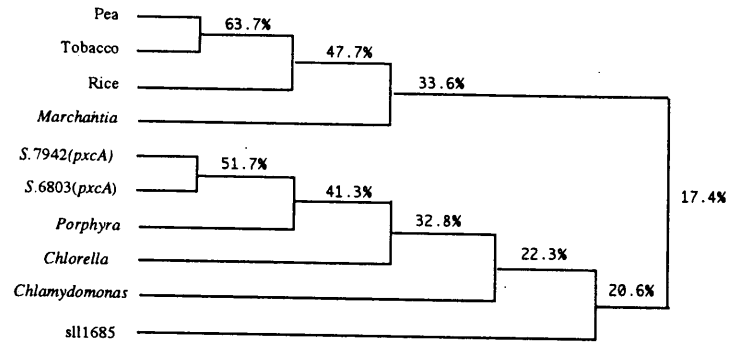

Figure 1. Phylogenetic tree for PxcA of cyanobacteria and CemA of plants and algae.

observed in the soluble fraction [16]. The antibody also reacted with the thylakoid membrane preparation. However, the cross reactivity was much less than with the cytoplasmic membrane and, therefore, is considered to be due to contamination of the cytoplasmic membrane. The 52-kDa band was not detected on the Coomassie brilliant blue staining profiles of the WT membranes. The amount of PxcA appears to be low.

3.3. GROWTH CHARACTERISTICS OF THE *pxcA*$^-$ MUTANTS

Mutants were constructed by substituting *pxcA* in the WT cells of *Synechocystis* and *Synechococcus* with the omega fragment. Both mutants were unable to grow in BG11 medium (N- Na^+; ~17 mM Na^+) at pH 6.5 or, at any pH in a low Na^+ (L- Na^+; ~100 μM Na^+) under aeration with 3% (vol/vol) CO_2 in air [9,10]. The WT cells grew well in the pH range between 6.5 and 8.5 in BG11 medium but only at alkaline pH in the low Na^+ medium.

3.4. ABSENCE OF LIGHT-DEPENDENT PROTON EXTRUSION IN THE *pxcA*$^-$ MUTANTS

Light-dependent proton extrusion, which has been observed with various cyanobacteria strains, was observed with the WT cells of *Synechocystis* and *Synechococcus*. Illumination of WT cells of *Synechocystis* resulted in an extrusion followed by an uptake of protons (Fig. 2, curve A). Similar profile was obtained for WT cells of *Synechococcus*. The light-dependent proton extrusion was not observed with the *pxcA*$^-$ mutants (curves B and C). These results indicated that *pxcA* is involved in light-dependent proton extrusion.

A mutant constructed by disrupting another *cemA* homologue in *Synechocystis* (sll1685) showed the WT phenotype; the mutant extruded protons in the light and grew normally at pH 6.5 or in L-Na^+ medium. Another mutant constructing by inactivating *pxcA* and sll1685 genes showed the phenotype of the *pxcA*$^-$ mutant.

3. 5. PHOTOSYSTEM II-DEPENDENT PROTON EXTRUSION

The proton extrusion was observed with WT cells in the presence of dimethylbenzoquinone (DMBQ; an electron acceptor from PS II) (curves A and B in Fig. 3) or with a PSI-deletion mutant(*psaAB*$^-$) (curve C). The result indicated that linear electron transport *via* PS II is essential to this reaction and that the proton extrusion proceeds without PSI

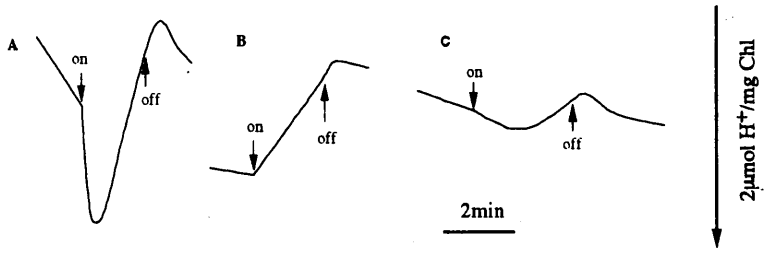

Figure 2. Net proton movements in cell suspensions of the WT (A) and *pxcA*$^-$ mutant (B) of *Synechocystis* PCC6803 and *pxcA*$^-$ mutant of *Synechococcus* PCC7942 (C). Light was switched on and off as indicated.

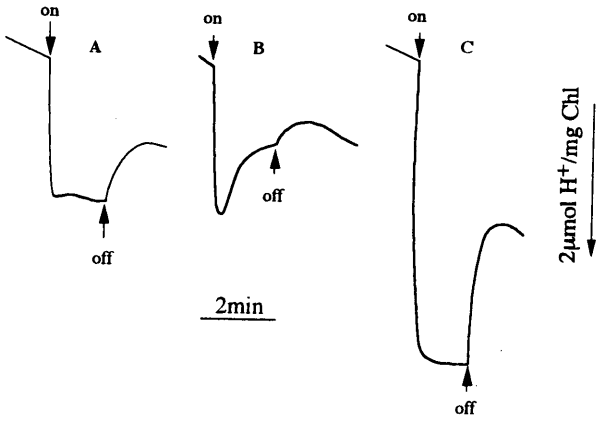

Figure 3. Net proton movement in the suspensions of WT Synechocystis (curveA) and Synechococcus (B) and *psaAB*$^-$ (C) cells upon switching the light on and off. Cells were suspended in 0.2 mM Tes-KOH containing 15 mM NaCl. DMBQ was added prior to illumination for curves A and B.

reaction. Curves A and C in Fig. 3 indicate that the net proton extrusion does not proceed continuously in the light but ceases after a minute of illumination. This suggests that in the light both extrusion and influx of protons occur, reaching a stationary level where there is no net proton exchange. The influx of proton in the light was clearly observed with *Synechococcus* cells (curveB). After the light is turned off (causing proton extrusion to cease) proton influx continues for a short time until new steady-state level is attained. Thus, proton extrusion and proton uptake proceed simultaneously in the light and proton uptake continues for a short period when proton extrusion was ceased. Probably, Δpmf produced by proton extrusion is utilized for proton uptake.

3.6. EFFECT OF Na^+ AND pH ON THE UPTAKE OF CO_2 AND NO_3^-.

Protons are produced during the transport of CO_2; protons are consumed when NO_3^- is reduced to NH_4 *via* NO_2^-. Cells have a mechanism to maintain a homeostasis with respect to the intracellular pH and electroneutrality during these processes. To test whether the PxcA-dependent proton exchange is involved in maintaining this homeostasis, the uptake of CO_2 and NO_3^- was monitored as a function of the activity of proton exchange. For this purpose, the uptake of CO_2 and NO_3^- in WT and the *pxcA*$^-$ strain was measured at pH 8.0 and 6.5 in the presence of normal concentration (15 mM) of NaCl (N-Na^+) or KCl with a low contaminating (~100μM) concentration of Na^+ (L-Na^+). At L-Na^+, the activity of NO_3^- uptake was very low in *pxcA*$^-$ at pH 8.0 and was zero at pH 6.5 (lower columns in Fig. 4). At N-Na^+, no significant effect of *pxcA* inactivation was observed on CO_2 and NO_3^- uptake at pH 8.0 but CO_2-uptake activity was reduced significantly at pH 6.5 (upper and lower columns). No CO_2 uptake was observed in the mutant at pH 6.5 and L-Na^+. It is evident that the inactivation of *pxcA* strongly affected the CO_2 uptake under acidic conditions and the NO_3^- uptake at low Na^+ concentrations.

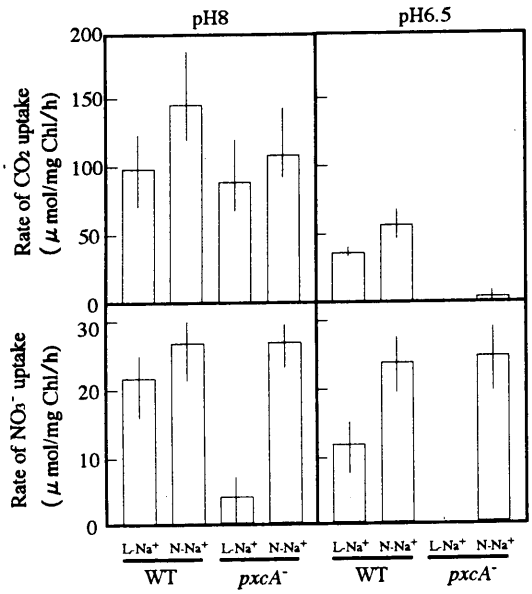

Figure 4. The rates of CO_2 and NO_3^- uptake in the WT and *pxcA*$^-$ cells of *Synechocystis* at pH 8.0 and 6.5 in the presence of 15 mM NaCl (N-Na^+) or KCl (L-Na^+).

4. Discussion

Cells have a mechanism to keep their intracellular homeostasis against various environmental changes. PxcA-dependent proton exchange system may be involved in keeping intracellular pH and charge homeostasis. Another system involved in such homeostasis would be Na^+/H^+ antiport. The activity of both systems are dependent on Na^+ concentration in the medium. The hypothesis that the PxcA-dependent and Na^+/H^+ antiport-dependent proton exchange are involved in pH homeostasis may explain the growth characteristics of the WT and *pxc*- mutant. The ability of cells to keep their intracellular pH homeostasis depends on the presence of the system(s) and on Na^+ concentration in the medium. The ability would be in the following order:

$$\text{WT(N-Na}^+\text{)>WT (L-Na}^+\text{], } pxcA^- \text{ (N-Na}^+\text{) >}pxcA^- \text{ (L-Na}^+\text{)}$$

The highest ability will be attained by WT cells at N-Na^+ (~15 mM) and the lowest ability by the *pxcA*$^-$ mutant at L-Na^+. This may explain why WT cells grow at wide range of pHs in BG11 medium and the mutant cells are unable to grow at any pHs in the L-Na^+ medium [9,10]. This model could be verified by studying the characteristics of disruption mutants of Na^+/H^+ antiporter genes. *Synechocystis* PCC 6803 possesses at least 5 Na^+/H^+ antiporter(-like) genes. We are now trying to construct such mutants.

There is no ATP-binding motif in PxcA, which suggested that PxcA is not a proton transporter driven by ATP. It is possible that PxcA plays a role in regulating or acti-

vating an H^+-ATPase or it could be a new type of proton pump. Further studies are in progress to answer these questions on the role of PxcA.

5. Acknowledgement

This study was supported by Grants-in Aid for Scientific Research (No. 09640767) from the Ministry of Education, Science, Sports and Culture of Japan and by grants from the New Energy and Industrial Technology Development Organization (NEDO) of Japan and from the Human Frontier Science Program.

6. References

1. Sasaki, Y., Sekiguchi, K., Nagano, Y.and Matsuno, R. (1993) Chloroplast envelope protein encoded by chloroplast genome. *FEBS Lett.* **316,** 93-98.
2. Willey, D.L. and Gray, J.C. (1990) An open reading frame encoding a putative haem-binding polypeptide is cotranscribed with the pea chloroplast gene for apocytochrome f. *Plant Mol. Biol.* **15,** 347-356.
3. Shinozaki, K., Ohme, M., Tanaka, M., Wakasugi, T., Hayashida, N., Matsubayashi, T., Zaita, N., Chunwongse, J., Obokata, J., Yamaguchi-Shinozaki, K., Ohto, C., Torazawa, K., Meng, B.Y., Sugita, M., Deno, H., Kamogashira, T., Yamada, K., Kusuda, J., Takaiwa, F., Kato, A., Tohdoh, N., Shimada, H. and Sugiura, M. (1986) The complete nucleotide sequence of the tobacco chloroplast genome: its gene organization and expression. *EMBO J.* **5,** 2043-2049.
4. Hiratsuka, J., Shimada, H., Whittier, R., Ishibashi, T., Sakamoto, M., Mori, M., Kondo, C. Honji, Y., Sun, C.R., Meng, B.Y., Li, Y.Q., Kanno, A., Nishizawa, Y., Hirai, A., Shinozaki, K. and Sugiura, M. (1989) The complete sequence of the rice (*Oryza sativa*) chloroplast genome: intermolecular recombination between distinct tRNA genes accounts for a major plastid DNA inversion during the evolution of the cereals. *Mol. Gen. Genet.* **217,** 185-194.
5. Ohyama, K., Fukuzawa, H., Kohchi, T., Shirai, H., Sano, T., Sano, S., Umesono, K., Shiki, Y., Takeuchi, M., Chang, Z., Aota, S., Inokuchi,H. and Ozeki, H. (1986) Chloroplast gene organization deduced from complete sequence of liverwort *Marchantia polymorpha* chloroplast DNA. *Nature* **322,** 572-574.
6. Rolland, N., Dorne, A.-J., Amoroso, G., Sultemeyer, D.F., Joyard, J. and Rochaix, J.-D. (1997) Disruption of the plastid *ycf10* open reading frame affcts uptake of inorganic carbon in the chloroplast of *Chlamydomonas. The EMBO J.* **16,** 6713-6726.
7. Reith M.E. and Munholland J. (1995) Complete nucleotide sequence of the *Porphyra purpurea* chloroplast genome. *Plant Mol. Biol. Rep.* **13,** 333-335.
8. Wakasugi, T., Nagai,T., Kapoor, M., Sugita, M., Ito, M., Ito, S., Tsudzuki, J., Nakashima, K., Tsudzuki, T., Suzuki, Y., Hamada, A., Ohta, T., Inamura, A., Yoshinaga, K.and Sugiura, M. (1997) Complete nucleotide sequence of the chloroplast genome from the green alga *Chlorella vulgaris.* The existence of genes possibly involved in chloroplast division. *Proc.Natl.Acad.Sci.U.S.A.* **94,** 5967-5972.
9. Katoh, A., Lee, K.S., Fukuzawa, H. Ohyama, K. and Ogawa, T. (1996) A *cemA* homologue essential to CO_2 transport in the cyanobacterium, *Synechocystis* PCC6803. *Proc. Natl. Acad. Sci. USA* **93,** 4006-4010.
10. Sonoda, M., Katoh, H., Ohkawa, H. and Ogawa, T. (1997) Cloning of *cotA* gene of *Synechococcus* PCC7942 and complementation of a *cotA*-less mutant of *Synechocystis* PCC6803 with chimeric genes of the two strains. *Photosynth. Res.* **54,** 99-105.
11. Shen, G., Boussiba, S. and Vermaas, W.F.J. (1993) *Synechocystis* sp. PCC6803 strains lacking photosystem I and phycobilisome function. *Plant Cell* **5,** 1853-1863.
12. Stanier, R.Y., Kunisawa, R., Mandel, M. and Cohen-Bazire, G. (1971)Purification and properties of unicellular blue-green algae (order *Chroococcales*). *Bacteriol. Rev. 35,* 171-205.
13. Katoh, A., Sonoda, M., Katoh, H. and Ogawa, T. (1996) Absence of light-induced proton extrusion in *cotA*-less mutant of *Synechocystis* sp. strain PCC6803. *J. Bacteriol.* **178,** 5452-5455.
14. Sonoda, M., Katoh, H., Vermaas, W., Schmetterer, G. and Ogawa, T. (1998) Photosynthetic Electron Transport Involved in the PxcA-Dependent Proton Extrusion in *Synechocystis* sp. PCC6803: Effect of *pxcA* Inactivation on CO_2, HCO_3^- and NO_3^- Uptake*J. Bacteriol.* in press.
15. Kaneko, T., Sato, S., Kotani, H., Tanaka, A., Asamizu, E., Nakamura, Y., Miyajima, N., Hirosawa, M., Sugiura, M., Sasamoto, S., Kimura, T., Hosouchi, T., Matsuno, A., Muraki, A., Nakazaki, N., Naruo, K., Okumura, S., Shimpo, S., Takeuchi, C., Wada, T., Watanabe, A., Yamada, M., Yasuda, M. and S. Tabata, S. (1996) Sequence analysis of the genome of the unicellular cyanobacterium *Synechocystis* sp. strain PCC6803. II. Sequence determination of the entire genome and assignment of potential protein-coding regions. *DNA Research* **3,** 109-136.
16. Sonoda, M., Kitano, K., Katoh, A., Katoh, H., Ohkawa, H. and Ogawa, T. (1997) Size of *cotA* and identification of the gene Product in *Synechocystis* sp. strain PCC6803. *J. Bacteriol.* **179,** 3845-3850.